



# **Evolution, function and manipulation of methyl halide production in plants**

**Evelyn Koerner**

A thesis submitted to the University of East Anglia for the degree of  
Doctor of Philosophy

John Innes Centre  
Norwich, UK

September 2012

© This copy of the thesis has been supplied on condition that anyone who consults it is understood to recognise that its copyright rests with the author and that use of any information derived there from must be in accordance with current UK Copyright Law. In addition, any quotation or extract must include full attribution.

## **Acknowledgements**

Firstly, I would like to thank my supervisor Lars Østergaard for giving me the opportunity to work on this exciting project in his lab and for his guidance and support. I would also like to thank current and past members of the Østergaard lab for their help, especially Pauline Stephenson, Thomas Girin, Sara Fuentes and Alice Baillie. A special thanks goes to Bill Sturges, Hannah Newton and Stephen Humphrey for analysing the methyl halide samples. I would also like to thank Anna Jordan, Gavin Hatt and Ian Bedford for their help with the insect experiments, and Andrzej Tkacz and Phil Poole for hosting me in their lab to do the rhizosphere work. Moreover, I would like to thank Rene Dreos and Sam Mugford for their help with the microarray analysis.

I am grateful to Nick Brewin, Mike Merrick, Rita Galhano, Ane Sesma, Georgina Fabro and Jonathan Jones for making the Rotation Year such a fantastic experience and another thank you to Jonathan for his support as my secondary supervisor.

I would also like to thank Chie Hattori, Anastasia Gardiner, Cintia Kawashima and Kate Bailey for cheering me up during lunch or tea breaks when things were not going so well.

Finally, I would like to thank my parents, my sister and my partner Moritz for their love and support during the last couple of years.

The work presented here was funded by the John Innes Foundation and the Earth and Life Systems Alliance (ELSA).

## Abstract

Methyl halides (CH<sub>3</sub>Cl, CH<sub>3</sub>Br and CH<sub>3</sub>I) are a group of volatile organic compounds which contribute to natural ozone degradation in the atmosphere. Plants are important emitters of these compounds due to the activity of halide/thiol methyltransferases (HTMTs), however, the function of HTMTs or methyl halide production is not known. In *Arabidopsis thaliana*, one HTMT is primarily responsible for the production of methyl halides and encoded by the *HARMLESS TO OZONE LAYER (HOL)* gene.

In this study, an *A. thaliana hol* mutant and *35S::HOL* lines were used to investigate the function of HOL. No support was found for the hypothesis that HOL contributes to salt stress tolerance via the disposal of excessive amounts of halides. On the contrary, increased HOL activity made *35S::HOL* plants more susceptible towards salt stress. Despite the toxicity of methyl halides, differences in HOL activity in *hol* mutant and *35S::HOL* plants did not affect the performance of insect herbivores, nor did it alter the microbial diversity of the rhizosphere in these lines. Microarray analysis of WT and *hol* mutant plants pointed to a function of HOL in starch/carbon metabolism and stress response pathways in *A. thaliana*.

*Brassica* crops are significant emitters of methyl halides. A *HOL*-homologous gene (*BraA.HOL.a*) was identified in *Brassica rapa*. It was confirmed that this gene contributes to methyl halide production in *B. rapa* since *braA.hol.a* mutants had significantly reduced emission levels compared to WT.

*HOL*-homologous genes were also found in various plant species throughout the plant kingdom including the moss *Physcomitrella patens*, which was shown to produce CH<sub>3</sub>Br. These data show that methyl halide production is an ancient mechanism in land plants. Moreover, phylogenetic analysis revealed a clear separation between HTMTs from glucosinolate (GL)-containing plants and HTMTs from eudicots without GLs supporting the hypothesis of a novel function of HTMTs in the order Brassicales.

## Table of Contents

Acknowledgements.....	i
Abstract.....	ii
Table of Figures .....	vii
Table of Tables .....	x
List of Abbreviations .....	xi
<b>Chapter 1 – General Introduction.....</b>	<b>1</b>
1.1 Methyl halides and ozone degradation.....	1
1.2 Sources and sinks of methyl halides .....	3
1.3 Abiotic methyl halide production from senescent and dead leaves .....	7
1.4 Production of methyl halides by methyltransferases .....	9
1.5 Function of methyl halide production and HTMTs .....	12
1.6 Objectives of this thesis .....	16
<b>Chapter 2 – Materials and Methods.....</b>	<b>17</b>
2.1 Plant material and growth conditions.....	17
2.1.1 <i>Arabidopsis thaliana</i> .....	17
2.1.2 <i>Brassica rapa</i> .....	17
2.1.3 <i>Oryza sativa</i> .....	17
2.1.4 <i>Physcomitrella patens</i> .....	18
2.2 DNA extraction.....	18
2.3 RNA extraction and cDNA synthesis .....	19
2.4 Creation of transgenic <i>A. thaliana</i> lines.....	19
2.4.1 Plasmid construction.....	19
2.4.1.1 Generation of <i>35S::HOL</i> , <i>35S::PpHOL</i> , <i>35S::OsHOL1</i> , <i>35S::OsHOL2</i> and <i>35S::PtHTMT</i> constructs.....	19
2.4.1.2 Generation of <i>HOL::GUS</i> construct.....	20
2.4.1.3 Generation of <i>HOL::HOL:GFP</i> and <i>35S::GFP</i> constructs.....	20
2.4.2 Sequencing.....	20
2.4.3 Transformation into <i>A. thaliana</i> .....	21
2.5 Creation of <i>DR5::GFP</i> x <i>hol</i> and <i>DR5::GFP</i> x <i>35S::HOL</i> crosses .....	21
2.6 Generation of <i>Physcomitrella Pphol</i> knockout lines .....	21
2.7 Genotyping of <i>braA.hol.a</i> mutants.....	22
2.8 RT-PCR and Quantitative Real-Time PCR .....	22
2.9 Microarray analysis.....	23
2.10 Methyl halide measurements .....	24
2.11 Salt stress and KSCN experiments.....	25

2.12 Sucrose experiment .....	25
2.13 Auxin experiments .....	25
2.14 Chlorophyll measurements .....	26
2.15 Glucosinolate analysis .....	26
2.16 GUS activity.....	26
2.17 Iodine staining for visualisation of starch .....	27
2.18 Microscopy .....	27
2.19 Herbivore experiments.....	28
2.20 Rhizosphere community profiling .....	28
2.20.1 Experimental setup.....	28
2.20.2 Bacterial count .....	29
2.20.3 DNA extraction and ARISA .....	29
2.20.4 Generation of plots and statistical analysis .....	30
2.20.5 PCR amplification of <i>cmuA</i> .....	31
2.21 Phylogenetic analysis.....	31
2.22 Statistical analysis.....	32
<b>Chapter 3 – Characterisation and manipulation of <i>HOL</i> gene expression in <i>Arabidopsis thaliana</i> .....</b>	<b>33</b>
3.1 Introduction.....	33
3.1.1 Properties of <i>A. thaliana</i> <i>HOL</i> methyltransferases .....	33
3.1.2 Objectives of this chapter.....	35
3.2 Results.....	35
3.2.1 Characterisation of <i>HOL</i> gene expression and <i>HOL</i> protein localisation.....	35
3.2.2 Generation and characterisation of <i>35S::HOL</i> lines .....	38
3.2.3 Microarray analysis of the <i>hol</i> mutant .....	40
3.2.4 Identification of potential functions of <i>HOL</i> from public microarray data.....	45
3.3 Discussion.....	46
<b>Chapter 4 – Exploring potential functions of <i>HOL</i> and methyl halide emissions in <i>Arabidopsis thaliana</i>: Part I .....</b>	<b>51</b>
4.1 Introduction.....	51
4.1.1 Methyl halide production and salt stress.....	51
4.1.2 Objectives of this chapter.....	54
4.2 Results.....	54
4.2.1 <i>HOL</i> and salt stress tolerance.....	54
4.2.1.1 Effects of salt stress on the growth of <i>hol</i> mutant and <i>35S::HOL</i> plants .....	54
4.2.1.2 Effects of salt stress on <i>HOL</i> expression.....	58
4.2.1.3 Why are <i>35S::HOL</i> lines more susceptible to salt stress?.....	61

4.2.2 HOL and starch metabolism .....	64
4.2.3 HOL and auxin.....	66
4.3 Discussion.....	69
<b>Chapter 5 – Exploring potential functions of HOL and methyl halide emissions in <i>Arabidopsis thaliana</i>: Part II.....</b>	<b>75</b>
5.1 Introduction.....	75
5.1.1 Production and role of volatiles emitted by plants.....	75
5.1.2 Methyl halides - a novel type of plant volatiles involved in plant defence against herbivores or pathogens? .....	76
5.1.3 Methylation of glucosinolate hydrolysis products by HOL.....	77
5.1.4 Objectives of this chapter.....	79
5.2 Results.....	80
5.2.1 HOL and GL metabolism.....	80
5.2.2 HOL and plant-insect interactions .....	82
5.2.3 Influence of methyl halide production on rhizosphere bacteria.....	84
5.3 Discussion.....	88
<b>Chapter 6 – Characterisation and manipulation of methyl halide production in <i>Brassica rapa</i>, <i>Oryza sativa</i> and the moss <i>Physcomitrella patens</i> .....</b>	<b>93</b>
6.1 Introduction.....	93
6.1.1 Methyl halide production in crop plants .....	93
6.1.2 The moss <i>Physcomitrella patens</i> – a model for understanding the molecular basis of plant development and evolution.....	95
6.1.3 Objectives of this chapter.....	95
6.2 Results.....	96
6.2.1 Manipulation of methyl halide production in <i>Brassica rapa</i> .....	96
6.2.2 Characterisation and manipulation of methyl halide production in rice ( <i>Oryza sativa</i> ).....	99
6.2.3 Characterisation and manipulation of methyl halide production in the moss <i>Physcomitrella patens</i> .....	101
6.3 Discussion.....	103
<b>Chapter 7 – Evolution and functional diversity of <i>HOL</i>-homologous genes in plants.....</b>	<b>107</b>
7.1 Introduction.....	107
7.1.1 Plant halide/thiol methyltransferases – a unique class of SAM-dependent methyltransferases .....	107
7.1.2 Objectives of this chapter.....	108
7.2 Results.....	108
7.2.1 Natural variation in the <i>HOL</i> gene among <i>A. thaliana</i> accessions.....	108

7.2.2 Phylogenetic analysis of HTMT proteins .....	109
7.2.3 Analysis of the putative nucleophile-binding site of HTMT proteins .....	112
7.2.4 Cross-species complementation experiments .....	113
7.2.4.1 Generation and characterisation of <i>35S::OsHOL1</i> and <i>35S::OsHOL2</i> lines ....	114
7.2.4.2 Generation and characterisation of <i>35S::PpHOL</i> lines .....	116
7.2.4.3 Generation and characterisation of <i>35S::PtHTMT</i> lines .....	117
7.3 Discussion .....	118
<b>Chapter 8 – Conclusion and Outlook.....</b>	<b>122</b>
8.1 Summary .....	122
8.2 Future directions .....	124
<b>Appendix – Supplemental Figures and Tables.....</b>	<b>127</b>
Chapter 2 .....	127
Chapter 3 .....	130
Chapter 4 .....	140
Chapter 5 .....	143
Chapter 6 .....	147
Chapter 7 .....	154
<b>References.....</b>	<b>158</b>

## Table of Figures

<b>Figure 1.1</b>	Chemical structure, global emissions and properties of methyl halides with regard to ozone depletion .....	1
<b>Figure 1.2</b>	The Antarctic ozone hole .....	2
<b>Figure 1.3</b>	Recovery of the ozone layer .....	3
<b>Figure 1.4</b>	Contribution of known natural and human-made sources to the total amount of methyl halides found in the atmosphere .....	6
<b>Figure 1.5</b>	Temperature-dependent production of CH <sub>3</sub> Cl during heating of pectin and chloride .....	8
<b>Figure 1.6</b>	Production of methyl halides and sulphur volatiles by S-Adenosyl-L-methionine-dependent methyltransferases .....	10
<b>Figure 1.7</b>	The <i>HOL</i> gene controls methyl halide production in <i>A. thaliana</i> .....	12
<b>Figure 1.8</b>	CH <sub>3</sub> Cl-dependent methylation reactions catalysed by the wood-rotting fungus <i>P. pomaceus</i> .....	13
<b>Figure 1.9</b>	Survival of <i>A. thaliana</i> WT and <i>hol</i> mutant seedlings after infection with <i>Pseudomonas syringae</i> pv. <i>maculicola</i> .....	14
<b>Figure 1.10</b>	Production of methyl thiocyanate in <i>A. thaliana</i> WT and <i>hol</i> mutant plants and their susceptibility towards potassium thiocyanate.....	15
<b>Figure 2.1</b>	Collection of air samples for methyl halide analysis.....	24
<b>Figure 3.1</b>	Structure and active site of the <i>A. thaliana</i> <i>HOL</i> methyltransferase .....	34
<b>Figure 3.2</b>	Tissue-specific <i>HOL</i> gene expression in <i>HOL::GUS</i> reporter lines .....	36
<b>Figure 3.3</b>	Localisation of <i>HOL</i> protein in roots .....	37
<b>Figure 3.4</b>	Overexpression of <i>HOL</i> in <i>A. thaliana</i> .....	39
<b>Figure 3.5</b>	Susceptibility of WT, <i>hol</i> and <i>35S::HOL</i> lines to KSCN.....	40
<b>Figure 4.1</b>	CH <sub>3</sub> Cl emissions from <i>Brassica rapa</i> after salt treatment .....	53
<b>Figure 4.2</b>	Growth of WT, <i>hol</i> and <i>35S::HOL</i> seedlings on sodium chloride .....	55
<b>Figure 4.3</b>	Germination of WT, <i>hol</i> and <i>35S::HOL</i> lines on various salts .....	56
<b>Figure 4.4</b>	Growth and germination of WT, <i>hol</i> and <i>35S::HOL</i> lines on potassium iodide.....	57
<b>Figure 4.5</b>	Growth of WT, <i>hol</i> and <i>35S::HOL</i> seedlings on sodium bromide.....	58
<b>Figure 4.6</b>	Expression patterns of <i>HOL</i> in a <i>HOL::GUS</i> reporter line under NaCl stress .....	59
<b>Figure 4.7</b>	Expression of <i>HOL</i> after treatment with various salts.....	60
<b>Figure 4.8</b>	Expression of <i>HOL</i> after treatment with potassium iodide .....	61
<b>Figure 4.9</b>	Effects of KSCN, methionine and polyamines (spermine or spermidine) on KI-mediated growth inhibition in <i>35S::HOL</i> lines.....	63



<b>Figure 4.10</b>	Effect of gibberellic acid (GA <sub>3</sub> ) on the germination of WT, <i>hol</i> and <i>35S::HOL</i> lines under KI stress .....	64
<b>Figure 4.11</b>	<i>QQS</i> expression and starch accumulation in WT and <i>hol</i> plants.....	65
<b>Figure 4.12</b>	<i>EXL1</i> expression in WT and <i>hol</i> plants and their response to sucrose .....	66
<b>Figure 4.13</b>	Effect of auxin on root and hypocotyl growth of WT, <i>hol</i> and <i>35S::HOL</i> plants.....	67
<b>Figure 4.14</b>	Auxin response in WT, <i>hol</i> and <i>35S::HOL</i> lines containing the <i>DR5::GFP</i> reporter gene.....	68
<b>Figure 5.1</b>	Multiple functions of plant volatiles .....	76
<b>Figure 5.2</b>	Methylation of GL hydrolysis products by TMT/HOL.....	78
<b>Figure 5.3</b>	Glucosinolate content in WT, <i>hol</i> and <i>35S::HOL</i> plants.....	81
<b>Figure 5.4</b>	<i>Plutella xylostella</i> performance on WT and <i>hol</i> mutant plants .....	82
<b>Figure 5.5</b>	<i>Bradysia paupera</i> survival and choice assay on WT, <i>hol</i> and <i>35S::HOL</i> plants.....	83
<b>Figure 5.6</b>	Non-metric MDS plots of bacterial community profiles in the rhizosphere of WT, <i>hol</i> and <i>35S::HOL</i> plants.....	85
<b>Figure 5.7</b>	Distribution of individual ISR fragments among WT, <i>hol</i> and <i>35S::HOL</i> rhizosphere samples.....	87
<b>Figure 6.1</b>	Global production rates for oilseed rape and rice from 1961-2010.....	94
<b>Figure 6.2</b>	Phylogenetic relationship between <i>HOL</i> -homologous genes from <i>A. thaliana</i> , <i>B. rapa</i> and <i>B. oleracea</i> .....	97
<b>Figure 6.3</b>	Methyl halide emissions from <i>B. rapa</i> WT and <i>hol.a</i> mutants .....	98
<b>Figure 6.4</b>	Methyl halide emissions from different rice varieties.....	100
<b>Figure 6.5</b>	Methyl halide emissions from <i>P. patens</i> .....	102
<b>Figure 6.6</b>	Generation of <i>PpHol</i> knockout lines.....	103
<b>Figure 7.1</b>	Phylogenetic relationship of the species used in this study.....	110
<b>Figure 7.2</b>	Phylogenetic tree of plant HTMT proteins.....	111
<b>Figure 7.3</b>	Overexpression of rice <i>HOL</i> genes in <i>A. thaliana</i> .....	114
<b>Figure 7.4</b>	Methyl halide emissions from <i>35S::OsHOL1</i> and <i>35S::OsHOL2</i> lines .....	115
<b>Figure 7.5</b>	Susceptibility of <i>35S::OsHOL1</i> and <i>35S::OsHOL2</i> lines towards KSCN .....	116
<b>Figure 7.6</b>	Overexpression of <i>PpHOL</i> in <i>A. thaliana</i> and susceptibility of <i>35S::PpHOL</i> lines towards KSCN .....	117
<b>Figure 7.7</b>	Whole-genome duplication events in seed plants and flowering plants.....	119
<b>Supplemental Figure 3.1</b>	<i>A. thaliana</i> <i>HOL</i> and <i>HOL-like</i> genes.....	130
<b>Supplemental Figure 3.2</b>	Methyl halide emissions from WT and <i>hol</i> seedlings.....	131

<b>Supplemental Figure 3.3</b>	Verification of expression levels of six genes differentially expressed in the <i>hol</i> mutant (microarray) ..... 132
<b>Supplemental Figure 4.1</b>	Root growth of WT and <i>hol</i> seedlings on sodium chloride .... 140
<b>Supplemental Figure 4.2</b>	Growth of WT, <i>hol</i> and <i>35S::HOL</i> seedlings on various salts and mannitol ..... 141
<b>Supplemental Figure 4.3</b>	Growth of WT and <i>35S::HOL</i> seedlings on sodium iodide ..... 142
<b>Supplemental Figure 4.4</b>	Expression patterns of <i>HOL</i> in a <i>HOL::GUS</i> reporter line under NaBr stress..... 142
<b>Supplemental Figure 5.1</b>	Bacterial population count in the rhizosphere of WT, <i>hol</i> and <i>35S::HOL</i> roots ..... 143
<b>Supplemental Figure 5.2</b>	Examples of ARISA profiles ..... 144
<b>Supplemental Figure 5.3</b>	Examples of <i>cmuA</i> fragments obtained by PCR from DNA extracted from rhizosphere samples of <i>A. thaliana</i> ..... 146
<b>Supplemental Figure 6.1</b>	Alignment of <i>HOL</i> and <i>HLL</i> protein sequences from <i>A. thaliana</i> , <i>B. rapa</i> and <i>B. oleracea</i> ..... 147
<b>Supplemental Figure 6.2</b>	<i>B. rapa</i> <i>HOL</i> and <i>HOL-like</i> genes ..... 148
<b>Supplemental Figure 6.3</b>	Genomic DNA sequence of <i>BraA.HOL.a</i> showing the mutations identified in the TILLING assay ..... 149
<b>Supplemental Figure 6.4</b>	Amino acid substitutions in <i>B. rapa hol.a</i> mutant lines identified in the TILLING assay ..... 150
<b>Supplemental Figure 6.5</b>	Alignment of <i>HOL</i> and <i>HLL</i> protein sequences from <i>A. thaliana</i> and <i>O. sativa</i> ..... 151
<b>Supplemental Figure 6.6</b>	Rice <i>HOL</i> genes..... 152
<b>Supplemental Figure 6.7</b>	Location, structure and predicted transcripts of the <i>P. patens HOL</i> gene..... 152
<b>Supplemental Figure 6.8</b>	Alignment of <i>HOL</i> and <i>HLL</i> protein sequences from <i>A. thaliana</i> and <i>P. patens</i> ..... 153
<b>Supplemental Figure 7.1</b>	Alignment of HTMT protein sequences used for phylogenetic analysis..... 155
<b>Supplemental Figure 7.2</b>	Maximum Likelihood tree of plant HTMT proteins..... 157

## Table of Tables

<b>Table 1.1</b>	Temperature-dependent production of CH <sub>3</sub> Cl from dead and senescent leaves of various plant species and from pectin .....	9
<b>Table 1.2</b>	Affinity of halide/thiol methyltransferases towards different substrates in several species of fungi, plants and marine algae .....	11
<b>Table 3.1</b>	Genes down-regulated in the <i>hol</i> mutant.....	41
<b>Table 3.2</b>	Genes up-regulated in the <i>hol</i> mutant.....	43
<b>Supplemental Table 2.1</b>	List of <i>Arabidopsis thaliana</i> lines used in this study.....	127
<b>Supplemental Table 2.2</b>	List of primers used in this study.....	128
<b>Supplemental Table 3.1</b>	Treatments which produce similar changes to genes down-regulated in the <i>hol</i> mutant .....	133
<b>Supplemental Table 3.2</b>	Treatments which produce similar changes to genes up-regulated in the <i>hol</i> mutant.....	134
<b>Supplemental Table 3.3</b>	Genes which are co-expressed with <i>HOL</i> (positive correlation).....	135
<b>Supplemental Table 3.4</b>	Genes which are co-expressed with <i>HOL</i> (negative correlation).....	137
<b>Supplemental Table 3.5</b>	Treatments and genotypes which down-regulate <i>HOL</i> .....	138
<b>Supplemental Table 3.6</b>	Treatments and genotypes which up-regulate <i>HOL</i> .....	139
<b>Supplemental Table 5.1</b>	MANOVA p-values for pairwise comparisons between genotypes and time points .....	145
<b>Supplemental Table 7.1</b>	Names and sources of HTMT protein sequences used for phylogenetic analysis in this study.....	154

**List of Abbreviations**

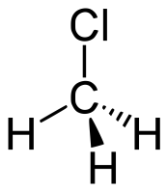
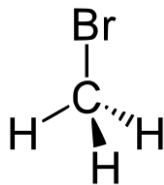
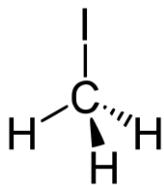
ANOVA	Analysis of variance
ARISA	Automated ribosomal spacer analysis
CDS	Coding sequence
EMS	Ethyl methanesulfonate
EXL	EXORDIUM-LIKE
GA	Gibberellic acid
GFP	Green fluorescent protein
GL	Glucosinolate
GUS	$\beta$ -glucuronidase
HLL	HOL-LIKE
HOL	HARMLESS TO OZONE LAYER
HTMT	Halide/thiol methyltransferase
IAA	Indole-3-acetic acid
iGA	Iterative group analysis
ISR	Intergenic spacer region
MANOVA	Multivariate analysis of variance
MCT	Methyl chloride transferase
MDS	Multi-dimensional-scaling
ML	Maximum Likelihood
MT	Methyltransferase
MU	4-methyl-umbelliferone
MUG	Methyl-umbelliferyl- $\beta$ -D-glucuronide
ODS	Ozone-depleting substance
PCR	Polymerase chain reaction
qPCR	Quantitative real-time PCR
QQS	QUA-QUINE STARCH
SAH	S-Adenosyl-L-homocysteine
SAM	S-Adenosyl-L-methionine
TILLING	Targeting induced local lesions in genomes
TMT	Thiol methyltransferase
WT	Wild-type

## Chapter 1 – General Introduction

### 1.1 Methyl halides and ozone degradation

Methyl halides (also known as halomethanes) are a group of volatile organic compounds derived from methane which contain one halogen atom (Fig. 1.1). Methyl chloride ( $\text{CH}_3\text{Cl}$ ), methyl bromide ( $\text{CH}_3\text{Br}$ ) and methyl iodide ( $\text{CH}_3\text{I}$ ) occur naturally in the atmosphere and contribute together with other, mainly human-made halogen source gases such as chlorofluorocarbons (CFCs) to ozone ( $\text{O}_3$ ) degradation (Davis *et al.*, 1996; Montzka *et al.*, 2011).

$\text{CH}_3\text{I}$  has only a small ozone depletion potential since it has a short atmospheric lifetime and thus hardly reaches the stratosphere, where ozone is most abundant (Fig. 1.1) (Youn *et al.*, 2010). In contrast,  $\text{CH}_3\text{Cl}$  and  $\text{CH}_3\text{Br}$  are long-lived halogenated compounds which contributed to 17% of the chlorine and 34% of the bromine found in the stratosphere in 2008 and therefore have a large impact on ozone degradation in the atmosphere.  $\text{CH}_3\text{Br}$  is a particular powerful ozone-depleting substance (ODS) as bromine atoms are more destructive to stratospheric ozone than chlorine atoms (Fig. 1.1) (Fahey and Hegglin, 2011).

	 Methyl chloride	 Methyl bromide	 Methyl iodide
Global emissions (kilotonnes/year)	3600-4600 <sup>a</sup>	110-150 <sup>a</sup>	260-610 <sup>b,c</sup>
Atmospheric lifetime (days)	365 <sup>a</sup>	292 <sup>a</sup>	7-14 <sup>a,b</sup>
Ozone depletion potential	0.02 <sup>a</sup>	0.66 <sup>a</sup>	0.017 <sup>b</sup>

**Figure 1.1. Chemical structure, global emissions and properties of methyl halides with regard to ozone depletion.** Global emissions include both human-made and natural sources. The ozone depletion potential (ODP) represents the relative effectiveness of halogen source gases to destroy stratospheric ozone. The ODP is calculated relative to CFC-11, whose ODP value is defined to be 1. ODP values are calculated for emissions of an equal mass of each gas. <sup>c</sup>Butler *et al.*, 2007; <sup>b</sup>Youn *et al.*, 2010; <sup>a</sup>Fahey and Hegglin, 2011.

About 90% of ozone is found in the stratosphere at an altitude of 15-35 km which is often referred to as the ozone layer. It protects life on earth from harmful ultraviolet-B radiation. The remaining 10% occur in the troposphere near the Earth's surface, where it is formed by reactions involving human-made pollutant gases. Tropospheric ozone is considered “bad ozone” as it is harmful to living organisms, especially plants. It is known to seriously affect the yield of agricultural crops and represents a significant risk to food security (Feng and Kobayashi, 2009; Fahey and Hegglin, 2011).

After the discovery that chlorine and bromine-containing gases cause stratospheric ozone depletion in the 1970s, and the appearance of a growing “ozone hole” (Fig. 1.2) over Antarctica in the 1980s, international efforts were launched in 1987 (Montreal Protocol) to restrict the release of ODSs caused by human activities.

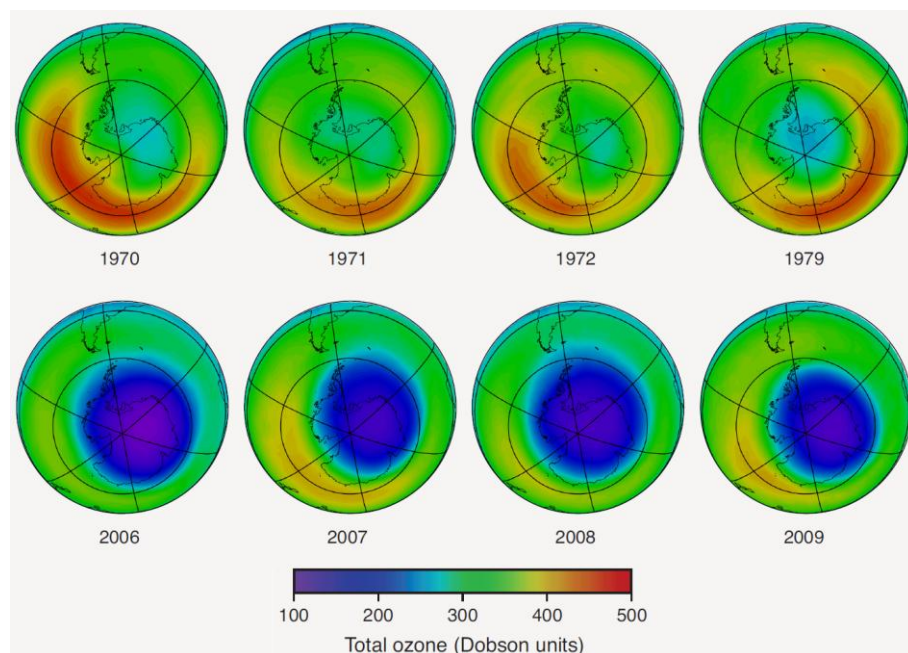


**Figure 1.2. The Antarctic ozone hole.** Average total ozone levels over Antarctica in October in the 1970s and in recent years (2006-2009). In the 1970s, no ozone hole was observed. In the 1980s, the ozone hole began to appear and nowadays extends to a size of 25 million km<sup>2</sup>. The ozone hole appears over Antarctica in late winter/early spring due to unique atmospheric and chemical conditions in this region (e.g. low temperatures, polar stratospheric clouds) which increase the effectiveness of ozone destruction by reactive halogen gases. Image taken from Fahey and Hegglin (2011).

As a result, the overall abundance of ODSs has decreased in the last 10 years (Fig. 1.3). However, due to the longevity of many ODSs, it will take several decades before the ozone layer will have recovered. Current projections estimate that total global and Antarctic ozone levels will return to 1980 values by the middle of this century assuming global compliance with the Montreal protocol and unchanged contribution of ODSs from natural sources (Fig. 1.3) (Dameris, 2010; Fahey and Hegglin, 2011).

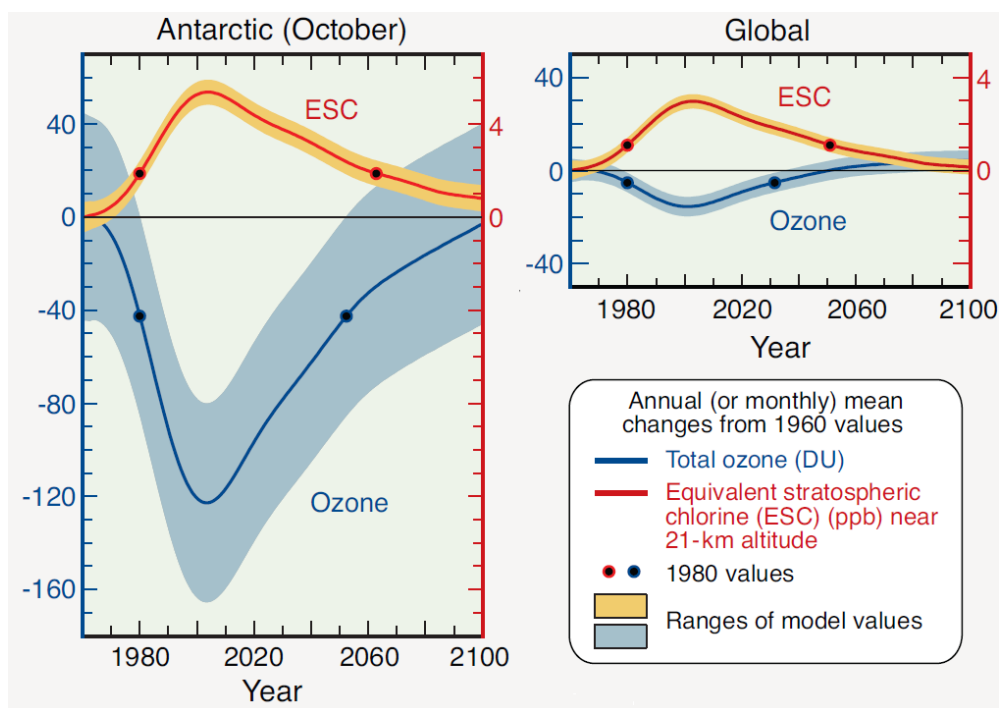


**Figure 1.3. Recovery of the ozone layer.** Long-term changes in global and Antarctic ozone (blue line) and equivalent stratospheric chlorine (ESC) (orange line) predicted by chemistry-climate models. ESC is an estimate of the amount of halogens available in the stratosphere to deplete ozone. Image taken from Fahey and Hegglin (2011).

## 1.2 Sources and sinks of methyl halides

Methyl halides are produced by both natural and anthropogenic sources (Fig. 1.4) and much progress has been made in the last two decades to identify the sinks and sources of these compounds in the environment. Overall, large uncertainties remain in the global atmospheric budgets of  $\text{CH}_3\text{Cl}$ ,  $\text{CH}_3\text{Br}$  and  $\text{CH}_3\text{I}$  regarding the relative contribution of known sources and the exact mechanism leading to the production of methyl halides in nature (Montzka *et al.*, 2011). Moreover, in the case of  $\text{CH}_3\text{Br}$ , known

sinks still outweigh best estimates of known sources indicating that some natural sources have not been identified yet.

CH<sub>3</sub>Cl is the most abundant methyl halide in the atmosphere with estimated global emissions of 3600-4600 kilotonnes (kt) per year (Fig. 1.1). It is also the most abundant chlorine-containing organic compound accounting for 17% of the total chlorine found in the stratosphere in 2008 (Fahey and Hegglin, 2011). Tropical and subtropical forests are the predominant source of CH<sub>3</sub>Cl emissions (Fig. 1.4 A) with approximately 1500-2900 kt originating from tropical plants such as tree ferns and halophytes (Yokouchi *et al.*, 2002; Saito and Yokouchi, 2006; Yokouchi *et al.*, 2007; Blei *et al.*, 2010), and 1400-2500 kt being produced by dead and senescent leaves each year (see section 1.3) (Keppler *et al.*, 2005; Saito and Yokouchi, 2008). Other significant sources include oceans, wetlands and salt marshes, and anthropogenic emissions from biomass burning and industry (Fig. 1.4 A). The sinks of CH<sub>3</sub>Cl (total amount of ~ 4400 kt/year) are oxidation by hydroxyl radicals in the atmosphere (91%) and microbial degradation in soils (6%) and oceans (3%) (Yoshida *et al.*, 2004; Clerbaux *et al.*, 2007; Schäfer *et al.*, 2007).

CH<sub>3</sub>Br is the most abundant bromine-containing compound accounting for 34% of the total bromine found in the stratosphere in 2008 (Fahey and Hegglin, 2011). Although total global emissions of this gas (110-150 kt/year) are much lower compared to CH<sub>3</sub>Cl (Fig. 1.1), CH<sub>3</sub>Br is of great importance due to its high ozone depletion potential and since significant amounts are produced by humans (e.g. biomass burning, combustion of leaded gasoline and fumigation) (Fig. 1.4 B). The use of CH<sub>3</sub>Br as a pesticide for soil fumigation and postharvest treatment of durable and perishable commodities (Taylor, 1994; Ristaino and Thomas, 1997) is controlled under the Montreal Protocol. Therefore, the contribution from fumigation has declined in recent years (Fahey and Hegglin, 2011). The main natural source of CH<sub>3</sub>Br are oceans (42 kt/year) (Fig. 1.4 B), where phytoplankton, algae and marine bacteria have been reported to produce these compounds (Itoh *et al.*, 1997; Laturus *et al.*, 1998; Colomb *et al.*, 2008; Fujimori *et al.*, 2012). Other significant natural sources include coastal salt marshes, mangroves, shrublands, wetlands and fungi (Montzka *et al.*, 2011). Interestingly, crop plants are also known to be significant CH<sub>3</sub>Br producers (Fig. 1.4 B): Rice and oilseed rape contribute about 0.7 kt (~1%) and 5.1 kt (~4%), respectively, to the global CH<sub>3</sub>Br budget each year (Redeker and Cicerone, 2004; Lee-Taylor and Redeker, 2005; Mead *et al.*, 2008). Other crop plants such as cabbage and mustard have



also been reported to emit  $\text{CH}_3\text{Br}$ , however, global emission levels are estimated to be  $< 0.1$  kt/year (Mead *et al.*, 2008). Similar to  $\text{CH}_3\text{Cl}$ , the main sinks of  $\text{CH}_3\text{Br}$  are photolysis and oxidation by hydroxyl radicals (64 kt/year), and uptake and microbial degradation in soils (32 kt/year) and oceans (49 kt/year) (Montzka *et al.*, 2011).

Estimated global emissions of  $\text{CH}_3\text{I}$  range between 260-610 kt/year. Due to its short atmospheric lifetime, the ozone depletion potential of  $\text{CH}_3\text{I}$  is very small (Fig. 1.1). The majority  $\text{CH}_3\text{I}$  (224 kt/year) is produced in oceans (Fig. 1.4 C) both by abiotic reactions involving photochemically produced methyl radicals and iodine atoms (Moore and Zafiriou, 1994), and by living organisms such as algae and marine bacteria (Manley *et al.*, 1992; Itoh *et al.*, 1997; Laturus *et al.*, 1998; Amachi *et al.*, 2001; Toda and Itoh, 2011; Fujimori *et al.*, 2012). Other natural sources of  $\text{CH}_3\text{I}$  are coastal and inland wetlands (Dimmer *et al.*, 2001; Cox *et al.*, 2004). The contribution from anthropogenic sources such as biomass burning and combustion of wood is relatively small (Fig. 1.4 C), however,  $\text{CH}_3\text{I}$  is currently being licensed as a replacement for  $\text{CH}_3\text{Br}$  as a fumigant. Therefore, fumigation may become a significant source in the future. Interestingly, large amounts of  $\text{CH}_3\text{I}$  (16-29 kt/year) are also emitted by rice paddies (Lee-Taylor and Redeker, 2005) (Fig. 1.4 C). The main sink of  $\text{CH}_3\text{I}$  is its photolysis in the atmosphere (Bell *et al.*, 2002). It has also been reported that  $\text{CH}_3\text{I}$  is converted to  $\text{CH}_3\text{Cl}$  via a nucleophilic substitution reaction of  $\text{CH}_3\text{I}$  with chloride ions because of the high concentration of chloride in seawater (Toda and Itoh, 2011).

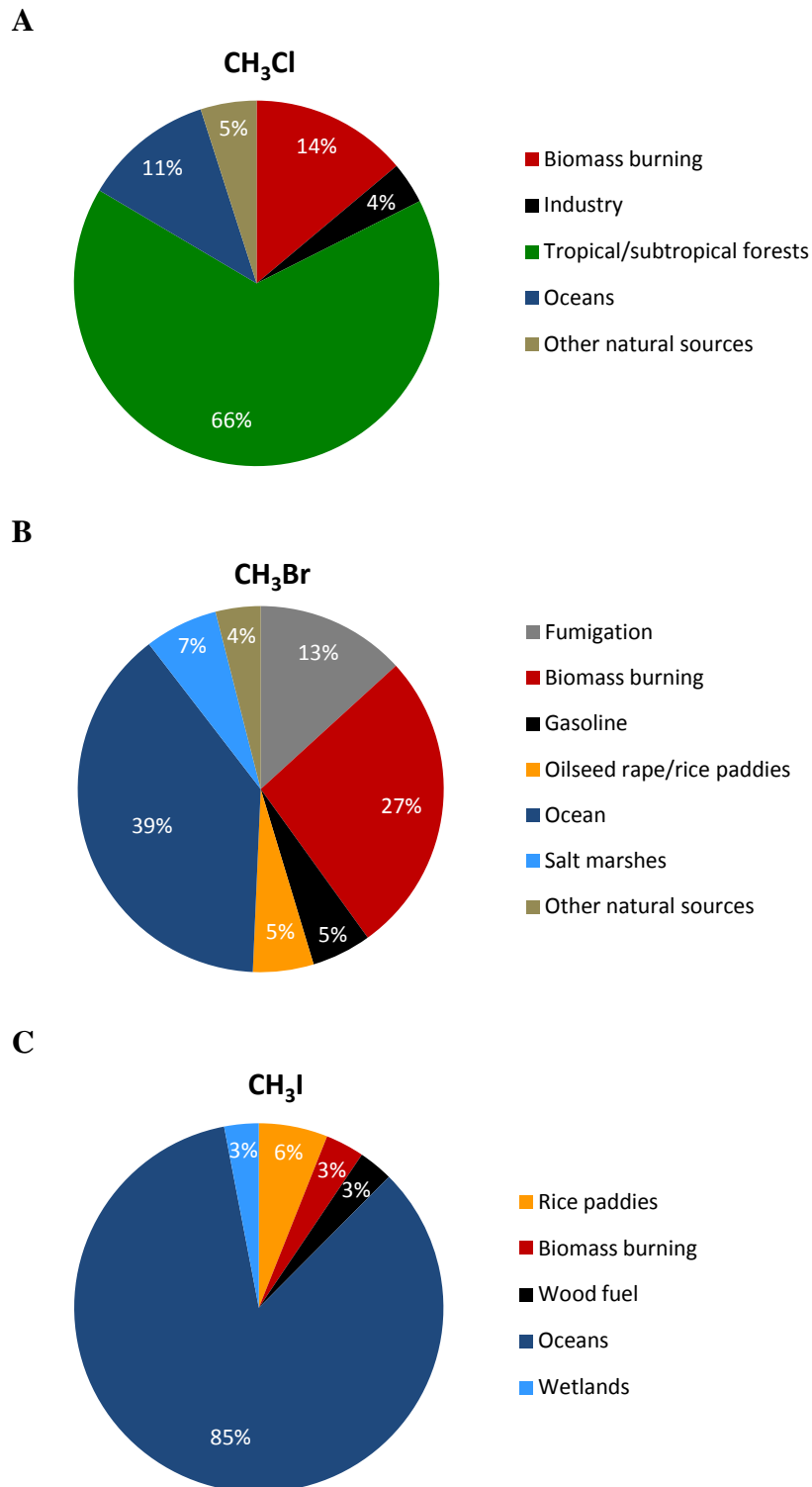


**Figure 1.4.** Contribution of known natural and human-made sources to the total amount of methyl halides found in the atmosphere. (A) Sources of CH<sub>3</sub>Cl based on Yoshida *et al.* (2004), Clerbaux *et al.* (2007). (B) Sources of CH<sub>3</sub>Br based on Montzka *et al.* (2011). (C) Sources of CH<sub>3</sub>I based on Youn *et al.* (2010).

It is generally expected that the abundance of methyl halides in the atmosphere will remain constant in the future if the balance of its natural production and loss processes does not change (Fahey and Hegglin, 2011). However, some concerns have been raised regarding the impact of changes in agricultural practices, and the effect of climate change on the production of methyl halides (Montzka *et al.*, 2011) as those factors have not been included in models predicting the recovery of the ozone layer. The increased cultivation of crop plants which emit methyl halides (e.g. rice, oilseed rape) to feed an increasing human population could pose a risk in the future. Moreover, it has been shown previously that methyl halide production in plants positively correlates with the concentration of halide ions in the soil or growth medium (Gan *et al.*, 1998; Rhew *et al.*, 2003; Redeker and Cicerone, 2004; Armeanu-D'Souza, 2009). Thus, with increasing salinisation of soils through irrigation, coastal inundation or deliberate cultivation of poorer soils, methyl halide emissions could increase in the future. It has also been shown that methyl halide emissions from rice are strongly influenced by temperature (Redeker and Cicerone, 2004), and it was estimated that a temperature increase of 1°C could increase CH<sub>3</sub>Br and CH<sub>3</sub>I emissions from this crop by 10% (Lee-Taylor and Redeker, 2005). Moreover, the abiotic production of methyl halides in leaf litter is also positively correlated with temperature (see section 1.3).

### **1.3 Abiotic methyl halide production from senescent and dead leaves**

Large amounts of methyl halides are released by biomass burning (Fig. 1.4), but for a long time it was not known how they are formed in this process. Hamilton *et al.* (2003) finally discovered that CH<sub>3</sub>Cl is produced in plant tissue by a methylation reaction involving chloride ions and methyl groups present in pectin of plant cell walls (Fig. 1.5). Similarly, heating of pectin with Br<sup>-</sup> or I<sup>-</sup> led to the release of CH<sub>3</sub>Br and CH<sub>3</sub>I, respectively.

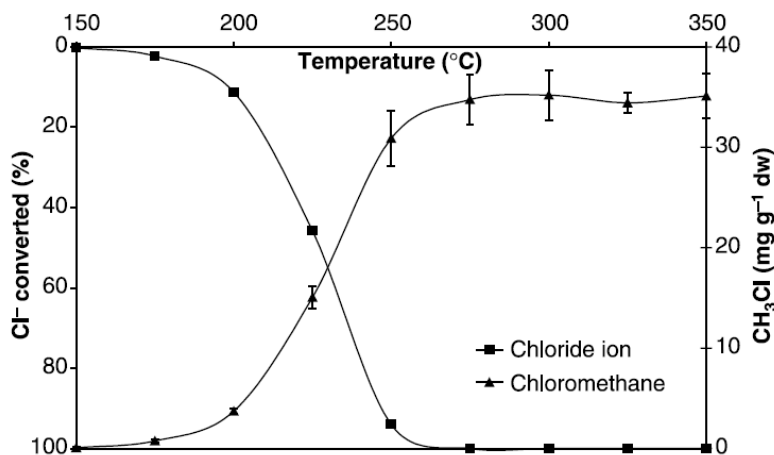


**Figure 1.5. Temperature-dependent production of CH<sub>3</sub>Cl during heating of pectin and chloride.** Image taken from Hamilton *et al.* (2003).

Interestingly, the same study showed that CH<sub>3</sub>Cl is also produced in dead and senescent leaves of various plant species at lower temperatures (30°C - 50°C). Emission rates were positively correlated with temperature and tissue chloride content (Table 1.1). It was also ruled out that CH<sub>3</sub>Cl was released by microorganisms since leaves sterilised with gamma radiation or incubated with N<sub>2</sub> showed similar CH<sub>3</sub>Cl emission profiles as untreated leaves incubated with air. Based on these observations, it was concluded that abiotic CH<sub>3</sub>Cl production in subtropical and tropical regions, where leaf surface temperatures can reach up to 50°C, significantly contributes to global atmospheric CH<sub>3</sub>Cl (Hamilton *et al.* 2003). Indeed, recent studies estimated that approximately 1400-2500 kt CH<sub>3</sub>Cl are produced by senescent leaves and leaf litter in tropical and subtropical ecosystems each year (Keppler *et al.*, 2005; Saito and Yokouchi, 2008).

Recently, it was also shown that CH<sub>3</sub>Br is produced from dried leaves of tomato, ash and saltwort at temperatures between 25°C and 50°C via the same abiotic mechanism involving bromide ions and pectin. CH<sub>3</sub>Br emissions increased exponentially with rising temperature (Wishkerman *et al.*, 2008). The significance of this source with respect to the global CH<sub>3</sub>Br budget has not been established yet.

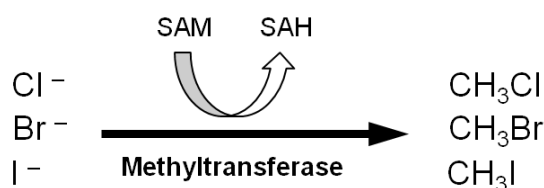
**Table 1.1. Temperature-dependent production of CH<sub>3</sub>Cl from dead and senescent leaves of various plant species and from pectin.** Emission rates were measured over 48 h from either freshly fallen leaves (tree species) or from air-dried leaf material (*D. glomerata*, *B. maritima*). Data taken from Hamilton *et al.* (2003).

Plant species	Temperature (°C)	CH <sub>3</sub> Cl (ng/g DM/d)	Chloride content (mg/g DM)
Ash ( <i>Fraxinus excelsior</i> )	30	13	6.9
Ash ( <i>Fraxinus excelsior</i> )	40	64	6.9
Ash ( <i>Fraxinus excelsior</i> )	50	115	6.9
Oak ( <i>Quercus robur</i> )	40	5	0.3
Cock's foot ( <i>Dactylis glomerata</i> )	40	49	10.3
Cock's foot ( <i>Dactylis glomerata</i> )	50	140	10.3
Saltwort ( <i>Batis maritima</i> )	30	2700	283
Saltwort ( <i>Batis maritima</i> )	50	31000	283
Apple pectin + NaCl	40	3300	25

#### 1.4 Production of methyl halides by methyltransferases

Despite that fact that vast amounts of methyl halides are produced by living organisms, the exact mechanisms of their production remained unknown for a long time. In 1990, it was discovered that methyl halides are produced by S-Adenosyl-L-methionine (SAM)-dependent methyltransferases (MTs) which catalyse the transfer of a methyl group from SAM to chloride, bromide and iodide ions (Fig. 1.6 A). Methyl chloride transferase activity was detected in whole cells and cell extracts of the fungus *Phellinus pomaceus*, the marine algae *Endocladia muricata* and the plant *Mesembryanthemum crystallinum*. It was also shown that the *E. muricata* methyl chloride transferase (MCT) was able to produce CH<sub>3</sub>Br and CH<sub>3</sub>I when incubated with bromide or iodide ions (Wuosmaa and Hager, 1990). In subsequent years, methyl halide transferase activity was confirmed in various other species including bacteria (Table 1.2 and references therein) (Amachi *et al.*, 2001) which confirmed that the enzymatic biogenesis of methyl halides is a widespread mechanism.

A



B

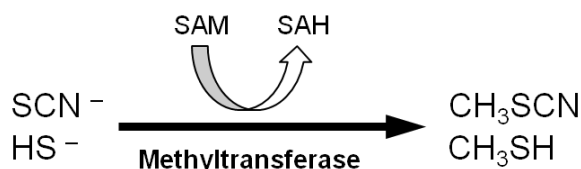


**Figure 1.6. Production of methyl halides and sulphur volatiles by S-Adenosyl-L-methionine (SAM)-dependent methyltransferases (MTs).** A unique class of SAM-dependent MTs in plants are able to methylate halide ions (A) and in some cases thiol compounds (B) in a nucleophilic substitution reaction to produce methyl halides and sulphur volatiles. SAM is used as the methyl donor and is converted to S-Adenosyl-L-homocysteine (SAH) in the process.

Interestingly, the majority of methyl halide transferases are also able to methylate sulphur-containing ions such as thiocyanate (SCN<sup>-</sup>) and bisulfide (HS<sup>-</sup>) (Fig. 1.6 B, Table 1.2). This was first observed by a survey of *in vivo* methyl iodide production from leaf discs of diverse plant species which showed that methanethiol (CH<sub>3</sub>SH) was produced when leaf discs from 20 different plant species were incubated with HS<sup>-</sup> ions instead of I<sup>-</sup> ions (Saini *et al.*, 1995). Subsequently, it was confirmed by *in vitro* enzyme kinetic studies that the same enzyme in cabbage (*Brassica oleracea*) can mediate the SAM-dependent methylation of both halides and HS<sup>-</sup> (Attieh *et al.*, 1995), and further sulphur-containing methyl acceptors such as thiocyanate (SCN<sup>-</sup>) were later identified for this enzyme (Attieh *et al.*, 2000a).

The first gene encoding a methyl chloride transferase was cloned in the salt-tolerant plant *Batis maritima*, and it was shown that this enzyme shares three conserved motifs with other SAM-dependent MTs (Ni and Hager, 1998). Since then, other halide/thiol MTs (HTMTs) have been cloned in *B. oleracea* (Attieh *et al.*, 2002), *Arabidopsis thaliana* (Rhew *et al.*, 2003; Nagatoshi and Nakamura, 2009), radish (*Raphanus sativus*) (Itoh *et al.*, 2009), rice (*Oryza sativa*) (Takekawa and Nakamura, 2012) and the diatom *Phaeodactylum tricornutum* (Toda and Itoh, 2011). Moreover, the kinetic properties of these enzymes have been characterised in detail (Table 1.2).

**Table 1.2. Affinity of halide/thiol methyltransferases towards different substrates in several species of fungi, plants and marine algae.** The Michaelis constant ( $K_m$ ) is the substrate concentration at which the reaction rate is at half-maximum, thus a small  $K_m$ -value indicates high affinity.

Species	$K_m$ (mM) of substrate					
	Cl <sup>-</sup>	Br <sup>-</sup>	I <sup>-</sup>	HS <sup>-</sup>	SCN <sup>-</sup>	SAM
<i>Phellinus pomaceus</i> <sup>1</sup>	300	10	0.3	n.a.	n.a.	0.005
<i>Batis maritima</i> <sup>2</sup>	100	25	6.5	n.d.	n.a.	0.23
<i>Brassica oleracea</i> <sup>3</sup>	85	29	1.3	4.7	n.a.	0.03
<i>Brassica oleracea</i> (TMT1) <sup>4</sup>	n.a.	n.a.	8.0	n.a.	0.002	0.052
<i>Arabidopsis thaliana</i> (HOL) <sup>5</sup>	280	n.a.	n.a.	0.3	0.062	0.092
<i>Arabidopsis thaliana</i> (HLL1) <sup>5</sup>	36	n.a.	n.a.	1.1	1.8	0.049
<i>Arabidopsis thaliana</i> (HLL2) <sup>5</sup>	n.d.	n.a.	n.a.	1.3	3.1	0.04
<i>Raphanus sativus</i> <sup>6</sup>	1657	177	4.5	12.2	0.04	0.19
<i>Oryza sativa</i> (HOL1) <sup>7</sup>	n.d.	45	0.07	n.a.	0.145	0.013
<i>Oryza sativa</i> (HOL2) <sup>7</sup>	n.d.	34	1.1	n.a.	0.246	0.03
<i>Endocladia muricata</i> <sup>8</sup>	5	40	n.a.	n.a.	n.a.	0.016
<i>Phaeodactylum tricornutum</i> <sup>9</sup>	638	73	8.6	9.9	7.9	0.016

<sup>1</sup>Crude enzyme extracts (Saxena *et al.*, 1998), <sup>2</sup>recombinant protein MCT (Ni and Hager, 1999), <sup>3</sup>crude enzyme extracts (Attieh *et al.*, 1995), <sup>4</sup>recombinant protein TMT1 (Attieh *et al.*, 2002), <sup>5</sup>recombinant proteins HOL, HLL1 and HLL2 (Nagatoshi and Nakamura, 2009), <sup>6</sup>recombinant protein HTMT (Itoh *et al.*, 2009), <sup>7</sup>recombinant proteins HOL1 and HOL2 (Takekawa and Nakamura, 2012), <sup>8</sup>crude enzyme extracts (Wuosmaa and Hager, 1990), <sup>9</sup>recombinant protein PtHTMT (Toda and Itoh, 2011), n.a. – not available, n.d. – not detected.

So far, only one study has shown that HTMTs catalyse the formation of methyl halides *in vivo*. In *A. thaliana*, a gene encoding a HTMT was identified and named *HARMLESS TO OZONE LAYER (HOL)*, based on the expected effect of its loss of function. Indeed, it was confirmed that *HOL* controls the production of methyl halides since *hol* mutant plants showed strongly reduced emissions of CH<sub>3</sub>Cl, CH<sub>3</sub>Br and CH<sub>3</sub>I to less than 1% of WT levels in adult plants (Fig. 1.7). Moreover, it was shown that CH<sub>3</sub>Br emissions increased more than a thousand-fold when plants were transferred to a 50 mM NaBr solution (Rhew *et al.*, 2003). In addition to *HOL*, two other genes, *HOL-LIKE 1* and *2 (HLL1, HLL2)*, can be found in the *A. thaliana* genome. The enzymes encoded by these genes possess HTMT activity *in vitro* (Table 1.2) (Nagatoshi and Nakamura, 2007, 2009), however, they do not play a significant role in methyl halide production *in vivo* since CH<sub>3</sub>Cl, CH<sub>3</sub>Br and CH<sub>3</sub>I emissions were strongly reduced in the *hol* mutant.

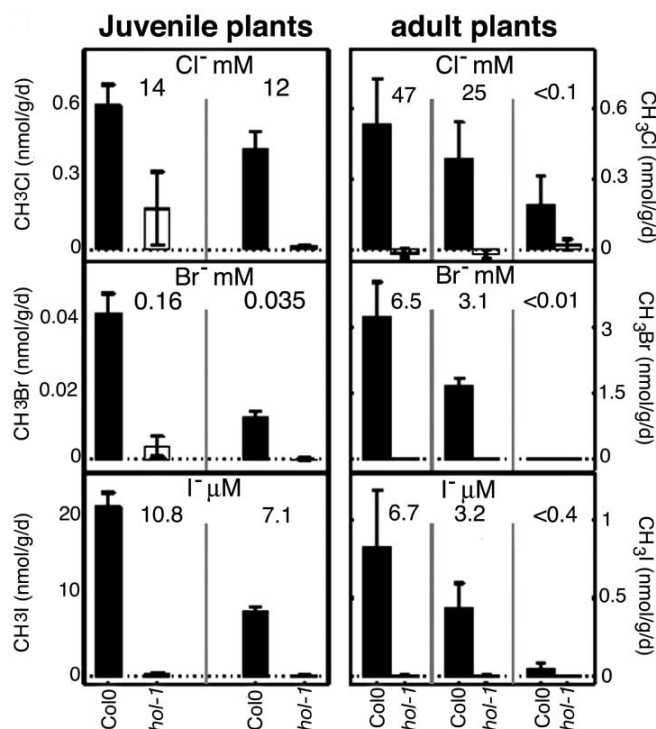


**Figure 1.7. The *HOL* gene controls methyl halide production in *A. thaliana*.** CH<sub>3</sub>Cl, CH<sub>3</sub>Br and CH<sub>3</sub>I emissions from WT and *hol* mutant plants. The numbers represent the average concentration of halide ions in the growth medium. Image taken from Rhew *et al.* (2003).

## 1.5 Function of methyl halide production and HTMTs

To date only one function of methyl halide production has been described: It was shown by isotopic labelling of methyl halides that in wood-rotting fungi (e.g. *Phellinus pomaceus*, *Phanerochaete chrysosporium*), CH<sub>3</sub>Cl acts as a methyl donor in the biosynthesis of methyl esters and anisoles (Fig. 1.8), or veratryl alcohol, the latter known to be an important component of the lignin degradation pathway (Harper *et al.*, 1989; Harper *et al.*, 1990). Interestingly, CH<sub>3</sub>Br and CH<sub>3</sub>I were also able to act as methyl donors in the synthesis of methyl butyrate from butyric acid, although with lower efficiency than CH<sub>3</sub>Cl (Harper *et al.*, 1989). The exact mechanisms of these reactions are not known.



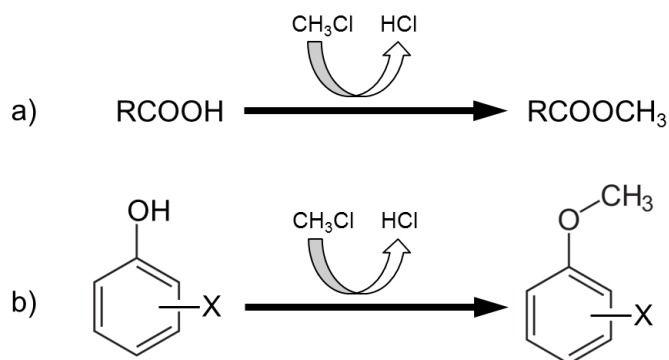


**Figure 1.8.**  $\text{CH}_3\text{Cl}$ -dependent methylation reactions catalysed by the wood-rotting fungus *P. pomaceus*. Production of methyl esters **a)** and anisoles **b)**, R can be a variety of alkyl or aryl groups; X can be a variety of substituents.

The purpose of methyl halide production in plants remains unknown. At least in *A. thaliana*, methyl halides do not seem to play a major role in plant development under optimal growth conditions since the *hol* mutant did not show any obvious growth defects. The following hypotheses have been proposed regarding the function of methyl halide production and HTMTs in plants: Manley (2002) suggested that methyl halides are simply “accidents of metabolism” caused by non-specific methylation of halide ions. However, Ni and Hager (1998, 1999) proposed that the production of  $\text{CH}_3\text{Cl}$  by a *Batis maritima* methyl chloride transferase provides a mechanism for halophytic plants to dispose of excessive chloride ions and thus to maintain homeostatic levels of  $\text{Cl}^-$  in the cytoplasm. Accordingly, in *Arabidopsis*, in several *Brassica* crops and in rice, it was shown that methyl halide emissions positively correlate with the concentration of halide ions in the growth medium or soil (Gan *et al.*, 1998; Rhew *et al.*, 2003; Redeker and Cicerone, 2004; Armeanu-D'Souza, 2009). Moreover, ecosystems with high soil salinity, such as salt marshes and mangrove forests, have been reported to be significant methyl halides sources (Fig. 1.4) (Rhew *et al.*, 2000; Yokouchi *et al.*, 2000; Manley *et al.*, 2006; Manley *et al.*, 2007).

In addition to a function in salt tolerance, methyl halide production could also contribute to resistance against biotic stress.  $\text{CH}_3\text{Br}$  and  $\text{CH}_3\text{I}$  have been used as pesticides for soil fumigation and for postharvest treatment of durable and perishable commodities. They are effective against various plant pathogens, insects and nematodes (Taylor, 1994; Ohr *et al.*, 1996; Ristaino and Thomas, 1997). It is therefore possible that

plants produce toxic methyl halides as a defence mechanism. Interestingly, this hypothesis is supported by the study of Nagatoshi and Nakamura (2009) who showed that *A. thaliana hol* seedlings had a reduced survival rate when infected with *Pseudomonas syringae* pv. *maculicola* (Fig. 1.9). However, this particular experiment can be criticised as the authors did not use the standard procedure of monitoring bacterial growth by infiltrating the pathogen into the plant and determining number of colony-forming units in plant extracts a few days later.

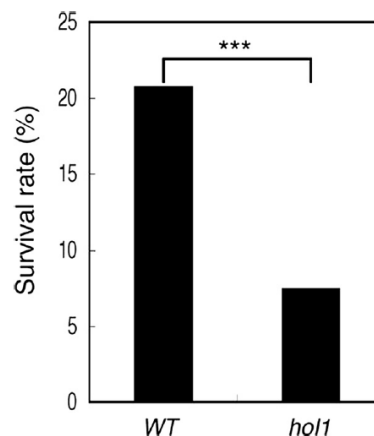


**Figure 1.9. Survival of *A. thaliana* WT and *hol* mutant seedlings after infection with *Pseudomonas syringae* pv. *maculicola*.** Seeds were sown on MS medium and infested with a droplet of a bacterial suspension of the pathogen. After 19 days the survival rate of the seedlings was evaluated based on the emergence of true leaves. Asterisks represent significant differences from WT ( $\chi^2$  test,  $p < 0.001$ ). Image taken from Nagatoshi and Nakamura (2009).

Alternatively, it is possible that plants produce methyl halides to attract bacteria which use these volatiles as a carbon and energy source. Numerous bacteria which are able to utilise methyl halides have been isolated from soils (Schäfer *et al.*, 2007). Recently, methyl-halide degrading bacteria were also isolated from the leaf surface of *A. thaliana* plants (Nadalig *et al.*, 2011). It is possible that such bacteria could act as biocontrol microorganisms in the rhizosphere or phyllosphere of plants by impairing the growth of pathogens e.g. due to competition for nutrients (Lindow and Brandl, 2003; Bais *et al.*, 2006; Raaijmakers *et al.*, 2009).

Given that many HTMTs are able to methylate sulphur-containing ions *in vitro* to produce sulphur volatiles (Fig. 1.6 B, Table 1.2), it has been proposed that this mechanism could have a specific purpose in glucosinolate (GL)-containing plants, such

as the *Brassicaceae*, since  $\text{SCN}^-$  and  $\text{HS}^-$  occur naturally in this group of plants as a result of GL hydrolysis after wounding (Attieh *et al.*, 2000a). In *A. thaliana*, it was confirmed that HOL catalyses the conversion of  $\text{SCN}^-$  into  $\text{CH}_3\text{SCN}$  since leaf extracts from *hol* mutant plants did not produce  $\text{CH}_3\text{SCN}$  upon wounding (Fig. 1.10 A) (Nagatoshi and Nakamura, 2009). It has also been proposed that sulphur volatiles such as  $\text{CH}_3\text{SCN}$  and  $\text{CH}_3\text{SH}$  could attract predators (parasitoids) of feeding insects, or suppress the spread of pathogens due to their toxicity (Attieh *et al.*, 2002; Nagatoshi and Nakamura, 2009), however, very little is known about  $\text{CH}_3\text{SCN}$  and  $\text{CH}_3\text{SH}$  emissions in living plants and their role in plant defence. Moreover, it has been proposed that the methylation of toxic GL hydrolysis products by HTMTs is a detoxification mechanism (Attieh *et al.*, 2000a). The observation that *A. thaliana hol* mutant plants are more susceptible towards  $\text{SCN}^-$  than WT plants supports this hypothesis (Fig. 1.10 B) (Nagatoshi and Nakamura, 2009).

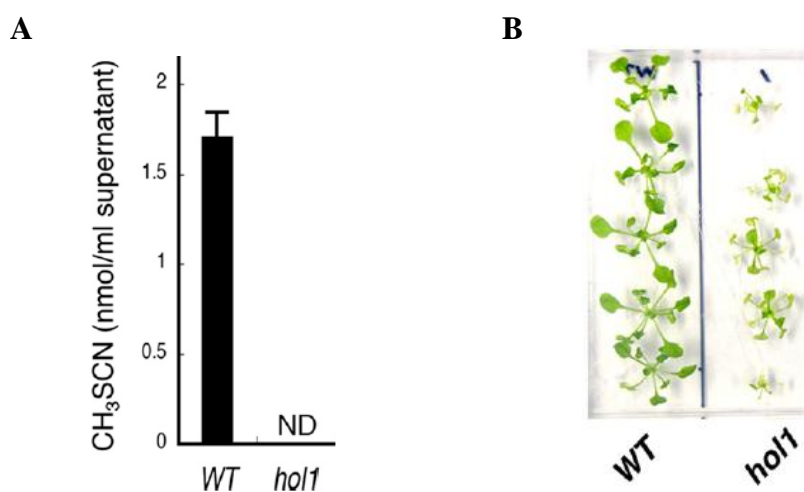


**Figure 1.10. Production of methyl thiocyanate ( $\text{CH}_3\text{SCN}$ ) in *A. thaliana* WT and *hol* mutant plants and their susceptibility towards potassium thiocyanate (KSCN). (A)  $\text{CH}_3\text{SCN}$  production was measured from the supernatant of homogenised leaves. ND – not detected. (B) Two-week-old seedlings were transferred to MS medium containing 1 mM KSCN and pictures taken after 12 days. Images taken from Nagatoshi and Nakamura (2009).**

## 1.6 Objectives of this thesis

To date, none of the proposed hypotheses described here have been investigated thoroughly. The main aim of this thesis was to use WT, *hol* mutant and *35S::HOL* lines of the model plant *Arabidopsis thaliana* to shed light on the function of HTMTs and methyl halide production in plants. The main focus was directed towards the function of HOL in salt stress tolerance, and how HOL could affect the outcome of plant-insect or plant-microbe interactions in *A. thaliana*. This included a thorough characterisation of *HOL* expression patterns under normal growth conditions and under stress. Moreover, microarray analysis of WT and *hol* mutant plants was performed to identify potential functions of HOL.

Secondly, since the two crop plants oilseed rape (*Brassica napus*) and rice (*Oryza sativa*) are significant producers of methyl halides, we wanted to assess the consequences to plant development and stress tolerance in the absence of methyl halide emissions in these plants. To achieve this, we aimed at identifying the genes involved in the production of methyl halides based on homology to the *A. thaliana* *HOL* gene and subsequently isolating and characterising putative *hol* mutants from TILLING populations of *B. rapa* and rice. The diploid *B. rapa* is an ancient progenitor of *B. napus* and has been chosen here to simplify genetics compared to the polyploid *B. napus*.

Finally, the diversity and evolutionary relationship of HTMTs in land plants was characterised by conducting phylogenetic analyses of known and new *A. thaliana* *HOL*-homologous protein sequences retrieved from sequenced plant genomes. We also tested if methyl halide production can be detected in the moss *Physcomitrella patens* to elucidate whether methyl halide production is an ancient mechanism in land plants. Moreover, it was investigated if the putative *HOL* homologues in rice, *P. patens* and the diatom *Phaeodactylum tricorutum* are capable of producing methyl halides and detoxifying  $\text{SCN}^-$  *in planta* to answer the question whether  $\text{SCN}^-$  detoxification evolved specifically in GL-containing plants such as the *Brassicaceae*. This was tested by developing and characterising *A. thaliana* lines overexpressing these genes.

## Chapter 2 – Materials and Methods

### 2.1 Plant material and growth conditions

#### 2.1.1 *Arabidopsis thaliana*

*A. thaliana* lines (Col-0) used in this study are shown in Supplemental Table 2.1. Seeds were surface-sterilised in 70% ethanol for 2 min and then in a bleach solution (15% bleach, 0.01% Tween 20) for further 10 min. Seeds were washed with sterile water five times and sown on MS media (4.4 g/l Murashige and Skoog basal salt mixture (Duchefa), 10 g/l sucrose, 0.5 g/l MES, 8 g/l agar, pH 5.7). Unless otherwise stated, plates were stratified at 4°C for 3 days and then transferred to a 23°C growth chamber with a day/night cycle of 16 h/8 h. When plants were grown to maturity, seedlings were transferred to pots containing a Levington F2 compost/grit mix after ten days and grown in the glasshouse at 22°C/16 h light - 18°C/8 h dark.

#### 2.1.2 *Brassica rapa*

Seeds of *Brassica rapa* var. R-o-18 wild-type and *braA.hol.a* mutant lines were sown in Levington F2 compost and grown in the glasshouse at 18°C with a day/night cycle of 16 h/8 h. The *braA.hol.a* mutants were obtained from the JIC TILLING population generated by EMS mutagenesis (Stephenson *et al.*, 2010). Mutants were back-crossed to WT to reduce the mutation load and homozygous individuals of the F<sub>2</sub> and F<sub>3</sub> generation were used for the experiments.

#### 2.1.3 *Oryza sativa*

Seeds of three different cultivars of *Oryza sativa* (Nipponbare, CO39 and Bala), kindly provided by Ane Sesma (JIC), were sown in pots containing a John Innes No. 1 compost/silver sand mix and grown in a growth room at 28°C/12 h light - 24°C/12 h dark.

### 2.1.4 *Physcomitrella patens*

The Gransden wild-type strain of *Physcomitrella patens* (Hedw.) Bruch and Schimp was used in this study. One ml of spore suspension (~20 spores), kindly provided by Liam Dolan (University of Oxford), was plated on PPNO3 media (0.8 g/l CaNO<sub>3</sub>·4H<sub>2</sub>O, 0.25 g/l MgSO<sub>4</sub>·7H<sub>2</sub>O, 0.0125 g/l FeSO<sub>4</sub>·7H<sub>2</sub>O, 0.055 mg/l CuSO<sub>4</sub>·5H<sub>2</sub>O, 0.055 mg/l ZnSO<sub>4</sub>·7H<sub>2</sub>O, 0.614 mg/l H<sub>3</sub>BO<sub>3</sub>, 0.389 mg/l MnCl<sub>2</sub>·4H<sub>2</sub>O, 0.055 mg/l CoCl<sub>2</sub>·6H<sub>2</sub>O, 0.028 mg/l KI, 0.025 mg/l Na<sub>2</sub>MoO<sub>4</sub>·2H<sub>2</sub>O, 0.25g/l KH<sub>2</sub>PO<sub>4</sub> (pH 7), 7 g/l agar). Cultures were grown in a 23°C growth chamber with a day/night cycle of 16 h/8 h. Single gametophores were sub-cultured regularly on fresh PPNO3 media for maintenance.

## 2.2 DNA extraction

In most cases, DNA was extracted using a modified version of Edwards' protocol (1991). Briefly, leaf material (~50 mg) was collected in an Eppendorf tube and snap-frozen in liquid nitrogen. After grinding, 400 µl of extraction buffer (200 mM Tris HCl pH 7.5, 50 mM NaCl, 25 mM EDTA, 0.5% SDS) were added and the sample vortexed for 5 sec. After centrifugation at 13,000 rpm for 1 min, 300 µl of the supernatant were transferred to a new Eppendorf tube, mixed with 300 µl isopropanol and left at room temperature for 2 min. The sample was then centrifuged at 13,000 rpm for 5 min and the supernatant discarded. The pellet was washed with 300 µl 70% ethanol and centrifuged for another 5 min before removing the supernatant. After drying, the pellet was dissolved in 50 µl water.

This method was also used to extract DNA from the diatom *Phaeodactylum tricorutum*. A small culture of the *P. tricorutum* strain CCMP 632 was kindly provided by Rob Utting (UEA). Five ml of culture ( $2.5 \times 10^6$  cells/ml) were centrifuged at 13,000 rpm for 5 min and the supernatant discarded. The pellet was then dissolved in 600 µl extraction buffer and incubated at 50°C for 10 min. After centrifugation at 13,000 rpm for 1 min, 500 µl of the supernatant were transferred to a new Eppendorf tube and DNA was precipitated with 500 µl isopropanol and washed as described above.

To extract DNA from a large number of leaf samples for single use in PCR (e.g. genotyping), the Chelex method was used. A small leaf disc (ø ~0.5 cm) was collected in an Eppendorf tube containing 50 µl of 10% (w/v) Chelex resin (BioRad). The leaf

sample was then punched with a pipette tip several times and boiled for 5-10 min at 99°C. After centrifugation at 13,000 rpm for 30 sec, 1 µl of supernatant was used for a standard 20-µl PCR reaction.

### 2.3 RNA extraction and cDNA synthesis

Total RNA was extracted from ground plant material (50-100 mg) using the RNeasy Plant Mini Kit (Qiagen) according to manufacturer's instructions including on-column DNase digestion. cDNA was synthesised from 4 µg of total RNA using an oligo dT primer (T<sub>18</sub>V) and M-MLV reverse transcriptase (Invitrogen) in a 20-µl reaction volume according to the manufacturer's protocol. After heat inactivation, 180 µl water were added to the reaction. The resulting cDNA solution is used for subsequent methods described in this chapter.

### 2.4 Creation of transgenic *A. thaliana* lines

#### 2.4.1 Plasmid construction

The names and sequences of the primers used in this study are summarised in Supplemental Table 2.2.

##### 2.4.1.1 Generation of 35S::HOL, 35S::PpHOL, 35S::OsHOL1, 35S::OsHOL2 and 35S::PtHTMT constructs

The *HOL* (At2g43910.1) coding sequence (CDS) was amplified from Col-0 cDNA using primers MCT1 and MCT2. The *PpHOL* (Pp1s304\_15V6.1) CDS was amplified from *P. patens* cDNA using primers PpHOL\_F1 and PpHOL\_R1. The *OsHOL1* (Os03g62670.1) and *OsHOL2* (Os06g06040.1) CDS were amplified from rice (Nipponbare) cDNA using primers OsHOL1\_F1, OsHOL1\_R1 and OsHOL2\_F1, OsHOL2\_R1, respectively. The *PtHTMT* (EEC49246.1) CDS was amplified from *P. tricornutum* genomic DNA using primers PtHTMT\_F1 and PtHTMT\_R1. The resulting fragments were inserted between the *Bam*HI and *Sal*I sites of the pBIN-JIT binary vector, a pBIN19 (Clontech) derivative containing a tandem repeat of the cauliflower mosaic virus (CaMV) 35S promoter.

#### 2.4.1.2 Generation of *HOL::GUS* construct

Primers HOLP1 and HOLP2 were used to amplify 2.4 kb of *HOL* promoter sequence upstream of the start codon from genomic Col-0 DNA. The promoter fragment was inserted between the *Hind*III and *Bam*HI sites of the pBI101.1 binary vector (Jefferson *et al.*, 1987) containing the CDS of the  $\beta$ -Glucuronidase (*GUS*) gene.

#### 2.4.1.3 Generation of *HOL::HOL:GFP* and *35S::GFP* constructs

Nested PCR was performed using primers HOL\_F2 and HOL\_R2 (1<sup>st</sup> round), and primers HOL\_F1\_A and HOL\_R1 (2<sup>nd</sup> round) to amplify a 4.4 kb genomic DNA fragment (*HOL::HOL*) starting from 2 kb upstream of the start codon and terminating just before the stop codon of *HOL* (At2g43910.1). This fragment was then inserted between the *Xba*I and *Bam*HI sites of pBluescript II KS vector (Stratagene) to yield the pBS-HOL vector. The CDS (without start codon) of *GFP* (version mGFP5, Haseloff, 1999) was amplified from a plasmid kindly provided by Nicolas Arnaud (JIC) using primers GFP\_F2 and GFP\_R2. This fragment was then inserted between the *Bam*HI and *Pst*I sites of pBS-HOL yielding the pBS-HOL-GFP vector containing the complete *HOL::HOL:GFP* construct. The *HOL::HOL:GFP* construct was then subcloned between the *Kpn*I and *Xba*I sites of the pCGN18 binary vector (Krizek and Meyerowitz, 1996) replacing the 35S promoter.

To generate the *35S::GFP* construct, primers GFP\_F4 and GFP\_R4 were used to amplify *GFP* CDS (with start codon) from the pBS-HOL-GFP vector. This fragment was then inserted between the *Bam*HI and *Xba*I sites of the original pCGN18 binary vector, placing it under the control of the 35S promoter.

### **2.4.2 Sequencing**

All inserted fragments in the vectors were fully sequenced. Sequencing reactions (10  $\mu$ l) contained 1  $\mu$ l Big Dye v3.1, 1.5  $\mu$ l 5x sequencing buffer, 0.3  $\mu$ l primer (10  $\mu$ M) and approx. 100-200 ng/ $\mu$ l plasmid DNA. The sequencing reaction was performed in a G-STORM GS482 thermal cycler with initial denaturation at 96°C for 1 min, followed by 30 cycles of 96°C for 30 sec, 55°C for 15 sec and 60°C for 4 min. Sequencing was performed by Genome Enterprise Ltd.



### 2.4.3 Transformation into *A. thaliana*

A modified version of the floral dip method (Clough and Bent, 1998) was used for *Arabidopsis* transformation. A 200-ml culture of *Agrobacterium* strain AGL1 carrying the binary vector with the construct of interest was grown in LB media with appropriate antibiotics for 16-24 h at 28°C to OD<sub>600</sub> ~1.6. Cultures were then centrifuged for 20 min at 3500 rpm and the pellet resuspended in a 5% sucrose solution to OD<sub>600</sub> ~ 0.8 to make a 400-ml infiltration solution. Before dipping, Silwet L-77 was added to the infiltration solution to a final concentration of 0.03%. Flowering plants (5-6-week-old) were then fully dipped into the infiltration solution for several seconds with gentle agitation. Plants were then covered with a plastic bag for 1 day to maintain humidity before being returned to the glasshouse. Seeds were harvested and sown on MS agar containing 50 µg/ml kanamycin. It was also verified by PCR that resistant plants contained the transgene of interest. Homozygous T3 plants were used for the experiments.

### 2.5 Creation of *DR5::GFP x hol* and *DR5::GFP x 35S::HOL* crosses

Homozygous plants of *DR5::GFP* and *hol*, and *DR5::GFP* and *35S::HOL* (196-11) were crossed to generate the *DR5::GFP x hol* and the *DR5::GFP x 35S::HOL* crosses, respectively. Segregating F2 and F3 plants were genotyped for the presence of the *GFP* transgene using primers eGFP\_F1 and eGFP\_R1 and for the presence of either the T-DNA insertion of *hol* mutants using primers JMLB2 and HOL\_R8 or the *35S::HOL* transgene using primers AtHOL1\_F and AtHOL1\_R. Lines homozygous for both loci were used for experiments.

### 2.6 Generation of *Physcomitrella Pphol* knockout lines

To generate a gene targeting construct for transformation of *P. patens*, a 0.9 kb genomic fragment of *PpHOL* (Fragment 1), starting from 1.5 kb upstream of the start codon, was amplified from genomic *P. patens* DNA using primers PpHOL\_KO\_F1 and PpHOL\_KO\_R1. A second 0.8 kb genomic fragment (Fragment 2), starting from 0.5 kb downstream of the stop codon, was amplified using primers PpHOL\_KO\_F2 and PpHOL\_KO\_R2. Fragment 1 and 2 were inserted between the *NcoI* and *SpeI* sites, and *XbaI* and *HindIII* sites, respectively, of the pBHrev vector (also known as pBHSNR)

flanking the hygromycin resistance gene cassette (Fig. 6.6) (Menand *et al.*, 2007). Transformation of *P. patens* protoplasts and selection of transformants was carried out in Liam Dolan's Lab (University of Oxford) as described in Menand *et al.* (2007).

## 2.7 Genotyping of *braA.hol.a* mutants

A small piece (~ 1 cm<sup>2</sup>) of a young *B. rapa* leaf was collected and the DNA extracted using the Edwards protocol as described above. A 1.2-kb fragment of the *BraA.HOL.a* gene containing the mutations identified in the mutants in the TILLING screen was amplified in a 20- $\mu$ l PCR reaction containing 12.3  $\mu$ l water, 2  $\mu$ l DNA, 2  $\mu$ l 10x Ex Taq buffer, 1.6  $\mu$ l dNTP mixture (2.5 mM each), 0.1  $\mu$ l Takara Ex Taq polymerase and 1  $\mu$ l of each of the primers (10  $\mu$ M) BrHOLa\_F1 and BrHOLa\_R1. The PCR was performed in a G-STORM GS482 thermal cycler with initial denaturation at 95°C for 2 min, followed by 30 cycles of 95°C for 15 sec, 55°C for 30 sec and 72°C for 1 min 30 sec. After PCR, 1  $\mu$ l of the reaction and the BrHOLa\_F1 primer were used for sequencing as described above. Chromatograms were viewed with FinchTV software (Geospiza) to distinguish WT, homozygous and heterozygous individuals at the mutation site.

## 2.8 RT-PCR and Quantitative Real-Time PCR

For reverse transcription PCR (RT-PCR), 1  $\mu$ l of cDNA was mixed with 14.5  $\mu$ l water, 2  $\mu$ l 10x Standard Taq buffer (NEB), 0.4  $\mu$ l dNTP mixture (10 mM each), 0.1  $\mu$ l Standard Taq polymerase (NEB) and 1  $\mu$ l of each primer (10  $\mu$ M) in a 20- $\mu$ l reaction volume. The PCR was performed in a G-STORM GS482 thermal cycler with initial denaturation at 95°C for 2 min, followed by 35 cycles of 95°C for 15 sec, 55°C for 30 sec and 72°C for 30 sec.

For quantitative real-time PCR (qPCR), 2  $\mu$ l of cDNA was mixed with 10  $\mu$ l SYBR Green JumpStart Taq ReadyMix (Sigma), 0.4  $\mu$ l of each primer (10  $\mu$ M) and 7.2  $\mu$ l water in a 20- $\mu$ l reaction volume. The reactions were set up in a 96-well plate using primers to amplify the target template and a reference template (see Suppl. Table 2.2 for primer sequences). The PCR was run and fluorescence measured in a Chromo4 Real-Time PCR Detector (Biorad) with initial denaturation at 95°C for 2 min, followed by 45 cycles of 95°C for 10 sec, 55°C for 10 sec and 72°C for 20 sec. Melting curve analysis was also performed at the end of the run to verify that only one product was amplified.

PCR efficiencies and expression levels were calculated for the target gene and reference gene from a serial dilution of one cDNA sample. Target gene transcript levels were normalised to the transcript level of one reference gene or to the geometric average of the transcript levels of multiple reference genes (Vandesompele *et al.*, 2002).

## 2.9 Microarray analysis

*Arabidopsis* WT and *hol* seedlings were grown on MS media for 7 days. Six seedlings (roots inclusive) were pooled per Eppendorf tube and a total of 3 (pooled) biological replicates per genotype were harvested. RNA was extracted as described above and ATH1 *Arabidopsis* genome arrays (Affymetrix) were hybridised by Rene Dreos (JIC) according to manufacturer's instructions.

Data were analysed using the *affy*, *limma*, *gcrma*, *arrayQualityMetrics* and *annotate* packages available from the open source software platform Bioconductor (Gentleman *et al.*, 2004). Raw data were normalised using the Robust Multichip Average (RMA) method (Irizarry *et al.*, 2003). Differentially expressed genes in *hol* seedlings compared to WT were identified with the *limma* package (Smyth, 2005) from the means of 3 biological replicates applying a Benjamini and Hochberg (BH)-corrected t-test (P-value < 0.05) and log<sub>2</sub> of fold change [log(FC)] >1 or < -1.

Additionally, iterative group analysis (iGA) (Breitling *et al.*, 2004) was employed to identify treatments from the AtGenExpress database that most resemble the *hol* mutant in terms of transcriptome responses. To do so, all genes were first sorted according to their log fold-change value: One list from lowest to highest value (down-regulated) and a second list from highest to lowest value (up-regulated). Each gene is assigned to one or more functional classes. In this case, a functional class is defined as a hormone or stress treatment which causes a significant up/down-regulation in particular genes based on datasets of 268 different treatments in the AtGenExpress database (Mugford *et al.*, 2009; Koprivova *et al.*, 2010). The iGA software then calculates which classes, i.e. treatments (and the number of members in each class) are significantly overrepresented at the top part of each gene list. Since there are two lists of genes, we identified (1) treatments that produce similar changes to genes up-regulated in the *hol* mutant and (2) treatments that produce similar changes to genes down-regulated in the *hol* mutant.

## 2.10 Methyl halide measurements

To collect air samples, plants were fully enclosed in bags made from Teflon sheet for several hours as indicated in the figure legends. The bags were sealed to plant pots or beakers using electrical tape or elastic bands (Fig. 2.1). Control pots or Petri dishes without plants were also bagged and samples collected to determine background methyl halide levels in the air and to account for any emissions caused by abiotic or biotic processes in the soil alone. These background methyl halide levels were then subtracted from the levels detected from enclosed plants. Each bag was fitted with a Teflon valve from which the sample was extracted. Samples were taken into evacuated 1-litre or 2-litre SilcoCans via a piece of Teflon tubing. Upon opening the negative pressure of the canister drew in approximately 1 or 2 litre of air, respectively, from the plant's headspace. If possible, a pump was used to facilitate the extraction and to pressurise the canisters. 200 ml of air samples were analysed for methyl halides at UEA on a fully-automated Entech GC-MS system as described in Newton (2011).

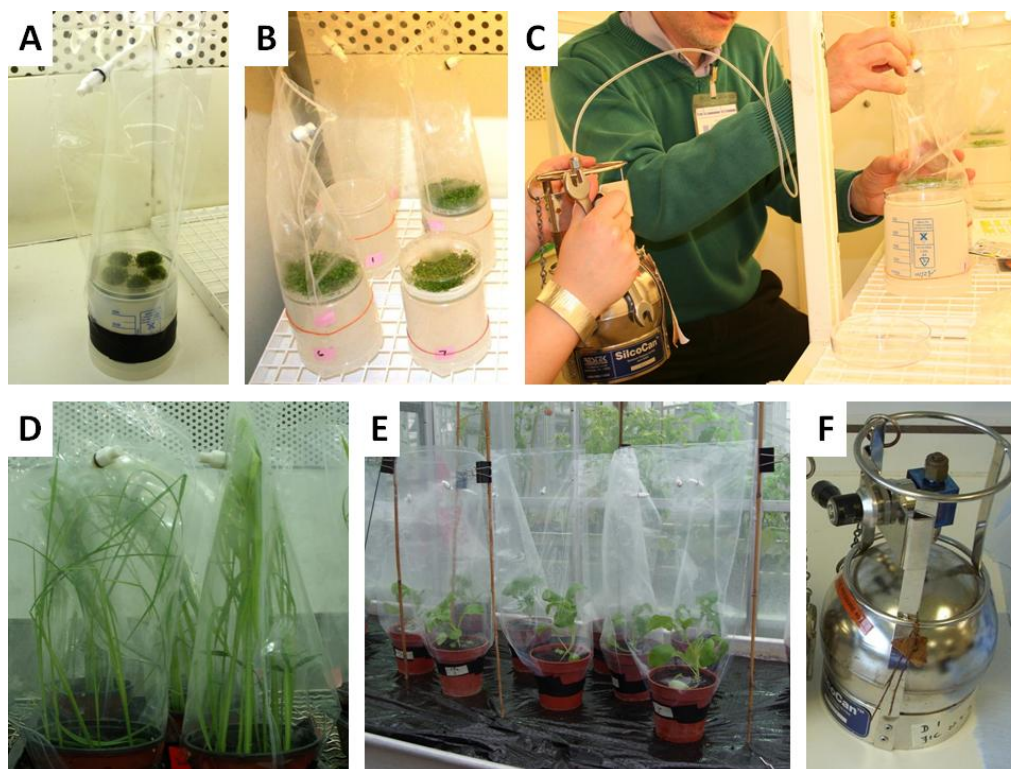


**Figure 2.1.** Collection of air samples for methyl halide analysis. Moss (A) and *Arabidopsis* (B) were grown on agar in Petri dishes. Rice (D) and *Brassica rapa* (E) were grown in compost. All plants were enclosed in Teflon bags for several hours. Samples were taken from the valve of each bag into evacuated SilcoCans (F) via a piece of Teflon tubing (C).

## 2.11 Salt stress and KSCN experiments

For the *A. thaliana* experiments in Petri dishes, unless otherwise stated, seedlings were grown on MS media for 4-5 days and were then transferred to fresh MS media supplemented with varying concentrations of KSCN, NaCl, KCl, CaCl<sub>2</sub>, Na<sub>2</sub>SO<sub>4</sub>, NaBr, KBr, KI, NaI or mannitol as indicated in the figure legends. If the media was supplemented with methionine, spermidine, spermine or GA<sub>3</sub>, filter-sterilised stock solutions were made of these compounds and added to the media after autoclaving. Pictures were taken using a Samsung S85 digital camera. Plant material for RNA extraction, GUS staining, chlorophyll measurements or weighing was harvested at the time points indicated in the figure legends. Fresh mass of the seedlings was determined by dividing the total weight of pooled seedlings on each plate by the number of seedlings. Root length of NaCl-treated seedlings was measured using millimetre paper. For germination assays, seeds were sterilised as described above and stratified for 3 days at 4°C in sterile water before sowing on MS agar. For salt stress experiments in the glasshouse, 2-week-old-plants were watered every 3-4 days with 10 ml NaCl solution for 4 weeks. At the first time of treatment 50 mM NaCl solution was used for watering the plants and this amount was then gradually increased to 100 mM and finally to 200 mM at the next two treatment time points for the respective treatment groups. For the KSCN experiments with *B. rapa* in the glasshouse, 7-day-old plants were watered every 2-3 days with 20 ml KSCN solution (10 mM) or water for 9 days.

## 2.12 Sucrose experiment

Seeds were sown on half-strength MS medium supplemented with 0.2%, 0.5% or 1% sucrose. After stratification, seedlings were allowed to grow for 14 days at the standard growth condition described above. Fresh mass of the seedlings was then determined by dividing the total weight of pooled seedlings on each plate by the number of seedlings.

## 2.13 Auxin experiments

Seeds were sown on MS media containing different concentrations of indole-3-acetic acid (IAA) as indicated in the figure legends. Plates were stratified for 3 days at 4°C and then placed vertically in a 23°C growth chamber with a day/night cycle of 16 h/8 h.

After 6 days pictures were taken using a Samsung S85 digital camera and root length measured using ImageJ (Abramoff *et al.*, 2004). For measurement of hypocotyl growth in the dark, plates were transferred to a 23°C growth chamber and exposed to light for 1h. Afterwards, plates were wrapped in aluminium foil and placed vertically. Pictures were taken after 5 days and hypocotyl length measured using ImageJ.

## 2.14 Chlorophyll measurements

Ground plant material (100 mg) was extracted with 2 ml 95% ethanol at 4°C for 16 h. After centrifugation at 13,000 rpm for 5 min, 200 µl of the supernatant were transferred to a 96-microwell plate and absorbance measured at 664 nm (chlorophyll *a*) and 648 nm (chlorophyll *b*) using a plate reader (Tecan). The total amount of chlorophyll was calculated as follows (Lichtenthaler, 1987):  $C_{a+b}$  (µg/ml) =  $5.24 \cdot A_{664} + 22.24 \cdot A_{648}$ .

## 2.15 Glucosinolate analysis

Leaf material was harvested from 5-week-old plants grown in a growth room at 22°C/10 h light - 22°C/14h dark and glucosinolate analysis conducted by the Stan Kopriva Lab (JIC) as described in Mugford *et al.* (2009).

## 2.16 GUS activity

For visualising GUS activity, sample tissue was fixed in ice-cold 90% acetone for 20 min at room temperature. After rinsing with GUS-buffer (50 mM phosphate-buffer (pH 7.2), 0.2% Triton-X-100, 5 mM  $K_4Fe(CN)_6$ , 5 mM  $K_3Fe(CN)_6$ ), GUS staining buffer was added (GUS-buffer with 2 mM X-Gluc [5-bromo-4-chloro-3-indolyl-β-D-glucuronide]) and samples vacuum-infiltrated for 15 min. Samples were incubated at 37°C for 16 h and then washed several times with 70% ethanol.

For quantification of GUS activity, a novel fluorometric assay (Fior and Gerola, 2009) that corrects for inhibitors of GUS activity in plant extracts was applied. To extract protein, plant tissue (~80 mg) was ground in liquid nitrogen and 700 µl extraction buffer (100 mM phosphate-buffer (pH 7.0), 10 mM EDTA, 5.6 mM β-mercaptoethanol) were added. Samples were vortexed for 5 min and then centrifuged at 13,000 rpm for 20 min at 4°C and the supernatant collected. Assays were performed at

room temperature in 96-well plates. Three reaction mixtures were set up in parallel and used to calculate GUS activity and to correct for inhibitory activity of plant extracts: (1) Ten  $\mu\text{l}$  of a 10 mM 4-methyl-umbelliferyl- $\beta$ -D-glucuronide (MUG) solution were added to 90  $\mu\text{l}$  supernatant. (2) Three  $\mu\text{l}$  of commercial *E. coli* GUS (100 U/ml) were mixed with 90  $\mu\text{l}$  of supernatant and 10  $\mu\text{l}$  MUG were added. (3) The activity of *E. coli* GUS was measured separately (90  $\mu\text{l}$  extraction buffer + 3  $\mu\text{l}$  *E. coli* GUS + 10  $\mu\text{l}$  MUG). Fluorescence of the produced 4-methyl-umbelliferone (MU) was measured in 10-min-intervals after addition of MUG for one hour using a TECAN plate reader at 360/480 nm excitation/emission wavelengths. The amount of MU produced ( $\mu\text{g}/\text{min}$ ) was calculated using a standard curve (fluorescence measurements of seven different concentrations of MU ranging from 0.17 – 34  $\mu\text{g}/\text{ml}$ ). Corrected GUS activity ( $V_c$ ) was calculated as follows: Firstly, an activity coefficient (a) for the *E. coli* GUS in the plant extract (supernatant) was calculated:  $a = [\text{GUS activity (2)} - \text{GUS activity (1)}] / \text{GUS activity (3)}$ . This coefficient was then used to calculate corrected GUS activity:  $V_c = \text{GUS activity (1)} / a$ .

### 2.17 Iodine staining for visualisation of starch

Plants were decolourised in boiling 100% ethanol and then incubated in Lugol's solution for 15 min. Plants were washed with water several times before pictures were taken.

### 2.18 Microscopy

Images of GUS stained samples were taken using the Leica MZ 16 microscope with Leica DFC280 digital camera or the Nikon Eclipse 800 microscope with Pixera Pro 600ES digital camera. Confocal imaging was performed using a Zeiss 510 meta laser scanning confocal microscope. GFP was excited using the 488 nm excitation and emission was collected between 505 - 550 nm. Images were processed using ImageJ (Abramoff *et al.*, 2004).

## 2.19 Herbivore experiments

Plants were grown in Levington M2 compost in a growth room at either 22°C/10 h light - 22°C/14 h dark (short days) or 23°C/16 h light - 20°C/8 h dark (long days) and experiments conducted there. For the caterpillar experiment, plants were grown under long days. One first-instar larva of *Plutella xylostella* was placed on a rosette leaf of a 3-week-old plant and a small plastic cage was attached to the leaf to prevent movement of the caterpillar to other leaves. After 3 days, the infested leaf was photographed and the amount of consumed leaf area estimated. The cage was then removed and the caterpillar allowed to feed on the whole plant for further 5 days. At the end of the experiment (Day 8), photos were taken of the whole plant and consumed leaf area estimated. The weight of the caterpillar was also measured.

For the Sciarid survival assay, three plants were grown per pot for 7 weeks under short days to establish a good root system. Twenty newly-laid *Bradysia paupera* eggs were then washed onto the soil of each pot. After one week, pots were given a sticky trap and bagged up. The number of adult flies emerging from each pot was counted four weeks after infestation with the eggs.

For the Sciarid choice assay, three plants were grown per pot for 11 weeks under short days. For infestation, pots were transferred to long-day conditions, randomised within a tray in a cage and 50 large females and 15 males were added. After two weeks, any remaining adults were removed and pots transferred back to short-day conditions. Pots were given a sticky trap and bagged up. The number of adult flies emerging from each pot was counted four weeks later.

## 2.20 Rhizosphere community profiling

### 2.20.1 Experimental setup

The soil (Bawburgh soil) used as an inoculum in this experiment was collected from a depth of 5-10 cm from a natural grassland site at the JIC Church Farm at Bawburgh, 2 miles west of Norwich and stored at 4°C. This soil was then thoroughly mixed with autoclaved Levington F2 compost to yield a mixture containing 5% Bawburgh soil. The soil/compost mixture was filled into autoclaved 50 ml plastic beakers and watered with sterile water. One 10-day-old *A. thaliana* seedling grown previously on MS media was transferred to each beaker. Moreover, some beakers were left unplanted as a control.



Beakers were then placed in trays in a randomised order and transferred to a growth chamber at 23°C/12 h light - 23°C/12 h dark and watered with sterile water every day. Rhizosphere soil samples and soil samples from the unplanted beakers were collected after 1, 2 and 4 weeks. To collect rhizosphere soil, plants were uprooted and gently shaken to remove the majority of soil. The shoot was then cut off and the root with attached soil (or a similar amount of soil from unplanted beakers) was transferred into 50 ml tubes containing 10 ml phosphate buffered saline (PBS). Samples were vortexed for 10 min and the root removed afterwards. After centrifugation at 4,000 rpm for 5 min, the supernatant was discarded and 1 g (wet weight) of soil was used for DNA extraction and determination of colony-forming units (cfu), respectively.

### **2.20.2 Bacterial count**

One gram of rhizosphere soil was thoroughly mixed in 1 ml of sterile water. A dilution series ranging from  $10^{-1}$  to  $10^{-8}$  was made from this soil solution and 20  $\mu$ l of each dilution dropped onto TY agar plates and allowed to spread and dry naturally (Miles *et al.*, 1938). Plates were placed into the plant growth chamber room (23°C) and cfu counted 1 day after inoculation.

### **2.20.3 DNA extraction and ARISA**

DNA extraction was performed using a modified version of the protocol described in Griffiths *et al.* (2000). Briefly, one g of soil was transferred to a 2-ml screw-top tube containing a mixture of small silica beads and glass beads (ca.  $1/6^{\text{th}}$  of the tube volume) and one big glass bead (0.5 mm). Samples were snap-frozen in liquid nitrogen and stored at -80°C if necessary. To extract DNA, 500  $\mu$ l hexadecyltrimethylammonium bromide (CTAB) buffer and 500  $\mu$ l phenol:chloroform:isoamyl alcohol (25:24:1) (pH8) were added to the sample. CTAB buffer was made by mixing equal amounts of 10% (w/v) CTAB in 0.7 M NaCl with 240 mM potassium phosphate buffer (pH 8). Samples were lysed on a FastPrep homogeniser for 30 sec at speed 5.5. After centrifugation at 14,000 rpm at 4°C for 5 min, the top aqueous layer of the supernatant was transferred to a new Eppendorf tube, mixed with an equal volume of chloroform:isoamyl alcohol (24:1) and centrifuged again at 14,000 rpm at 4°C for 5 min. The top layer was transferred to a new Eppendorf tube and DNA precipitated by adding 2 volumes of

polyethylene glycol (PEG) solution (30% (w/v) PEG 6000 in 1.6 M NaCl) for 2 h at room temperature. The sample was then centrifuged at 14,000 rpm for 10 min and the supernatant discarded. The pellet was washed with 200  $\mu$ l 70% ethanol and centrifuged for another 5 min before removing the supernatant. After drying, the pellet was dissolved in 100  $\mu$ l water. The DNA was then further cleaned using the OneStep PCR Inhibitor Removal Kit (Zymo Research) according to manufacturer's instructions.

The DNA was then subjected to Automated Ribosomal Intergenic Spacer Analysis (ARISA). Primers ITSF (labelled with the fluorescent dye 6-carboxyfluorescein) and ITSReub were used to amplify the 16S-23S intergenic spacer region (ISR) from the bacterial rRNA operons (Cardinale *et al.*, 2004). The length of the ISR varies between different species and this feature can be used to characterise the structure of bacterial communities (Fisher and Triplett, 1999). ISR fragments were amplified in a 11- $\mu$ l PCR reaction containing 3  $\mu$ l water, 1  $\mu$ l DNA, 5  $\mu$ l GoTaq mix (Promega) and 1  $\mu$ l of each of the primers (10  $\mu$ M). The PCR was performed with initial denaturation at 95°C for 5 min, followed by 30 cycles of 94°C for 1 min, 55°C for 1 min and 72°C for 2 min. After PCR, 1  $\mu$ l of the reaction was mixed with 10  $\mu$ l Hi-Di formamide (Life Technologies) and 0.4  $\mu$ l 1200 LIZ size standard (Applied Biosystems). ARISA profiles of these samples were then generated by capillary electrophoresis by Genome Enterprise Ltd.

#### **2.20.4 Generation of plots and statistical analysis**

Raw ARISA profile data were modified by excluding ISR sizes of < 100 bp and those with fluorescence (i.e. peak area) of < 25 units. These profiles were then aligned using the T-Align web tool (Smith *et al.*, 2005). Fluorescence data were normalised by dividing the fluorescence of each ISR by the total fluorescence of all ISRs to give relative fluorescence (%).

For the comparison of ARISA profiles, only the 100 most abundant ISR sizes (i.e. those with highest fluorescence) of each ARISA profile were chosen for statistical analysis. Statistical analysis was performed using the software package PRIMER 6 as described in Micallef *et al.* (2009b). A similarity matrix was constructed by calculating similarities between each pair of ARISA profiles based on the relative fluorescence of the 100 most abundant ISR sizes. Similarity was calculated from square-root-transformed data using the Bray-Curtis coefficient. Data transformation down-weights

the dominance of the most abundant ISR sizes. To illustrate the similarity between samples (profiles) non-metric Multi-Dimensional-Scaling (MDS) was used. The closer two points (i.e. samples) are in a MDS plot, the higher is their similarity. Moreover, multivariate analysis of variance (MANOVA) was used for significance testing. MANOVA was performed using the R package *vegan* (Oksanen *et al.*, 2010) as described in Osborne *et al.* (2011).

To illustrate the distribution of individual ISR sizes, ternary plots were generated using a script developed by Andrzej Tkacz and Jitender Cheema at JIC (unpublished). Only ISR fragments showing a relative fluorescence of > 1% in at least one sample were included in the plot. Circle sizes indicate the dominance of each ISR fragment i.e. large circles depict high total fluorescence.

### 2.20.5 PCR amplification of *cmuA*

A 807-bp fragment of the *cmuA* gene was amplified in a 20- $\mu$ l PCR reaction containing 13.5  $\mu$ l water, 2  $\mu$ l DNA, 2  $\mu$ l 10x Taq buffer, 0.4  $\mu$ l dNTP mixture (10 mM each), 0.1  $\mu$ l Taq polymerase (NEB) and 1  $\mu$ l of each of the primers (10  $\mu$ M) *cmuA*802f and *cmuA*1609r (Miller *et al.*, 2004). The PCR was performed in a G-STORM GS482 thermal cycler with initial denaturation at 95°C for 2 min, followed by 35 cycles of 95°C for 15 sec, 55°C for 30 sec and 72°C for 1 min 30 sec.

### 2.21 Phylogenetic analysis

The *A. thaliana* HOL and HLL protein sequences were retrieved from the MIPS *A. thaliana* genome database (<http://mips.helmholtz-muenchen.de/plant/genomes.jsp>). The protein sequence of AtHOL was used to perform a BLAST search on the NCBI ([www.ncbi.nlm.nih.gov](http://www.ncbi.nlm.nih.gov)) and Phytozome (<http://www.phytozome.net>) databases to retrieve protein sequences of known and putative *HOL*-homologous genes from other plants species. The names and sources of the sequences used for the phylogenetic analyses are summarised in Supplemental Table 7.1.

Sequences were prealigned using MUSCLE v3.6 (Edgar, 2004). The alignment was then manually edited in BioEdit v7.0 (Hall, 1999) to remove ambiguously aligned positions. Conserved regions in the alignment were highlighted using the BOXSHADE tool ([http://www.ch.embnet.org/software/BOX\\_form.html](http://www.ch.embnet.org/software/BOX_form.html)) which highlights identical

and similar amino acids residues in black or grey, respectively. The Jones, Taylor and Thornton (JTT) model with  $\alpha = 1.35$  and  $p\text{-inv} = 0.1$  was chosen as the best-fitting evolutionary model in ProtTest (Abascal *et al.*, 2005).

The Bayesian analysis was performed with MrBayes (v3.2.1, Huelsenbeck and Ronquist, 2001) with the settings “rates=invgamma” and “Aamodelpr=fixed (Jones)”. Two independent runs were computed for 200,000 generations at which point the standard deviation was  $< 0.03$ . One tree was saved every 100 generations. A “burnin=500” was chosen to give the final tree.

The Maximum Likelihood (ML) analysis was performed with PhyML v3.0 (Guindon and Gascuel, 2003) using the JTT model, estimated  $\alpha$  and  $p\text{-inv}$  values, a SPR search with 5 random input trees and bootstrapping (100 replicates). All trees were visualised using the programme FigTree (<http://tree.bio.ed.ac.uk/software/figtree/>).

## **2.22 Statistical analysis**

Data were analyzed with GenStat v13. Two-sample t-tests or ANOVA with Bonferroni-corrected or Fisher’s protected LSD post-hoc tests were used. To ensure homogeneity of variances, data were log-transformed if necessary.

## Chapter 3 – Characterisation and manipulation of *HOL* gene expression in *Arabidopsis thaliana*

### 3.1 Introduction

In the last three decades the well-established model plant *Arabidopsis thaliana* has helped us to understand how plants work and the availability of a wide range of resources and tools (e.g. seed stock centres, internet databases) continue to facilitate further breakthroughs in the field of plant biology (Koornneef and Meinke, 2010). The discovery that *A. thaliana* produces and emits methyl halides and the identification of the *HOL* gene, which controls the production of these compounds (Rhew *et al.*, 2003), render *A. thaliana* a useful tool to help us understand the function and purpose of methyl halide production in plants.

#### 3.1.1 Properties of *A. thaliana* *HOL* methyltransferases

Three genes encoding HTMTs (At2g43910, At2g43920 and At2g43940, referred to as *HOL*, *HLL1* and *HLL2*, respectively) can be found in close proximity on chromosome II in the *A. thaliana* genome (Suppl. Fig. 3.1). The amino acid sequences of *HLL1* and *HLL2* are 83% and 61% identical to *HOL*, respectively. It has been shown that all three HTMTs are capable of methylating iodide and thiocyanate ( $\text{SCN}^-$ ) when assayed *in vitro* as recombinant proteins previously expressed in *E. coli* (Nagatoshi and Nakamura, 2007, 2009). Interestingly, only *HOL* and *HLL1*, but not *HLL2*, are able to methylate chloride (Table 1.2). These results showed that all three proteins are functional *in vitro* and possess halide and thiol methyltransferase activity, however, only little is known about the exact function of *HOL*, *HLL1* and *HLL2* *in planta*.

Analysis of publicly available microarray data sets showed that all three genes are ubiquitously expressed in *A. thaliana*. However expression levels of *HLL1* and *HLL2* are very low compared to expression levels of *HOL* (Nagatoshi and Nakamura, 2007). Most importantly, *HOL* is almost solely responsible for the production of methyl halides in *A. thaliana* since in the *hol* mutant,  $\text{CH}_3\text{Cl}$ ,  $\text{CH}_3\text{Br}$  and  $\text{CH}_3\text{I}$  emission levels are strongly reduced to less than 1% of WT levels in adult plants (Fig. 1.7) (Rhew *et al.*, 2003). Similarly, the ability to detoxify  $\text{SCN}^-$  *in vivo* is attributed to the function of *HOL* only since the *hol* mutant is more susceptible to  $\text{SCN}^-$  than WT plants, whereas

*hll1* and *hll2* mutants are not (Fig. 1.10) (Nagatoshi and Nakamura, 2009). These data imply that there is no functional redundancy between the different HTMT proteins, and that HOL alone is the major player in methylating halide ions and  $\text{SCN}^-$  in *A. thaliana*. Possible functions of HOL and/or methyl halide emissions are thoroughly discussed in Chapter 4 and 5.

Three different transcripts encoding slightly different proteins are predicted to be produced from the *HOL* gene (Suppl. Fig. 3.1). The protein sequence predicted by gene model At2g43910.1 shares the highest similarity with the protein sequences of previously cloned *HOL*-homologous genes in *Batis maritima* (Ni and Hager, 1998) and *Brassica oleracea* (Attieh *et al.*, 2002), and therefore genomic and coding sequences of this gene model were used in this study for generation of *35S::HOL* and *HOL::HOL:GFP* lines. According to this model, the *A. thaliana* *HOL* gene consists of 8 exons and 7 introns and encodes a protein of 227 amino acids with a predicted molecular weight of 25 kDa. Recently, the crystallographic structure of HOL was described and putative active sites of the enzyme predicted (Fig. 3.1) (Schmidberger *et al.*, 2010). The same study also tested, by using site-directed mutagenesis, whether some of the residues in the active site determine substrate specificity. It was found that the Tyr172 residue was important for the binding of the smaller chloride nucleophile since the Tyr172Phe variant showed reduced efficiency with chloride ions compared to the WT variant of the enzyme.

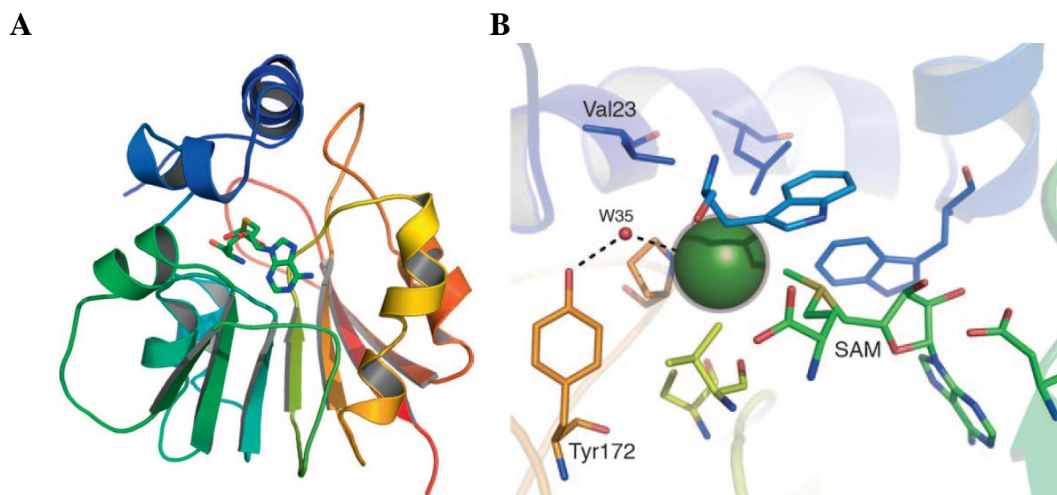


**Figure 3.1. Structure and active site of the *A. thaliana* HOL methyltransferase.** (A) The diagram is coloured in a spectrum from N-terminus (blue) to C-terminus (red) and the putative active site is occupied by S-Adenosyl-L-homocysteine (SAH). (B) Close-up of the active site binding S-Adenosyl-L-methionine (SAM) and chloride (green sphere). Images taken from Schmidberger *et al.* (2010).

### 3.1.2 Objectives of this chapter

The first objective of this chapter was to thoroughly characterise the tissue-specific expression patterns of the *A. thaliana* *HOL* gene using *HOL::GUS* reporter lines. Moreover, the localisation and expression of the *HOL* protein was investigated using *HOL::HOL:GFP* lines. Secondly, transgenic lines overexpressing the *HOL* gene (*35S::HOL*) were generated in order to test if increased *HOL* activity raises emission levels of methyl halides and promotes  $\text{SCN}^-$  tolerance. Finally, to identify potential functions of *HOL* in *A. thaliana*, microarray analysis of WT and *hol* mutant plants was performed to gain more insight into the global effects of *HOL* activity and/or methyl halide production on the transcriptome of *A. thaliana*. Moreover, publicly available microarray data sets were analysed to identify treatments (e.g. stress, hormones) which affect *HOL* gene expression, and to identify genes which are co-expressed with *HOL*.

## 3.2 Results

### 3.2.1 Characterisation of *HOL* gene expression and *HOL* protein localisation

It has previously been shown by northern blot analysis that the *HOL* gene is expressed in young seedlings and in all above-ground tissue in 4-week-old plants (Rhew *et al.*, 2003). To further characterise the expression pattern of *HOL*, *HOL::GUS* reporter lines containing 2.4 kb of promoter sequence fused to the *GUS* reporter gene were generated. Tissue from different developmental stages was then harvested and stained to monitor *GUS* activity. Two independent transgenic lines were tested and both showed the same expression pattern.

The most prominent observation was the high expression of *HOL* in the roots throughout the whole life cycle of the plant (Fig. 3.2). *GUS* activity was already detected in the root meristem of stratified seeds before sowing (Fig. 3.2 A) and gradually increased in the vasculature of the root and hypocotyl during germination and early seedling growth (Fig. 3.2 B-D). After germination, *GUS* expression was also detected in the hydathodes and vascular tissue of leaves (Fig. 3.2 D-E). Young, developing leaves showed higher expression compared to older leaves (Fig. 3.2 E). In mature plants (5 weeks after sowing), *GUS* activity was not detected in leaves anymore, but could still be found in roots (data not shown). Interestingly, *HOL* was also

expressed in the stamens of flowers at a very specific point at the border of the filament and anther structure (Fig. 3.2 F, G).

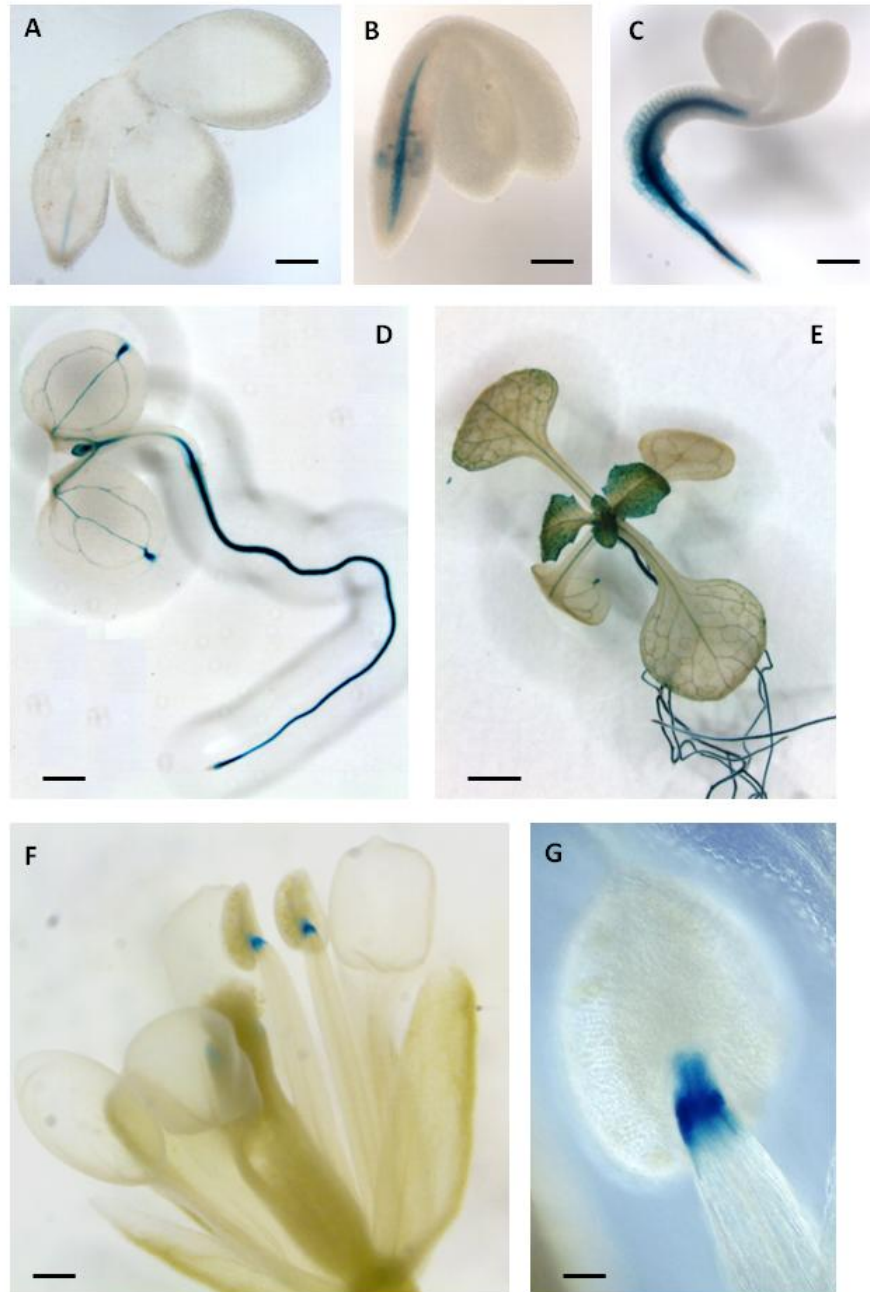


**Figure 3.2. Tissue-specific *HOL* gene expression in *HOL::GUS* reporter lines.** Tissue from different developmental stages was harvested and stained for GUS activity. (A) to (E): Seeds were sown on MS plates and stratified for 3 days at 4°C and seedlings stained 0 h (A), 24 h (B), 48 h (C), 72h (D) and 9 days (E) after transfer to the growth room. (F) and (G): GUS activity in the stamens of flowers harvested from five-week-old plants. Scale bars = 0.1 mm in (A) and (B), 0.2 mm in (C) and (F), 0.4 mm in (D), 1.5 mm in (E) and 0.05 mm in (G).



To determine the tissue-specific expression of HOL protein and its subcellular localisation, transgenic lines expressing a GFP-tagged HOL protein under the control of the HOL promoter (*HOL::HOL:GFP*) were generated. Moreover, *35S::GFP* lines were generated as a control. Several independent transgenic lines were tested for each construct and all showed the same expression pattern.

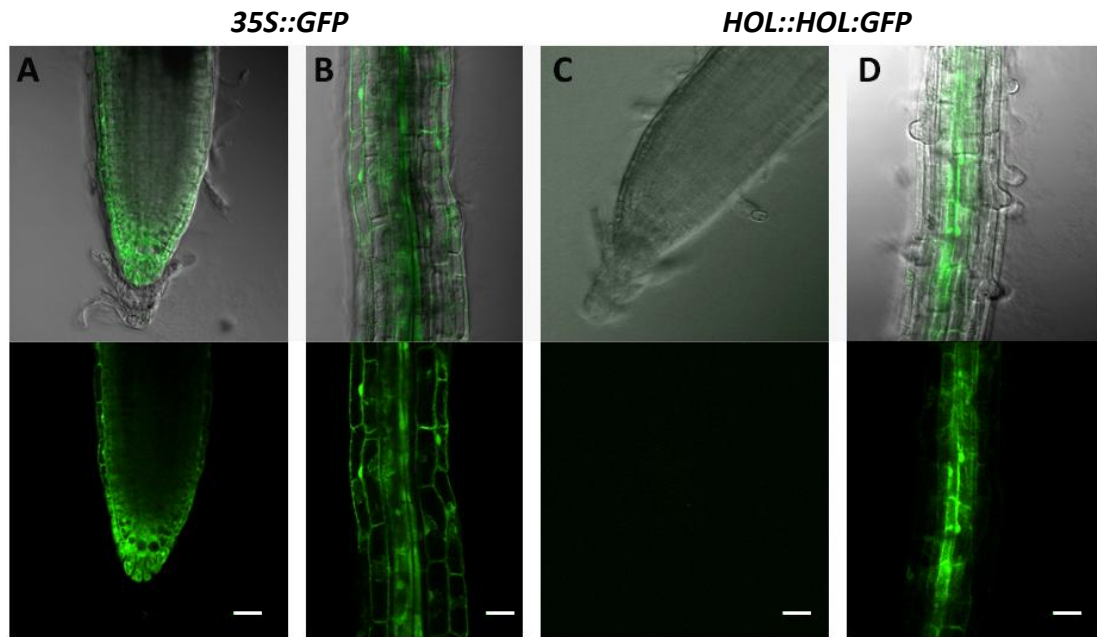


**Figure 3.3. Localisation of HOL protein in roots.** Confocal images of GFP expression in *35S::GFP* (Control) (A) and (B), and in *HOL::HOL:GFP* roots (C) and (D). Images were taken from the root tip (A) and (C), and the root (B) and (D) of 11-day-old seedlings. Merged images of GFP and bright field (top) and GFP alone (bottom) are shown. Scale bar = 30  $\mu$ m.

Confocal imaging of GFP in roots showed that HOL is localised in the cell cytosol (Fig. 3.3 D), similar to GFP alone (Fig. 3.3 B). This is in accordance with the HOL localisation predicted by the TargetP server (Emanuelsson *et al.*, 2007) which did not identify any obvious trafficking signal motifs in the amino acid sequence of HOL. It is not surprising that GFP was also detected in the nucleus since HOL is a relatively small protein (25 kDa) and can therefore probably passively diffuse into the nucleus. These images also showed that HOL protein expression is restricted to the vasculature in the roots (Fig. 3.3 D) and cannot be detected in root tips (Fig. 3.3 C), whereas, as expected, GFP alone is ubiquitous in the roots and root tips of *35S::GFP* lines (Fig. 3.3 A, B). Overall, HOL protein expression in roots is similar to the pattern of *HOL* gene

expression observed in roots of *HOL::GUS* reporter lines. However, in contrast to GUS accumulation (Fig. 3.2 A-D), GFP was not detected in the vasculature near the root tip (Fig. 3.3 C), and no GFP was found in very young seedlings (i.e. younger than 10 days) (data not shown).

### 3.2.2 Generation and characterisation of 35S::*HOL* lines

Initially, a reliable sampling method for methyl halide measurements from plants had to be established. Therefore, *A. thaliana* WT and *hol* seedlings were grown to collect air samples. It has been shown that in the *hol* mutant, CH<sub>3</sub>Cl, CH<sub>3</sub>Br and CH<sub>3</sub>I emissions are strongly reduced (Fig. 1.7) (Rhew *et al.*, 2003). In our set-up, seedlings were densely grown on agar plates for 20 days and each plate was then enclosed in Teflon bags fitted with a valve, from which air samples were collected at several time points (see Chapter 2). Using this method, we were able to detect CH<sub>3</sub>Cl, CH<sub>3</sub>Br and CH<sub>3</sub>I emitted from the seedlings. There was a positive linear correlation between methyl halide concentration and enclosure time. Moreover, as expected, methyl halide emissions from the *hol* mutant were strongly reduced compared to WT or, in the case of CH<sub>3</sub>I, did not exceed atmospheric background levels (Suppl. Fig. 3.2).

In order to test if the overexpression of *HOL* causes an increase in methyl halide emissions, two independently transformed lines (196-9 and 196-11) expressing the full-length CDS of *HOL* under the control of the cauliflower mosaic virus (CaMV) 35S promoter were generated. *HOL* transcript levels were 60-fold and 140-fold higher in 196-9 and 196-11, respectively, compared to WT transcript levels (Fig. 3.4 A). Accordingly, CH<sub>3</sub>Cl and CH<sub>3</sub>Br emissions were increased 20-fold and 50-fold in 196-9 and 196-11, respectively, and CH<sub>3</sub>I emission levels were elevated three-fold in both overexpressor lines compared to WT methyl halide levels (Fig. 3.4 B-D). These data confirm the positive correlation between *HOL* gene expression levels and methyl halide production in *A. thaliana*.

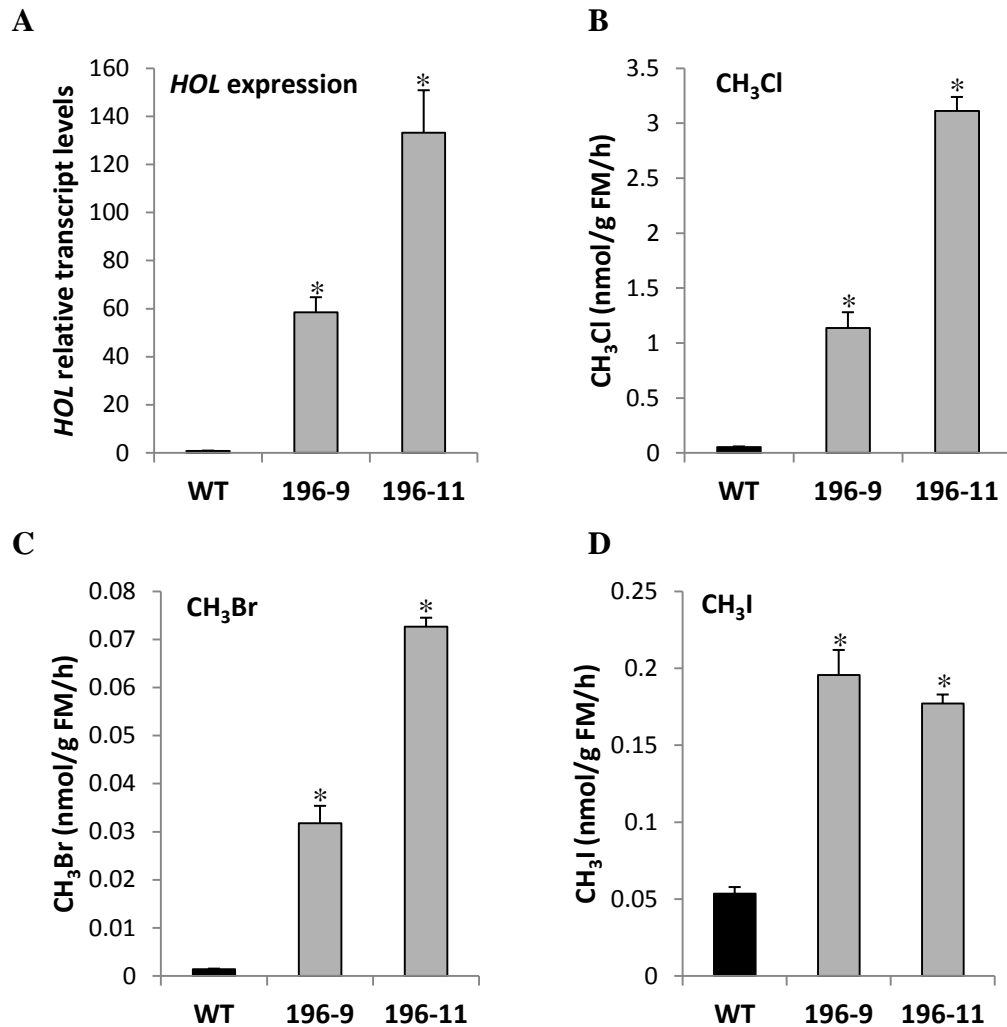


**Figure 3.4. Overexpression of *HOL* in *A. thaliana*.** Relative *HOL* expression levels (A) and emission profiles of CH<sub>3</sub>Cl (B), CH<sub>3</sub>Br (C) and CH<sub>3</sub>I (D) in *A. thaliana* WT and *35S::HOL* lines (196-9, 196-11). Transcript levels were determined in 12-day-old seedlings by qPCR and *HOL* expression normalised to expression of *EF1α*. Methyl halide emissions were measured from 10-day-old seedlings grown on agar plates. Air samples were taken 8 h after enclosure. Background methyl halide emissions were also determined from agar control and subtracted from the amounts detected from enclosed plants. Data points are the mean ± s.e. of three biological replicates. Asterisks represent significant differences from WT (t-test,  $p < 0.001$ ).

It has previously been shown that the overexpression of *HOL* leads to an increased tolerance towards SCN<sup>-</sup> in *A. thaliana* (Nagatoshi and Nakamura, 2009). Therefore, WT, *hol* and *35S::HOL* seedlings were grown on MS media supplemented with KSCN. As expected, *hol* was highly sensitive towards low KSCN concentrations (Fig. 3.5 A), whereas both overexpressor lines grew well on 1 mM and 2.5 mM KSCN (Fig. 3.5), and also survived on 5 mM KSCN (data not shown).

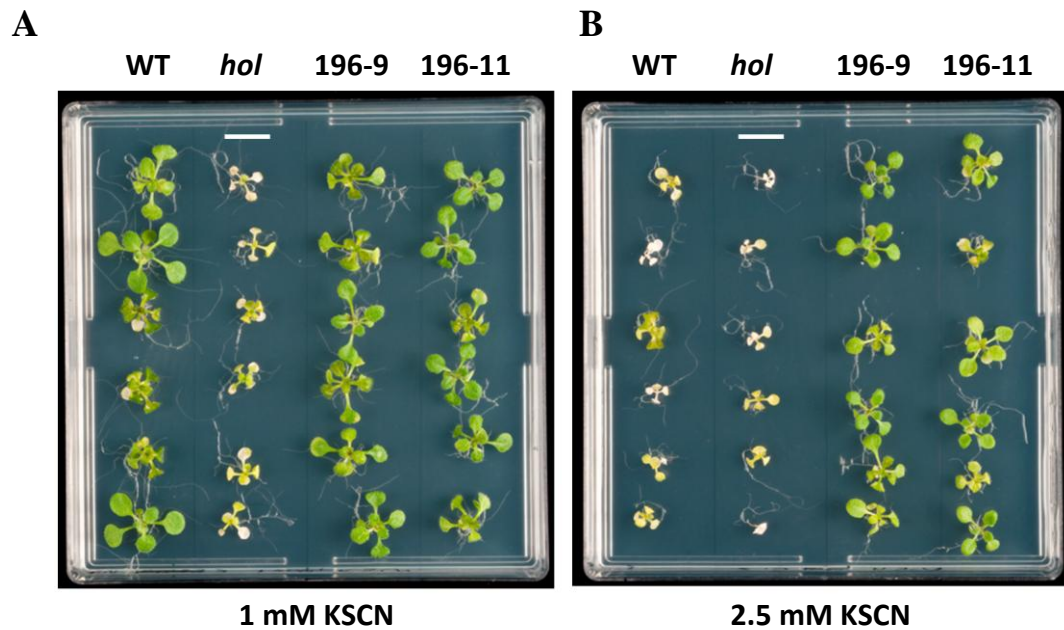


**Figure 3.5. Susceptibility of WT, *hol* and 35S::*HOL* lines (196-9, 196-11) to KSCN.** Five-day-old seedlings were transferred to MS media containing 1 mM (A) or 2.5 mM (B) KSCN and pictures taken 7 days later. Scale bar = 1 cm.

Taken together, these data confirm that the 35S::*HOL* lines generated in this study are fully functional and show the expected phenotypes associated with increased HOL activity.

### 3.2.3 Microarray analysis of the *hol* mutant

To gain more insight into the global effects of HOL activity and/or methyl halide production on the transcriptome of *A. thaliana*, microarray analysis was performed using the Affymetrix ATH1 *Arabidopsis* genome array. RNA was extracted from whole, seven-day-old WT and *hol* mutant seedlings grown on MS media. Differentially expressed genes were identified that satisfied the criteria of both a > 2-fold difference between *hol* and WT seedlings and a P-value < 0.05 (Benjamini-Hochberg-corrected t-test). These genes were then classified into functional classes (Tables 3.1 and 3.2) based on information available at TAIR ([www.arabidopsis.org](http://www.arabidopsis.org)) and links to publications therein. Overall, 32 genes were down-regulated (Table 3.1) and 49 genes up-regulated (Table 3.2) in the *hol* mutant compared to WT. The expression patterns of the four most up-regulated and four most down-regulated genes were verified by qPCR (Suppl. Fig. 3.3, Fig. 4.11 and Fig. 4.12).

**Table 3.1. Genes down-regulated in the *hol* mutant.** Fold change is calculated from the signal ratio of *hol* over WT from the means of 3 biological replicates applying a fold change threshold < 0.5 and a P-value < 0.05 (Benjamini-Hochberg-corrected t-test).

<b>AGI code</b>	<b>Functional classes and gene description</b>	<b>Fold change</b>	<b>P-value</b>
At2g43910	HOL	0.08	6.5E-09
<b>Metabolism</b>			
At3g30720	QUA-QUINE STARCH (QQS)	0.02	4.0E-12
<b>Anthocyanin biosynthesis</b>			
At5g54060	Anthocyanin xylosyltransferase (UGT79B1)	0.29	0.009
At1g56650	Myb transcription factor (PAP1)	0.31	2.9E-04
At1g03495	Anthocyanin coumaroyltransferase	0.31	0.037
At4g14090	Anthocyanin glucosyltransferase (UGT75C1)	0.35	0.017
At3g29590	Anthocyanin malonyltransferase (At5MAT)	0.41	0.006
At4g22880	Anthocyanidin synthase	0.41	0.005
At5g17220	Glutathione-S-transferase (TT19)	0.42	0.029
<b>Response to abiotic/biotic stress</b>			
At1g60190	U-Box E3 Ubiquitin Ligase (PUB19)	0.24	1.7E-04
At4g03060	2-oxoglutarate dependent dioxygenase (AOP2)	0.31	0.003
At3g49580	RESPONSE TO LOW SULFUR 1 (LSU1)	0.35	0.001
At5g15950	SAM decarboxylase (AdoMetDC 2)	0.44	0.002
At3g44450	UV-B-responsive protein	0.44	0.004
At5g42760	Leucine carboxyl methyltransferase	0.44	0.022
At3g47420	Glycerol-3-phosphate permease (AtG3Pp1)	0.44	0.012
At5g20150	SPX domain-containing protein (SPX1)	0.45	0.023
At5g24660	RESPONSE TO LOW SULFUR 2 (LSU2)	0.45	0.005
At3g22840	EARLY LIGHT-INDUCED PROTEIN 1 (ELIP1)	0.48	0.021
At5g01820	CBL-interacting protein kinase (CIPK14)	0.48	0.004
At5g48850	SULPHUR DEFICIENCY-INDUCED 1 (SDI1)	0.48	2.0E-04
At1g05170	Galactosyltransferase	0.50	0.005
<b>Response to light/auxin</b>			
At2g44910	Homeodomain-leucine zipper protein (ATHB4)	0.29	0.002
At4g16780	Homeodomain-leucine zipper protein (ATHB2)	0.42	4.5E-04
<b>Circadian Clock</b>			
At2g46790	PSEUDO-RESPONSE REGULATOR 9 (PRR9)	0.44	0.002
<b>Structure/Cell wall</b>			
At1g60590	Polygalacturonase	0.37	0.002
<b>Signalling component</b>			
At5g10930	CBL-interacting protein kinase (CIPK5).	0.44	0.005

AGI code	Functional classes and gene description	Fold change	P-value
<b>Unknown</b>			
At2g15020	Unknown protein	0.41	0.002
At5g01790	Unknown protein	0.46	0.001
At4g01080	TRICHOME BIREFRINGENCE-LIKE 26 (TBL26)	0.47	0.029
At1g20070	Unknown protein	0.47	0.014
At5g46690	Basic HLH protein (BHLH071)	0.47	1.7E-04

Firstly, microarray analysis confirmed that *HOL* gene expression was reduced in the *hol* mutant (Table 3.1). Since the probe for *HOL* on the chip also binds transcripts of *HLL1* (At2g43920), the differences in *HOL* expression between WT and the mutant were not accurately depicted. In fact, qPCR analysis confirmed that *HOL* transcript levels were very strongly reduced in the *hol* mutant (relative expression levels (mean  $\pm$  s.e.): WT =  $0.9 \pm 0.07$ , *hol* =  $0.0004 \pm 0.0002$ , n = 3).

Secondly, the gene whose expression was primarily affected in the *hol* mutant (only 2% of WT transcript levels) was the *QUA-QUINE STARCH (QQS)* gene (Table 3.1). The precise function of this gene remains unknown, but it has been proposed that it regulates starch metabolism in response to cold (Li *et al.*, 2009; Seo *et al.*, 2011). *QQS* is believed to be repressed by EXORDIUM-LIKE 1 (EXL1), a protein that promotes growth during low carbon availability in *A. thaliana* (Schröder *et al.*, 2011). Accordingly, *EXL1* was up-regulated in the *hol* mutant (Table 3.2). A thorough investigation of *QQS* and *EXL1* expression in WT and the *hol* mutant and possible effects on carbon metabolism in these plants are further described in Chapter 4.

Overall, several genes involved in anthocyanin biosynthesis which are known to be coexpressed in *A. thaliana* (Yonekura-Sakakibara *et al.*, 2012) were down-regulated in the *hol* mutant. In addition, genes associated with the circadian clock, e.g. *PRR5* and *PRR9* (Nakamichi *et al.*, 2010), and the photoperiodic control of plant growth and/or shade avoidance, such as *ATHB2*, *ATHB4* and *IAA29* (Sorin *et al.*, 2009; Kunihiro *et al.*, 2011), were also differentially expressed in the *hol* mutant (Table 3.1 and 3.2).

By far, the largest number of genes (13 down and 18 up-regulated) whose transcript levels were altered in the *hol* mutant were genes responding to abiotic and/or biotic stresses. For example, expression of *PUB19*, which negatively regulates ABA and drought responses in *Arabidopsis* (Liu *et al.*, 2011), was reduced to one-fourth compared to WT. Interestingly, three genes, *LSU1*, *LSU2* and *SDII*, which are known

to respond to sulphur deficiency (Maruyama-Nakashita *et al.*, 2005; Howarth *et al.*, 2009) were down-regulated in the *hol* mutant. Moreover, two genes, *AOP2* and *CYP81F2*, involved in the biosynthesis of glucosinolates (Pfalz *et al.*, 2009; Neal *et al.*, 2010), sulphur-containing metabolites important in plant defence against pathogens and herbivores (see Chapter 5), also showed altered expression levels in the mutant (Table 3.1 and 3.2).

**Table 3.2. Genes up-regulated in the *hol* mutant.** Fold change is calculated from the signal ratio of *hol* over WT from the means of 3 biological replicates applying a fold change threshold > 2 and a P-value < 0.05 (Benjamini-Hochberg-corrected t-test).

AGI code	Functional classes and gene description	Fold change	P-value
<b>Metabolism</b>			
At3g47340	Glutamine-dependent asparagine synthetase (ASN1)	4.14	0.005
At1g35140	EXORDIUM-LIKE 1 (EXL1)	4.13	2.8E-04
At1g02660	Alpha/beta-hydrolase protein	2.89	2.8E-04
At5g56870	Beta-galactosidase (BGAL4)	2.66	0.042
At1g10070	Amino acid aminotransferase (BCAT-2)	2.28	0.015
At1g23870	Trehalose-phosphate synthase (TPS9)	2.25	0.002
<b>Response to abiotic/biotic stress</b>			
At4g35770	Senescence-associated gene (SEN1)	3.50	1.5E-05
At1g21910	Transcription factor (DREB26)	2.65	0.002
At5g20250	Glycosyl hydrolase (DIN10)	2.56	3.9E-04
At2g26560	Phospholipase A 2A (PLA IIA)	2.55	0.004
At4g04330	Chaperone (RbcX1)	2.48	0.003
At4g31800	Transcription factor (WRKY18)	2.47	0.008
At1g76650	CALMODULIN-LIKE 38 (CML38)	2.44	0.011
At1g79700	Integrase-type DNA-binding protein	2.35	2.9E-04
At3g62550	Adenine nucleotide alpha hydrolases-like protein	2.31	0.001
At4g27450	Aluminium induced protein	2.22	0.001
At5g06690	Thioredoxin (WCRKC1)	2.21	0.003
At1g72060	Serine-type endopeptidase inhibitor	2.20	0.024
At3g15450	Aluminium-induced protein	2.19	0.004
At5g20230	BLUE-COPPER-BINDING PROTEIN (BCB)	2.17	0.029
At5g57220	Cytochrome P450 monooxygenase (CYP81F2)	2.16	0.010
At2g15890	Maternal effect embryo arrest 14 (MEE14)	2.11	0.001
At2g18700	Trehalose-phosphate synthase (TPS11)	2.08	0.004
At3g48360	Transcription factor (BT2)	2.02	0.004

<b>AGI code</b>	<b>Functional classes and gene description</b>	<b>Fold change</b>	<b>P-value</b>
<b>Response to light/auxin</b>			
At2g33830	Dormancy/auxin-associated protein	5.22	1.7E-04
At3g03840	SAUR-like auxin-responsive protein	3.14	0.005
At4g32280	Auxin inducible protein (IAA29)	3.06	4.1E-04
At1g29440	SAUR-like auxin-responsive protein	2.28	0.004
At3g19850	Phototropic-responsive NPH3 family protein	2.02	0.001
<b>Circadian clock</b>			
At5g24470	PSEUDO-RESPONSE REGULATOR 5 (PRR5)	2.48	0.002
<b>Structure/Cell wall</b>			
At1g02640	BETA-XYLOSIDASE 2 (BXL2)	3.05	4.8E-04
At5g49360	BETA-XYLOSIDASE 1 (BXL1)	2.35	0.001
At3g45970	EXPANSIN-LIKE A1 (EXPL1)	2.32	0.004
At2g30600	BTB/POZ domain-containing protein	2.01	0.029
<b>Signalling component</b>			
At5g24240	Phosphatidylinositol 3- and 4-kinase	3.25	0.003
At3g59350	Protein kinase	2.29	0.006
<b>Transport</b>			
At1g11260	H <sup>+</sup> /hexose cotransporter (STP1)	2.76	0.003
At1g57980	Nucleotide-sugar transporter family protein	2.60	0.004
At1g22570	Proton-dependent oligopeptide transport family protein	2.39	0.007
<b>Protein processing</b>			
At2g28120	Nodulin family protein	2.07	0.013
At5g21170	Encodes subunit of the SnRK1 kinase (AKINbeta1)	2.06	0.001
<b>Unknown</b>			
At5g62280	Unknown protein	3.16	3.2E-04
At1g50040	Unknown protein	2.65	0.001
At1g28330	DORMANCY-ASSOCIATED PROTEIN 1 (DRM1)	2.45	0.011
At3g19680	Unknown protein	2.34	0.031
At2g34510	Unknown protein	2.26	0.017
At5g14120	Nodulin family protein	2.15	0.002
At5g22920	Zinc finger protein	2.14	0.002
At3g15630	Unknown protein	2.03	0.008



The analysis described above only takes into account genes which show a two-fold change in expression in *hol* seedlings compared to WT. However, it can be useful to search the whole data set for a concerted expression change of genes belonging to the same functional class by using the Iterative Group Analysis (iGA) approach (Breitling *et al.*, 2004). In this case, the functional class is defined as a stress or hormone treatment which causes a significant up/down-regulation of particular genes based on the AtGenExpress database (Mugford *et al.*, 2009; Koprivova *et al.*, 2010). Thus, iGA identified treatments which most resemble the *hol* mutant in terms of transcriptome responses.

In accordance to the results described above, iGA revealed that there was a high overlap between genes differentially expressed in the *hol* mutant and genes up/down-regulated by various stress and light treatments (Suppl. Tables 3.1 and 3.2). Interestingly, genes that are down-regulated by specific light treatments (red, far red, white, blue or UV light) were generally up-regulated in the *hol* mutant and vice versa. No such clear correlation was found with regards to abiotic/biotic stress treatments, but the genes that showed differential expression in the *hol* mutant (both up and down-regulated genes) were generally down-regulated by stress.

Overall, the results obtained from microarray analysis indicate that *HOL* could regulate responses to various stresses and light/auxin in *A. thaliana*.

#### **3.2.4 Identification of potential functions of *HOL* from public microarray data**

Publicly available microarray data sets from the Genevestigator database (Hruz *et al.*, 2008) were also analysed to shed light on potential functions of *HOL* in *A. thaliana*. Firstly, co-expression analysis was conducted to identify genes whose expression patterns positively or negatively correlate with *HOL* expression. In accordance with the results from the microarray analysis of the *hol* mutant, several genes responsive to various stresses or light/auxin were found to be co-expressed with *HOL* (Suppl. Tables 3.3 and 3.4). With respect to genes of sulphur metabolism and GL synthesis only one gene, *UGT74C1*, which is involved in GL synthesis (Gachon *et al.*, 2005) was identified (Suppl. Table 3.3). The expression of this gene positively correlated with *HOL* expression. Interestingly, two genes, *TCPI4* and *EMB 1273*, which regulate embryo development (Tzafrir *et al.*, 2004; Tatematsu *et al.*, 2008) were also co-expressed with *HOL* (Suppl. Table 3.3).

The Genevestigator database was also used to identify treatments (e.g. stress, hormones) or genotypes (e.g. mutants) which alter *HOL* expression patterns in *A. thaliana*. Again, in accordance to the results from the iGA analysis, *HOL* expression was regulated by abiotic/biotic stress treatments and specific light treatments (Suppl. Tables 3.5 and 3.6). Moreover, *HOL* was strongly down-regulated by the application of the plant hormones abscisic acid (ABA) or brassinolide (BL) (Suppl. Table 3.5), and the GA-synthesis-inhibitor paclobutrazole. *HOL* was up-regulated in the auxin-resistant mutant *axr1-12* and in the *max4* mutant, which exhibits increased and auxin-resistant bud growth (Sorefan *et al.*, 2003). Heat treatment also up-regulated *HOL* expression (Suppl. Table 3.6). Interestingly, *HOL* expression was down-regulated in leaf samples inoculated with the pathogen *Pseudomonas syringae* pv. *tomato* compared to mock-treated leaf samples (Suppl. Table 3.5), whereas *HOL* expression was up-regulated in leaf samples inoculated with *P. syringae* pv. *tomato* mutant strains that have reduced virulence (due to mutations in the type III secretion system) compared to samples inoculated with WT strains of this pathogen (Suppl. Table 3.6). This suggests that the down-regulation of *HOL* is dependent on the presence of a functional type III secretion system in *P. syringae* pv. *tomato*.

Overall, these results support the data obtained from the transcriptome analysis of the *hol* mutant and indicate that *HOL* regulates responses to various stresses and light/auxin in *A. thaliana*.

### 3.3 Discussion

The first objective of this chapter was to thoroughly characterise the tissue-specific expression patterns of the *A. thaliana* *HOL* gene, both on the transcript and the protein level. Using *HOL::GUS* reporter lines, it was shown that *HOL* is mainly expressed in roots and in young leaves. Within the roots, expression is restricted to the vascular tissue. This observation was also confirmed on the protein level since GFP-tagged *HOL* was mainly found in the vasculature of roots. These results are in accordance with *A. thaliana* microarray data from the Genevestigator database (Hruz *et al.*, 2008) which show highest *HOL* expression levels in seedlings, roots and leaf primordia.

Some discrepancies were observed between GFP expression in roots of *HOL::HOL:GFP* lines and GUS expression in roots of *HOL::GUS* lines. In contrast to

GUS accumulation, GFP was not detected in the vasculature near the root tip and no GFP was found in very young seedlings. This could be caused by the higher stability of GUS compared to GFP (Jefferson *et al.*, 1987; Verkhusha *et al.*, 2003) or by the regulation of *HOL* gene expression on the translational level.

Little is known about the tissue-specific activity or expression of HTMTs in other plants. The *HOL*-homologous gene *TMT1* of *Brassica oleracea* showed gene expression and enzyme activity in various tissues including roots, stems and leaves. *TMT1* expression and enzyme activity were stronger in seedlings than in mature plants (Attieh *et al.*, 2002) which is similar to the expression patterns observed in *A. thaliana* in this study. Contrarily, in *Raphanus sativus*, HTMT activity was high in leaves, but could not be detected in roots (Itoh *et al.*, 2009).

Imaging of GFP-tagged *HOL* protein in *HOL::HOL:GFP* lines showed that the protein is located in the cytosol. This is in accordance with the *HOL* localisation predicted by the TargetP server (Emanuelsson *et al.*, 2007) which did not identify any obvious trafficking signal motifs in the amino acid sequence of *HOL*. Since *HOL* and some HTMTs from other plants can methylate both halide ions and HS<sup>-</sup> ions (Table 1.2), it was originally postulated that they may play a role in the detoxification of excess HS<sup>-</sup> produced upon sulphate reduction in chloroplasts (Attieh *et al.*, 2000a). However, the latter study showed that in *B. oleracea*, HTMT activity was only detected in the cytosol and not in purified chloroplast. Accordingly, our data show that *A. thaliana* *HOL* is not targeted to plastids.

Overall, the observation that *HOL* is mainly expressed in roots suggests that *HOL* functions in this organ, and that the majority of methyl halides are produced by the root in *A. thaliana*. However, further experiments are needed to verify this. Interestingly, in *Brassica* crops, CH<sub>3</sub>Br emissions were not detected from roots when the shoot was cut off, indicating that in these plants, CH<sub>3</sub>Br is released from the aboveground part of the plant (Gan *et al.*, 1998).

The second objective of this chapter was to generate and characterise transgenic lines overexpressing the *HOL* gene (*35S::HOL* lines). These lines were generated to test if we could corroborate the relationship between *HOL* activity and methyl halide production in *A. thaliana* and to provide, together with the *hol* mutant, a useful tool to identify potential functions of *HOL* and methyl halide production in this plant.

Initially, a reliable sampling method for methyl halide measurements from living plants had to be established. Enclosing agar plates with *A. thaliana* seedlings in Teflon bags for several hours turned out to be suitable to get sufficient, measurable quantities of CH<sub>3</sub>Cl, CH<sub>3</sub>Br and CH<sub>3</sub>I in the air samples extracted from the plant's headspace. Moreover, the quantities measured in WT and *hol* seedlings were comparable to the absolute quantities previously reported in *A. thaliana* and are also in accordance with relative emissions of CH<sub>3</sub>I > CH<sub>3</sub>Cl > CH<sub>3</sub>Br (Fig. 1.7) (Rhew *et al.*, 2003).

The same experimental set-up was used to measure methyl halide emissions from two independent *35S::HOL* lines (196-9, 196-11) generated in this study. Both lines showed strongly increased emissions for all methyl halides in comparison to WT. Line 196-11 was the strongest emitter of both lines, and it also had the highest *HOL* transcript levels. These data confirm the positive correlation between *HOL* gene expression levels and methyl halide production in *A. thaliana*. Interestingly, CH<sub>3</sub>I emissions from *35S::HOL* lines were lower than CH<sub>3</sub>Cl emissions in this particular experiment. It is possible that the initial iodide content of the MS agar (~100 nmol) was already depleted at the time of air sample collection due to the high methyltransferase activity in the overexpressor lines and therefore reducing the amount of CH<sub>3</sub>I produced in these plants.

The susceptibility of *35S::HOL* lines to SCN<sup>-</sup> was also tested since it was shown that overexpression of *HOL* leads to an increased tolerance towards SCN<sup>-</sup> (Nagatoshi and Nakamura, 2009). As expected, both lines, 196-9 and 196-11, showed a higher tolerance to KSCN than WT seedlings confirming that the *35S::HOL* lines generated in this study are fully functional and show the expected phenotype associated with increased *HOL* activity.

The final objective of this chapter was to conduct microarray analysis on WT and *hol* mutant plants in order to gain more insight into the global effects of *HOL* activity and/or methyl halide production on the transcriptome of *A. thaliana* and therefore helping us to identify potential functions of *HOL* in this plant. Moreover, publicly available microarray data sets were analysed to identify treatments (e.g. stress, hormones) which affect *HOL* gene expression, and to identify genes which are co-expressed with *HOL*.

Two different approaches for the computational analysis of the microarray data from the *hol* mutant were used. Firstly, the conventional approach of finding individual

genes significantly up or down-regulated in the *hol* mutant was applied and these genes were then divided into functional classes. A total of 81 genes were up or down-regulated in the *hol* mutant compared to WT. Apart from *HOL*, the gene whose expression was primarily affected in the *hol* mutant was the *QQS* gene. The precise function of this gene is not known, but it is believed to regulate starch metabolism in response to cold in *A. thaliana* (Li *et al.*, 2009; Seo *et al.*, 2011). A possible link between starch metabolism and *HOL* was further investigated and discussed in Chapter 4.

Seven genes (e.g. *UGT79B1*) involved in anthocyanin biosynthesis and known to be co-expressed in *A. thaliana* (Yonekura-Sakakibara *et al.*, 2012) were down-regulated in the *hol* mutant. Generally, the accumulation of anthocyanins (purple coloration) can be seen in hypocotyls and cotyledons of WT seedlings when they are grown on high sucrose media (Solfanelli *et al.*, 2006), and this phenotype is absent in *ugt79b1* mutants (Yonekura-Sakakibara *et al.*, 2012). However, despite the fact that several anthocyanin biosynthesis genes were down-regulated in *hol*, no differences in the purple-coloration phenotype were seen between WT and the *hol* mutant when seedlings were grown on high sucrose concentrations (data not shown) suggesting that the down-regulation does not impair anthocyanin synthesis in the *hol* mutant.

By far the largest number of genes differentially regulated in the *hol* mutant was classified as being responsive to various abiotic and biotic stresses. This trend was also confirmed by Iterative Group Analysis (iGA), the second approach used in this study to analyse the microarray dataset from the *hol* mutant. Moreover, analysis of public microarray data showed that various stress treatments and the application of hormones involved in stress-signaling such as ABA regulate *HOL* expression, and that several stress-responsive genes were co-expressed with *HOL*. Interestingly, among the stress-responsive genes that were differentially regulated in the *hol* mutant were several genes associated with sulphur deficiency and GL metabolism. Moreover, one gene, encoding a UDP-Glucosyltransferase involved in GL biosynthesis, was co-expressed with *HOL*.

Several hypotheses have been proposed about the function of *HOL* with regard to abiotic and biotic stress: Firstly, it has been proposed that methyl halide production could be involved in salt stress tolerance as halide ions such as chloride are consumed and released into the air. Secondly, methyl halides or sulphur volatiles such as methyl thiocyanate (CH<sub>3</sub>SCN) and methanethiol (CH<sub>3</sub>SH), which are produced by *HOL*, could act as allelochemicals or airborne plant-insect signals and thus contribute to defence

against herbivores and pathogens. The observation that *HOL* is mainly expressed in roots suggests that *HOL* functions in this organ and supports these ideas as roots are directly exposed to both abiotic and biotic stresses, and to various pathogens and herbivores. Interestingly, the specific expression of *HOL* in the root vasculature is similar to the expression of adenosine-5'-phosphosulphate kinases (APK1, APK2 and APK3) which are also expressed in and around the vasculature in roots and play a major role in the synthesis of secondary sulphated metabolites such as GLs (Mugford *et al.*, 2009). The proposed role of *HOL* in salt stress tolerance and in plant defence, and other potential functions of *HOL* which are pointed out by the microarray dataset in this chapter are thoroughly tested and discussed in Chapter 4 and 5.

Overall, it remains to be investigated whether the observed differences in the transcriptome of the *hol* mutant are caused by the lack of *HOL* itself or by the lack of production of methyl halides. In the microarray experiment described here, WT and *hol* seedlings were grown in separate Petri dishes, thus ambient methyl halide concentrations were very low in the *hol* seedlings. To answer this question, it would be interesting to investigate the changes in the transcriptome of *hol* plants when they are grown together with WT plants and thus are exposed to methyl halides.

## **Chapter 4 – Exploring potential functions of HOL and methyl halide emissions in *Arabidopsis thaliana*: Part I**

### **4.1 Introduction**

Despite the high production rates of methyl halides from a variety of biological sources and the discovery of SAM-dependent halide/thiol methyltransferases in bacteria, fungi, algae and plants (see Chapter 1), the physiological and ecological roles of methyl halides remain largely unknown. So far, a distinct metabolic function for CH<sub>3</sub>Cl has only been found in wood-rotting fungi such as *Phellinus pomaceus*. There, methyl chloride can act as a methyl donor in the biosynthesis of methyl esters (Harper *et al.*, 1989) and veratryl alcohol, the latter known to be an important component of the lignin degradation pathway (Fig. 1.8) (Harper *et al.*, 1990).

In *A. thaliana*, HOL does not seem to play a major role in plant development under optimal growth conditions since *hol* mutant and *35S::HOL* plants did not show any obvious growth defects. However, several hypotheses have been proposed about the biological function of *HOL/HTMT* genes in plants with regard to stress conditions which are discussed below and in the next chapter (Chapter 5). This chapter focuses on investigating the effects of HOL activity/methyl halide production on salt stress tolerance and explores further potential functions of this gene in *A. thaliana* plant metabolism and development based on the alterations observed in the transcriptome of the *hol* mutant (see Chapter 3). In Chapter 5, the effects of HOL/methyl halides on plant-insect and plant-microbe interactions are described.

#### **4.1.1 Methyl halide production and salt stress**

Soil salinity is a major abiotic stress that negatively affects plant growth. It is caused by natural processes such as the accumulation of salts in arid regions, weathering of rocks or the deposition of oceanic salts carried by wind and rain, but it can be aggravated in agricultural soils by certain irrigation and fertilisation practices (Kafkafi *et al.*, 2001; Munns, 2002; Munns and Tester, 2008). Accumulation of high levels of salt (mainly in the form of NaCl) causes drought stress in plants by lowering the water potential of the soil and thus impairing water uptake. Moreover, the accumulation of ions such as Na<sup>+</sup>,

$Mg^{2+}$ ,  $K^+$ ,  $Ca^{2+}$ ,  $Cl^-$  and  $SO_4^{2-}$  in plant cells affects cell membrane properties and protein functions (Chinnusamy and Zhu, 2004).

Salt tolerant plants have developed various strategies to cope with salinity such as (1) controlling the uptake and transport of ions, (2) the production of organic solutes for osmotic adjustment and (3) the compartmentalisation of toxic ions, e.g. by the sequestration of  $Na^+$  into vacuoles (Flowers and Colmer, 2008; Munns and Tester, 2008). Unfortunately, most research on salt tolerance has focussed on  $Na^+$  rather than  $Cl^-$ . Thus, mechanisms of  $Cl^-$  tolerance in plants are still poorly understood (Teakle and Tyerman, 2010), and only recently new insights have been gained. For example, in *A. thaliana*, a cation-chloride cotransporter (CCC) and a chloride channel (CLCc) contribute to salt tolerance by regulating chloride homeostasis (Colmenero-Flores *et al.*, 2007; Jossier *et al.*, 2010).

Whereas chloride is an abundant nutrient in natural soils with an average concentration of ~100 mg/kg soil (Kafkafi *et al.*, 2001), average bromide and iodide concentrations are much lower with ~1 mg/kg and ~5 mg/kg soil, respectively (Whitehead, 1984; Flury and Papritz, 1993). Nevertheless, bromide concentrations may reach harmful concentrations in some agricultural soils due to excessive application of bromine-containing pesticides and fertilisers (Flury and Papritz, 1993). Unfortunately, only very little is known about the effects of  $I^-$  and  $Br^-$  on plant metabolism. The growth and metabolism of the salt-tolerant plant *Salicornia brachiata* was not negatively affected by the application of up to 600 mM NaBr (Reddy, 2009), but some glycophytes including vegetables such as bean, cabbage, potato and spinach have been shown to be sensitive towards  $Br^-$  in the soil and showed symptoms of toxicity similar to those of NaCl stress (Flury and Papritz, 1993). Studies about iodine fortification of crops by adding iodide to the soil showed that iodide tolerance varies strongly between plant species (Zhu *et al.*, 2003; Blasco *et al.*, 2008; Landini *et al.*, 2011; Landini *et al.*, 2012). Tomato was able to tolerate up to 20 mM KI in the growth medium without severe injuries (Landini *et al.*, 2011), whereas the biomass of lettuce was reduced when grown on 80  $\mu$ M KI (Blasco *et al.*, 2008). Thus, it is important to include the effects of bromide and iodide salts when studying salt stress responses and tolerance mechanisms in plants.

Since halide ions such as  $Cl^-$ ,  $Br^-$  and  $I^-$  are consumed and released into the air, it has been proposed that methyl halide production could be involved in salt stress tolerance in organisms producing those gases (Harper, 1985). This hypothesis was



supported by the cloning and characterisation of a methyl chloride transferase (MCT) in the halophytic plant *Batis maritima* (Ni and Hager, 1998, 1999), whose amino acid sequence is 69% identical to *A. thaliana* HOL. The BmMCT enzyme functioned well under high NaCl concentrations and kinetic analysis revealed that it could use chloride, bromide and iodide, but not sulfide as substrates (Table 1.2). Moreover, in several *Brassica* crops and in rice, it was shown that methyl halide emissions positively correlate with the concentration of halide ions in the growth medium or soil (Gan *et al.*, 1998; Redeker and Cicerone, 2004). Accordingly, in *A. thaliana*, the application of 50 mM NaBr caused a thousand-fold increase in CH<sub>3</sub>Br emissions (Rhew *et al.*, 2003). Similarly, the watering of *Brassica rapa* plants with different concentrations of NaCl caused a significant increase in CH<sub>3</sub>Cl emissions (Fig. 4.1) (Armeanu-D'Souza, 2009).

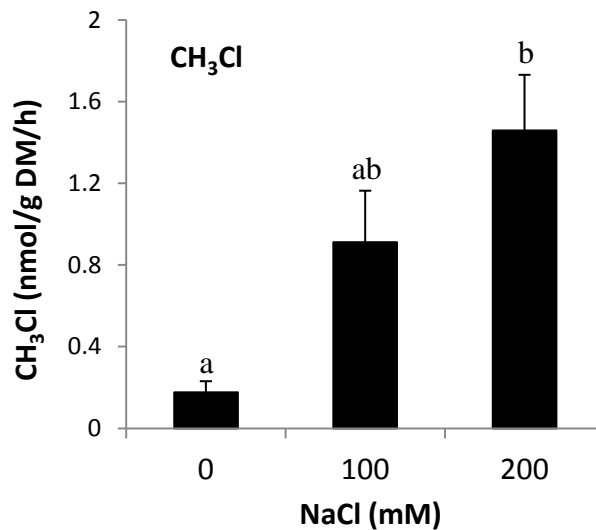


**Figure 4.1. CH<sub>3</sub>Cl emissions from *Brassica rapa* after salt treatment.** Three-week old plants were watered with solutions containing 0, 100 or 200 mM NaCl for 15 days. Air samples were taken 4 h after enclosure. Background methyl halide emissions were also determined from soil control and subtracted from the amounts detected from enclosed plants. Data points are the mean  $\pm$  s.e. of three biological replicates. Different letters indicate significant differences between treatments (ANOVA with Fisher's protected LSD post-hoc test,  $p < 0.05$ ). Data taken from Armeanu-D'Souza *et al.* (2009).

### 4.1.2 Objectives of this chapter

The main aim of this chapter was to thoroughly investigate the relationship between HOL and salt stress tolerance in *A. thaliana* by studying the response of WT, *hol* mutant and *35S::HOL* lines to various salt stresses. Moreover, two other potential functions of this gene in *A. thaliana* plant metabolism and development based on the alterations observed in the transcriptome of the *hol* mutant were studied: The link between (1) HOL and starch metabolism and (2) HOL and auxin responses.

## 4.2 Results

### 4.2.1 HOL and salt stress tolerance

#### 4.2.1.1 Effects of salt stress on the growth of *hol* mutant and *35S::HOL* plants

In order to test if methyl halide production and/or HOL activity contribute to salt tolerance, five-day-old WT, *hol* and *35S::HOL* seedlings were transferred to MS media containing various concentrations of NaCl. As expected, salt treatment caused a reduction in growth and severe chlorosis in the seedlings, but no differences were observed between the genotypes (Fig. 4.2).

Similarly, root growth of WT and *hol* seedlings was strongly reduced upon NaCl stress, however, *hol* roots did not show a stronger reduction in growth in comparison to WT (Suppl. Fig. 4.1). Long-term salt stress experiments were also conducted with WT, *hol* and *35S::HOL* plants grown in soil in the glasshouse. Two-week-old plants were watered with NaCl solutions ranging from 0-200 mM NaCl for 4 weeks. Again, no differences in susceptibility towards NaCl were observed between the genotypes within each treatment group (data not shown). These results suggest that HOL does not contribute to NaCl stress in *A. thaliana*, however, it could not be ruled out that the toxic effects of Na<sup>+</sup> could mask any beneficial effects of HOL activity on chloride homeostasis.

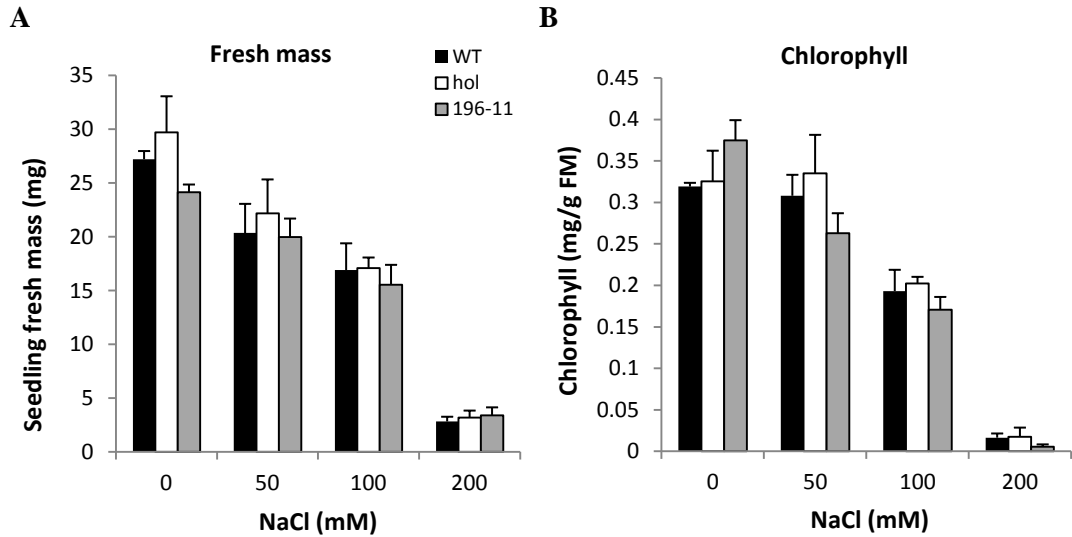


**Figure 4.2. Growth of WT, *hol* and 35S::HOL (196-11) seedlings on sodium chloride (NaCl).** Five-day-old seedlings were transferred to MS agar plates containing 0, 50, 100 or 200 mM NaCl and fresh mass (A) and chlorophyll content (B) determined after 7 days. Data points are the mean  $\pm$  s.e. of three independent experiments each evaluating 18 seedlings. No significant differences were observed between genotypes within a treatment group (ANOVA).

To address this problem, the effects of various chloride salts on the germination, growth and survival of WT, *hol* and 35S::HOL seedlings were tested. Moreover, mannitol and Na<sub>2</sub>SO<sub>4</sub> were used to account for the specific effects of osmotic stress and Na<sup>+</sup> stress. As expected, survival and growth of seedlings were reduced when seedlings were grown on MS media containing various salts or mannitol (Suppl. Fig. 4.2). Seed germination was also severely inhibited by the various salt treatments (Fig. 4.3). However, no significant differences between genotypes were observed in any of the treatments. Taken together, these results suggest that there is no significant contribution of HOL or methyl halide production in promoting tolerance towards chloride salts in *A. thaliana*.

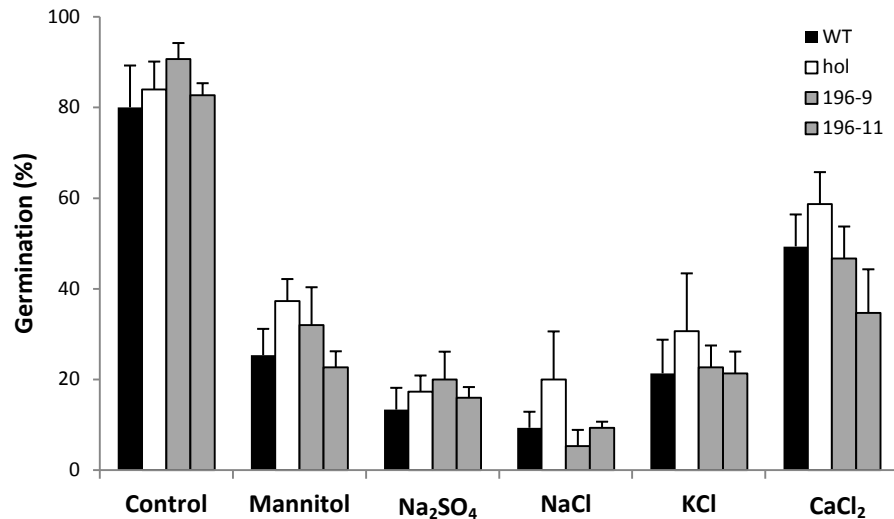


**Figure 4.3. Germination of WT, *hol* and *35S::HOL* lines (196-9, 196-11) on various salts.** Seeds were stratified for 3 days and then sown on MS agar plates containing no salt (control), 100 mM NaCl, 100 mM KCl, 50 mM CaCl<sub>2</sub>, 50 mM Na<sub>2</sub>SO<sub>4</sub> or 200 mM mannitol. Data points are the mean  $\pm$  s.e. of three plates each evaluating 25 seeds. No significant differences were observed between genotypes within each treatment group (ANOVA).

Given that the *A. thaliana* HOL enzyme is able to methylate not only chloride but also bromide (Br<sup>-</sup>) and iodide (I<sup>-</sup>) (Fig. 1.6 A) (Rhew *et al.*, 2003), the tolerance of WT, *hol* and *35S::HOL* seedlings towards these ions was tested. Both Br<sup>-</sup> and I<sup>-</sup> are readily taken up by plants, but only little is known about the concentration levels that cause toxicity and how high levels of these ions affect plant metabolism (Whitehead, 1984; Flury and Papritz, 1993). To test the tolerance of WT, *hol* and *35S::HOL* lines towards I<sup>-</sup>, seedlings were transferred to plates containing various concentrations of potassium iodide (1, 5 or 10 mM KI). Generally, the application of 1 mM KI caused a reduction in growth and mild chlorosis in all genotypes (data not shown). Surprisingly, at higher concentrations ( $\geq$  5 mM KI), *35S::HOL* seedlings were more susceptible towards KI. They gained only about 50% of the fresh mass of WT seedlings and showed severe chlorosis (Fig. 4.4 A, B). Similarly, germination was also strongly reduced in *35S::HOL* seeds compared to WT seeds when sown on agar containing 5 mM or 10 mM KI (Fig. 4.4 C). No differences in germination rates and growth were detected between WT and *hol* seedlings when subjected to KI stress. To confirm that the observed phenotype in *35S::HOL* lines upon KI stress is linked to the toxicity of I<sup>-</sup> rather than K<sup>+</sup>, the growth of *35S::HOL* seedlings on media containing 10 mM sodium iodide (NaI) was observed. As expected, *35S::HOL* seedlings showed stronger chlorosis than WT seedlings (Suppl. Fig. 4.3).

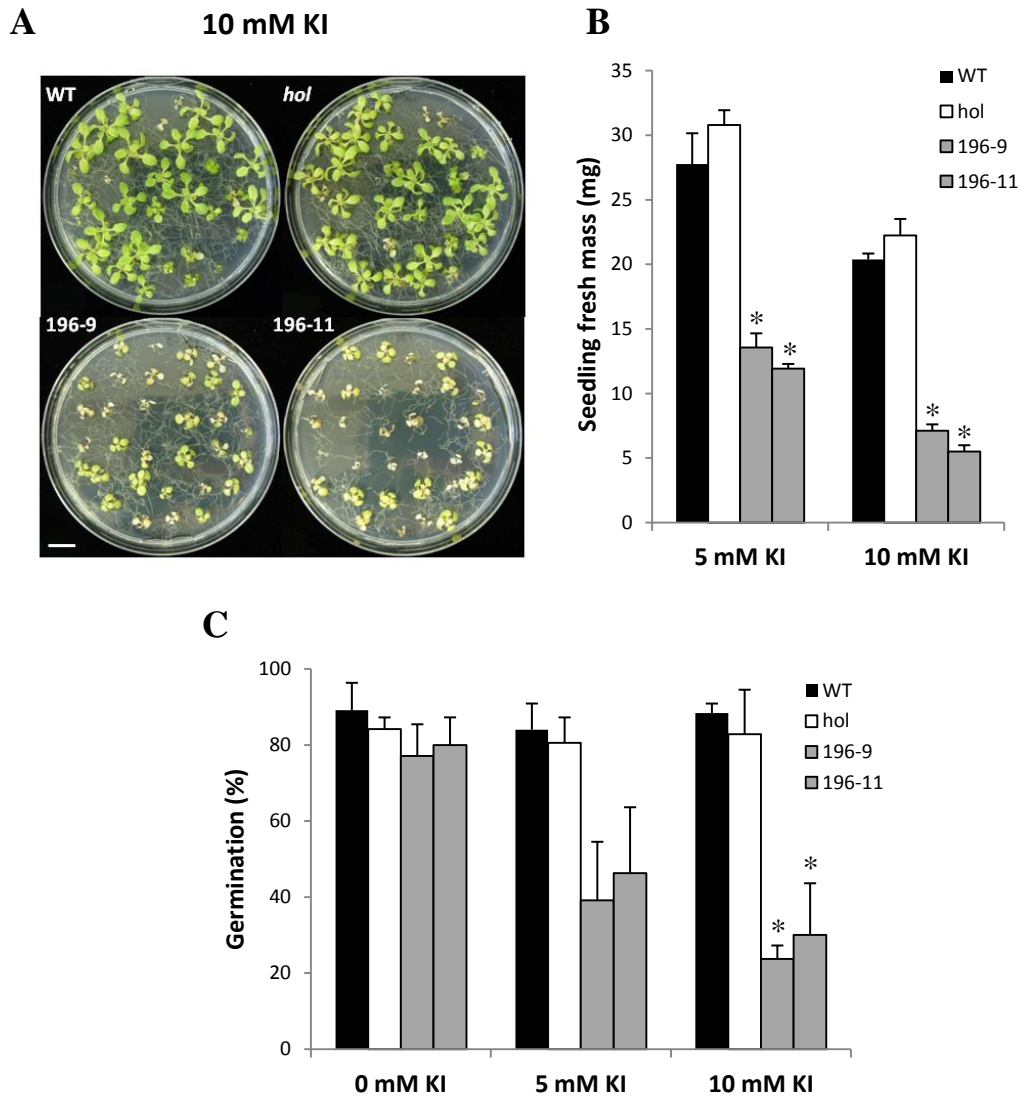


**Figure 4.4. Growth and germination of WT, *hol* and *35S::HOL* lines (196-9, 196-11) on potassium iodide (KI).** Four-day-old seedlings were transferred to MS agar plates containing 5 or 10 mM KI. Pictures (**A**) were taken and seedling weight (**B**) determined after 13 days of treatment. Scale bar = 1 cm. Data points are the mean  $\pm$  s.e. of two independent experiments. (**C**) Germination rate was recorded 2 days after the sowing on MS agar plates containing 0, 5 or 10 mM KI. Data points are the mean  $\pm$  s.e. of two independent experiments evaluating 55 and 100 seeds, respectively. Asterisks represent significant differences from WT within a treatment group (ANOVA with Fisher's protected LSD post-hoc test,  $p < 0.05$ ).

Finally, the susceptibility of WT, *hol* and *35S::HOL* lines towards  $\text{Br}^-$  was tested by subjecting the seedlings to NaBr stress. No differences in the growth and survival between WT and *hol* were observed, but *35S::HOL* seedlings showed slightly reduced growth and stronger chlorosis compared to WT (Fig. 4.5), although the symptoms caused by  $\text{Br}^-$  were less pronounced than the symptoms observed upon iodide stress in *35S::HOL* seedlings. Once more, KBr treatment had a similar effect on *35S::HOL* plants as NaBr confirming that the phenotype is linked with  $\text{Br}^-$  stress (data not shown).

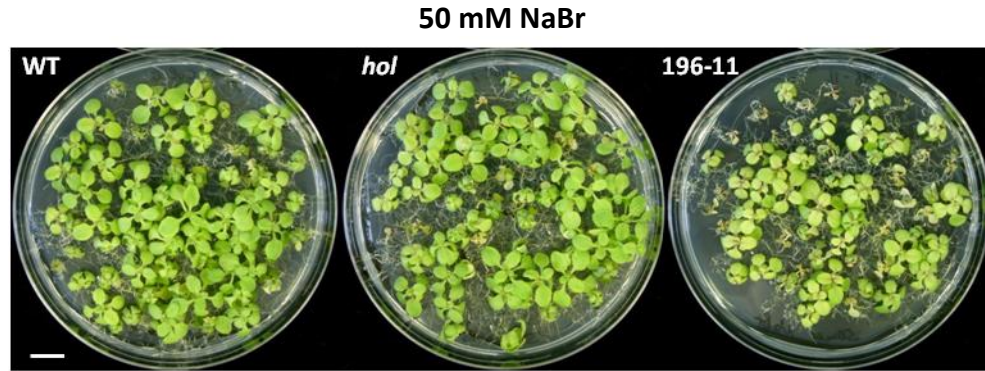


**Figure 4.5. Growth of WT, *hol* and 35S::*HOL* (196-11) seedlings on sodium bromide (NaBr).** Four-day-old seedlings were transferred to MS agar plates containing 50 mM NaBr. Pictures were taken after 13 days of treatment. Scale bar = 1 cm.

All in all, these data do not support the hypothesis that *HOL* or methyl halide emissions contribute to salt tolerance in *A. thaliana*, because *hol* mutants were not more sensitive to salt stress than the WT. Moreover, the overexpression of *HOL*, which causes increased methyl halide emissions in 35S::*HOL* plants, did not make these plants more salt tolerant, on the contrary, it made them more susceptible towards bromide and iodide salts.

#### 4.2.1.2 Effects of salt stress on *HOL* expression

To further elucidate the involvement of *HOL* in salt stress responses, expression patterns of the gene were investigated by measuring GUS activity in *HOL*::GUS reporter plants and by qPCR analysis of WT seedlings after salt treatment. Firstly, *HOL*::GUS seedlings grown on media containing various concentration of NaCl (0-200 mM) were stained for GUS expression. Interestingly, GUS activity was reduced in the leaves and partially in roots upon NaCl stress. This effect was particularly apparent in seedlings treated with 100 mM NaCl (Fig. 4.6 A). Quantitative measurements using MUG assays showed that GUS activity was reduced by 50 % in seedlings treated with 100 mM NaCl (Fig. 4.6 B). Similar effects were also seen in plants grown in soil in the glasshouse. GUS staining was reduced in the roots of 5-week-old *HOL*::GUS plants after 12 days of 100 and 200 mM NaCl treatment (data not shown).

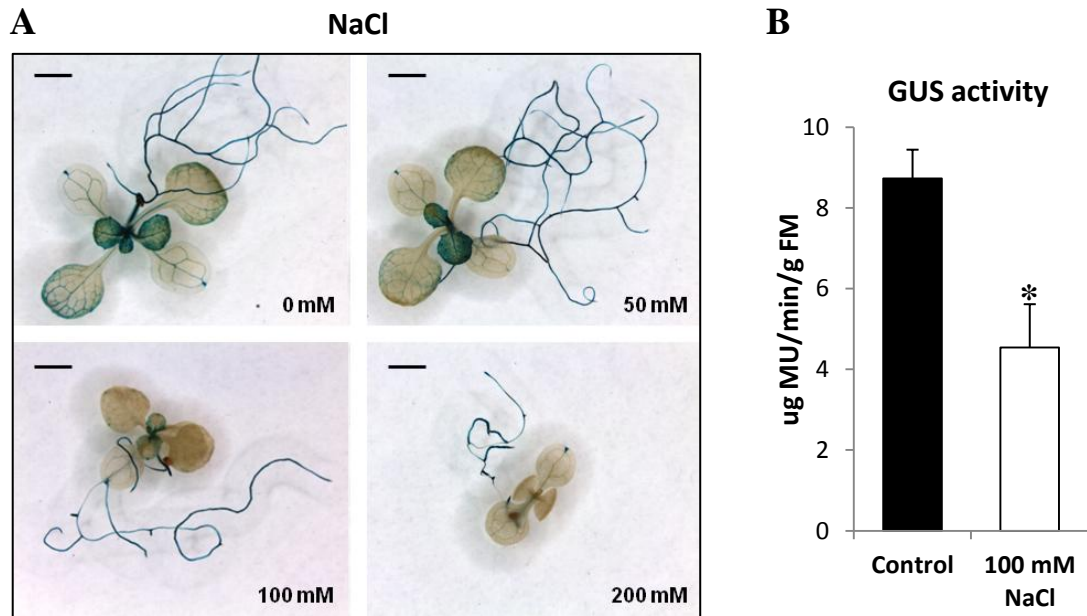


**Figure 4.6. Expression patterns of *HOL* in a *HOL::GUS* reporter line under NaCl stress.** Four-day-old seedlings were transferred to MS agar plates containing 0, 50, 100 or 200 mM NaCl. After 5 days seedlings were either stained (A) or GUS activity determined quantitatively using a MUG assay (B). Data points are the mean  $\pm$  s.e. of three biological replicates. Asterisks represent significant differences from control (t-test,  $p < 0.05$ ). Scale bars = 1.5 mm.

Secondly, to test whether the suppression of *HOL* is caused by  $\text{Cl}^-$  stress rather than  $\text{Na}^+$  or osmotic stress, *HOL::GUS* seedlings were exposed to various chloride salts,  $\text{Na}_2\text{SO}_4$  or mannitol, and GUS expression determined by staining. Interestingly, GUS expression was only reduced in the leaves of seedlings which were treated with chloride salts, whereas mannitol or  $\text{Na}_2\text{SO}_4$  treatment did not cause a reduction in GUS expression (Fig. 4.7 A). Similar effects were seen when *HOL* transcript levels were quantified in WT seedlings by qPCR upon salt treatment. Generally, all stress treatments caused a significant reduction in *HOL* expression compared to untreated seedlings (control). But NaCl, KCl and  $\text{CaCl}_2$ -treated seedlings had significantly lower *HOL* transcript levels than  $\text{Na}_2\text{SO}_4$  or mannitol-treated seedlings (Fig. 4.7 B).

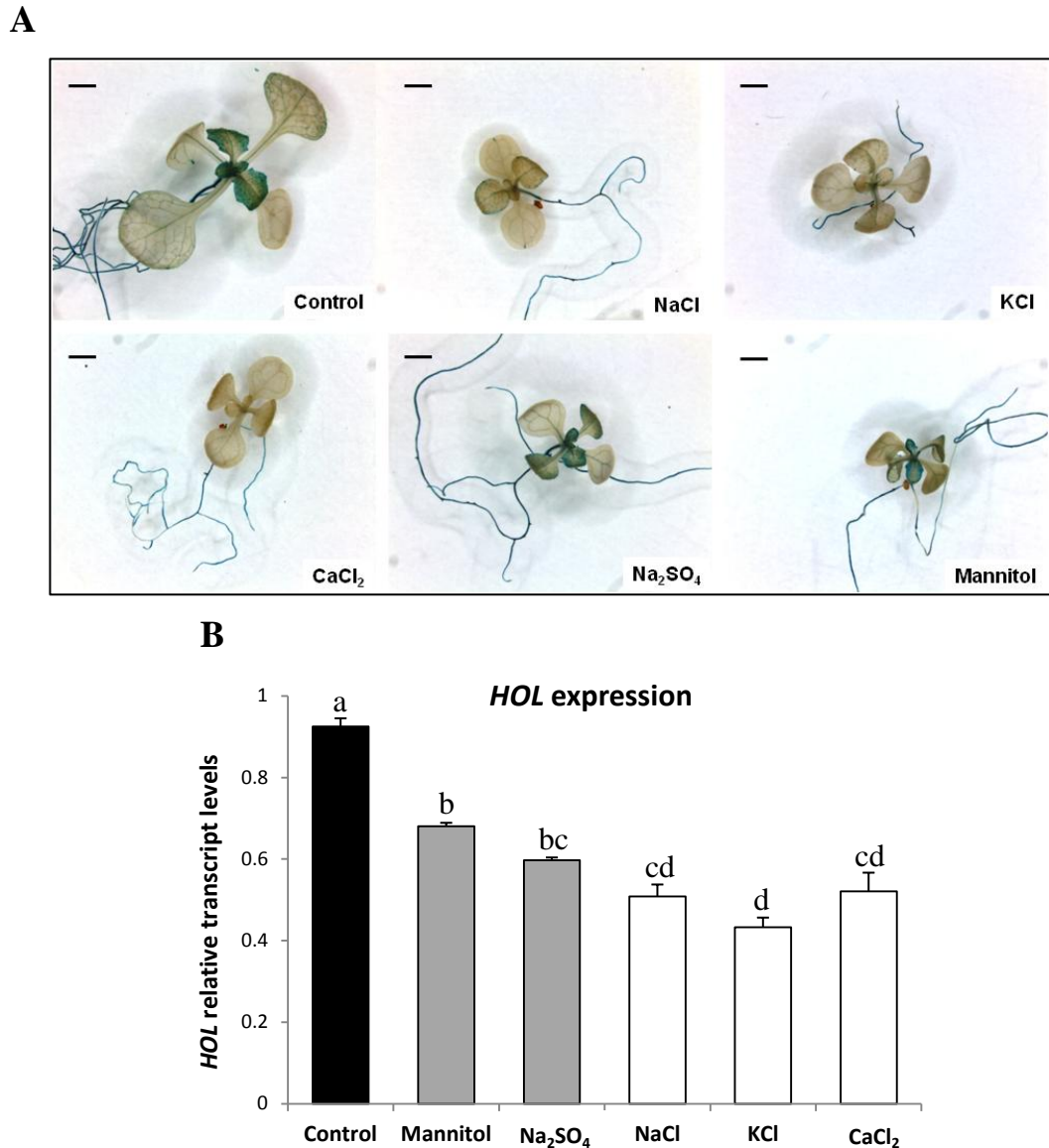


**Figure 4.7. Expression of *HOL* after treatment with various salts.** Four-day-old seedlings were transferred to MS agar plates containing no salt (control), 100 mM NaCl, 100 mM KCl, 50 mM CaCl<sub>2</sub>, 50 mM Na<sub>2</sub>SO<sub>4</sub> or 200 mM mannitol. **(A)** *HOL::GUS* reporter seedlings were stained for GUS activity after 5 days of treatment. Scale bars = 1 mm. **(B)** Transcript levels were determined in WT seedling (without roots) after 5 days of treatment by qPCR. *HOL* expression was normalised to the geometric mean of *EF1α* and *UBQ10* expression. Data points are the mean ± s.e. of three biological replicates. Different letters indicate significant differences between treatments (ANOVA with Bonferroni-corrected post-hoc test,  $p < 0.05$ )

Finally, the effects of Br<sup>-</sup> and I<sup>-</sup> on *HOL* expression were investigated. NaBr treatment also caused a reduction of GUS activity in *HOL::GUS* seedlings compared to untreated seedlings (Suppl. Fig. 4.4). Surprisingly, KI treatment did not significantly alter *HOL* expression, neither in *HOL::GUS* reporter lines nor in WT seedlings (Fig. 4.8).



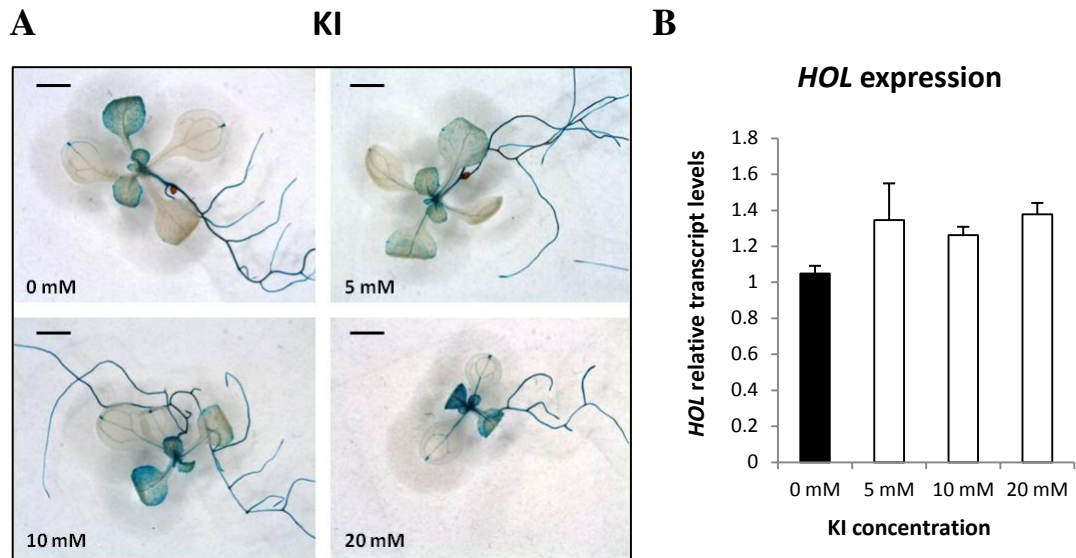


**Figure 4.8. Expression of *HOL* after treatment with potassium iodide (KI).** Four-day-old seedlings were transferred to MS agar plates containing 0, 5, 10 or 20 mM KI. (A) *HOL::GUS* reporter seedlings were stained for GUS activity after 5 days of treatment. Scale bars = 1 mm. (B) Transcript levels were determined in WT seedling after 5 days of treatment by qPCR. *HOL* expression was normalised to the expression of *EF1 $\alpha$* . Data points are the mean  $\pm$  s.e. of three biological replicates. No significant differences were observed between treatments (ANOVA).

All in all, these data suggest that salt treatment suppresses *HOL* expression in most cases and that the suppression is linked to the specific effects of halide ions such as  $\text{Cl}^-$  or  $\text{Br}^-$ , and not to the effects of osmotic stress or cations such as  $\text{Na}^+$ . Surprisingly, but in accordance with the observed effects of halide ions on the growth and survival of *35S::HOL* lines, it can be proposed that methyl halide emissions need to be lowered in *A. thaliana* when plants are exposed to salt stress.

#### 4.2.1.3 Why are *35S::HOL* lines more susceptible to salt stress?

The higher susceptibility of *35S::HOL* lines towards bromide and iodide was an unexpected observation. Nevertheless, this phenotype was investigated further to understand how increased *HOL* activity affects plant metabolism. Two reasons could account for the negative impacts on plant growth and germination in *35S::HOL* lines when subjected to salts stress.

Firstly, excessive amounts of methyl halides, which are produced upon salt stress in plants (Fig. 4.1) (Rhew *et al.*, 2003), could accumulate to toxic levels in the plant tissue. Methyl halides are known to be toxic to a wide range of organisms, and

methyl bromide and methyl iodide have been used as pesticides and for weed control for many decades (Ristaino and Thomas, 1997; Zhang *et al.*, 1997). In *A. thaliana*, it has been shown that the application of NaSCN inhibits the production of methyl halides (Rhew *et al.*, 2003) due to the higher affinity of HOL towards  $\text{SCN}^-$  than to halide ions (Table 1.2). To test if the application of  $\text{SCN}^-$  could improve the survival of *35S::HOL* lines subjected to KI stress, seedlings were transferred to media containing 10 mM KI or 10 mM KI + 1 mM KSCN and fresh mass recorded after 13 days. No differences in the fresh mass of *35S::HOL* seedlings were observed between treatments indicating that the reduction in growth is probably not linked to the accumulation of methyl iodide (Fig. 4.9 A). However, methyl iodide emissions before and after the application of KSCN need to be determined to support this hypothesis.

Secondly, it is possible that *35S::HOL* lines suffer from SAM depletion due to the high activity of HOL (Fig. 1.6 A). In addition to providing a methyl group for the production of methyl halides, SAM is also an essential substrate in numerous metabolic pathways including the biosynthesis of polyamines (Roje, 2006). Polyamines have been shown to have regulatory functions in abiotic stress tolerance (Alcazar *et al.*, 2010). Therefore, the metabolism of *35S::HOL* lines could be severely affected by the lack of SAM and it was tested if *35S::HOL* seedlings can be rescued by applying methionine, a precursor in SAM synthesis. Seedlings were transferred to media containing 10 mM KI or 10 mM KI + 0.5 mM methionine and seedling weight determined after 10 days. No differences in seedling weight of *35S::HOL* lines were observed between the two treatments (Fig. 4.9 B). Similarly, the exogenous application of polyamines (spermine or spermidine) did not rescue *35S::HOL* lines from KI-hypersensitivity (Fig. 4.9 C). Taken together these results suggest that *35S::HOL* lines are not affected by SAM depletion.

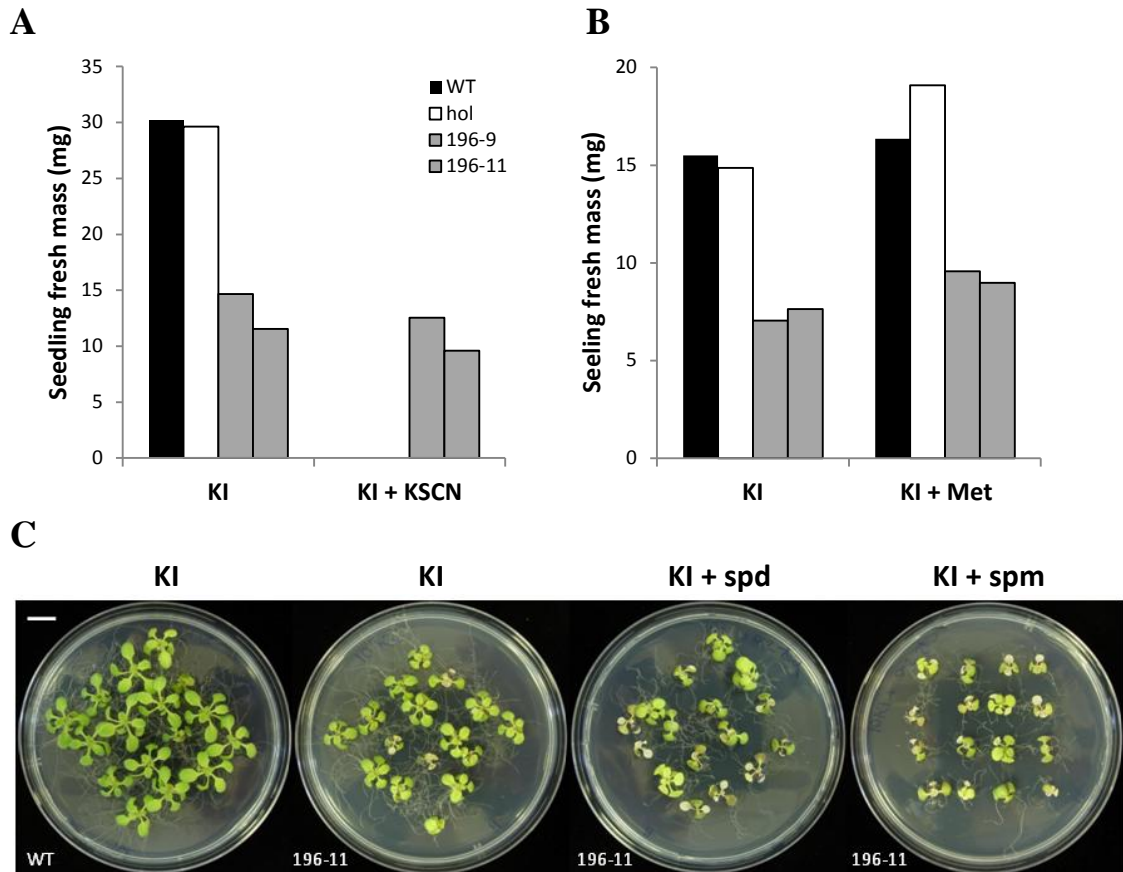


**Figure 4.9. Effects of KSCN, methionine and polyamines (spermine or spermidine) on KI-mediated growth inhibition in 35S::HOL lines.** (A) Four-day-old seedlings of Col-0, *hol* and 35S::HOL lines (196-9, 196-11) were transferred to MS agar plates containing 5 mM KI or 5 mM KI + 1 mM KSCN and seedling weight determined after 13 days. No data are shown for WT and *hol* when grown on KI + KSCN due to the inhibition of growth by KSCN in these lines. (B) Four-day-old seedlings were transferred to MS agar plates containing 10 mM KI or 10 mM KI + 0.5 mM methionine (Met) and seedling weight determined after 10 days. Average seedling weight was calculated by dividing the total fresh mass of pooled seedlings by the number of seedlings. (C) Six-day-old seedlings of Col-0, *hol* and 35S::HOL line (196-11) were transferred to MS agar plates containing 10 mM KI, 10 mM KI + 0.5 mM spermidine (spd) or 10 mM KI + 0.5 mM spermine (spm) and pictures taken after 10 days.

Finally, we wanted to test if the low germination rate of 35S::HOL lines could be rescued by the application of gibberellic acid (GA). In *A. thaliana* seeds, GA promotes embryo growth and the breakage of the seed coat during germination (Sun, 2008). Recently, it has also been shown that GA treatment can counteract the inhibitory effects of abiotic stress treatments such as NaCl on seed germination (Alonso-Ramirez *et al.*, 2009). However, in our experiment GA application did not rescue the low germination rate observed in 35S::HOL seeds subjected to KI stress (Fig. 4.10) indicating that the reduction of germination rates in 35S::HOL seeds is probably not linked to a reduction of GA levels.

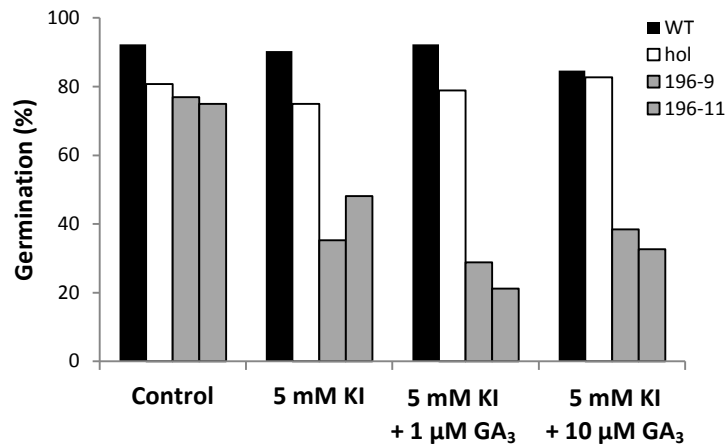


**Figure 4.10. Effect of gibberellic acid (GA<sub>3</sub>) on the germination of WT, *hol* and 35S::*HOL* lines (196-9, 196-11) under KI stress.** Seeds were stratified for 3 days and then sown on MS agar plates containing 0 (Control), 5 mM KI, 5 mM KI + 1 μM GA<sub>3</sub> or 5 mM KI + 10 μM GA<sub>3</sub>. Germination rate was recorded 2 days after sowing. 52 seeds were scored.

#### 4.2.2 HOL and starch metabolism

Microarray analysis revealed that the expression of the *QUA-QUINE STARCH (QQS)* gene was strongly reduced in the *hol* mutant (Chapter 3). The precise function of this gene is still not known, but it has been suggested that this gene is involved in the regulation of starch synthesis in *A. thaliana* since *qqs* mutants accumulated higher levels of starch at the end of the day compared to WT (Li *et al.*, 2009). To verify the data from the microarray experiment, qPCR analysis was used to accurately measure expression levels of *QQS* in WT and the *hol* mutant. Indeed, in the *hol* mutant, *QQS* transcript levels were strongly reduced to less than 1% of WT transcript levels (Fig. 4.11 B). Moreover, it was tested if the *hol* mutant accumulated higher levels of starch at the end of the day, similar to *qqs* mutants. However, iodine staining of WT and *hol* plants did not show any strong differences between the genotypes (Fig. 4.11 A).

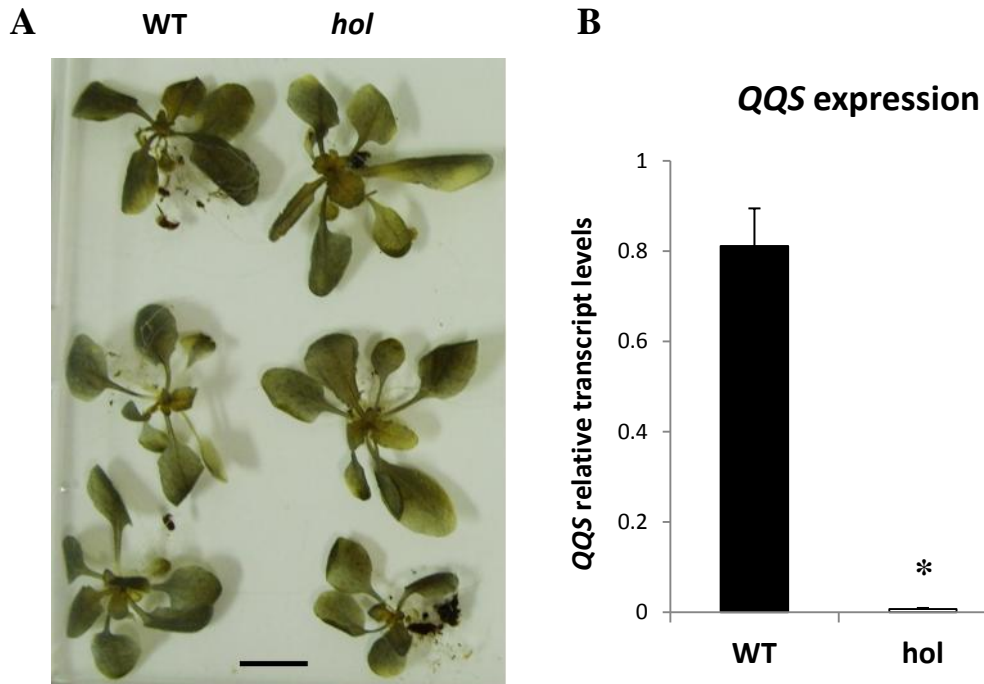


**Figure 4.11. *QQS* expression and starch accumulation in WT and *hol* plants.** (A) Iodine staining of leaf starch of 3-week-old plants grown at a 16 h light - 8h dark regime. Plants were harvested at the end of the light period. Scale bar = 1 cm. (B) Transcript levels were determined in 7-day-old seedlings grown on MS media by qPCR. *QQS* expression was normalised to the expression of *EF1α*. Data points are the mean  $\pm$  s.e. of four biological replicates. Asterisks represent significant differences from WT (t-test,  $p < 0.001$ ).

Microarray analysis also showed that the gene *EXORDIUM-LIKE 1 (EXL1)* is differentially regulated in the *hol* mutant. Expression analysis using qPCR confirmed that *EXL1* transcript levels are 3-fold higher than WT *EXL1* levels (Fig. 4.12 B). *EXL1* is believed to suppress the expression of *QQS* (Schröder *et al.*, 2011). Thus, our data are in accordance with this observation since *QQS* levels are strongly reduced in the *hol* mutant. *EXL1* promotes growth during low carbon availability in *A. thaliana*, we therefore wanted to test the response of *hol* seedlings to low sucrose levels similar to the experiments conducted by Schröder *et al.* (2011). To do so, WT and *hol* seedlings were grown on MS media supplemented with 0.2%, 0.5% or 1% sucrose. However, no differences in growth were observed between the genotypes (Fig. 4.12 A).

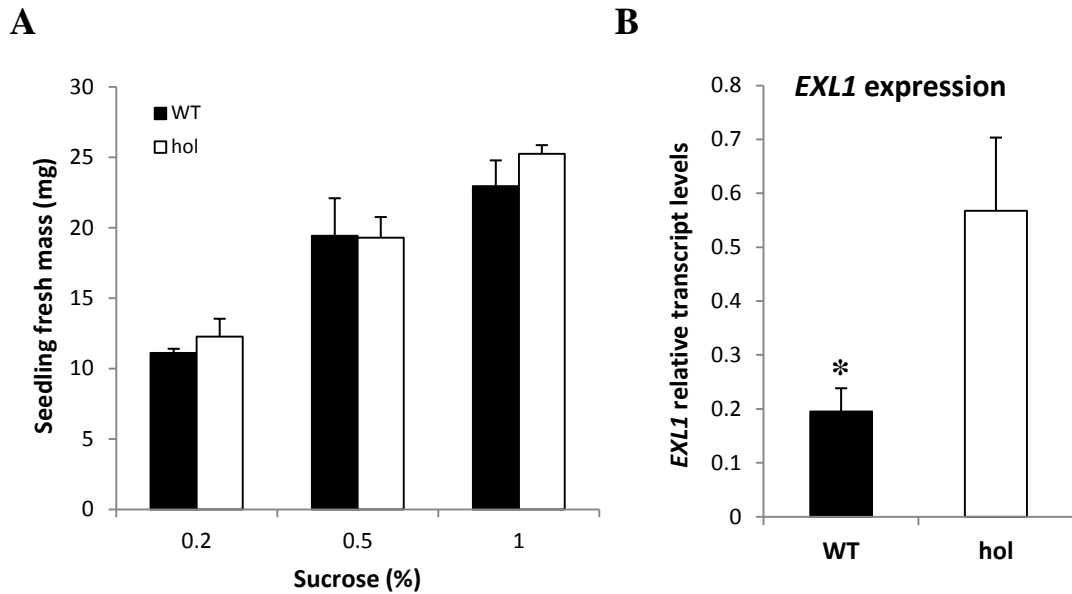


**Figure 4.12. *EXL1* expression in WT and *hol* plants and their response to sucrose. (A)** Seedlings were grown on half-strength MS medium supplemented with 0.2% , 0.5% or 1% sucrose for 14 days. Data points are the mean  $\pm$  s.e. of three plates containing 14-16 plants each. No significant differences were observed between treatments (t-test). **(B)** Transcript levels were determined in 7-day-old seedlings grown on MS media by qPCR. *EXL1* expression was normalised to the expression of *EF1a*. Data points are the mean  $\pm$  s.e. of four biological replicates. Asterisks represent significant differences from WT (t-test,  $p < 0.05$ ).

Taken together, these results show that *EXL1* and *QOS* expression levels are strongly altered in the *hol* mutant compared to WT. A first look at the phenotypic features linked to these genes in the *hol* mutant did not reveal any significant differences compared to WT, however, both genes and their functions are not yet fully understood and further experiments are necessary to understand the involvement of HOL in regulating the expression or action of any of these genes.

#### 4.2.3 HOL and auxin

The plant hormone auxin regulates diverse developmental processes including flower and fruit development, root growth, hypocotyl elongation and phototropic and gravitropic responses (Jensen *et al.*, 1998; Muday, 2001; Tanimoto, 2005; Sorefan *et al.*, 2009; Ding *et al.*, 2011; Girin *et al.*, 2011). Microarray analysis showed that several genes differentially expressed in the *hol* mutant could be assigned to a class of auxin/light-responsive genes. It was therefore tested if WT, *hol* and *35S::HOL* seedlings

responded differently to the application of auxin. Firstly, root length was measured in seedlings grown on MS media containing various concentrations of indole-3-acetic acid (IAA). As expected, application of IAA caused a suppression of root growth in all genotypes (Fig. 4.13 A). However, root length of *hol* seedlings was increased by 35% compared to WT when 1  $\mu$ M IAA was applied suggesting that the *hol* mutant is less sensitive to the application of auxin. No differences were observed between WT and *35S::HOL* seedlings (Fig. 4.13 A). Secondly, hypocotyl elongation of seedlings grown in the dark in response to IAA was assessed. As expected, hypocotyl growth was inhibited by IAA, but again, the *hol* mutant showed slightly reduced sensitivity to the application of 5  $\mu$ M IAA (Fig. 4.13 B). The application of IAA did not cause any differences between WT and *35S::HOL* seedlings, but interestingly, line 196-11 showed stronger hypocotyl growth in the dark when no IAA was applied Fig. 4.13 B).

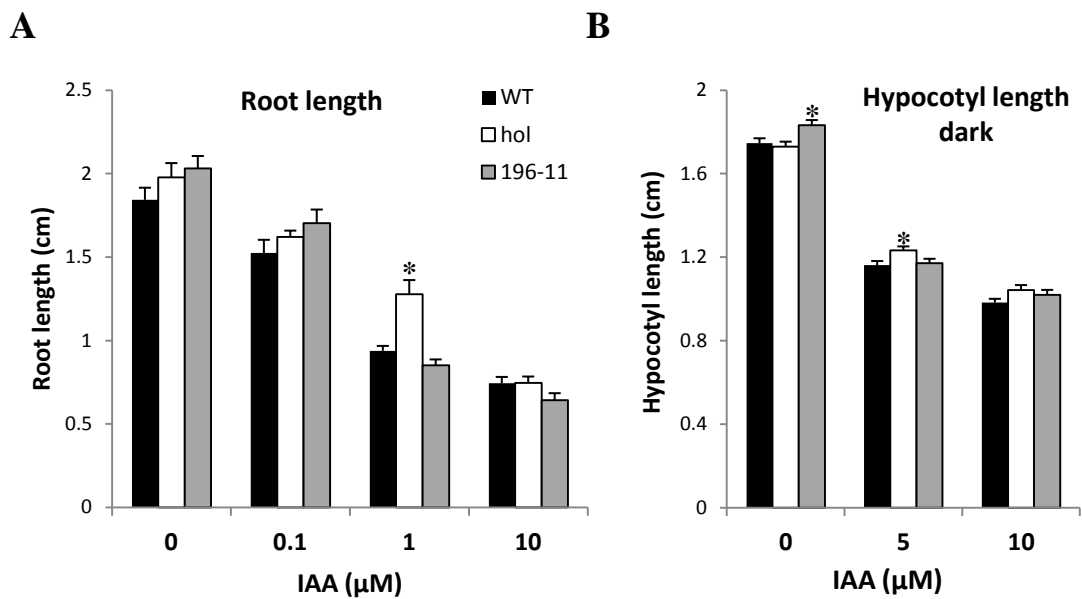


**Figure 4.13. Effect of auxin on root and hypocotyl growth of WT, *hol* and *35S::HOL* line (196-11).** (A) Seedlings were grown on MS agar plates containing 0, 0.1, 1 or 10  $\mu$ M IAA at a 16 h light - 8h dark regime and root length measured after 6 days. Data points are the mean  $\pm$  s.e. of 20-30 seedlings. Asterisks represent significant differences from WT within a treatment group (ANOVA with Fisher's protected LSD post-hoc test,  $p < 0.001$ ). (B) Seedlings were grown in the dark on MS agar plates containing 0, 5 or 10  $\mu$ M IAA and hypocotyl length measured after 5 days. Data points are the mean  $\pm$  s.e. of 60-80 seedlings. Asterisks represent significant differences from WT within a treatment group (ANOVA with Fisher's protected LSD post-hoc test,  $p < 0.05$ ).

To obtain further insight into the relationship between HOL activity and auxin, the *hol* mutant and the *35S::HOL* line 196-11 were crossed with a *DR5::GFP* reporter line (Friml *et al.*, 2003), thus making it possible to visualise auxin responses in *hol* mutant and *35S::HOL* plants. Generally, auxin activity is high in the apical root meristem and in lateral root primordia (Vanneste and Friml, 2009). Therefore, GFP fluorescence was examined at these sites in *DR5::GFP* x *hol* and *DR5::GFP* x *35S::HOL* crosses. No differences in GFP fluorescence at the apical root meristem or at the lateral root primordia were observed between the different genotypes under normal growth conditions (Fig. 4.14, data not shown).

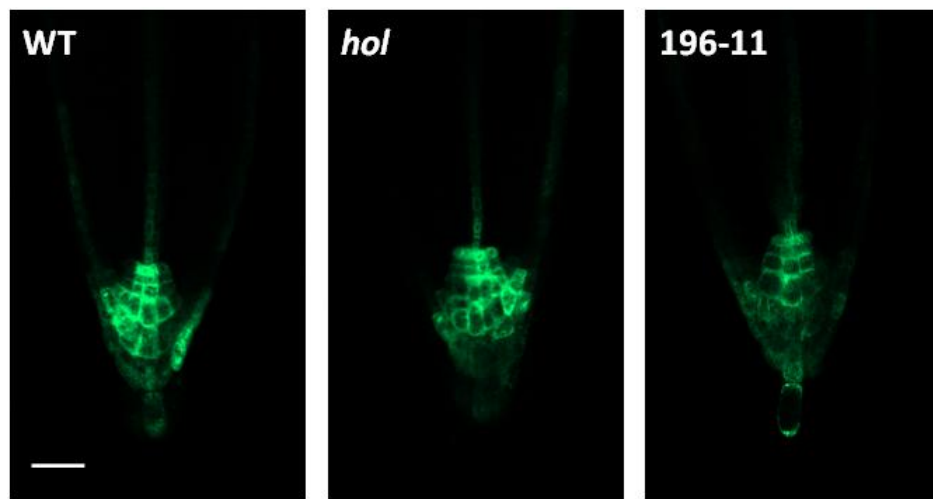


**Figure 4.14. Auxin response in WT, *hol* and *35S::HOL* (196-11) lines containing the *DR5::GFP* reporter gene.** Confocal images of *DR5::GFP* expression in roots of 5-day-old seedlings of WT, *hol* and 196-11 grown on MS agar. Scale bar = 30  $\mu$ m.

All in all, these data show that the *hol* mutant is slightly less sensitive to the application of auxin. More experiments are needed to understand this phenomenon. So far, it seems that at least auxin signalling *per se* was not impaired in the roots of *hol* seedlings under normal growth conditions.



### 4.3 Discussion

The main aim of this study was to investigate potential functions of methyl halide production in *A. thaliana*. Firstly, the effects of HOL activity/methyl halide production on salt stress tolerance were investigated. The cloning of a *HOL*-orthologous gene (*BmMCT*) in the halophytic plant *Batis maritima* and the subsequent characterisation of the enzyme consolidated the hypothesis that methyl halide production contributes to stress tolerance in plants (Ni and Hager, 1998, 1999). However, at the start of this project, no thorough investigation of this hypothesis had been conducted. The availability of *hol* mutant and overexpressor lines in *A. thaliana*, which show reduced or increased HOL activity and methyl halide production rates, respectively, made it possible to thoroughly test the involvement of HOL in salt stress tolerance in this plant.

No differences in germination rates or growth were observed between WT and *hol* plants when they were subjected to various salt stresses (chloride, bromide and iodide salts). Therefore, our data do not support the hypothesis that an increase in methyl halide production upon salt stress contributes to salt tolerance in *A. thaliana* by regulating  $\text{Cl}^-$ ,  $\text{Br}^-$  or  $\text{I}^-$  homeostasis, because the *hol* mutant was not more sensitive to salt stress than the WT. Moreover, the overexpression of *HOL*, which causes increased methyl halide emissions in *35S::HOL* plants, did not make these plants more salt tolerant, on the contrary, it made them more susceptible towards bromide and iodide, but not to chloride salts. These observations are in accordance with a study by Nagatoshi and Nakamura (2009) which did not find any differences in growth between WT, *hol* and *35S::HOL* seedlings when they were subjected to various concentrations of KCl and NaCl.

Another argument, proposed by Harper (2000), for dismissing any function of HOL in salt stress tolerance is the fact that the loss of a  $\text{CH}_3$  group provided by the energetically expensive SAM would be a high price to pay for the elimination of halide ions. Nevertheless, he did not rule out that HOL activity could be confined to small cellular compartments particularly vulnerable to high levels of halide ions. However, this is not supported by the expression patterns of *HOL*, which show high expression levels in the vasculature of roots and young leaves, and the lack of targeting of HOL to any particular compartment or organelle in *A. thaliana* (Chapter 3).

Finally, the suppression of *HOL* by  $\text{Cl}^-$  and  $\text{Br}^-$  also contradicts an involvement of this gene in salt stress tolerance. Interestingly, the down-regulation was linked

specifically to these two substrates of HOL and not to any osmotic or cation ( $\text{Na}^+$ ) effects. These results are in accordance with microarray data from the *A. thaliana* eFP browser (Winter *et al.*, 2007) which showed a permanent down-regulation of *HOL* in roots and shoots after application of 150 mM NaCl. Surprisingly, *HOL* transcript levels were not altered by KI treatment, but it is necessary to collect more expression data at different time points after the start of salt treatments to get an accurate picture about how salt treatment affects *HOL* gene expression.

Overall, our data support the view of Manley (2002) who denotes methyl halides as “accidents of metabolism” without any particular function due to the insertion of halides into the active site of numerous methyl transferases. Moreover, he proposed, based on the comparison of tissue halide levels with methyl halide production rates in several plant species, that the loss of halides in the form of methyl halides is only minimal in plant tissues. Based on our own measurements, *A. thaliana* WT plants produce only about 1 nmol of  $\text{CH}_3\text{Cl}$  per day per g FM, which is indeed only a small fraction of the total chloride content ( $\sim 88 \mu\text{mol/g}$  FM) found in *A. thaliana* roots treated with 50 mM NaCl (Jossier *et al.*, 2010). However, it is necessary to quantify  $\text{CH}_3\text{Cl}$  emissions from *A. thaliana* upon NaCl stress to get an accurate picture of chlorine stoichiometry. In *B. rapa*, 100 mM NaCl treatment caused only a 5-fold increase in methyl halide emissions (Fig. 4.1), whereas in *A. thaliana*, a 1000-fold increase in  $\text{CH}_3\text{Br}$  emissions was observed after the application of 50 mM NaBr (Rhew *et al.*, 2003). The quantification of halide ion content in *hol* mutant and *35S::HOL* plants after salt treatment could give further information about the effectiveness of methyl halide production on halide removal. A recent study about iodine biofortification in plants showed that *A. thaliana* plants genetically modified to assimilate large amounts of iodine, via the overexpression of a sodium-iodide symporter (NIS), did not accumulate more iodine in the tissue than WT plants. Instead, iodine was removed as  $\text{CH}_3\text{I}$  due to the activity of HOL, and this problem was only overcome by making a *NISxhol* cross which was then able to accumulate high levels of iodine in its tissue (Landini *et al.*, 2012).

We were intrigued by the hypersensitivity of *35S::HOL* lines towards  $\text{I}^-$  and  $\text{Br}^-$  and investigated further to understand why increased methyl halide emissions/HOL activity negatively affected plant growth and therefore probably caused a down-regulation of *HOL* in *A. thaliana* upon salt stress. Two possibilities were tested: Firstly, the high

production rates of methyl halides in *35S::HOL* lines, which probably increase immensely after application of salts, were considered a factor contributing to hypersensitivity of those plants towards salts. Methyl halides are known to be toxic to a wide range of organisms, and methyl bromide and methyl iodide have been used as pesticides and for weed control for many decades (Ristaino and Thomas, 1997; Zhang *et al.*, 1997). It is believed that methyl halides react with functional groups such as  $\text{NH}_2$  and  $\text{SH}$  in various amino acids and peptides such as glutathione (Price, 1985). Glutathione is a key antioxidant in many tissues and its production is induced under stress conditions including salt stress (Noctor *et al.*, 1998; Koprivova *et al.*, 2008). It was shown that fumigation of lemons with  $\text{CH}_3\text{I}$  reduced glutathione concentrations to less than 5% of the control value (Ryan *et al.*, 2007). Thus, it is possible that the observed symptoms in *35S::HOL* lines upon salt stress are due to a decrease in glutathione levels and it will be interesting to test this hypothesis in future experiments. Reactivity of methyl halides is expected to be  $\text{CH}_3\text{I} > \text{CH}_3\text{Br} > \text{CH}_3\text{Cl}$  due to the chemical properties of the various halide anions. This is consistent with our observation that iodide in the medium had the strongest effect on *35S::HOL* lines even at low concentrations compared to the other halides. A simple method to block methyl halide production by HOL is the addition of the competitive inhibitor  $\text{SCN}^-$  (Rhew *et al.*, 2003). For this reason, we tested if the addition of KSCN could rescue *35S::HOL* lines, however, this was not the case as no differences were observed between *35S::HOL* seedlings grown on KI or KI+KSCN media. Therefore, we did not find support for methyl halide toxicity in these plants at this stage. Future work needs to verify if  $\text{CH}_3\text{I}$  emissions in *35S::HOL* lines are indeed reduced by the application of KSCN to KI media.

Secondly, it was hypothesised that *35S::HOL* seedlings suffer from SAM depletion due to the high activity of *HOL*. In addition to providing a methyl group for the production of methyl halides, SAM is also an essential substrate in numerous metabolic pathways including the biosynthesis of polyamines (Roje, 2006). Polyamines have been shown to have regulatory functions in abiotic stress tolerance (Alcazar *et al.*, 2010). SAM is synthesised from methionine and ATP by SAM synthetase. Generally, SAM is not thought to be a limiting resource as long as the transmethylation cycle mediates the recycling of thiol and adenylyl groups to regenerate methionine (Moffatt and Weretilnyk, 2001). However, under stress conditions the recycling mechanism may be disturbed. Moreover, reduced levels of SAM could reduce the production of polyamines

which may lead to KI-hypersensitivity (Yamaguchi *et al.*, 2006). Again, we did not find any support for this hypothesis. The application of methionine or polyamines did not rescue *35S::HOL* seedlings upon KI stress. However, further experiments such as the quantification of SAM levels in *35S::HOL* lines before and after application of KI are necessary to falsify our hypothesis.

Finally, we wanted to test if the low germination rate of *35S::HOL* lines could be rescued by the application of gibberellic acid (GA). In *A. thaliana* seeds, GA promotes embryo growth and the breakage of the seed coat during germination (Sun, 2008). Recently, it has also been shown that GA treatment can counteract the inhibitory effects of abiotic stress treatments such as NaCl on seed germination (Alonso-Ramirez *et al.*, 2009). Interestingly, *HOL* is already expressed in the root of the embryo before germination indicating a possible function of *HOL* in regulating germination. Moreover, iterative group analysis of the microarray data showed an overlap between genes differently expressed in the *hol* mutant and genes up/down-regulated by treatments with various plant hormones or hormone inhibitors (Suppl. Table 3.1, 3.2). It is therefore possible that *HOL* might be involved in plant responses to hormones such as GA or auxin (see below). However, in our experiment, GA application did not rescue the low germination rate observed in *35S::HOL* seeds subjected to KI stress, indicating that the reduction of germination rates in *35S::HOL* is probably not linked to a reduction of GA levels in these lines. Further experiments including the measurement of hormone levels are necessary to understand why germination of *35S::HOL* seeds is inhibited.

Further potential functions of the *HOL* gene in *A. thaliana* plant metabolism and development were explored based on the alterations observed in the transcriptome of the *hol* mutant (see Chapter 3). One gene initially annotated to encode a protein of unknown function was particularly down-regulated in the *hol* mutant. A recent study revealed that the gene encodes a small protein which appears to be a novel regulator of starch synthesis in *A. thaliana* and was named QUA-QUINE STARCH (QQS) (Li *et al.*, 2009). It was shown that the leaf starch content of *QQS* RNAi mutant lines was increased by 30%, whereas in *35S::QQS* plants, starch content was reduced compared to WT (Li *et al.*, 2009; Seo *et al.*, 2011). So far, it is not known how *QQS* influences starch metabolism, and surprisingly, no *QQS*-homologous genes have been found in other plant species yet.

Quantitative PCR confirmed that in the *hol* mutant, *QQS* transcript levels were strongly reduced to less than 1% of WT transcript levels. However, we did not observe any differences in the starch content between WT and *hol* plants when iodine staining was used. Further experiments which accurately quantify starch levels in the *hol* mutant at several time points during the light and dark period are necessary to verify if starch content is altered in these plants.

Furthermore, it would be interesting to explore how HOL activity might affect *QQS* activity. Recently, it was shown that two splice variants ( $\alpha$  and  $\beta$ ) of the INDETERMINATE DOMAIN 14 (IDD14) transcription factor regulate *QQS* expression and starch accumulation in response to cold stress. IDD14 $\alpha$  activates *QQS* expression by binding to the *QQS* promoter. However, under cold stress conditions IDD14 $\beta$  is increasingly produced and binds to IDD14 $\alpha$ . The IDD14 $\alpha$ -IDD14 $\beta$  heterodimer has reduced binding affinity to the *QQS* promoter and therefore *QQS* expression is reduced leading to a lower starch degradation rate during the night. It was proposed that this mechanism could help plants to maintain starch reserves under stress conditions such as cold (Seo *et al.*, 2011). In the *hol* mutant, *IDD14* expression was not altered based on the microarray data, however, it could be interesting to specifically check the expression patterns of both IDD14 splicing variants in *hol* and *35S::HOL* plants by qPCR. Perhaps it could be speculated that changes in methyl halide emissions, e.g. under salt stress conditions, could modulate the expression of *QQS* and thus help plants to adjust their energy reserves.

Another gene, *EXORDIUM-LIKE 1 (EXL1)*, which is also involved in balancing carbon and energy supply in *A. thaliana* under unfavourable environmental conditions (Schröder *et al.*, 2011) was significantly up-regulated in the *hol* mutant. *EXL1* expression is increased during low carbon and low energy availability, and *exl1* mutants showed reduced growth under light-limited conditions and when grown on low sucrose levels. We tested if *hol* seedlings had increased growth rates compared to WT on media supplemented with low amounts of sucrose, however, no differences were detected between the genotypes indicating that up-regulation of *EXL1* in *hol* plants does not increase biomass production under low sucrose levels. The mode of action of *EXL1* is not known. Interestingly, *EXL1* seems to suppress the expression of *QQS* as *exl1* mutants had increased *QQS* transcript levels compared to WT (Schröder *et al.*, 2011). Our data are in accordance with this observation since *QQS* levels are strongly reduced in the *hol* mutant. Thus, it remains to be investigated if *EXL1* regulates starch

metabolism by modulating *QQS* expression under unfavourable environmental conditions and whether methyl halides directly influence the expression or action of any of these genes.

Finally, it was tested if there is any relationship between HOL and auxin signalling in *A. thaliana*. Microarray data indicated that a number of auxin/light-responsive genes were differentially regulated in the *hol* mutant (Chapter 3). In accordance with these data, we found that the *hol* mutant was slightly less sensitive to exogenous application of auxin, and *35S::HOL* lines showed increased hypocotyl growth in the dark. One of the genes down-regulated in the *hol* mutant encodes the transcription factor ATHB2 (also named HAT4). ATHB2 is known to regulate hypocotyl and root growth, presumably by altering auxin transport (Schena *et al.*, 1993; Steindler *et al.*, 1999; Köllmer *et al.*, 2011). Recently, it was also proposed that the auxin-inducible protein IAA29 integrates auxin and light stimuli to regulate the elongation of hypocotyls (Kunihiro *et al.*, 2011). *IAA29* was significantly up-regulated in the *hol* mutant (Chapter 3). Aux/IAA proteins are involved in the early steps of auxin signal transduction (Mockaitis and Estelle, 2008), however, we did not find any differences in auxin signalling in *hol* or *35S::HOL* plants harbouring the *DR5::GFP* reporter gene under normal growth conditions. The data presented here only give a first glimpse of a potential involvement of HOL in auxin signalling and encourage further experiments. It could be interesting to test if *DR5::GFP* expression is altered when *hol* or *35S::HOL* plants are stressed. At this stage, it is difficult to imagine how HOL could influence auxin-signalling pathways. One hypothesis is that methyl halides could be signalling molecules/hormones themselves modulating auxin responses via hormonal crosstalk.

## **Chapter 5 – Exploring potential functions of HOL and methyl halide emissions in *Arabidopsis thaliana*: Part II**

### **5.1 Introduction**

This chapter focuses on investigating the effects of HOL activity on (1) plant-herbivore interactions and (2) on the microbial diversity of the rhizosphere in *A. thaliana*. We propose that HOL can affect the outcome of such interactions via the production of methyl halides or sulphur volatiles.

#### **5.1.1 Production and role of volatiles emitted by plants**

Plants release a variety of different volatiles into the atmosphere. To date, approximately 1700 volatile compounds have been identified in more than 90 plant families (Knudsen *et al.*, 2006; Schiestl, 2010). Most of these compounds belong to the groups of terpenoids, fatty acids derivatives, benzenoids or phenylpropanoids, but low-molecular-weight volatiles such as ethylene, methanol or acetone are also emitted by plants (Fall, 2003; Laothawornkitkul *et al.*, 2009).

Plant volatiles fulfil several functions in plants (Fig. 5.1) (Dudareva *et al.*, 2006; Laothawornkitkul *et al.*, 2009; Unsicker *et al.*, 2009; Dicke and Baldwin, 2010; Wenke *et al.*, 2010): They act as signalling compounds within the plant (e.g. ethylene, methyl jasmonate, methyl salicylate), they attract pollinators and seed disseminators, and play an important role in plant defence against pathogens and insect herbivores, both aboveground and belowground. Interestingly, upon herbivore attack, specific blends of volatiles are produced which can directly affect the survival and performance of herbivores due to their toxic or repelling properties, or they can protect the plant from further damage by attracting natural enemies of the attacking herbivore such as parasitoids. Moreover, herbivore-induced plant volatiles can activate or prime defence responses in undamaged parts of the plant or in neighbouring plants (Baldwin *et al.*, 2006; Dicke and Baldwin, 2010). It has also been shown that volatile isoprenoids confer a protective effect on photosynthesis under abiotic stress conditions such as thermal and oxidative stress (Vickers *et al.*, 2009).

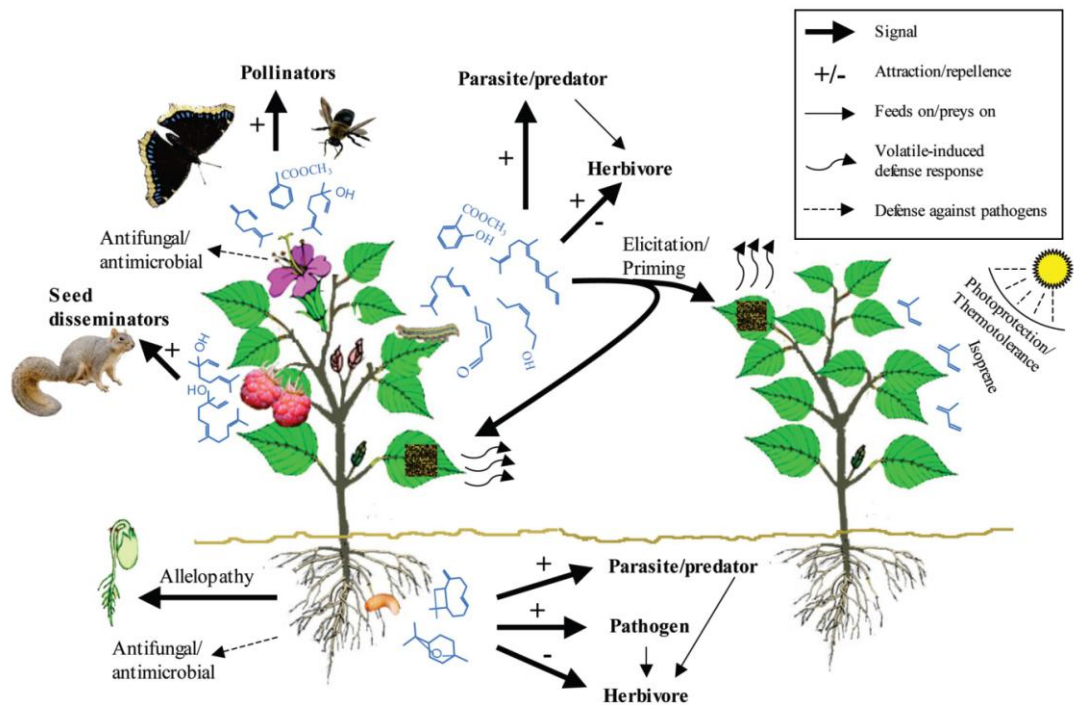


**Figure 5.1. Multiple functions of plant volatiles.** Plant volatiles attract pollinators and seed disseminators. They are also involved in plant defence against herbivores and pathogens either by directly affecting them due to their toxic or repelling properties or by attracting natural enemies (e.g. parasitoids). Volatiles can also act as signals within a plant or between plants and elicitate or prime defence responses in undamaged parts of the plant or in neighbouring plants. Moreover, volatile isoprenoids can protect plants against abiotic stress such as high temperatures. Image taken from Dudareva *et al.* (2006).

### 5.1.2 Methyl halides - a novel type of plant volatiles involved in plant defence against herbivores or pathogens?

Methyl halide emissions are widespread in the plant kingdom and have been reported for several plant species including dicots, monocots, ferns, mosses and green algae (see Chapter 1, 6 and 7). We propose that methyl halides could affect the outcome of plant-herbivore or plant-microbe interactions in two ways. Firstly, it is possible that they could act as toxins and therefore be an important part of plant defence against herbivores and pathogens.  $\text{CH}_3\text{Br}$  and  $\text{CH}_3\text{I}$  have been used as pesticides for soil fumigation and for postharvest treatment of durable and perishable commodities. They are effective against various plant pathogens, insects and nematodes (Taylor, 1994; Ohr *et al.*, 1996; Ristaino and Thomas, 1997). This hypothesis is supported by the study of Nagatoshi and Nakamura (2009) which showed that *A. thaliana hol* seedlings had a reduced survival rate when infected with *Pseudomonas syringae* pv. *maculicola* (Fig. 1.9). Moreover, it was shown that fumigation of soil samples with  $\text{CH}_3\text{Br}$  and  $\text{CH}_3\text{I}$



significantly reduced soil microbial diversity compared to untreated soil samples (Ibekwe *et al.*, 2001; Ibekwe *et al.*, 2010). Interestingly, in marine algae, other volatile halogenated compounds such as bromoform (CHBr<sub>3</sub>) or dibromochloromethane (CHBr<sub>2</sub>Cl) have been shown to possess antimicrobial activity and to function as herbivore deterrents (Paul *et al.*, 2006a; Paul *et al.*, 2006b).

Secondly, it is possible that plants produce methyl halides to attract bacteria which use these volatiles as a carbon and energy source. Numerous bacteria which are able to utilise methyl halides have been isolated from soils (Schäfer *et al.*, 2007). Recently, methyl-halide degrading bacteria were also isolated from the leaf surface of *A. thaliana* plants (Nadalig *et al.*, 2011). It is possible that such bacteria could act as biocontrol microorganisms in the rhizosphere or phyllosphere of plants by impairing the growth of pathogens e.g. due to competition for nutrients (Lindow and Brandl, 2003; Bais *et al.*, 2006; Raaijmakers *et al.*, 2009).

### 5.1.3 Methylation of glucosinolate hydrolysis products by HOL

Glucosinolates (GLs) are sulphur-rich secondary metabolites found mainly in a few angiosperm families from the order Brassicales such as *Brassicaceae*, *Capparaceae* and *Caricaceae* (Fahey *et al.*, 2001). They define the flavours of cabbage, broccoli, cauliflower and other *Brassica* vegetables and possess antioxidant and cancer-preventing activities (Vig *et al.*, 2009), therefore playing an important part in a healthy diet. In plants, GLs contribute to defence against various herbivores, bacteria, fungi and pathogens (Brown and Morra, 1997; Halkier and Gershenzon, 2006; Bednarek *et al.*, 2009).

Approximately 130 different GLs have been identified to date (Agerbirk and Olsen, 2012). They all share a chemical structure consisting of a  $\beta$ -D-glucopyranose residue linked via a sulphur atom to a (Z)-N-hydroximosulphate ester plus a variable R group (Fig. 5.2). GLs are synthesised from various amino acids and classified accordingly: (1) Aliphatic GLs derived from Ala, Leu, Ile, Met or Val, (2) aromatic GLs derived from Phe or Tyr, and (3) indolic GLs derived from Trp. Most of the biological activities of GLs such as their toxicity towards herbivores are attributed to the compounds released upon enzymatic hydrolysis of GLs by myrosinases. In intact plant tissue, myrosinases are inactivated or spatially separated from GLs, however, upon tissue damage, myrosinases are released and GLs converted to toxic compounds such as

isothiocyanates, thiocyanates and nitriles (Halkier and Gershenzon, 2006). These hydrolysis compounds can degrade further to form thiocyanate ions ( $\text{SCN}^-$ ), bisulphide ions ( $\text{HS}^-$ ) or organic thiols (Fig. 5.2) (Attieh *et al.*, 2000a; Agerbirk *et al.*, 2009). Interestingly, these ions are physiological substrates of HOL and other HTMTs from various species (Table 1.2).

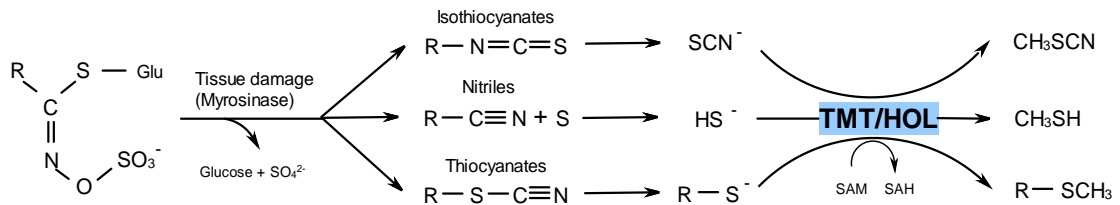


**Figure 5.2. Methylation of GL hydrolysis products by TMT/HOL.** Upon tissue damage myrosinases are released and GLs converted to toxic compounds such as isothiocyanates, thiocyanates and nitriles. These hydrolysis compounds can degrade further to form thiocyanate ions ( $\text{SCN}^-$ ), bisulphide ions ( $\text{HS}^-$ ) or organic thiols, which can then be methylated by TMT/HOL to form methyl thiocyanate, methanethiol or methylated organic thiols. Modified after Attieh *et al.* (2000a).

The capability of plants to methylate not only halide ions but also sulphur-containing ions (Fig. 5.2) was first observed by Saini *et al.* (1995). A survey of *in vivo* methyl iodide production from leaf discs of diverse plant species showed that methanethiol ( $\text{CH}_3\text{SH}$ ) was produced when leaf discs from 20 different plant species were incubated with  $\text{HS}^-$  ions instead of  $\text{I}^-$  ions. Subsequently, it was confirmed by *in vitro* enzyme kinetic studies that the same enzyme in *Brassica oleracea* can mediate the SAM-dependent methylation of both halides and  $\text{HS}^-$  (Attieh *et al.*, 1995), and further sulphur-containing methyl acceptors such as thiocyanate ( $\text{SCN}^-$ ) were later identified for this thiol methyltransferase (TMT) (Attieh *et al.*, 2000a). Several TMT isoforms have been identified in *B. oleracea*, and finally, two genes (*TMT1* and *TMT2*) were cloned in this species (Attieh *et al.*, 2000b; Attieh *et al.*, 2002), whose amino acid sequences are 87% and 84% identical to *A. thaliana* HOL, respectively.

Two hypotheses have been proposed regarding the function of TMTs in members of the *Brassicaceae*. Firstly, it was proposed that this mechanism could help plants to detoxify GL hydrolysis products (Attieh *et al.*, 2000b). GL hydrolysis products mainly occur after damage (see above), but are also known to be present in undamaged tissue due to endogenous catabolism and turnover of GLs (Petersen *et al.*, 2002). The

study of Nagatoshi and Nakamura (2009) showed that  $\text{SCN}^-$  was present in undamaged leaves of *A. thaliana*. As expected, the amount of  $\text{SCN}^-$  increased strongly in the leaf extracts after wounding. Moreover,  $\text{CH}_3\text{SCN}$  emissions were detected in leaf extracts of wounded leaves, but not in leaf extracts of undamaged leaves. It was then confirmed that HOL catalyses the conversion of  $\text{SCN}^-$  into  $\text{CH}_3\text{SCN}$  since leaf extracts from *hol* mutant plants did not produce  $\text{CH}_3\text{SCN}$  upon wounding (Fig. 1.10 A), and since the *hol* mutant was also more susceptible towards application of  $\text{SCN}^-$  than WT plants (Fig. 1.10 B) (Nagatoshi and Nakamura, 2009).

Secondly, it was proposed that sulphur volatiles such as  $\text{CH}_3\text{SCN}$  and  $\text{CH}_3\text{SH}$ , which are produced by TMTs, could attract predators (parasitoids) of the feeding insects or suppress the spread of pathogens (Attieh *et al.*, 2002; Nagatoshi and Nakamura, 2009), however, little is known about  $\text{CH}_3\text{SCN}$  and  $\text{CH}_3\text{SH}$  emissions in living plants and their role in plant defence.

#### 5.1.4 Objectives of this chapter

The main objectives of this chapter were to investigate the effects of HOL activity on (1) plant-herbivore interactions and (2) on the microbial diversity of the rhizosphere using WT, *hol* mutant and *35S::HOL* plants. Firstly, the GL content of the different *A. thaliana* genotypes was measured since HOL is involved in GL metabolism, and since GLs contribute to defence against pathogens and herbivores. Secondly, the survival and behaviour of the larvae of diamondback moth (*Plutella xylostella*) and black fungus gnat (*Bradysia paupera*) were tested when feeding on these plants. Finally, Automated Ribosomal Intergenic Spacer Analysis (ARISA) was performed on DNA samples extracted from rhizosphere soil of WT, *hol* mutant and *35S::HOL* plants. This technique involves PCR amplification of the 16S-23S intergenic spacer region (ISR) from the bacterial rRNA operons using primers which anneal to conserved regions in the 16S and 23S rRNA genes. The length of the ISR varies between different species, and this feature can therefore be used to characterise the structure of bacterial communities in the soil or rhizosphere (Fisher and Triplett, 1999; Ranjard *et al.*, 2001; Micallef *et al.*, 2009b).

## 5.2 Results

### 5.2.1 HOL and GL metabolism

First of all, it was tested if there were any differences in leaf GL content between WT, *hol* mutant and *35S::HOL* plants since GLs play an important part in plant defence. We also presumed that the *hol* mutant may accumulate less GLs in order to reduce the amount of toxic GL hydrolysis products which are normally catabolised by HOL in *A. thaliana* (Nagatoshi and Nakamura, 2009). Indeed, it was found that the total GL content was slightly reduced in *hol* plants compared to WT (Fig. 5.3 A), mainly due to a significant reduction of about 25% of 4-methylsulfinylbutyl-GL (4MSOB), the most abundant GL in *A. thaliana* (Fig. 5.3 C). Two of the indolic GLs, 4-hydroxy-indole-3-yl-methyl-GL (4OHI3M) and 1-methoxyindole-3-ylmethyl-GL (1MOI3M) were also reduced by 35% and 45%, respectively, in the *hol* mutant compared to WT (Fig. 5.3 E). These results therefore support our hypothesis that the *hol* mutant accumulates less GLs in order to reduce the amount of GL hydrolysis products. Total GL content of the *35S::HOL* line 196-11 did not differ from WT (Fig. 5.3 A), although two of the less abundant indolic GLs, 4-methoxyindole-3-yl-methyl-GL (4MOI3M) and 4OHI3M were reduced in line 196-11 compared to WT (Fig. 5.3 D, E).

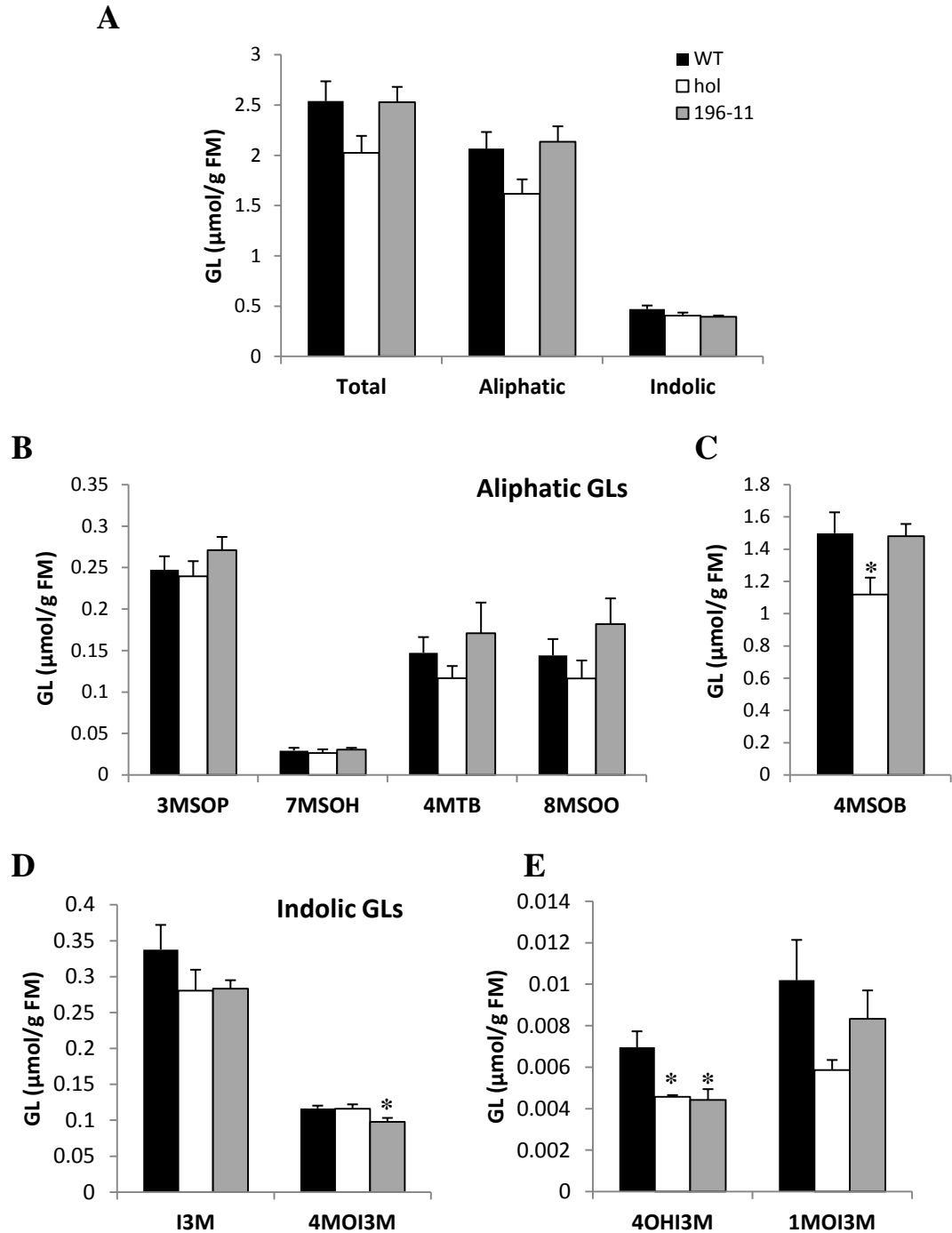


**Figure 5.3. Glucosinolate content in WT, *hol* and *35S::HOL* (196-11) plants.** Levels of total, aliphatic and indolic GLs (**A**) and levels of individual aliphatic (**B, C**) and indolic GLs (**D, E**) in leaves of 5-week-old plants. Asterisks represent significant differences from WT (ANOVA with Fisher's protected LSD post-hoc test,  $p < 0.05$ ). 3MSOP, 3-methylsulfinylpropyl-GL; 4MSOB, 4-methylsulfinylbutyl-GL; 7MSOH, 7-methylsulfinylheptyl-GL; 4MTB, 4-methylthiobutyl-GL; 8MSOO, 8-methylsulfinyloctyl-GL; I3M, indole-3-yl-methyl-GL; 4MOI3M, 4-methoxyindole-3-yl-methyl-GL; 4OHI3M, 4-hydroxy-indole-3-yl-methyl-GL; 1MOI3M, 1-methoxyindole-3-ylmethyl-GL.

### 5.2.2 HOL and plant-insect interactions

*A. thaliana* WT and *hol* plants were infested with larvae of the crucifer-specialist *Plutella xylostella* (diamondback moth, Lepidoptera: *Plutellidae*) in order to test if HOL activity affects the performance of this herbivore. Plant damage was recorded after 3 and 8 days and larval mass determined at the end of the experiment. No significant differences in plant damage were observed between genotypes (Fig. 5.4 A), and larvae gained the same weight when feeding on WT and *hol* mutant plants (Fig. 5.4 B).

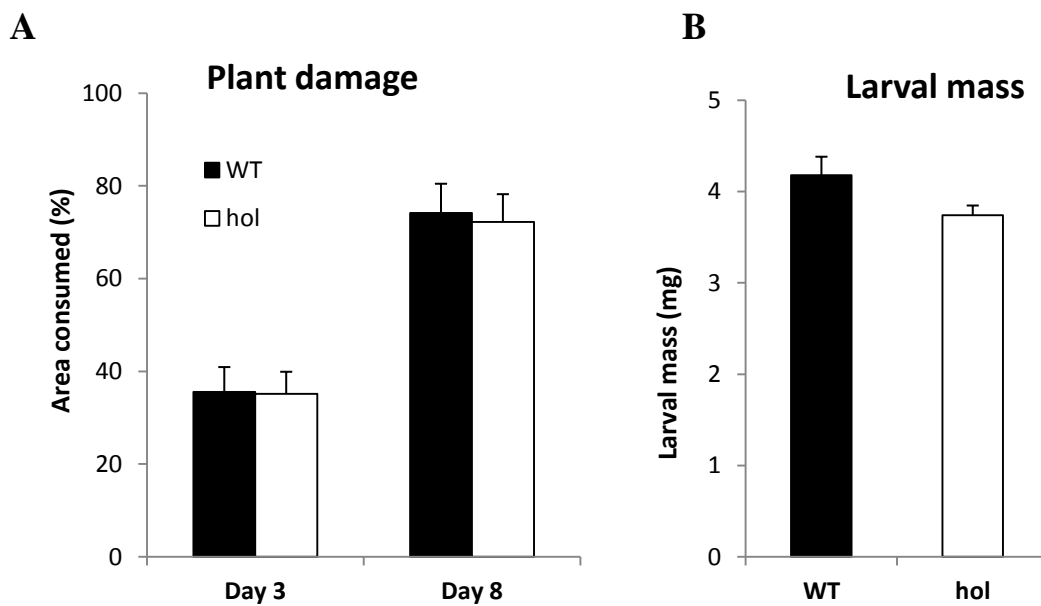


**Figure 5.4. *Plutella xylostella* performance on WT and *hol* mutant plants.** One larva was placed on a rosette leave of a three-week-old plant and the damage to the leaf or the whole plant recorded after 3 days or 8 days, respectively (A). Larval mass (B) was determined after 8 days of feeding. Data points are the mean  $\pm$  s.e. of 28 leaves/plants or 10 larvae, respectively. No significant differences were observed between WT and the *hol* mutant (t-test).

Since *HOL* is mainly expressed in the roots of *A. thaliana*, we also wanted to test the performance of the generalist root feeder *Bradysia paupera* (black fungus gnat, Diptera: *Sciaridae*) when feeding on WT, *hol* and *35S::HOL* roots. Plants roots were infested with *B. paupera* eggs, and the number of adult flies emerging from the soil was recorded. Overall, no significant differences in the survival rate were observed between larvae feeding on different plant genotypes. However, survival of *B. paupera* tended to be slightly higher when feeding on *35S::HOL* roots and lower when feeding on *hol* roots compared to WT (Fig. 5.5 A).

Additionally, in a choice assay, adult flies were allowed to choose between WT, *hol* and *35S::HOL* plants for oviposition. This experiment would show whether methyl halide volatiles attract or repel *B. paupera* flies when searching for a host plant. However, no differences were observed in the number of adult flies emerging from each plant indicating that similar numbers of eggs were laid on each genotype (Fig. 5.5 B).

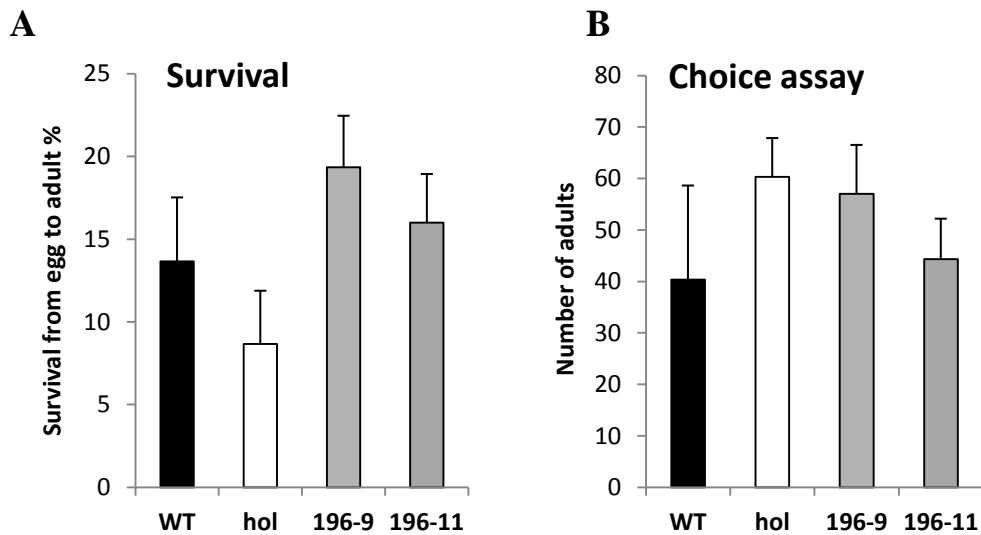


**Figure 5.5. *Bradysia paupera* survival and choice assay on WT, *hol* and *35S::HOL* (196-9, 196-11) plants. (A)** Twenty newly-laid eggs were washed onto the soil of each pot containing three 7-week-old plants grown under short-day conditions. The number of adult flies emerging from each pot was counted after 4 weeks. Data points are the mean  $\pm$  s.e. of 15 replicates. **(B)** Fifty large females and 15 males were allowed to infest 11-week-old plants grown under short-day conditions for 14 days and then removed. The number of adult flies emerging from each pot was counted after 4 weeks. Data points are the mean  $\pm$  s.e. of 3 replicates. No significant differences were observed between genotypes (ANOVA).

Taken together these results showed that neither *P. xylostella* nor *B. paupera* larvae are negatively affected by methyl halide emissions or other effects of HOL activity such as the differences in GL content or possible emissions of sulphur volatiles such as  $\text{CH}_3\text{SCN}$ . Moreover, methyl halides or sulphur volatiles did not affect the host searching behaviour of *B. paupera* flies.

### 5.2.3 Influence of methyl halide production on rhizosphere bacteria

The rhizosphere provides a habitat for a wide range of microbes, and plant roots excrete a number of chemically different compounds called root exudates which can facilitate positive interactions with symbionts such as plant growth promoting bacteria, or provide protection against pathogens (Bais *et al.*, 2006). Interestingly, *HOL* is strongly expressed in roots (Chapter 3) which suggests that methyl halides are mainly produced in this organ. To test whether the production of methyl halides could affect bacterial numbers or the composition of the microbial community in the rhizosphere of *A. thaliana*, WT, *hol* mutant and *35S::HOL* plants were grown in sterile compost mixed with soil collected from a natural grassland site.

Initially, the number of colony-forming units (cfu) in the rhizosphere of the different genotypes or the soil control was determined. The total number of cfu was slightly reduced in unplanted soil, however, no significant differences in the total number of cfu was found between rhizosphere samples of WT, *hol* mutant and *35S::HOL* lines (Suppl. Fig. 5.1).

To analyse the composition of the rhizobacterial community of WT, *hol* and *35S::HOL* plants, DNA was extracted from the soil firmly attached to the roots or from an unplanted soil control after 1, 2 and 4 weeks, and a profile of the bacterial community for each genotype created using ARISA. Examples of ARISA profiles obtained from the rhizosphere soil of WT, *hol* and *35S::HOL* plants or from the unplanted soil control are shown in Supplemental Figure 5.2.



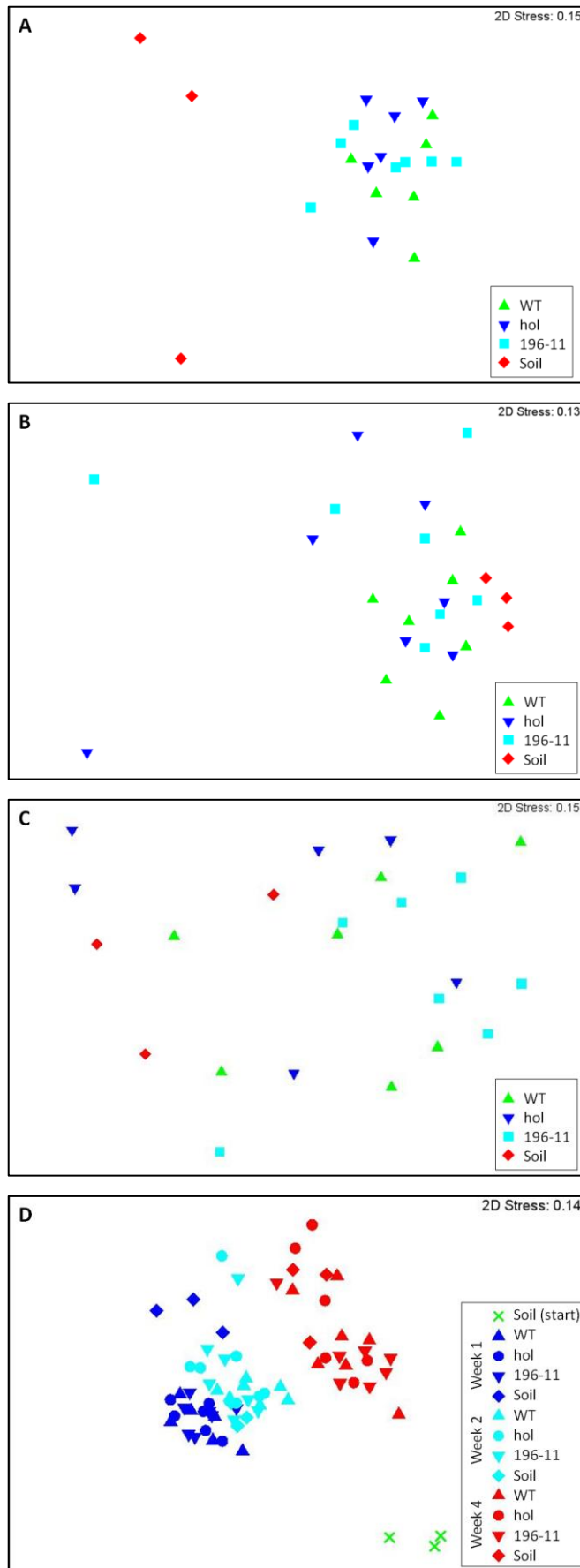


**Figure 5.6. Non-metric MDS plots of bacterial community profiles in the rhizosphere of WT, *hol* and 35S::*HOL* (196-11) plants.** Plots were generated from matrices of Bray-Curtis coefficients describing similarities between the ARISA profiles of each pair of samples. The closer two points (i.e. samples) are, the higher is their similarity. ARISA profiles were obtained from DNA extracted from the rhizosphere soil or from the unplanted soil control 1 week (A), 2 weeks (B) or 4 weeks (C) after the start of the experiment. Plot (D) combines the data of all time points including the soil control at the start of the experiment. Stress values of < 0.2 indicate that each plot is a good representation of the dataset. The results for the significance tests (MANOVA) are summarised in Supplemental Table 5.1.

Two approaches were used to characterise and compare ARISA profiles between the different genotypes. Firstly, similarity coefficients were generated by calculating similarities between each pair of ARISA profiles. These similarities were then illustrated in a non-metric Multi-Dimensional-Scaling (MDS) plot, and multivariate analysis of variance (MANOVA) was used for significance testing. This analysis showed that the composition of the bacterial communities of the rhizosphere significantly changed over the time course of the experiment (4 weeks) (Fig. 5.6 D, Suppl. Table 5.1). Generally, ARISA profiles of unplanted soil controls were different compared to ARISA profiles obtained from the rhizosphere samples, but these differences diminished during the time course of the experiment (Fig. 5.6, Suppl. Table 5.1). However, no significant differences between the rhizobacterial communities of WT, *hol* and *35S::HOL* plants were observed at any given time point. Overall, the variation within replicates of each genotype was large, especially 2 and 4 weeks after the start of the experiment (Fig. 5.6 B, C). These results suggest that methyl halides do not significantly alter the overall composition of the bacterial community of the *A. thaliana* rhizosphere.

It is possible that methyl halides only affect a minority of bacterial species which is not represented by the similarity coefficients shown in MDS plots. We therefore analysed the distribution of individual ISR fragments among WT, *hol* and *35S::HOL* rhizosphere samples to test if some of the ISR fragments only occur in one of the genotypes. As expected, the majority of ISR fragments, mainly the dominant ones (large circles), were found in all three genotypes, however, a small number of less abundant ISR fragments were genotype-specific (Fig. 5.7). For example, six ISR fragments were mainly found in the rhizosphere samples of *35S::HOL* plants harvested 2 weeks after the start of the experiment (Fig. 5.7 B).

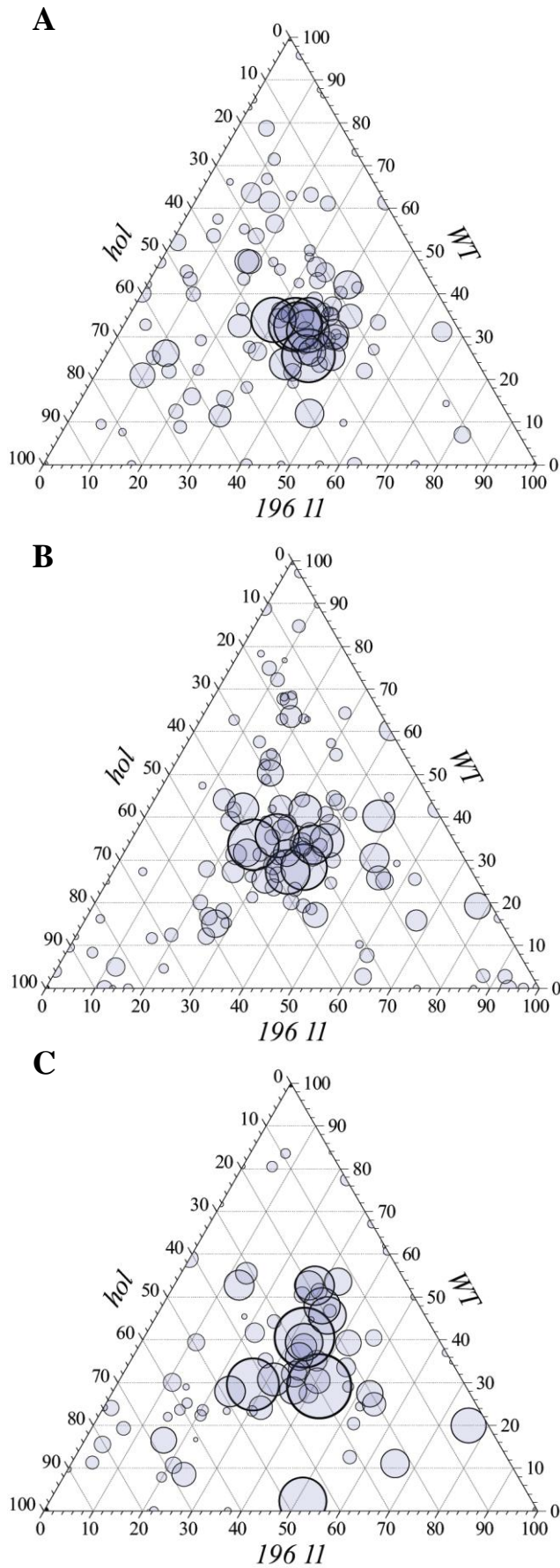


**Figure 5.7. Distribution of individual ISR fragments among WT, *hol* and *35S::HOL* (196-11) rhizosphere samples.** Ternary plots were generated from ISR fragments showing a relative fluorescence of > 1% in at least one sample. Circle sizes indicate the dominance of each ISR fragment i.e. large circles depict high total fluorescence. ARISA profiles were obtained from DNA extracted from the rhizosphere soil 1 week (**A**), 2 weeks (**B**) or 4 weeks (**C**) after the start of the experiment.

Further work is necessary to identify the species that are associated with the respective ISR fragments. For a start, we hypothesised that methyl-halide-degrading bacteria could be overrepresented in the *35S::HOL* rhizosphere. Numerous bacterial strains (e.g. *Methylobacterium*) which are able to utilise methyl halides have been isolated from soils (Schäfer *et al.*, 2007). Recently, methyl-halide-degrading bacteria were also isolated from the leaf surface of *A. thaliana* plants (Nadalig *et al.*, 2011). These bacteria all possess *cmu* gene clusters, which contain the genes that are essential for the utilisation of methyl halides. Primers which amplify the *cmuA* gene have been successfully employed to identify methyl-halide degrading bacteria (McAnulla *et al.*, 2001; Miller *et al.*, 2004; Nadalig *et al.*, 2011). We therefore used these primers to test our hypothesis and screened the DNA extracted from WT, *hol* and *35S::HOL* rhizosphere samples for the presence of the *cmuA* gene. Unfortunately, only a weak PCR product of the expected size was found in a few samples (Suppl. Fig. 5.3) indicating that methyl-halide degrading bacteria were not very common in our rhizosphere samples. Generally, the presence of the amplicon was not linked to the methyl halide phenotype as *cmuA* was detected in a few samples of all genotypes and the soil control (data not shown). However, further work is necessary to verify these results e.g. by sequencing the PCR products.

Taken together, we did not find evidence that methyl halides shape rhizobacterial communities in *A. thaliana*. Nevertheless, there are indications that a minority of bacteria might be affected by methyl halides, but which species belong to this minority is not clear at this stage.

### 5.3 Discussion

The main objectives of this chapter were to investigate the effects of HOL activity on (1) plant-herbivore interactions and (2) on the microbial diversity of the rhizosphere in *A. thaliana*. We proposed that HOL can affect the outcome of such interactions via the action of methyl halides and/or sulphur volatiles derived from GLs.

Since GLs play an important part in plant defence and due to the fact that HOL detoxifies GL breakdown products, the GL content of WT, *hol* and *35S::HOL* plants was quantified in order to test if there were any differences in GL content between the genotypes. We presumed that the *hol* mutant may accumulate less GLs to prevent the

accumulation of toxic GL hydrolysis products such as  $\text{SCN}^-$  which are normally catabolised by HOL (Nagatoshi and Nakamura, 2009). Indeed, it was found that the total GL content was reduced by 20% in the *hol* mutant compared to WT, mainly due to a significant reduction of 4MSOB. No major differences were observed between WT and *35S::HOL* lines.

Only two GL biosynthesis genes, *AOP2* and *CYP81F2*, were differentially regulated in the *hol* mutant (Chapter 3). *AOP2* catalyses the conversion of 4MSOB to 3-butenyl GL and could therefore affect 4MSOB levels, however, in Col-0, the *AOP2* allele encodes a non-functional protein (Neal *et al.*, 2010). *CYP81F2*, which was up-regulated in the *hol* mutant, catalyses the conversion of I3M to 4OHI3M (Pfalz *et al.*, 2009). Theoretically, the up-regulation of this gene should cause an increase in 4OHI3M levels, but the levels of 4OHI3M were reduced in the *hol* mutant. Taken together, the expression patterns of *AOP2* and *CYP81F2* did not explain the reduction of GL content in the mutant.

Alternatively, it is possible that the mode or rate of turnover of GLs is altered in the *hol* mutant, e.g. an increase in the rate of breakdown of GLs in *hol* plants could lower overall GL content. However, in that case, it is likely that the mode of breakdown does not involve the accumulation of GL hydrolysis products such as  $\text{SCN}^-$  since *hol* mutant plants grew well under normal conditions. Unfortunately, very little is known about GL catabolism in undamaged tissue of plants, but there is evidence for a steady turnover of GLs in intact tissue: It has been shown that the GL content and composition change during growth and development of *A. thaliana* (Petersen *et al.*, 2002). Moreover, GLs are a potential source of sulphur and nitrogen for other metabolic processes, and it has been shown that GLs are broken down when supply of these nutrients is limited (Falk *et al.*, 2007; Yan and Chen, 2007). The exact mechanisms of GL breakdown in undamaged tissues of plants remain unclear, but it is believed that myrosinases play a role (Yan and Chen, 2007; Janowitz *et al.*, 2009). In addition, it was proposed that some myrosinase-independent mechanisms exist in *A. thaliana* since myrosinase mutants still show GL turnover (Barth and Jander, 2006). Further work is necessary to shed light on the significance of HOL in GL catabolism. To begin with, it is of special interest to find out whether the detoxification of  $\text{SCN}^-$  is important in undamaged or damaged tissue. A thorough analysis of the accumulation of GL hydrolysis products in WT, *hol* and *35S::HOL* plants could help to answer this question.

To investigate the effects of HOL activity on plant-herbivore interactions, WT, *hol* and *35S::HOL* plants were subjected to herbivory. Two herbivores were tested. Firstly, the performance of *Plutella xylostella* larvae was tested when feeding on WT and *hol* plants. The crucifer specialist is not affected by GLs as it possesses a gut sulfatase which converts GLs to inactive desulfoglucosinolates, which cannot be hydrolysed by myrosinases (Ratzka *et al.*, 2002). Moreover, since *HOL* is mainly expressed in the roots of *A. thaliana*, we also tested the survival of the generalist root feeder *Bradysia paupera* when feeding on WT, *hol* and *35S::HOL* roots. Overall, our results indicate that neither *P. xylostella* nor *B. paupera* larvae were negatively affected by methyl halide emissions or other effects of HOL activity. Moreover, the choice experiment showed that methyl halides or sulphur volatiles neither attracted nor repelled *B. paupera* flies when searching for a host plant.

In future experiments, it could be interesting to monitor the performance of *P. xylostella* when feeding on *35S::HOL* lines. Moreover, the *B. paupera* experiments could be further improved. In our study, we monitored the emergence of adults from a constant number of eggs washed onto the soil. There was a large variance between the samples within one group, which could be caused by differences in egg viability and may blur any potential impact of methyl halides. A useful experimental set-up for future experiments could be the method described by Vaughan *et al.* (2011) which uses a relatively simple aeroponic culture system to study root herbivory in the *Bradysia-Arabidopsis* model system. In this set-up, plants are grown in Seramis clay granules and infested with large numbers of larvae. In addition to counting the emergence of flies, this system also allows monitoring of the feeding damage on the roots.

To test whether the production of methyl halides could affect the composition of the microbial community of the *A. thaliana* rhizosphere, DNA was extracted from rhizosphere soil of WT, *hol* mutant and *35S::HOL* plants, and a bacterial community profile generated using ARISA. We hypothesised that methyl halides could affect the composition of the rhizosphere community in two ways: (1) It is possible that methyl halides act as toxins to certain bacteria or (2) serve as an energy source for methyl-halide degrading bacteria. No significant differences were detected between the ARISA profiles of WT, *hol* mutant and *35S::HOL* rhizosphere samples 1, 2 or 4 weeks after the start of the experiment. However, there are indications that a minority of bacteria might be affected by methyl halides, especially within the first 2 weeks, however, it is not

clear at this stage which species belong to this minority. PCR amplification and sequencing of 16S rRNA fragments could help to identify these species. Using *cmuA* specific primers, we were unable to find evidence that methyl-halide degrading bacteria were attracted by methyl halide emissions in the roots.

Overall, we observed that the bacterial community structure varied significantly between sampling time points. ARISA profiles of unplanted soil controls were also different from the ARISA profiles obtained from the rhizosphere, however, these differences diminished during the time course of the experiment. These observations are in agreement with the study of Micallef (2009a), which proposed that this is caused by a reduction in the active release of root exudates as plants reach the end of their life-cycle.

To date, only a few studies have investigated the effects of different *A. thaliana* mutants or accessions on rhizobacterial communities, and experimental set-up such as plant growth conditions, type of soil inoculum and sampling techniques vary strongly between these studies (Hein *et al.*, 2008; Bressan *et al.*, 2009; Micallef *et al.*, 2009a; Micallef *et al.*, 2009b). In addition to the experimental set-up described in this study, we also created ARISA profiles from DNA extracted from the rhizosphere of plants grown in sand and watered with nutrient solution. In this case, soil solution was used as an inoculum at the start of the experiment. The rationale behind this experiment was to reduce the carbon content in the soil and therefore promote the growth of bacteria that associate with the root. However, in this set-up, plant growth was generally poor and variable, and ISR fragment numbers were too low to obtain reliable results (data not shown). Further work is necessary to improve the experimental design of such experiments. It could also be useful to monitor the succession of the bacterial community over a longer period of time using several generations of WT, *hol* and *35S::HOL* plants. This can be done by collecting a sample of the rhizosphere soil at the end of the life-cycle of *A. thaliana* and then use it as an inoculum for a new set of young plants.

Despite the fact that we did not find evidence for a role of HOL in plant-insect interactions or plant-microbe interactions in the rhizosphere, it is worth studying other biotic stressors in future experiments. WT, *hol* mutant and *35S::HOL* plants could be tested for their susceptibility towards plant-parasitic nematodes such as *Heterodera schachtii*. It has been shown that viability of *H. schachtii* eggs is significantly reduced by the application of 150 nmol CH<sub>3</sub>I per 50 ml of soil (Ohr *et al.*, 1996). We showed

that WT seedlings grown in Petri dishes produce up to 20 nmol CH<sub>3</sub>I per day, therefore this amount could certainly affect nematodes in close proximity to the roots. It could also be interesting to study the susceptibility of pathogens towards WT, *hol* mutant and *35S::HOL* plants. It has been shown that *hol* seedlings had a reduced survival rate when infected with *Pseudomonas syringae* pv. *maculicola* (Fig. 1.9) (Nagatoshi and Nakamura, 2009). However, this particular experiment can be criticised, as the authors did not use the standard procedure of monitoring bacterial growth by infiltrating the pathogen into the plant and determining number of colony-forming units in plant extracts a few days later.

Finally, future studies need to determine whether *A. thaliana* roots produce the majority of methyl halides as suggested by *HOL* expression patterns. It is also important to determine whether biotic stressors cause changes in *HOL* expression and/or methyl halide emissions.

Additionally, the production of sulphur volatiles such as CH<sub>3</sub>SCN and CH<sub>3</sub>SH needs to be measured from living plants before and after damage to evaluate the significance of these volatiles in plant defence against herbivores or pathogens. The study of Nagatoshi and Nakamura (2009) did only report CH<sub>3</sub>SCN emissions from leaf extracts of *A. thaliana*. CH<sub>3</sub>SCN emissions have been reported in *Brassica nigra* plants, but herbivory did not increase emission levels (Soler *et al.*, 2007). Unfortunately, in the same study, emissions were only measured from plants including the soil and not from soil alone. Thus, it cannot be ruled out that CH<sub>3</sub>SCN was produced by microorganisms in the soil. Similarly, CH<sub>3</sub>SH emissions have been detected from rice paddies (Nouchi *et al.*, 1997), but emission levels coincided with those from unvegetated sites indicating that CH<sub>3</sub>SH was emitted by algae, phytoplankton and microorganisms living in the flood water or soil.



## **Chapter 6 – Characterisation and manipulation of methyl halide production in *Brassica rapa*, *Oryza sativa* and the moss *Physcomitrella patens***

### **6.1 Introduction**

#### **6.1.1 Methyl halide production in crop plants**

Methyl halides contribute to ozone degradation in the atmosphere and extensive research has been conducted to identify the sinks and sources of these compounds in the environment (Chapter 1). It was discovered that significant amounts of methyl halides are produced by rice (*Oryza sativa*) and oilseed rape (*Brassica napus*). It is estimated that worldwide rice production is responsible for ca. 1% of atmospheric CH<sub>3</sub>Br and 6% of atmospheric CH<sub>3</sub>I concentrations (Redeker and Cicerone, 2004; Lee-Taylor and Redeker, 2005). Similarly, oilseed rape fields account for up to 4% of the global sources of CH<sub>3</sub>Br emissions (Gan *et al.*, 1998; Mead *et al.*, 2008). Although these numbers seem to be negligible at the moment, the production of methyl halides by crop plants could pose a risk in the future due to the steady increase of the human population and the demand for increased cultivation of crop plants. Production of oilseed rape has risen almost 20-fold from 3.6 million tonnes in 1961 to 59 million tonnes in 2010 (Fig. 6.1 A). It is not clear how long this trend is going to continue, but since oilseed rape is recently also being used for the production of biofuels, its cultivation will certainly further increase in the coming decades. Rice production has also steadily increased from 215 million tonnes to 672 million tonnes in the last 50 years (Fig. 6.1 B) and remains one of the most important food sources.

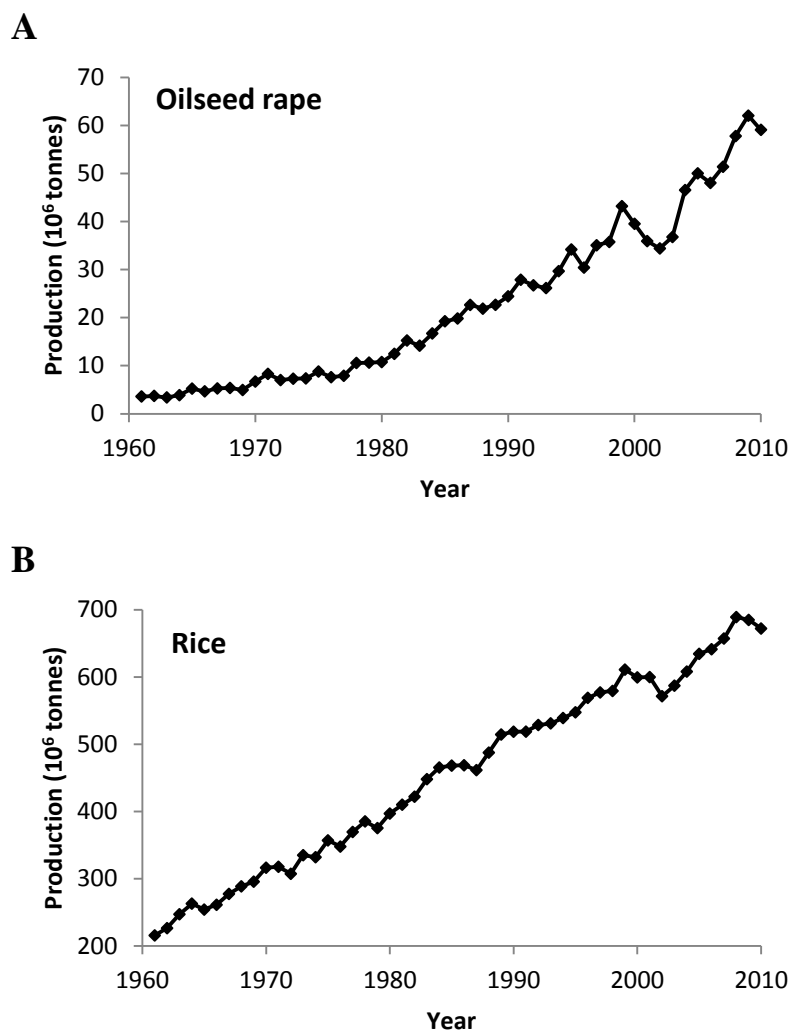


**Figure 6.1. Global production rates for oilseed rape and rice from 1961-2010.** Data for oilseed rape (**A**) and rice (**B**) were obtained from FAOSTAT (<http://faostat.fao.org/>).

In addition to an increased cultivation of oilseed rape and rice, the effects of climate change could also accelerate methyl halide production in these crops. It has been shown that methyl halide emissions from rice are strongly influenced by temperature (Redeker and Cicerone, 2004). It was estimated that a temperature increase of  $1^{\circ}\text{C}$  could increase  $\text{CH}_3\text{Br}$  and  $\text{CH}_3\text{I}$  emissions from this crop by 10% (Lee-Taylor and Redeker, 2005). Moreover, it has been shown previously that methyl halide production in *A. thaliana*, *B. rapa*, oilseed rape and rice positively correlates with the concentration of halide ions in the soil or growth medium (Gan *et al.*, 1998; Rhew *et al.*, 2003; Redeker and Cicerone, 2004; Armeanu-D'Souza, 2009). This highlights some potential risks associated with the development of salt tolerant crops which can be grown in saline soils (Flowers, 2004) as they could become significant emitters of methyl halides and threaten the ozone layer.

Taken together, these problems highlight the importance of identifying the genes that regulate the production of methyl halides in rice and oilseed rape as this could pave the way for the generation of “ozone-safe” crop varieties.

### **6.1.2 The moss *Physcomitrella patens* – a model for understanding the molecular basis of plant development and evolution**

Mosses (Bryophytes) represent one of the oldest groups of land plants. They are believed to have originated 400-450 million years ago (Kenrick and Crane, 1997). Their morphology and life cycle is distinct from that of higher plants. The haploid stage (gametophyte), comprising protonema and gametophores, is the dominant phase of the life cycle which facilitates mutagenesis and genetic analysis (Cove, 2005; Frank *et al.*, 2005). In the last 15 years, *Physcomitrella patens* has been established as a model organism and has been used to understand the evolution of genes and gene regulatory networks in plants (Sakakibara *et al.*, 2001; Nishiyama *et al.*, 2003; Cove, 2005; Menand *et al.*, 2007; Alboresi *et al.*, 2010). This development has been further accelerated by the release of the sequenced genome (Quatrano *et al.*, 2007).

*P. patens* could therefore be a valuable tool to understand the evolution and function of methyl halide production in plants. Methyl halide emissions have been reported for several plant species including dicots, monocots, ferns and green algae (Chapter 1), and *A. thaliana* *HOL*-homologous genes can be found in numerous plant species throughout the plant kingdom (Chapter 7). There are indications that mosses produce methyl halides since emissions have been detected in peatland ecosystems whose predominant vegetation consisted of mosses and grasses (Dimmer *et al.*, 2001), however, this has not been confirmed to date.

### **6.1.3 Objectives of this chapter**

The main objectives of this chapter were to characterise the production of methyl halides in the two crop plants *Brassica rapa* and rice (*Oryza sativa*) and to identify the genes involved in the production of these compounds by isolating and characterising putative *hol* mutants from TILLING populations of *B. rapa* and rice. The diploid *B. rapa* is an ancient progenitor of *B. napus* and has been chosen here to simplify genetics compared to the polyploid *B. napus*. Moreover, it was tested if methyl halide emissions

can be detected in the moss *Physcomitrella patens* to elucidate whether methyl halide production is an ancient mechanism that has evolved early in land plants.

## 6.2 Results

### 6.2.1 Manipulation of methyl halide production in *Brassica rapa*

Previous work in the lab has confirmed that various oilseed rape varieties and the *B. rapa* variety R-o-18 used in this study produce methyl halides (Fig. 4.1). Moreover, three *A. thaliana* *HOL*-homologous genes were identified and cloned in *B. rapa* (Armeanu-D'Souza, 2009). Analysis of the recently sequenced *B. rapa* genome revealed that there are in fact four *HOL*-homologous genes in this species. Phylogenetic analysis showed that two of these genes are more similar to *HOL*, whereas the other two are more similar to *HLL2* (Fig. 6.2, Suppl. Fig. 6.1). The genes were therefore named *BraA.HOL.a*, *BraA.HOL.b*, *BraA.HLL.a* and *BraA.HLL.b* according to the standardised *Brassica* gene nomenclature (Østergaard and King, 2008). *BraA.HOL.a* and *BraA.HLL.a* are located in tandem on chromosome A4. Similarly, *BraA.HOL.b* and *BraA.HLL.b* are located in tandem on chromosome A5 (Suppl. Fig. 6.2). These regions of chromosome A4 and A5 correspond to the region of chromosome II of *A. thaliana*, where *HOL* and *HLL2* are located (Parkin *et al.*, 2005). The amino acid sequences of *BraA.HOL.a* and *BraA.HOL.b* are 84% and 85% identical to *A. thaliana* *HOL*, respectively. As expected, phylogenetic analysis also showed that *BraA.HOL.a* and *BraA.HOL.b* are orthologous to *B. oleracea* *TMT2* and *TMT1*, respectively (Fig. 6.2).

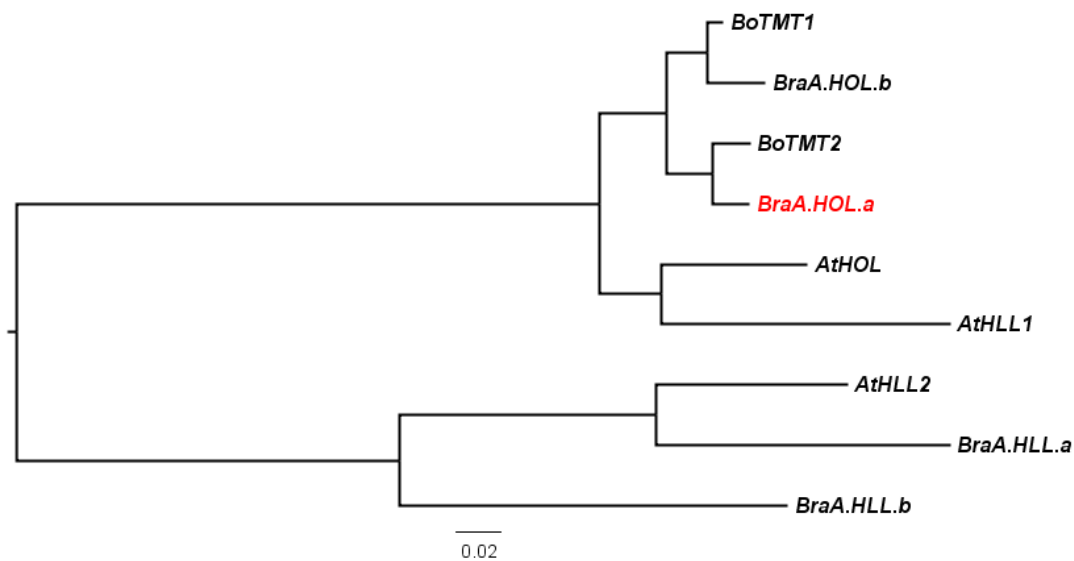


**Figure 6.2. Phylogenetic relationship between *HOL*-homologous genes from *A. thaliana*, *B. rapa* and *B. oleracea*.** Full-length protein sequences were aligned using ClustalX (Suppl. Fig. 6.1). The PHYLIP package was used to construct a neighbour-joining tree based on a JTT distance matrix. The gene targeted in the TILLING assay is highlighted in red. The scale bar refers to the number of amino acid substitutions per site.

To test if *BraA.HOL.a* has the same function as *A. thaliana HOL*, we identified and characterised putative loss-of-function mutants of this gene from a *B. rapa* TILLING population generated at JIC (Stephenson *et al.*, 2010). Previous work in the lab has confirmed that *BraA.HOL.a* is expressed in the plant (Armeanu-D'Souza, 2009). A 1.2-kb fragment of *BraA.HOL.a* was screened for point mutations and three alleles, *braA.hol.a-1*, *braA.hol.a-2* and *braA.hol.a-3* (for simplicity referred to as *hol.a-1*, *hol.a-2* and *hol.a-3*), were selected for further analysis. The *hol.a-1* allele has a mis-sense mutation changing glycine to aspartic acid (G33D), whereas *hol.a-3* allele has a mis-sense mutation in a conserved region changing proline to leucine (P128L) (Suppl. Fig. 6.3, 6.4). The *hol.a-2* allele has a splice-site mutation at the end of intron 1 (Suppl. Fig. 6.3) which is expected to abolish the function of the gene. The three mutant lines were back-crossed to WT to reduce the mutation load of the EMS mutagenesis and homozygous individuals were used for the analysis of methyl halide emissions.

Air samples for methyl halide emissions were collected from single plants grown in pots with soil. All three mutant lines showed a significant reduction in either CH<sub>3</sub>Cl or CH<sub>3</sub>Br emissions compared to WT (Fig. 6.3). CH<sub>3</sub>Cl emissions were reduced by 55% in *hol.a-1* and *hol.a-2*, and reduced by 30% in *hol.a-3* (Fig. 6.3 A). CH<sub>3</sub>Br

emissions of line *hol.a-1* were also significantly reduced by 60% compared to WT, whereas  $\text{CH}_3\text{Br}$  emissions of line *hol.a-2* and *hol.a-3* were only marginally lower compared to WT (Fig. 6.3 B). It was not possible to compare  $\text{CH}_3\text{I}$  emissions between genotypes since  $\text{CH}_3\text{I}$  emissions from all plants were too low to exceed background emission levels from unplanted soil control (data not shown). It is possible that the iodine content of the compost was too low and thus, only little  $\text{I}^-$  was taken up by the plants. However, halide ion content needs to be analysed in future experiments to verify this assumption.

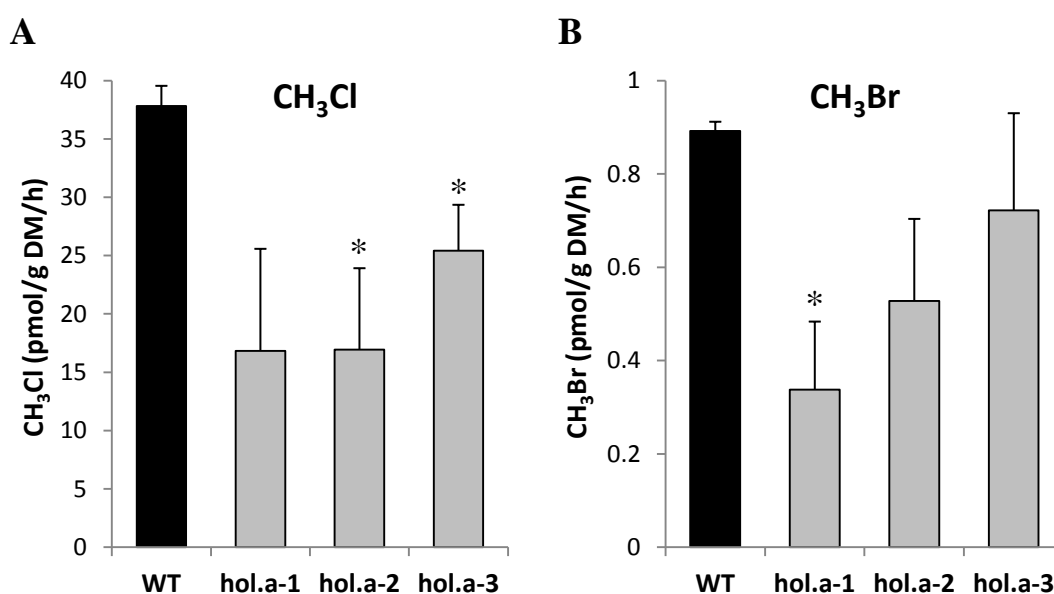


**Figure 6.3. Methyl halide emissions from *B. rapa* WT and *hol.a* mutants.**  $\text{CH}_3\text{Cl}$  (A) and  $\text{CH}_3\text{Br}$  (B) emissions were measured from 18-day-old plants grown in soil in the glasshouse.  $\text{CH}_3\text{I}$  emissions were not detected. Air samples were taken 6 h after enclosure. Background methyl halide emissions were also determined from soil control and subtracted from the amounts detected from enclosed plants. Data points are the mean  $\pm$  s.e. of three biological replicates. Asterisks represent significant differences from WT (t-test,  $p < 0.05$ ).

Since the *A. thaliana hol* mutant was less tolerant towards  $\text{SCN}^-$  than WT (Fig. 3.5), we wanted to test if the same is true for the *hol.a* mutants of *B. rapa*. Seven-day-old *B. rapa* seedlings of WT, *hol.a-1*, *hol.a-2* and *hol.a-3* were watered with either water (Control) or 10 mM KSCN for 9 days. As expected application of 10 mM KSCN inhibited plant growth and caused chlorosis in leaves, however, no significant differences were observed between WT and the *hol.a* mutant lines (data not shown) suggesting that *BraA.HOL.a* does not significantly contribute to KSCN tolerance in *B. rapa*.

Taken together, these results show that *BraA.HOL.a* is involved in methyl halide production in *B. rapa* and therefore has the same function as *A. thaliana HOL*. All three mutations discovered in the TILLING screen impaired the function of *BraA.HOL.a*, however *hol.a-1* and *hol.a-2* were the strongest alleles. Overall, the remainder of  $\text{CH}_3\text{Cl}$  or  $\text{CH}_3\text{Br}$  emission detected in *hol.a* mutants, and the lack of susceptibility towards  $\text{SCN}^-$  can probably be attributed to the activity of the other *HOL* homologue, *BraA.HOL.b*, indicating that *BraA.HOL.a* and *BraA.HOL.b* have a redundant function in methyl halide production and  $\text{SCN}^-$  detoxification in *B. rapa*.

### **6.2.2 Characterisation and manipulation of methyl halide production in rice (*Oryza sativa*)**

Methyl halide emissions from rice plants and rice paddies have been characterised previously (Muramatsu and Yoshida, 1995; Redeker *et al.*, 2000; Redeker *et al.*, 2002; Redeker and Cicerone, 2004; Redeker *et al.*, 2004). In this study, we analysed  $\text{CH}_3\text{Cl}$ ,  $\text{CH}_3\text{Br}$  and  $\text{CH}_3\text{I}$  emissions from three different cultivars of *Oryza sativa* (Nipponbare, CO39 and Bala) using the same sampling technique described for *A. thaliana* and *B. rapa* in this study. No differences in  $\text{CH}_3\text{Cl}$  emissions were detected between the cultivars (Fig. 6.4 A). However,  $\text{CH}_3\text{Br}$  and  $\text{CH}_3\text{I}$  emissions varied between the cultivars, being highest in CO39 and lowest in Nipponbare (Fig. 6.4 B, C). These observations indicate that there might be allelic variation in the genes that control methyl halide production in rice.

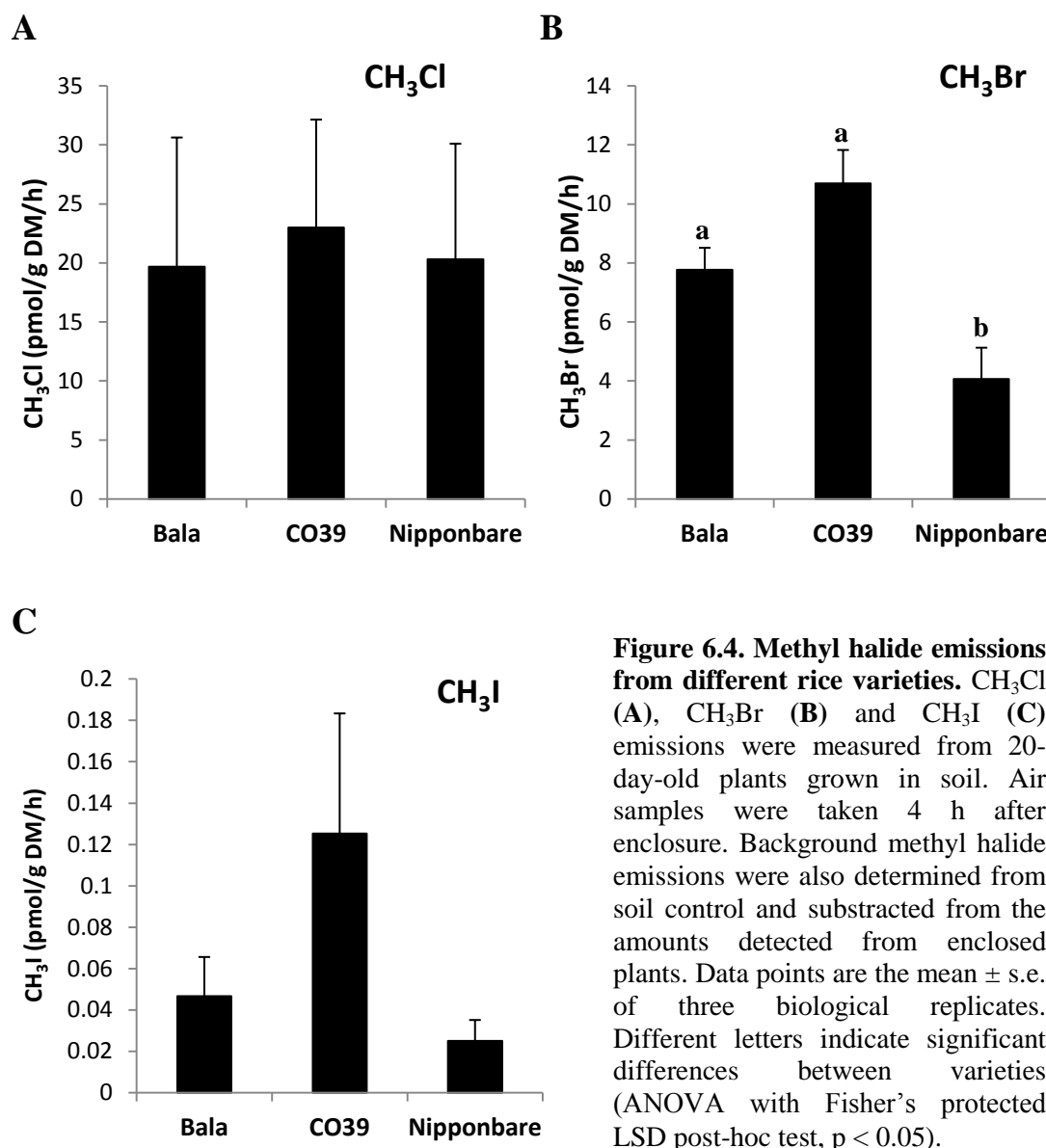


**Figure 6.4. Methyl halide emissions from different rice varieties.** CH<sub>3</sub>Cl (A), CH<sub>3</sub>Br (B) and CH<sub>3</sub>I (C) emissions were measured from 20-day-old plants grown in soil. Air samples were taken 4 h after enclosure. Background methyl halide emissions were also determined from soil control and subtracted from the amounts detected from enclosed plants. Data points are the mean  $\pm$  s.e. of three biological replicates. Different letters indicate significant differences between varieties (ANOVA with Fisher's protected LSD post-hoc test,  $p < 0.05$ ).

To identify the genes that control the production of methyl halides in rice, the rice genome was searched for the presence of *HOL*-homologous genes. Two genes, hereafter referred to as *OsHOL1* and *OsHOL2*, were found which are 51% and 57% identical to *A. thaliana* *HOL*, respectively, based on amino acid sequences (Suppl. Fig. 6.5). *OsHOL1* is located on chromosome III and *OsHOL2* is located on chromosome VI (Suppl. Fig. 6.6). Analysis of rice microarray data from the Genevestigator database (Hruz *et al.*, 2008) showed that *OsHOL1* is mainly expressed in the shoot and leaves and *OsHOL2* is mainly expressed in seedlings, the primary root and the pollen. It was also shown recently that both proteins encoded by these genes are capable of



methylating halide ions when assayed *in vitro* as recombinant proteins previously expressed in *E.coli* (Table 1.2) (Takekawa and Nakamura, 2012).

To test if these genes control methyl halide production *in vivo*, we tried to obtain loss-of-function mutants of *OsHOL1* and *OsHOL2* from a rice TILLING population generated at the University of California, Davis, USA (Till *et al.*, 2007). A 1.4-kb fragment of *OsHOL1* including exons 5-7 and a 1.3-kb fragment of *OsHOL2* including exons 6-8 were screened for point mutations. Unfortunately, only mutations in non-coding regions were identified in a screen of 768 individuals (data not shown).

### **6.2.3 Characterisation and manipulation of methyl halide production in the moss *Physcomitrella patens***

To test if methyl halide production has evolved early in land plants, we measured the production of methyl halides from the moss *Physcomitrella patens* when grown on agar (Fig. 6.5 A). CH<sub>3</sub>Cl, CH<sub>3</sub>Br and CH<sub>3</sub>I concentrations were very low in moss air samples and did not exceed background levels determined in air samples from agar control plates (Fig. 6.5 B, data not shown). This was probably due to the lack of halide ions in the moss as it was grown on minimal medium. We therefore added a 5 mM KBr solution to test if this treatment boosts the production of CH<sub>3</sub>Br. Indeed, the application of Br<sup>-</sup> caused a 16-fold increase in the production of CH<sub>3</sub>Br, whereas no changes were observed in the agar control (Fig. 6.5 B). These results confirm that *P. patens* is capable of producing CH<sub>3</sub>Br.

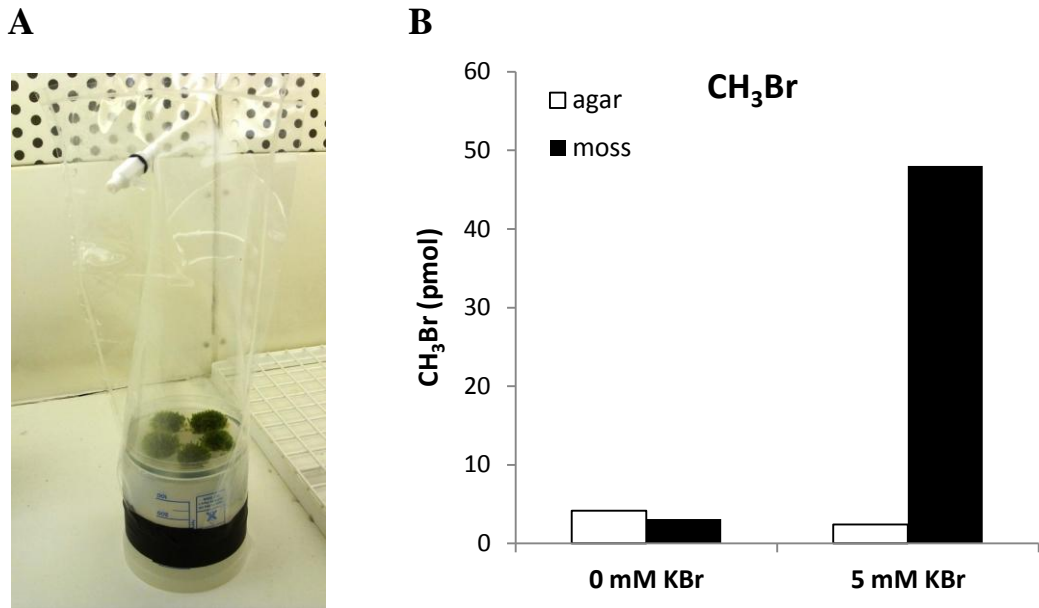


**Figure 6.5. Methyl halide emissions from *P. patens*.**  $\text{CH}_3\text{Br}$  concentrations (**B**) were measured in air samples collected from gametophore colonies grown on agar (**A**) and from agar plates alone (control). Air samples were initially taken from untreated plates (0 mM KBr) two days after enclosure and then for a second time after the addition of 4 ml sterile 5 mM potassium bromide (KBr) solution and enclosure for another two days.

To identify the genes that control the production of methyl halides in *P. patens*, the moss genome was searched for the presence of *HOL*-homologous genes. Only one gene, hereafter referred to as *PpHOL*, was found, which is 47% identical to *A. thaliana HOL*, based on amino acid sequences (Suppl. Fig. 6.7, 6.8). Analysis of *P. patens* microarray data from the Genevestigator database (Hruz *et al.*, 2008) showed that *PpHOL* is expressed in spores, the protonema and gametophores. To investigate if *PpHOL* controls the production of methyl halides in *P. patens*, *PpHol* knockout lines were generated. WT *P. patens* protoplasts were transformed with a gene targeting construct which replaces the endogenous *HOL* gene with an antibiotic resistance cassette by homologous recombination (Fig. 6.6). Transformants are currently being selected and methyl halide emissions will be measured from these lines soon.

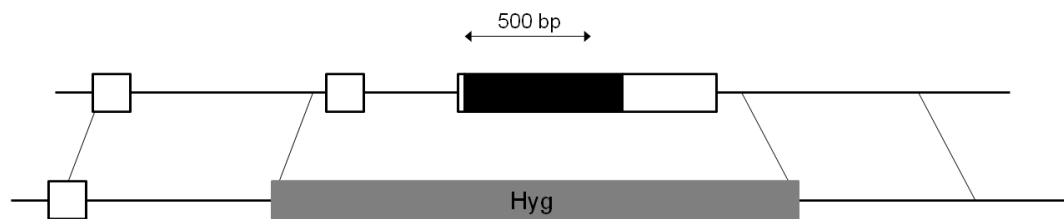


**Figure 6.6. Generation of *Pphol* knockout lines.** Structure of the *PpHOL* gene (Pp1s304\_15V6.2, Phypa\_60954) (up) and the expected results in the *Pphol* knockout after homologous recombination (down). The boxes represent exons with non-coding (white) and coding (black) regions. The grey box indicates the hygromycin resistance gene cassette. The regions of homology used for the gene replacement are delimited by grey lines.

### 6.3 Discussion

The main objectives of this chapter were to characterise the production of methyl halides in *B. rapa* and rice, and to identify the genes involved in the production of these compounds by isolating and characterising putative *hol* mutants from TILLING populations of *B. rapa* and rice.

Two putative *A. thaliana* *HOL*-orthologous genes, *BraA.HOL.a* and *BraA.HOL.b*, were identified in *B. rapa* and three *hol.a* mutant alleles were isolated from a TILLING population. Characterisation of methyl halide emissions from these mutants confirmed that *BraA.HOL.a* controls methyl halide production in *B. rapa* and therefore has the same function as *A. thaliana* *HOL*. Overall, methyl halide production was only reduced by 30-50% in *hol.a* mutants, and they did not show increased susceptibility towards KSCN compared to WT. This is most likely caused by the action of *BraA.HOL.b*. To test if *BraA.HOL.a* and *BraA.HOL.b* are indeed redundant, it is necessary to identify *hol.b* mutants from the TILLING population and to generate a double-mutant via crossing with *hol.a* which can then be tested for methyl halide production. It is also possible that the *HOL*-like genes *BraA.HLL.a* and *BraA.HLL.b* could contribute to methyl halide production in *B. rapa*. However, given that *HOL* alone is responsible for the bulk of methyl halide production in *A. thaliana*, it is likely that *BraA.HOL.a* and *BraA.HOL.b* are as well in *B. rapa*.

Interestingly, all three mutations discovered in the TILLING screen impaired the function of *BraA.HOL.a*. In the case of the *hol.a-2* mutant, this was expected as this line carries a splice-site mutation. The *hol.a-3* mutant has a mutation at a residue that is

conserved in all plant HTMTs except *Selaginella moellendorffii* *HOL* (Suppl. Fig. 6.4, Suppl. Fig. 7.1). This indicates that this residue is important for enzyme function, and our data suggest that it facilitates the binding of chloride since  $\text{CH}_3\text{Cl}$ , but not  $\text{CH}_3\text{Br}$  emissions, were reduced in the *hol.a-3* mutant. Surprisingly, the G33D mutation in the *hol.a-1* mutant also negatively affected the function of the enzyme despite the fact that the D-variant is present in HTMT proteins of monocots (Suppl. Fig. 6.4, Suppl. Fig. 7.1). It would be interesting to test in future experiments if  $\text{CH}_3\text{I}$  emissions are reduced in the *hol.a-1* mutant to test if this residue also affects the binding of iodide. Unfortunately, in our experiment  $\text{CH}_3\text{I}$  emissions from *B. rapa* plants were too low to exceed background emission levels from unplanted soil control. This problem can be avoided by application of small amounts of iodide to the soil in future experiments.

It is believed that the diploid *Brassica* genome has undergone a triplication event after diverging from the common ancestor of *Arabidopsis* and *Brassica* about 20 million years ago (Yang *et al.*, 1999; Lysak *et al.*, 2005; Parkin *et al.*, 2005). Therefore, up to three copies are expected to be found in diploid *Brassica* genomes for each single-copy *Arabidopsis* gene. Since we found only two *HOL*-orthologous genes in *B. rapa*, it is likely that one copy was lost. Similarly, only two *HOL*-like genes, *BraA.HLL.a* and *BraA.HLL.b* were identified in *B. rapa*. Based on phylogenetic analysis they are most closely related to *A. thaliana HLL2*. This suggests that one copy of this gene was also lost in *B. rapa*. Moreover, it is highly likely that *A. thaliana HLL1* originated from a duplication event after the divergence of *Arabidopsis* and *Brassica*.

The identification of one of the genes involved in methyl halide production in *B. rapa* provides the basis for identifying the relevant genes in *B. napus* (oilseed rape). *B. napus* is an amphidiploid species containing two diploid genomes (AACC) originating from the hybridisation of *B. rapa* (AA) and *B. oleracea* (CC) (U, 1935). So far, only two *A. thaliana HOL*-homologous genes, *TMT1* and *TMT2*, have been identified in *B. oleracea* (Attieh *et al.*, 2002). It is therefore likely that four genes contribute to methyl halide production in oilseed rape. The sequencing of the *B. napus* genome is ongoing and will be a useful resource to confirm how many genes control methyl halide production in this crop.

In addition to oilseed rape, rice has also been shown to be a strong producer of methyl halides. Most of the studies have focussed on quantifying the amounts emitted by rice paddies, and it was shown that  $\text{CH}_3\text{Br}$  and  $\text{CH}_3\text{I}$  are emitted by rice plants, whereas

CH<sub>3</sub>Cl is not since unplanted fields emitted as much CH<sub>3</sub>Cl as planted rice fields (Redeker *et al.*, 2000; Redeker and Cicerone, 2004; Redeker *et al.*, 2004). However, in this study, we showed that CH<sub>3</sub>Cl is produced by rice plants and was also the most abundant methyl halide. It is possible that algae or microorganisms in the water of the flooded rice fields masked CH<sub>3</sub>Cl emissions originating from the rice plants in previous studies, whereas the experimental set-up used in this study makes it possible to accurately quantify methyl halide emissions from rice. Overall, our results indicate that there might be allelic variation in the genes that control methyl halide production in rice since methyl halide emission profiles varied between different cultivars.

The methyl halide emission data obtained in this study have been used to estimate current and future global emissions of methyl halides from rice (Newton, 2011). Future rice yields were extrapolated using the linear upwards trend of rice production shown in Fig. 6.1 B. Current CH<sub>3</sub>Br emissions were estimated to be 1.1 kt/year which is similar to the value (0.7 kt/year) used in the current WMO report (Montzka *et al.*, 2011). CH<sub>3</sub>Cl estimates (1.6 kt/year) are slightly lower than the values (2.4-4.9 kt/year) reported by Lee-Taylor and Redeker (2005). Surprisingly, our estimated CH<sub>3</sub>I values (0.014 kt/year) were at least three orders of magnitude lower than figures (16-29 kt/year) reported previously from rice paddies (Lee-Taylor and Redeker, 2005). This suggests that large amounts of CH<sub>3</sub>I are produced by algae or microorganisms in the water of the flooded rice fields. Overall, it was predicted that methyl halide emissions are expected to increase 2.3-fold by the end of this century (Newton, 2011).

Analysis of the sequenced genome showed that there are two *A. thaliana* *HOL*-homologous genes, *OsHOL1* and *OsHOL2*, in rice. It was recently shown that both proteins encoded by these genes are capable of methylating halide ions when assayed in vitro as recombinant proteins previously expressed in *E.coli* (Table 1.2) (Takekawa and Nakamura, 2012). Unfortunately, no useful alleles were obtained for *OsHOL1* or *OsHOL2* from the UC Davis TILLING population. At the time when our TILLING screen was initiated (2009), the screening was still in the test phase and the screening of only 768 individuals lasted two years. Nowadays, 5000 individuals could be screened in about 3-6 months which could lead to the identification of potential mutant alleles of *OsHOL1* and *OsHOL2*. Alternatively, other mutant resources, such as T-DNA insertion lines, could be screened to identify mutant lines (Krishnan *et al.*, 2009) which could then be tested for their ability to produce methyl halides. Indeed, we identified a T-DNA

insertion line (03Z11CN32) in the rice mutant database of the National Centre of Plant Gene Research, Wuhan, China (<http://rmd.ncpgr.cn/>) with a putative T-DNA insertion in *OsHOL2*, but unfortunately the stock centre had lost this line.

Finally, it was tested if methyl halide emissions can be detected in the moss *Physcomitrella patens*. Initially we did not detect any CH<sub>3</sub>Cl, CH<sub>3</sub>Br and CH<sub>3</sub>I emissions when plants were grown on agar. However, the application of a KBr solution strongly increased CH<sub>3</sub>Br emissions confirming that *P. patens* is capable of producing CH<sub>3</sub>Br. This experiment also showed again the positive correlation between methyl halide emissions and halide content in the growth substrate. More experiments need to be conducted to analyse if *P. patens* also produces CH<sub>3</sub>Cl and CH<sub>3</sub>I. To do so, plants need to be grown in soil or in medium enriched with halide ions. Nevertheless, this initial experiment suggests that methyl halide production is an ancient mechanism that has evolved early in plants, and it is the first proof that mosses can also produce these ozone-depleting compounds.

One *A. thaliana* *HOL*-homologous gene was identified in the genome of *P. patens*. Several *Pphol* knockout lines were generated and are currently being selected. Analysis of methyl halide emissions from these lines will show if *PpHOL* controls the production of these compounds in the moss. Moreover, the knockout lines can then be used to further investigate the function of methyl halide production in plants.

## Chapter 7 – Evolution and functional diversity of *HOL*-homologous genes in plants

### 7.1 Introduction

#### 7.1.1 Plant halide/thiol methyltransferases – a unique class of SAM-dependent methyltransferases

S-Adenosyl-L-methionine (SAM)-dependent methyltransferases (MTs) are a diverse group of enzymes involved in the methylation of various substrates. Some MTs exhibit a strict specificity for one substrate, whereas others can methylate a wide range of substrates. Overall, MTs can be divided into specific groups according to their tertiary structure (Class I – V) or based on the atoms of the substrate they methylate (*O*-, *N*-, *C*- and *S*-MTs). The amino-acid sequence similarity between SAM-dependent MTs can be as low as 10%, even within a particular class, showing that the structural and catalytic requirements for methyltransfer from SAM are very flexible (Schubert *et al.*, 2003; Kozbial and Mushegian, 2005; Roje, 2006). In plants, *O*-MTs are involved in the biosynthesis of lignins and many plant secondary metabolites such as alkaloids and flavonoids. *N*-MTs act mainly on proteins, DNA and histones and therefore play an important part in the regulation of gene expression. *C*-MTs are known to be involved in the biosynthesis of lipids and vitamin E in plants (Roje, 2006).

The discovery of halide/thiol MTs (HTMTs) in plants such as *HOL* or TMTs (Chapter 1) revealed a novel class of SAM-dependent MTs who catalyse the production of ozone-depleting methyl halides and whose function remains puzzling. In addition to HTMTs, only a few other *S*-MTs have been described in plants e.g. methionine MT (Mudd and Datko, 1990) and a unique *S*-/*O*-MT in *Catharanthus roseus* (CrSMT1) of unknown function which can methylate both thiols and hydroxyl groups (Coiner *et al.*, 2006). Almost all HTMTs characterised to date in plants are capable of methylating both halide ions and thiols ( $\text{HS}^-$ ,  $\text{SCN}^-$ ) (Table 1.2). The only exception seems to be the methyl chloride transferase (MCT) from the salt-tolerant plant *Batis maritima* which can methylate halide ions but not  $\text{HS}^-$  (Ni and Hager, 1999). However, most of the enzyme kinetic data have been generated using recombinant proteins expressed in *E. coli*, therefore they can only give an indication about the real catalytic reactions that take place in living plant cells. Moreover, not all the known substrates of HTMTs have

been tested in most cases (Table 1.2). Nevertheless, thiol MT activity tends to be higher in glucosinolate (GL)-containing plants compared to plants without GLs (Table 1.2) (Saini *et al.*, 1995; Attieh *et al.*, 2000a) indicating that the ability to efficiently detoxify GL hydrolysis products may have only evolved in GL-containing plants.

### 7.1.2 Objectives of this chapter

Methyl halide emissions have been reported in numerous plant species throughout the plant kingdom including dicots, monocots, ferns and green algae, and HTMTs have been characterised in several plants species (Chapter 1). In this study, we have also shown that the moss *Physcomitrella patens* is capable of producing methyl halides (Chapter 6). The main objectives of this chapter were to characterise the diversity and evolutionary relationship of HTMTs in land plants. Firstly, natural variation in the *HOL* gene among *A. thaliana* accessions was investigated. Secondly, phylogenetic analyses of known and new *A. thaliana* *HOL*-homologous protein sequences retrieved from sequenced plant genomes were conducted. Moreover, we wanted to test if the putative *HOL* homologues in rice, *P. patens* and the diatom *Phaeodactylum tricorutum* are capable of producing methyl halides and detoxifying  $\text{SCN}^-$  *in planta*. The latter will show whether  $\text{SCN}^-$  detoxification evolved specifically in GL-containing plants such as the *Brassicaceae*. In order to answer this question, *A. thaliana* lines overexpressing these *HOL*-homologous genes were generated and characterised.

## 7.2 Results

### 7.2.1 Natural variation in the *HOL* gene among *A. thaliana* accessions

The diversity of the coding region of *HOL* among *A. thaliana* accessions was analysed using the *Arabidopsis* 1001 genomes browser (<http://signal.salk.edu/atg1001/3.0/gebrowser.php>). Ninety-nine of the 514 accessions show one or more mutations in the coding region of *HOL*, however, only one non-synonymous mutation was identified which leads to a V178D substitution in accessions Bik\_1, C24 and Co\_1. Bik\_1 originated from Lebanon and the other two accessions were found in Portugal. This mutation is therefore not related to a specific geographical region. These results show



that there is little genetic variation in the *HOL* gene among *A. thaliana* accessions. Moreover, the V178D substitution is unlikely to affect enzyme function, as this site is highly variable between HTMT proteins and the D-variant is also found in HTMTs of other members from the *Brassicaceae* family (Suppl. Fig. 6.4).

### 7.2.2 Phylogenetic analysis of HTMT proteins

To understand the diversity and evolutionary relationship of HTMTs in plants, we searched for *A. thaliana* *HOL*-homologous protein sequences in the sequenced genomes of the moss *Physcomitrella patens*, the lycophyte *Selaginella moellendorffii*, and several monocots and eudicots. Together with previously characterised HTMTs (Chapter 1) a total of 34 sequences were used for phylogenetic analyses (Suppl. Table 7.1) which represent the major evolutionary lineages of land plants (Fig. 7.1). The recently described HTMT in the diatom *Phaeodactylum tricornerutum* (Toda and Itoh, 2011), which is similar to HTMTs of higher plants, was included as an outgroup.

Overall, most species whose complete genomes have been sequenced possess only one HTMT gene. However, two or more copies of HTMT were found in *Oryza sativa*, *Setaria italica*, *Vitis vinifera*, *Carica papaya* and in several species within the *Brassicaceae* (see also Chapter 6). This supports the view that several whole-genome duplication events followed by gene loss have occurred during the evolution of flowering plants (Jaillon *et al.*, 2007; Barker *et al.*, 2009; Tang *et al.*, 2010; Jiao *et al.*, 2011).

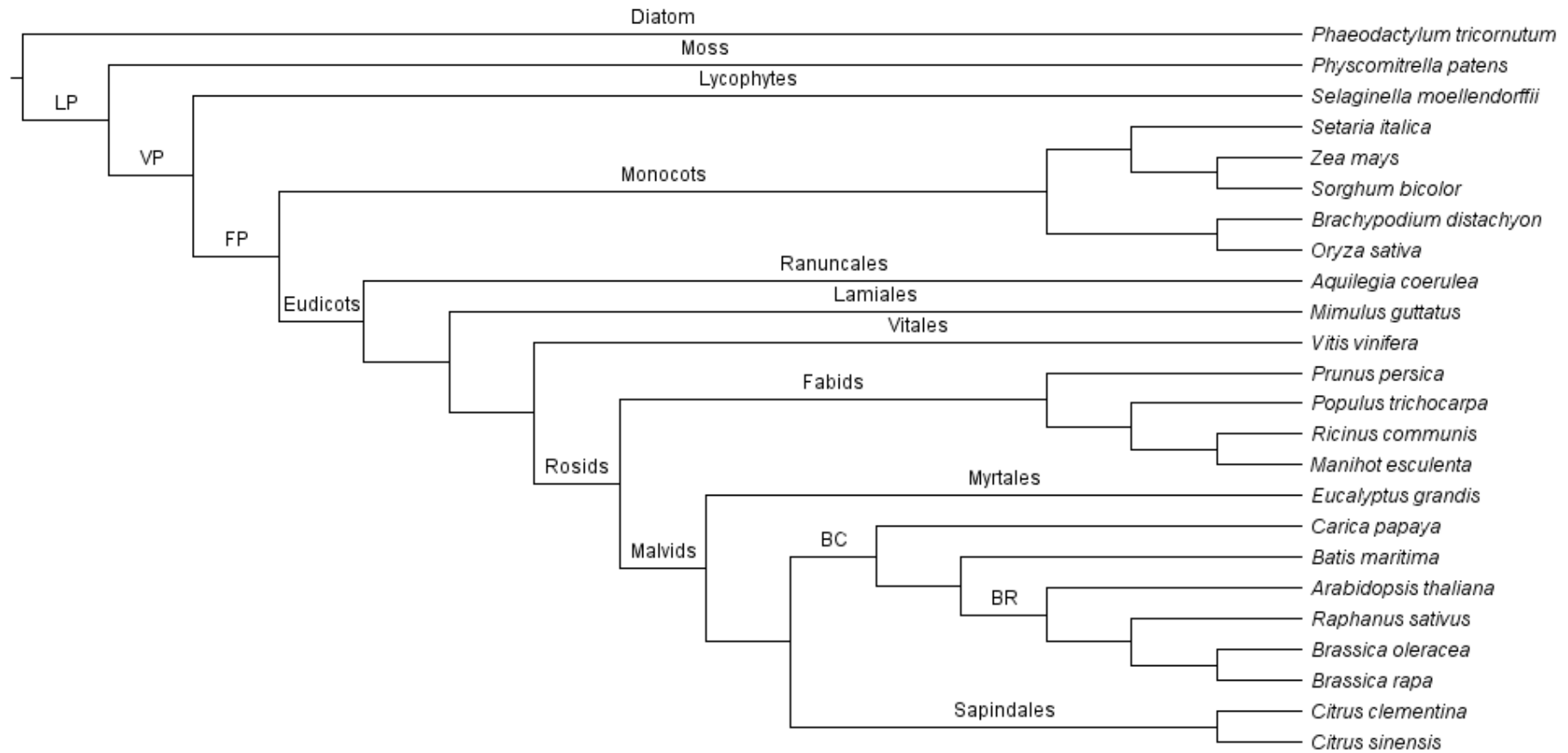


**Figure 7.1. Phylogenetic relationship of the species used in this study.** The cladogram was created using the NCBI Taxonomy browser (<http://www.ncbi.nlm.nih.gov/Taxonomy/CommonTree/wwwcmt.cgi>) and further modified using information available at the Angiosperm Phylogeny website (<http://www.mobot.org/MOBOT/research/APweb/>). LP, land plants; VP, vascular plants; FP, flowering plants; BC, Brassicales; BR, *Brassicaceae*.

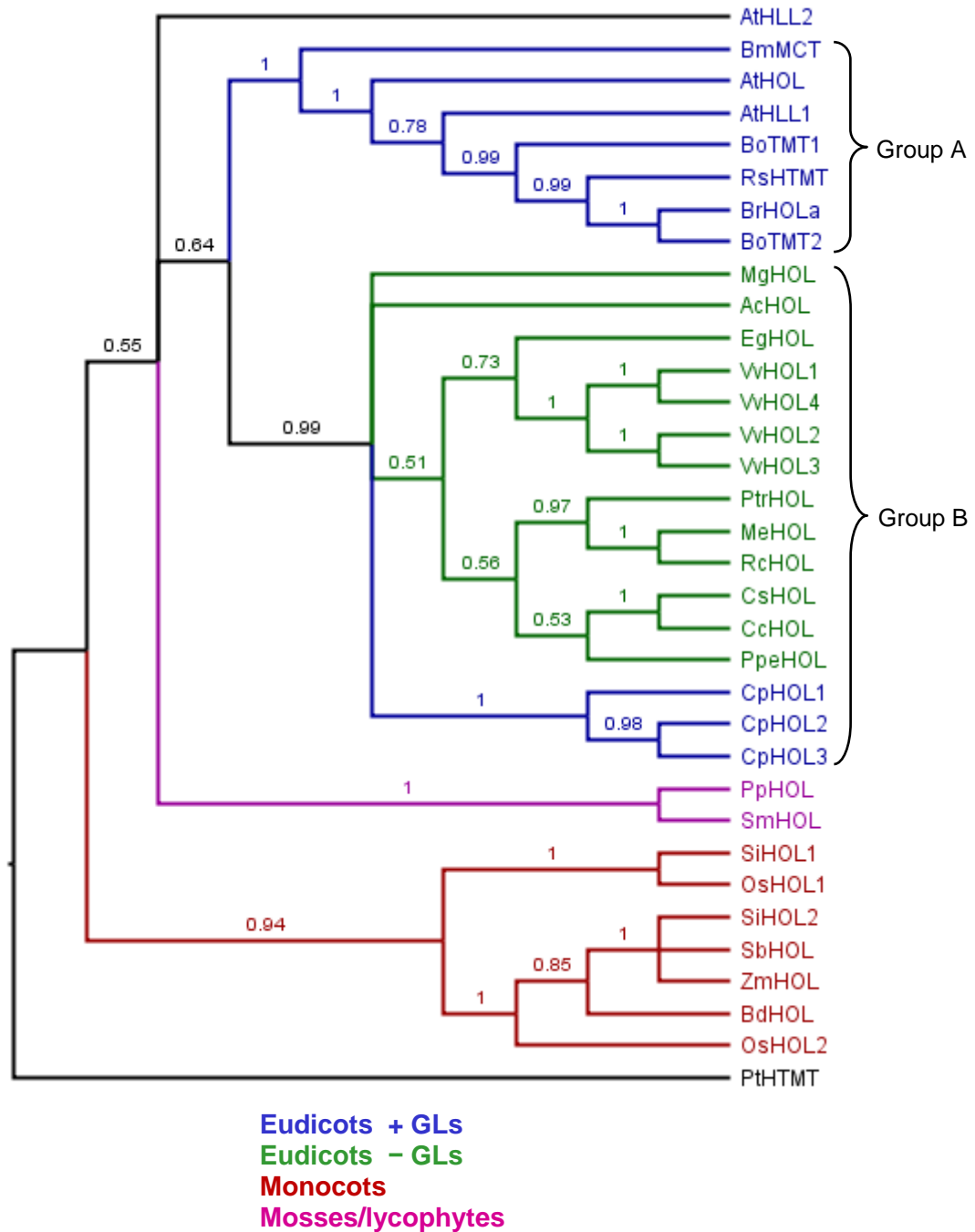


**Figure 7.2. Phylogenetic tree of plant HTMT proteins.** A Bayesian analysis was performed on an alignment of plant HTMT protein sequences (Suppl. Fig. 7.1). The tree was rooted using the *Phaeodactylum tricorutum* HTMT (diatom) as an outgroup. The numbers on the clades are posterior probability values. Clades with support values of less than 0.5 were collapsed. Species names: Ac, *Aquilegia coerulea*; At, *Arabidopsis thaliana*; Bd, *Brachypodium distachyon*; Bm, *Batis maritima*; Bo, *Brassica oleracea*; Br, *Brassica rapa*; Cc, *Citrus clementina*; Cp, *Carica papaya*; Cs, *Citrus sinensis*; Eg, *Eucalyptus grandis*; Me, *Manihot esculenta*; Mg, *Mimulus guttatus*; Os, *Oryza sativa*; Pp, *Physcomitrella patens*; Ppe, *Prunus persica*; Pt, *Phaeodactylum tricorutum*; Ptr, *Populus trichocarpa*; Rc, *Ricinus communis*; Rs, *Raphanus sativus*; Si, *Setaria italica*; Sm, *Selaginella moellendorffii*; Sb, *Sorghum bicolor*; Vv, *Vitis vinifera*; Zm, *Zea mays*.

Phylogenetic trees were computed from the alignment of HTMTs shown in Supplemental Figure 7.1 using Bayesian (Fig. 7.2) and Maximum Likelihood (ML) analysis (Suppl. Fig. 7.2). Both methods yielded trees with similar topology. Overall, the deep evolutionary relationships between most HTMTs were not resolved as most branches had low support values both in the Bayesian and the ML analysis. However, HTMTs of moss/lycophyte, monocots and eudicots all formed separate groups. Interestingly, within the eudicots, two distinct groups of HTMTs (A and B) are supported by both analyses (Fig. 7.2, Suppl. Fig. 7.2). Group A solely contains HTMTs from GL-containing plants (Brassicales), whereas group B contains mainly HTMTs from eudicots without GLs. It can be speculated that this separation reflects functional diversification; perhaps the evolution of the detoxification of GL hydrolysis products by HTMT proteins in GL-containing plants. The only exception is *Carica papaya* (*Caricaceae*) which produces GLs, but whose *HOL* proteins were assigned to group B. Within the Brassicales order, the *Caricaceae* is a sister family to the *Brassicaceae* and *Bataceae* (containing *Batis maritima*) families (Fig. 7.1) (Hall *et al.*, 2004). It can therefore be hypothesised that the potential new function of HTMTs has evolved after the divergence of *Caricaceae* from the common ancestor of *Brassicaceae* and *Bataceae*.

### 7.2.3 Analysis of the putative nucleophile-binding site of HTMT proteins

HTMT proteins have generally little sequence similarity with other SAM-dependent MTs apart from three motifs which are believed to be involved in SAM binding (Kagan and Clarke, 1994; Ni and Hager, 1998). However, amino acid sequence similarity is surprisingly high between HTMT proteins from different plant species and the diatom *P. tricornutum* (Suppl. Fig. 7.1).

Recently, amino acid residues that form the putative nucleophile-binding site in *A. thaliana* *HOL* have been described, and there are indications that variations in these amino acid residues could determine substrate specificity (Fig. 3.1) (Schmidberger *et al.*, 2010). The analysis of the alignment of HTMTs used for phylogenetic analyses in this study shows a high degree of conservation for most of those amino acid residues that form the active site of the enzyme (see black triangles in Suppl. Fig. 7.1). Interestingly, there are two exceptions (see red triangles in Suppl. Fig. 7.1): Firstly, half of the HTMTs have a phenylalanine (F) residue instead of tyrosine (Y) in the putative active site of the enzyme. Despite the fact that these two amino acids have similar

physicochemical properties, site-directed mutagenesis showed that in AtHOL, the tyrosine residue is important for the binding of the smaller chloride nucleophile since the Y172F variant showed reduced efficiency with chloride ions compared to the WT variant of the enzyme (Schmidberger *et al.*, 2010). The F-variant is found mainly in HTMTs belonging to group B, whereas the Y-variant is present in all HTMTs of group A and in monocots. Variation at this site might therefore affect the efficiency of methyl chloride production in different plant species.

Secondly, HTMTs from group A are the only members which have a valine (V) residue in the putative nucleophile-binding site, whereas all other HTMTs possess a threonine (T) residue instead. The physicochemical properties of these amino acids are different and could therefore affect substrate specificity. The valine residue may be the factor that enables HTMTs from group A to efficiently bind and methylate thiols.

#### **7.2.4 Cross-species complementation experiments**

Transgenic *A. thaliana* plants overexpressing *HOL*-homologous genes from rice, *P. patens* and the diatom *P. tricornutum* were generated to test if (1) these genes are capable of producing methyl halides *in planta* and (2) if the ability to efficiently detoxify GL hydrolysis products is confined to GL-containing plants such as *A. thaliana*.

Generally, the full-length coding sequences of each of the *HOL*/*HTMT* genes were cloned into the pBIN-JIT binary vector, which contains a tandem repeat of the CaMV 35S promoter and which was also used to generate the *35S::HOL* lines characterised in previous chapters. Both *A. thaliana* WT and the *hol* mutant were transformed with the constructs. Tests showed that the original *hol* mutant, which was obtained from the SALK T-DNA collection, had lost the kanamycin resistance provided by the T-DNA. However, when *hol* plants transformed with the pBIN-JIT plasmid were grown on kanamycin, it turned out that the kanamycin resistance gene of the plasmid was partially silenced making the selection of healthy transgenic seedlings difficult (data not shown). For this reason, homozygous transgenic lines in the WT background have only been obtained so far and were characterised in this study.

#### 7.2.4.1 Generation and characterisation of *35S::OsHOL1* and *35S::OsHOL2* lines

Two *A. thaliana* *HOL*-homologous genes were identified in rice and named *OsHOL1* and *OsHOL2* (Chapter 6). Two independently transformed lines (3-2 and 4-2) overexpressing *OsHOL1*, and two independently transformed lines (1-A and 3-C) overexpressing *OsHOL2* were generated. It was confirmed by qPCR that all *35S::OsHOL1* and *35S::OsHOL2* lines expressed the respective transgene, whereas no expression was detected in WT seedlings (Fig. 7.3). Transcript levels were quantified relative to *AtHOL* expression and ranged from 0.8 -1. Despite the fact that *OsHOL1* and *OsHOL2* were driven by the same promoter as *AtHOL* in *35S::HOL* lines, gene expression of *OsHOL1* and *OsHOL2* was not as strong. In *35S::HOL* lines, *AtHOL* transcript levels were up to 140-fold higher than WT *AtHOL* levels (Fig. 3.4).

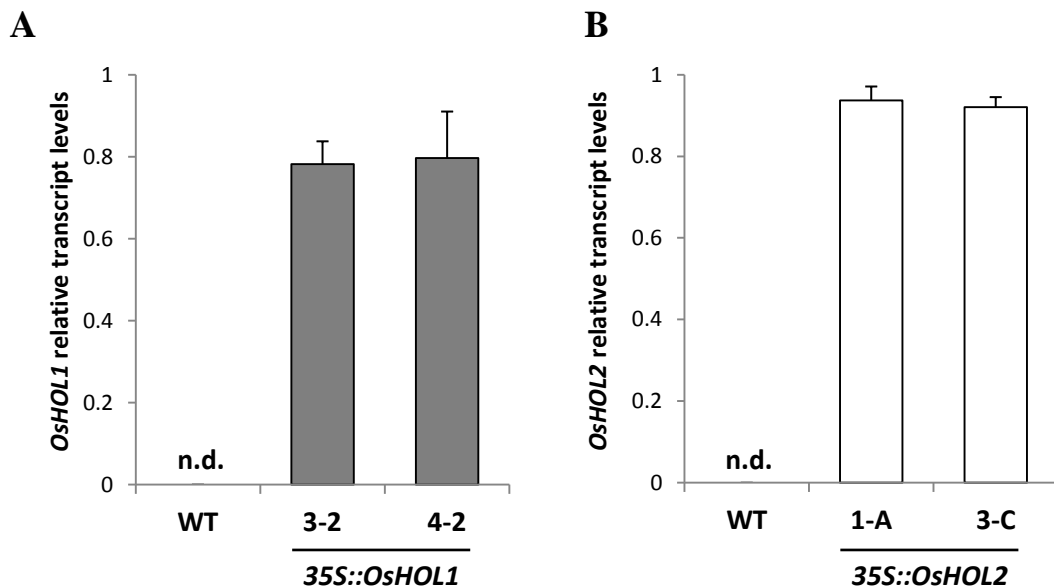
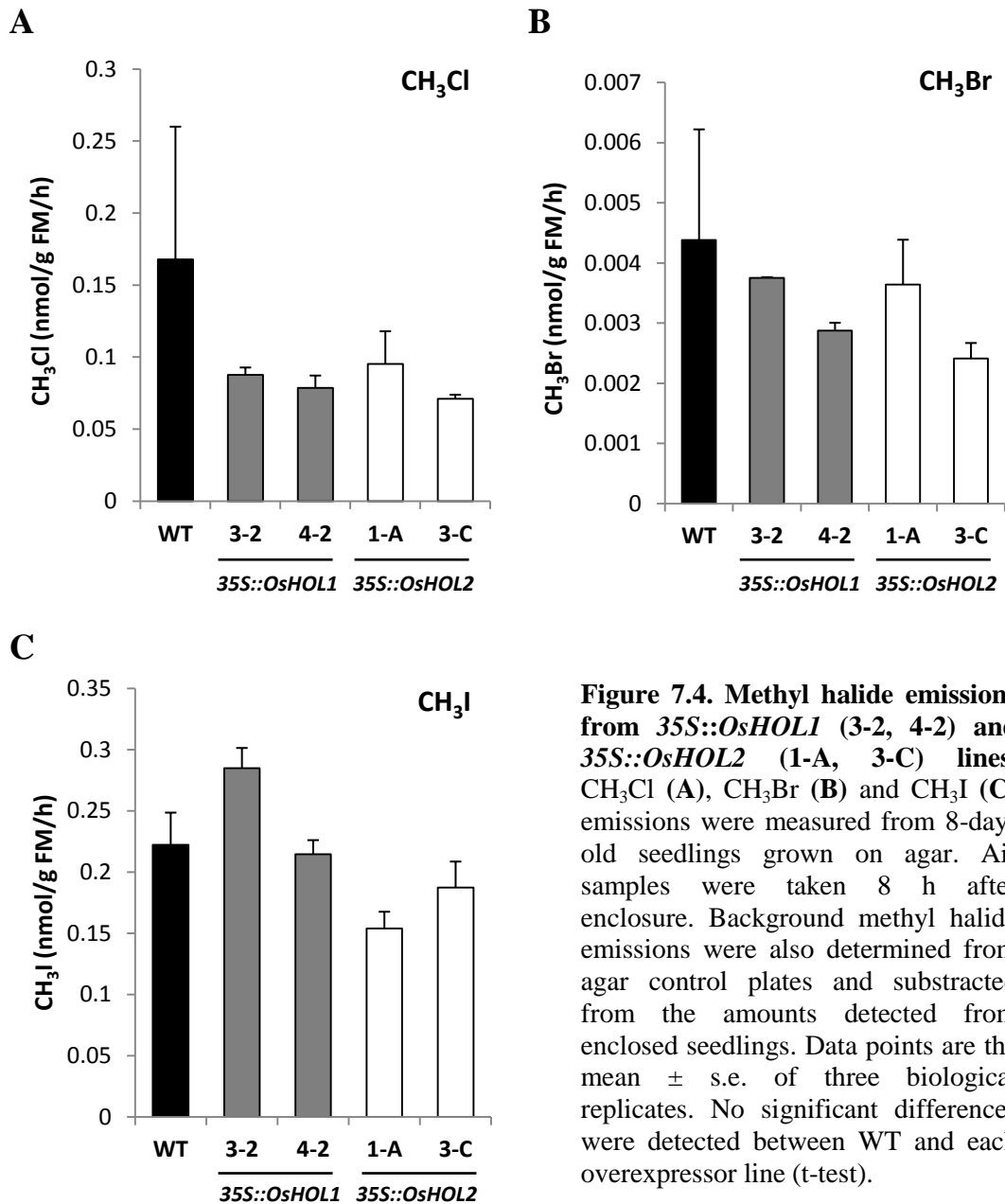


**Figure 7.3. Overexpression of rice *HOL* genes in *A. thaliana*.** Relative transcript levels of *OsHOL1* in *35S::OsHOL1* lines (3-2, 4-2) (**A**) and *OsHOL2* in *35S::OsHOL2* lines (1-A, 3-C) (**B**). Transcript levels were determined in 8-day-old seedlings by qPCR and *OsHOL1* and *OsHOL2* expression normalised to the transcript levels of *AtHOL*. Data points are the mean  $\pm$  s.e. of three biological replicates. n.d. - not detected.

To test if *OsHOL1* and *OsHOL2* control methyl halide production *in planta*,  $\text{CH}_3\text{Cl}$ ,  $\text{CH}_3\text{Br}$  and  $\text{CH}_3\text{I}$  emissions were measured from WT, *35S::OsHOL1* and *35S::OsHOL2* seedlings. No significant differences in methyl halide production were observed between the genotypes (Fig. 7.4). Since it was recently shown that *OsHOL1* and *OsHOL2* exhibit halide MT activity *in vitro* (Takekawa and Nakamura, 2012), our

results indicate that protein levels or enzyme activity of *OsHOL1* and *OsHOL2* might not be high enough in *35S::OsHOL1* and *35S::OsHOL2* plants, respectively, to produce methyl halide amounts that exceed background levels produced by endogenous *AtHOL*.



To test if *OsHOL1* and *OsHOL2* promote tolerance towards SCN<sup>-</sup>, WT, *35S::OsHOL1* and *35S::OsHOL2* seedlings were grown on MS media supplemented with 2.5 mM KSCN. Seedlings of line 196-11 (*35S::HOL*) were included as a positive control. Growth was observed for several days. Overall, *35S::OsHOL1* and *35S::OsHOL2* seedlings showed similar susceptibility towards SCN<sup>-</sup> than WT plants (Fig. 7.5)

indicating that neither *OsHOL1* nor *OsHOL2* contribute to  $\text{SCN}^-$  detoxification. However, protein levels of *OsHOL1* or *OsHOL2* need to be quantified to determine whether they are expressed sufficiently in *35S::OsHOL1* and *35S::OsHOL2* lines.

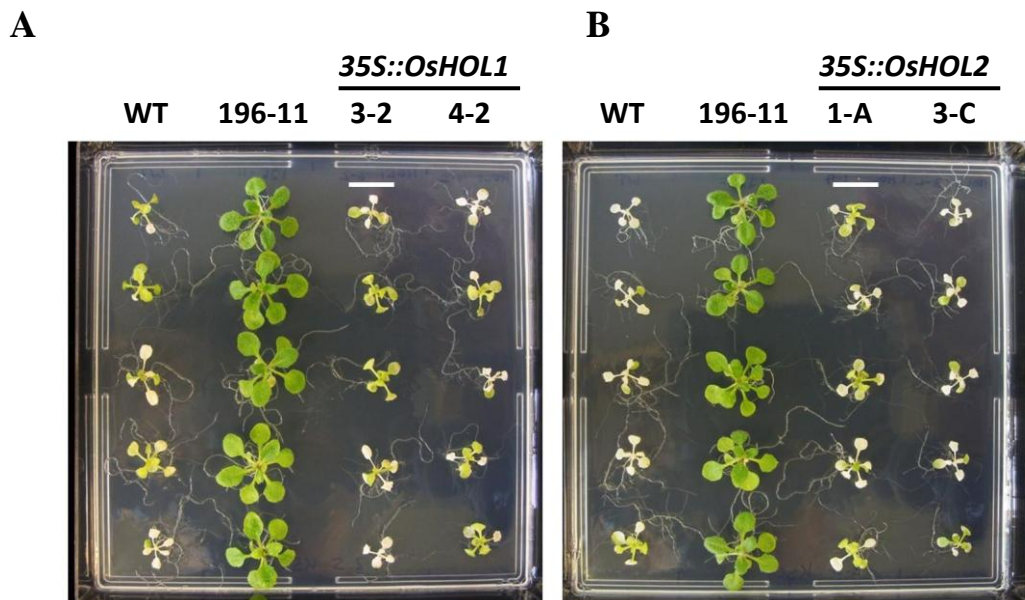


**Figure 7.5. Susceptibility of *35S::OsHOL1* and *35S::OsHOL2* lines towards KSCN.** Nine-day-old seedlings of WT, *35S::HOL* (196-11) and *35S::OsHOL1* (3-2, 4-2) (A) or *35S::OSHOL2* (1-A, 3-C) (B) were transferred to MS media containing 2.5 mM KSCN and pictures taken 7 days later. Scale bar = 1 cm.

#### 7.2.4.2 Generation and characterisation of *35S::PpHOL* lines

One *A. thaliana* *HOL*-homologous gene was identified in *P. patens* and named *PpHOL* (Chapter 6). Three independently transformed lines (1-1, 1-2 and 2-C) overexpressing *PpHOL* were generated. It was confirmed by qPCR that all *35S::PpHOL* lines expressed the transgene, whereas no expression was detected in WT seedlings (Fig. 7.6 A). Out of the three *35S::PpHOL* lines tested, line 2-C had the lowest *PpHOL* expression levels.

To test if *PpHOL* promotes tolerance towards  $\text{SCN}^-$ , WT, 196-11 and *35S::PpHOL* seedlings were grown on MS media supplemented with 2.5 mM KSCN. No differences in  $\text{SCN}^-$  tolerance were detected between WT and *35S::PpHOL* seedlings (Fig. 7.6 B) indicating that *PpHOL* does not contribute to  $\text{SCN}^-$  detoxification. Again, protein levels of *PpHOL* or methyl halide production need to be quantified to determine whether the protein is expressed sufficiently in *35S::PpHOL* lines. *PpHOL*



transcript levels ranged from 0.5-1 in the selected lines (Fig. 7.6 A), and therefore expression of the transgene was not as strong as expression of *AtHOL* in *35S::HOL* lines. Moreover, analysis of methyl halide production in *35S::PpHOL* lines needs to be quantified to test if the *PpHOL* gene controls methyl halide production and has the same function as *AtHOL*.

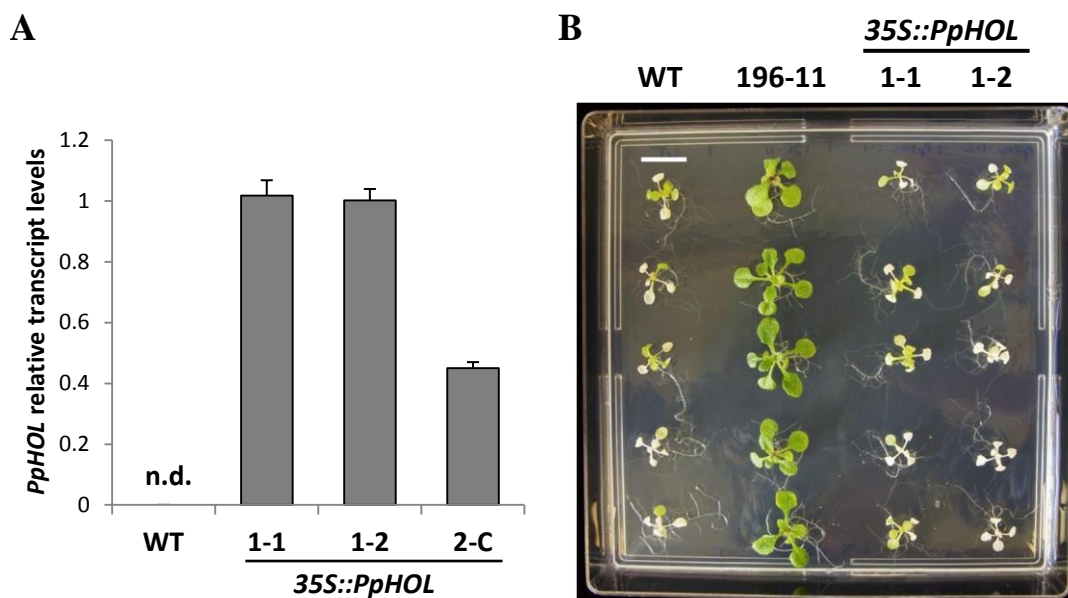


**Figure 7.6. Overexpression of *PpHOL* in *A. thaliana* and susceptibility of *35S::PpHOL* lines towards KSCN. (A)** Relative transcript levels of *PpHOL* in *35S::PpHOL* lines (1-1, 1-2, 2-C). Transcript levels were determined in 8-day-old seedlings by qPCR and *PpHOL* expression normalised to the expression of *AtHOL*. Data points are the mean  $\pm$  s.e. of three biological replicates. n.d. - not detected. **(B)** Eight-day-old seedlings of WT, *35S::HOL* (196-11) and *35S::PpHOL* (1-1, 1-2) were transferred to MS media containing 2.5 mM KSCN and pictures taken 7 days later. Scale bar = 1 cm.

#### 7.2.4.3 Generation and characterisation of *35S::PtHTMT* lines

Oceans are important sources of methyl halides and several marine macro- and microalgae have been reported to produce methyl halides and to possess HTMT activity (Chapter 1). Recently a gene which encodes a HTMT has been cloned in the diatom *Phaeodactylum tricorutum*. The gene shares high similarity with plant HTMT genes and it was shown that the PtHTMT protein is capable of methylating halides and thiol substrates when assayed *in vitro* as a recombinant protein previously expressed in *E.coli* (Table 1.2) (Toda and Itoh, 2011).

To test if PtHTMT is capable of producing methyl halides and to detoxify SCN<sup>-</sup> *in planta*, we overexpressed the full-length coding sequence of *PtHTMT* in *A. thaliana*. Several independently transformed lines of *35S::PtHTMT* were generated, and RT-PCR of hemizygous T2 lines confirmed that the transgene is expressed (data not shown). Homozygous plants are currently being obtained and will then be characterised for methyl halide production and SCN<sup>-</sup> tolerance. qPCR analysis will also be employed to quantify *PtHTMT* expression relative to *AtHOL* expression.

### 7.3 Discussion

The first objective of this chapter was to characterise the diversity and evolutionary relationship of HTMTs in land plants. Firstly, natural variation in the *HOL* gene among *A. thaliana* accessions was investigated. Little genetic variation in the coding sequence of *HOL* was found among 514 accessions. Only one non-synonymous mutation (V178D) was identified, however this mutation is unlikely to affect enzyme function, as the D-variant can be found in HTMTs of *B. rapa*, *B. oleracea* and *R. sativus*. These results suggest that all *A. thaliana* accessions produce methyl halides.

Secondly, phylogenetic analyses of known and new *A. thaliana* *HOL*-homologous protein sequences retrieved from sequenced plant genomes were conducted. Our analysis showed that most species whose complete genomes have been sequenced possess only one HTMT gene. However, two or more copies of HTMT were found in *Oryza sativa*, *Setaria italica*, *Vitis vinifera*, *Carica papaya* and in several species within the *Brassicaceae*. This supports the view that several whole-genome duplication events followed by gene loss have occurred during the evolution of flowering plants (Fig. 7.7) (Jaillon *et al.*, 2007; Barker *et al.*, 2009; Tang *et al.*, 2010; Jiao *et al.*, 2011).

Within the monocot clade we found support for one duplication event as two groups of *HOL* proteins, each comprising one of the two *HOL* proteins of *O. sativa* and *S. italica*, were identified by the phylogenetic analysis. Since both species belong to different clades (Fig. 7.1) (Bouchenak-Khelladi *et al.*, 2008) the gene duplication must have happened before the divergence of *O. sativa* and *S. italica* and indicates that the other monocot species analysed in this study have lost one copy of the *HOL* gene.

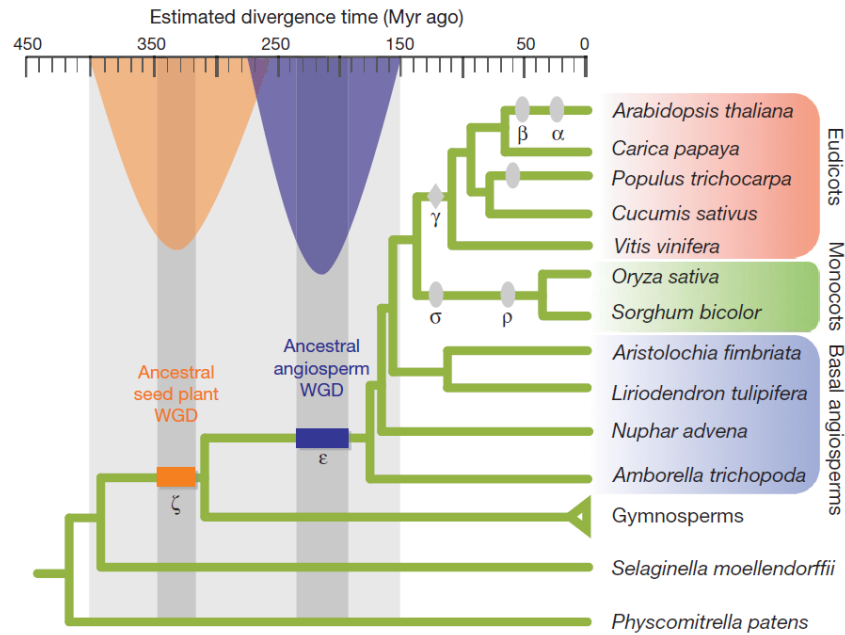


**Figure 7.7. Whole-genome duplication (WGD) events in seed plants and flowering plants.** In addition to two ancestral WGD events (blue and red box), several duplication events (ovals) and one triplication event (diamond) are believed to have occurred in flowering plants. Image taken from Jiao *et al.* (2011).

Within the eudicot clade we also found support for several duplication events as three *HOL/HLL* genes were found in *A. thaliana* and *C. papaya*, and 4 *HOL* genes in *V. vinifera*. However, since the evolutionary relationships are poorly resolved in some branches, especially in group B, it is hard to estimate when these duplication events have happened. Overall, it is likely that many species in the eudicot clade must have lost one or more copies of *HTMT* genes. Four *HOL* genes of *V. vinifera* were found at the NCBI database and included in the phylogenetic analysis, since it was shown that all four proteins possess halide MT activity when expressed and assayed in *E. coli* (Bayer *et al.*, 2009). However, according to the current version of the *V. vinifera* genome (Phytozome v8.0, <http://www.phytozome.net>), the existence of only two *HOL* genes (*VvHOL1* and *VvHOL2*) is supported. Since some parts of the protein sequence of *VvHOL3* and *VvHOL4* are identical to *VvHOL2* and *VvHOL1*, respectively (data not shown), it is possible that they are splicing variants of the latter.

As described in Chapter 6, it is believed that the genomes of the *Brassicaceae* tribe, which includes *B. rapa*, *B. oleracea* and *R. sativus* (Bailey *et al.*, 2006), have undergone a triplication event after the split from *A. thaliana* (Lysak *et al.*, 2005), and therefore up to three copies are expected to be found in those species for each single-

copy *Arabidopsis* gene. In *R. sativus*, only one *HTMT* gene has been cloned so far (Itoh *et al.*, 2009), but it is likely that more *HTMT* genes exist in this species as it is the case in *B. rapa* and *B. oleracea* (Fig. 6.2). Finally, the phylogenetic analysis also showed that AtHLL2 does not share much similarity with any of the HTMT proteins in group A or B. This result is in accordance with the phylogenetic analysis conducted in Chapter 6 (Fig. 6.2) which shows a clear separation between HOL and HLL proteins in the *Brassicaceae*. AtHLL2 showed only little or no MT activity towards halide ions and SCN<sup>-</sup> *in vitro* (Table 1.2) (Nagatoshi and Nakamura, 2007, 2009). It is therefore possible that AtHLL2 may have lost its function.

The most striking result of the phylogenetic analysis was the clear separation of HTMT proteins of eudicots into two groups (A and B). Group A solely contains HTMTs from GL-containing plants (Brassicales), whereas group B (with the exception of *C. papaya* HOL proteins) contains HTMTs from eudicots which do not produce GLs. This observation supports the hypothesis that HTMTs in group A have evolved a new function namely the detoxification of GL hydrolysis products. This hypothesis has been supported by other phylogenetic analyses (Nagatoshi and Nakamura, 2009; Takekawa and Nakamura, 2012), however, the work presented here is the first study that included an extensive list of HTMT genes from several plant species and conducted a thorough phylogenetic analysis using different methods and including statistical significance testing.

Neofunctionalisation of proteins to detoxify GL hydrolysis products is not an unknown phenomenon: Nitrilases, which are involved in the cyanide detoxification pathway by means of hydrolysing  $\beta$ -cyanoalanine, are ubiquitous in the plant kingdom. Interestingly, in the *Brassicaceae*, a new family of nitrilases has evolved which are not able to use  $\beta$ -cyanoalanine as a substrate. Instead they show high enzyme activities towards nitriles that originate from GL breakdown and thus are believed to function in GL catabolism (Janowitz *et al.*, 2009).

To further test the hypothesis that only HTMT proteins from group A are capable of efficiently detoxifying GL hydrolysis products, the HTMT genes of rice, *P. patens* and *P. tricornutum* were expressed in *A. thaliana* WT and the *hol* mutant. This approach also made it possible to investigate if these genes control methyl halide production *in planta*.

None of the overexpressor lines tested so far in the WT background (i.e. *35S::OsHOL1*, *35S::OsHOL2* and *35S::PpHOL*) survived on KSCN media indicating that *OsHOL1*, *OsHOL2* and *PpHOL* are not capable of detoxifying  $\text{SCN}^-$ . However, at this stage it is not clear whether the protein is expressed at sufficiently high levels in the plants to exceed background activity of endogenous *HOL* since *35S::OsHOL1* and *35S::OsHOL2* lines did not emit higher levels of methyl halides than WT plants, and methyl halide emissions have not been quantified in *35S::PpHOL* plants yet. qPCR analysis showed that mRNA from the transgenes did not accumulate to nearly as high levels as mRNA from the *AtHOL* gene in *35S::HOL* lines, although *OsHOL1*, *OSHOL2* and *PpHOL* were cloned and expressed using the same plasmid and 35S promoter. The stable expression of heterologous proteins is influenced by several factors (e.g. RNA stability, codon usage or sequences surrounding the start codon), and these features can vary between different plant species (Joshi *et al.*, 1997; Batard *et al.*, 2000; Desai *et al.*, 2010). Since only the CDS was used to generate the constructs, some of this information might be missing to efficiently express the *HOL* proteins from rice and moss in *A. thaliana*. It is also possible that some post-translational modifications are required for the stability and biological activity of the proteins. Work is currently underway to obtain homozygous lines of *35S::OsHOL1*, *35S::OsHOL2*, *35S::PpHOL* and *35S::PtHTMT* in the *hol* mutant background. Those lines will be subjected to methyl halide measurements and KSCN tests, and these data will then show whether the transgenes encode functional *HOL* proteins, and if the ability to detoxify  $\text{SCN}^-$  is restricted to GL-containing plants.

To find support for the hypothesis that the detoxification of thiol compounds has evolved in HTMTs belonging to group A, it would also be useful to generate *A. thaliana* lines expressing *HOL* genes of *Carica papaya*. Moreover, future experiments could employ site-directed mutagenesis to generate an *A. thaliana* line expressing a V140T variant of *AtHOL* in order to test if the valine at this putative nucleophile-binding site indeed confers resistance to thiol compounds.

## Chapter 8 – Conclusion and Outlook

### 8.1 Summary

Significant amounts of methyl halides are produced by plants in terrestrial ecosystems and therefore contribute to maintain the balance between natural ozone production and destruction in the atmosphere. History has taught us that this balance can be disturbed when increasing amounts of ozone-depleting substances are released into the atmosphere by human activities. It is therefore vital to identify unknown sources of methyl halide production in the environment and to understand the factors influencing the production of these compounds today and in the future.

This study has shown that methyl halide production is an ancient mechanism in plants as it was detected in mosses who have originated 400-450 million years ago. Moreover, genes encoding HTMTs, which control the production of methyl halides, are present in numerous plant species throughout the plant kingdom. This suggests that quantifying methyl halide production in other terrestrial plants harbouring *HTMT/HOL* genes in their genome can probably help to identify unknown natural sources of methyl halides.

We have confirmed by whole-plant measurements that in rice and *Brassica rapa*, significant amounts of methyl halides are produced by living plants rather than by microbial activity in the soil. Moreover, we identified a *HOL* gene (*BraA.HOL.a*) in *B. rapa* which contributes to methyl halide production in this plant. The current contribution of rice and *Brassica* crops to the global methyl halide budget appears to be negligible. However, the production of methyl halides by crop plants could pose a risk in the future, due to the increased cultivation of these plants to meet the demands of food and biofuels for a growing human population, and due to the effects of climate change (e.g. high temperatures) which could promote methyl halide production in crop plants and (most likely) other plants as well.

To shed light on the function of HTMTs and methyl halide production in plants, the model plant *Arabidopsis thaliana* was used. So far, the only described function of *HOL* on growth and development of *A. thaliana* appears to be the detoxification of GL hydrolysis products. Characterisation of *HOL::GUS* and *HOL::HOL:GFP* reporter lines

showed that *HOL* is strongly expressed in the roots. This observation suggested that *HOL* functions in this organ and that the majority of methyl halides are most likely produced by the root in *A. thaliana*. It also initially supported the hypotheses that *HOL* may (1) contribute to salt tolerance via the disposal of excessive amounts of halide ions accumulating in roots upon salt stress or (2) affect the outcome of plant-insect or plant-microbe interactions at the root-soil interface. These two main hypotheses were thoroughly tested in this study.

Overall, we did not find evidence that *HOL* promotes salt stress tolerance in *A. thaliana* since *HOL* expression was suppressed by halide treatment in WT plants, and since the *hol* mutant was not more sensitive to salt stress than WT plants. On the contrary, increased *HOL* activity made *35S::HOL* plants more susceptible towards Br<sup>-</sup> and I<sup>-</sup> ions. We were unable to find the cause which lead to salt hypersensitivity in *35S::HOL* plants, however, it is unlikely that increased methyl halide accumulation caused this phenotype as application of the competitive inhibitor SCN<sup>-</sup> did not rescue *35S::HOL* plants upon KI treatment. We also did not find support for the hypothesis that *35S::HOL* plants suffer from SAM depletion since application of methionine or polyamines did not improve the growth and survival of KI-stressed *35S::HOL* plants.

To investigate the effects of *HOL* activity on plant-herbivore interactions, WT, *hol* and *35S::HOL* plants were subjected to herbivory. No differences in the performance of the larvae of the crucifer specialist *Plutella xylostella* or the generalist root feeder *Bradysia paupera* were observed between genotypes, showing that methyl halide emissions or other effects of *HOL* activity do not affect these herbivores. However, *hol* mutant plants had lower levels of GLs compared to WT.

To test whether the production of methyl halides could affect the composition of the microbial community of the *A. thaliana* rhizosphere, ARISA profiles of rhizosphere bacteria were generated. Overall, no significant differences were detected between the ARISA profiles of WT, *hol* mutant and *35S::HOL* rhizosphere samples, however, slight differences in the distribution of ITS fragment were observed between genotypes.

We also conducted microarray analysis on WT and *hol* mutant plants in order to gain more insight into the global effects of *HOL* activity on the transcriptome of *A. thaliana*. Apart from *HOL*, the gene whose expression was strongly down-regulated in the *hol* mutant was the *QQS* gene which is believed to regulate starch metabolism in response to cold (Li *et al.*, 2009; Seo *et al.*, 2011). However, no differences in starch content were detected between WT and *hol* plants. Interestingly, the largest number of

genes differentially regulated in the *hol* mutant was classified as being responsive to various abiotic and/or biotic stresses. In addition, genes regulated by auxin and/or light were also differentially expressed in the *hol* mutant.

In accordance with these data, we found that the *hol* mutant was slightly less sensitive to exogenous application of auxin, and *35S::HOL* lines showed increased hypocotyl growth in the dark. At this stage, it is difficult to imagine how HOL may influence auxin/light-signalling pathways. We did not find any differences in auxin signalling in *hol* or *35S::HOL* plants harbouring the *DR5::GFP* reporter gene compared to WT under normal growth conditions.

In conclusion, the function of HTMTs and methyl halide production in plants remains puzzling. Phylogenetic analysis conducted in this study showed a clear separation of HTMT proteins of eudicots into two groups (A and B). Group A solely contains HTMTs from GL-containing plants (Brassicales), whereas group B (with the exception of *Carica papaya* HOL proteins) contains HTMTs from eudicots which do not produce GLs. This observation supports the hypothesis that HTMTs in group A have evolved a new function, namely the detoxification of GL hydrolysis products.

## 8.2 Future directions

This study and previous studies have shown that methyl halides are produced by species belonging to dicots, monocots, ferns, mosses or green algae, and several HTMT genes can be found throughout the plant kingdom. It is therefore hard to believe that these compounds are simply “accidents of metabolism” caused by non-specific methylation of halides. The dual activity of HTMTs i.e. the capability to methylate both halides and thiols is an intriguing feature of this enzyme.

So far, we were only able to study the function of *HOL* in *A. thaliana*. Since this plant produces GLs, the main function of HOL may be related to GL metabolism. In this respect, it is of special interest to find out whether the detoxification of GL hydrolysis products such as  $\text{SCN}^-$  is important in undamaged or damaged tissue. A thorough analysis of the accumulation of GL hydrolysis products in WT, *hol* and *35S::HOL* plants could help to answer this question. Additionally, the production of sulphur volatiles such as  $\text{CH}_3\text{SCN}$  and  $\text{CH}_3\text{SH}$  needs to be measured from living plants before and after damage to evaluate the significance of these volatiles in plant defence



against herbivores or pathogens. So far, CH<sub>3</sub>SCN emissions have only been reported from leaf extracts of *A. thaliana* (Nagatoshi and Nakamura, 2009).

However, microarray analysis pointed to potential functions of HOL unrelated to GL metabolism such as starch/carbon metabolism and auxin/light-responsive pathways. Preliminary experiments did not reveal any differences in the starch content between WT and *hol* plants when iodine staining was used. However, further experiments which accurately quantify starch levels in *hol* mutant plants at several time points during the light and dark period, and under normal and stress conditions are necessary to verify if starch content is altered in these plants. Further experiments are also needed to understand how HOL could influence auxin-signalling pathways. Firstly, it needs to be investigated whether the observed differences in the transcriptome of the *hol* mutant are caused by the lack of HOL itself or by the lack of production of methyl halides. In the microarray experiment described here, WT and *hol* seedlings were grown in separate Petri dishes, thus, ambient methyl halide concentrations were very low in *hol* seedlings. To answer this question, it would be interesting to investigate the changes in the transcriptome (or particular genes such as *QQS*) in *hol* plants when they are grown together with WT plants and thus are exposed to methyl halides. It could also be interesting to investigate whether methyl halides could have a protective effect against thermal and oxidative stress similar to isoprene, which is the most abundant volatile organic compound emitted from plants (Laothawornkitkul *et al.*, 2009; Vickers *et al.*, 2009).

In this study we developed new tools that can be used to investigate the function of methyl halide production in plants. *A. thaliana* lines overexpressing *HOL*-homologous genes from rice, *P. patens* or *P. tricornutum* can be used to test whether these genes contribute to salt stress tolerance, or rather show the same phenotype as *35S::HOL* lines under KI stress. Moreover, they can be used to assess if the ability to detoxify GL hydrolysis products is indeed restricted to HTMT proteins in GL-containing plants, as suggested by phylogenetic analysis.

Similarly, *Pphol* knockout lines and *braA.hol.a* mutants could be used to investigate the function of methyl halide production in plants. However, in the latter case, it would be useful to obtain *braA.hol.a/braA.hol.b* double-mutants because of the expected redundancy of *BraA.HOL.a* and *BraA.HOL.b* in controlling methyl halide emissions.

Finally, due to the concerns associated with increased methyl halide emissions from crop plants in the future, it is crucial to quantify emissions and find the genes which control the production of these compounds in crops. We have laid the foundations for identifying the genes in oilseed rape and rice and discovered a number of *HTMT* genes in other cereals and fruits of economic importance such as maize, cassava, peach or papaya. Understanding the genetic control of methyl halide production in these plants could pave the way for generating “ozone-safe” crop varieties.

## Appendix – Supplemental Figures and Tables

### Chapter 2

**Supplemental Table 2.1. List of *Arabidopsis thaliana* lines used in this study.** All transgenic lines were generated in this study except for *DR5::GFP* (Friml *et al.*, 2003). The *hol* mutant line was obtained from the SALK T-DNA collection as described in Rhew *et al.* (2003).

Name/Number	Comments
Col-0	WT
<i>hol</i> mutant	T-DNA insertion line
196-9	<i>35S::HOL</i>
196-11	<i>35S::HOL</i>
200-13	<i>HOL::GUS</i>
<i>35S::GFP</i>	
<i>HOL::HOL:GFP</i>	
<i>DR5::GFP</i>	
<i>DR5::GFP x 35S::HOL</i>	
<i>DR5::GFP x hol</i>	
3-2	<i>35S::OsHOL1</i>
4-2	<i>35S::OsHOL1</i>
1-A	<i>35S::OsHOL2</i>
3-C	<i>35S::OsHOL2</i>
1-1	<i>35S::PpHOL</i>
1-2	<i>35S::PpHOL</i>
2-C	<i>35S::PpHOL</i>

**Supplemental Table 2.2. List of primers used in this study.**

<b>Name</b>	<b>Sequence</b>	<b>Application</b>
HOLP1	TCCCTACAAAGTAGCTTTGTCTTCG	Creation of HOL::GUS construct
HOLP2	TTAATGGATCCGTTTCAGGGTTGGTCTTTCTTCTCG	Creation of HOL::GUS construct
MCT1	GTCGACATGGCTGAAGAACAACAAAACCTCAG	Creation of 35S::HOL construct
MCT2	GGATCCTCAATTGATCTTCTCCACCTTCC	Creation of 35S::HOL construct
HOL_F1_A	ATGCTCTAGAGGTACCTACTCTATTGATTGGTGTGG	Creation of HOL::HOL:GFP construct
HOL_R1	GCATGGATCCACCGCCACCATTGATCTTCTTCACCTTC	Creation of HOL::HOL:GFP construct
HOL_F2	CCACTCGTAAGGTACTGTGC	Creation of HOL::HOL:GFP construct
HOL_R2	TGTCTAACGTCACGTCGAAGC	Creation of HOL::HOL:GFP construct
HOL_F	AAGAAGTTGCTACGTTCTCTGC	Genotyping
HOL_R	AGCTAGAAGAAGACTGACTCC	Genotyping, sequencing
HOL_F3	CCAACTCGTAAGGTACAATAG	Sequencing
HOL_R3	TTGTATCTGGAGCAAGTTCG	Sequencing
HOL_R5	CGAGTGAGAGTGATTACAAGG	Sequencing
HOL_R6	AAGACCATGACTTATGACGCA	Sequencing
HOL_R7	AGGGTTGGTCTTTCTTTCTCG	Sequencing
HOL_R8	AGTGCGCTTTCGGAAATATCC	Genotyping, sequencing
M13_R	GGAAACAGCTATGACCATG	Sequencing
GFP_F2	GGCCGGATCCAGTAAAGGAGAAGAAGAACTTTT	Creation of HOL::HOL:GFP construct
GFP_R2	GCTCCTGCAGTCTAGATTATTTGTATAGTTCA TCCATGC	Creation of HOL::HOL:GFP construct
GFP_F1	CTGGAGTTGTCCCAATTCTTG	Genotyping
GFP_R1	TGATAATGATCAGCGAGTTGC	Genotyping, sequencing
GFP_F3	GCAACTCGCTGATCATTATCA	Sequencing
GFP_F4	TGGCCGGATCCATGAGTAAAGGAGAAGAAGAACTT	Creation of 35S::GFP construct, sequencing
GFP_R4	CGAATTCCTGCAGTCTAGAT	Creation of 35S::GFP construct
GFP_R5	CAAGAATTGGGACAACCTCCAG	Sequencing
oligo dT	TTTTTTTTTTTTTTTTTV	cDNA synthesis
AtHOL1_F	ATATTTCCGAAAGCGCACTCGCG	qPCR, genotyping
AtHOL1_R	TCTACTTTGTAGGGAGGTCCACCAA	qPCR, genotyping, sequencing
EF1a_F	GTCGATTCTGGAAAAGTCGACC	qPCR
EF1a_R	AATGTCAATGGTGATACCACGC	qPCR
UBQ10_F	AGAACTCTTGCTGACTACAATATCCAG	qPCR
UBQ10_R	ATAGTTTTCCAGTCAACGTCTTAAC	qPCR
QQS_F	ATGAAGACCAATAGAGAGCAGG	qPCR
QQS_R	CAGTAGTTGTAGAAGTGAAGCC	qPCR
EXL1_fw	TGGATCGGCTTGTACTGGAG	qPCR
EXL1_rev	GGGTCAAACAAGCCGGTAA	qPCR
eGFP_F1	GAAGCAGCACGACTTCTTCAAG	Genotyping
eGFP_R1	AACTCCAGCAGGACCATGTG	Genotyping
JMLB2	TTGGGTGATGGTTCACGTAGTGGGCCATCG	Genotyping

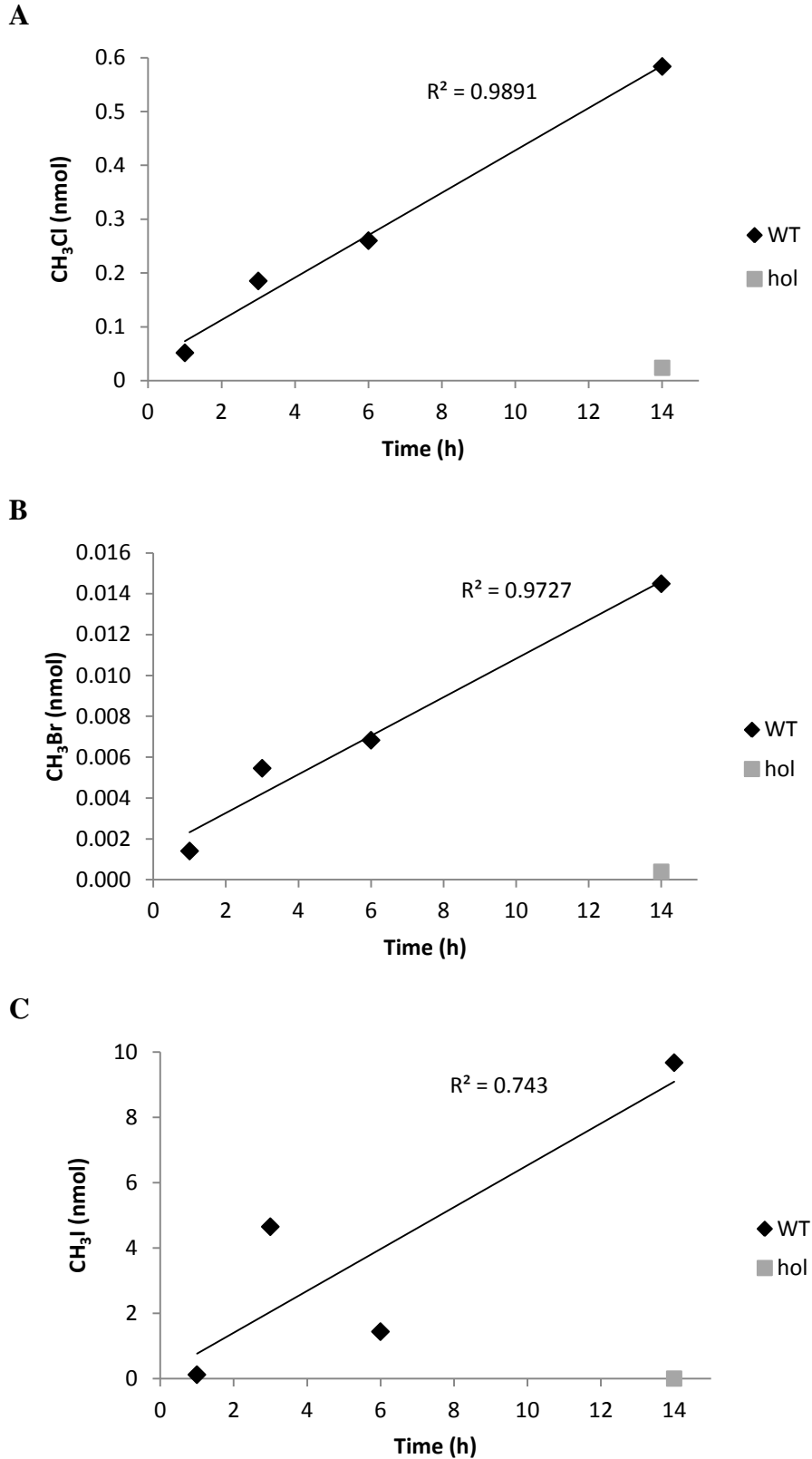
<b>Name</b>	<b>Sequence</b>	<b>Application</b>
BrHOLa_F1	TTTCGCGCTATATGGTTTCC	TILLING, genotyping, sequencing
BrHOLa_R1	CGGCTTAACTAATGCGAGCTT	TILLING, genotyping
PpHOL_F1	TACAGTCGACATGAGCTCCACAAATTCAGG	Creation of 35S::PpHOL construct
PpHOL_R1	ACTTAGATCTTTAGAAATGGCTCTCGCCCA	Creation of 35S::PpHOL construct
PpHOL_F2	AGAGGGCAAGGTTCTGTGC	Sequencing, genotyping
PpHOL_R2	GGGAAACATTAGAGTGATGAGC	Sequencing, genotyping, RT-PCR
PpHOL_F3	CTTCTTCTCGTATACTCCACC	RT-PCR
PpHOL_F4	TGCAACCTATGGACACTGCTTGGG	qPCR
PpHOL_R4	AACCAGGCACAAGAACCTTGCCC	qPCR
OsHOL1_F1	GCCGCTCGAGATGGCGTCGGCGATCGT	Creation of 35S::OsHOL1 construct
OsHOL1_R1	CACTGGATCCTTAGTCGGATTTTGTTCATCC	Creation of 35S::OsHOL1 construct
OsHOL1_F2	ACGATGTGGTTGCACTGTCC	Sequencing, genotyping, RT-PCR
OsHOL1_R2	CCTTCAGCCAAATACATGAGG	Sequencing, genotyping
OsHOL1_R3	AGATGAGATGGAACGGCTCC	RT-PCR
OsHOL1_F4	AGCATGGGCGAAGAGAATGGC	qPCR
OsHOL1_R4	GTTCAGCACCTCCTTGTAATCGAGC	qPCR
OsHOL2_F1	TACGGTCGACATGCACGCGCTGCCTCGCTC	Creation of 35S::OsHOL2 construct
OsHOL2_R1	CATCGGATCCTTATAGAGAAGATCCGGGTA	Creation of 35S::OsHOL2 construct
OsHOL2_F2	CGTTAAATCAGGAACCTCTCCC	Sequencing, genotyping
OsHOL2_R2	TAACTGTTTCTGCCCAAGCC	Sequencing, genotyping, RT-PCR, qPCR
OsHOL2_F3	TGGAGAAGGCTAAGCAGTGG	RT-PCR, qPCR
PtHTMT_F1	TACGGTCGACATGGCCATCGTGTTCGTGA	Creation of 35S::PtHTMT construct
PtHTMT_R1	GCATAGATCTTCAAGTATTCCACCAGCACA	Creation of 35S::PtHTMT construct
PtHTMT_F2	AGCATCCGTAACCTGGTTTGG	Sequencing, genotyping, RT-PCR
PtHTMT_R2	AGCAACAGTGATGTTTGACG	Sequencing, genotyping, qPCR
PtHTMT_R3	GATTCAAACAGAGCTTGTCG	RT-PCR
ITSF	GTCGTAACAAGGTAGCCGTA	ARISA
ITSReub	GCCAAGGCATCCACC	ARISA
cmuA802f	TTCAACGGCGAYATGTATCCYGG	cmuA PCR
cmuA1609r	TCTCGATGAACTGCTCRGGCT	cmuA PCR
PpHOL_KO_F1	AGTTCCATGGTCCCATGTGACATGAATTGG	Creation of PpHOL knock-out construct
PpHOL_KO_R1	AAGTACTAGTTTGGGCTATTTCTGGATACG	Creation of PpHOL knock-out construct
PpHOL_KO_F2	AGAATCTAGAAGGGAGGGAACACTTTGTGG	Creation of PpHOL knock-out construct
PpHOL_KO_R2	AGAAGGTCATCTCACAAACC	Creation of PpHOL knock-out construct
PpHOL_KO_F3	TGAGGGTCGATATGATTGGC	Sequencing
PpHOL_KO_R3	CCCAGAATAGTGAACCTGAGC	Sequencing
PpHOL_KO_F4	GGTGTTTTGTATCCCAATGC	Sequencing
PpHOL_KO_R4	GAAGCATATTGCTCAATAGGC	Sequencing
OsHOL1_F2	AGGCTGAAGGACAAGAGGCCGGG	TILLING
OsHOL1_R2	CGCCTGTATGGCAATCCTTACCTGC	TILLING
OsHOL2_F2	CAGTGACCAAGAAGGAGGACCACC	TILLING
OsHOL2_R2	TGGCCCATCTGTCTAGAGGAACAGGC	TILLING

Name	Sequence	Application
UGT79B1_F1	GAGAGGGTTCAAGGACGTGG	qPCR
UGT79B1_R1	CATCTCCTCCGTCATCAGCC	qPCR
ASN1_F1	CGGACGAGATCTTTGGAGGG	qPCR
ASN1_R1	GGAACACGTGCCTCTAGTCC	qPCR
SEN_F1	AGGAAAAGCAACGACAACAAGC	qPCR
SEN_R1	ACGTTGATGGCTCTAGTCGG	qPCR
DAA_F1	CGCGTAAGGAAAACGTGTGG	qPCR
DAA_R1	GGTGCTTGCTCCTAGTGTCG	qPCR
ATHB4_F3	CTGACCGAGGAGAATCGACG	qPCR
ATHB4_R3	CAGAGGAGGAGACACGTTTCG	qPCR
PUB19_F2	TCGACACGTTTCCAGTCAGG	qPCR
PUB19_R2	TAGCTCGTTTGTCTCGTCTCGG	qPCR

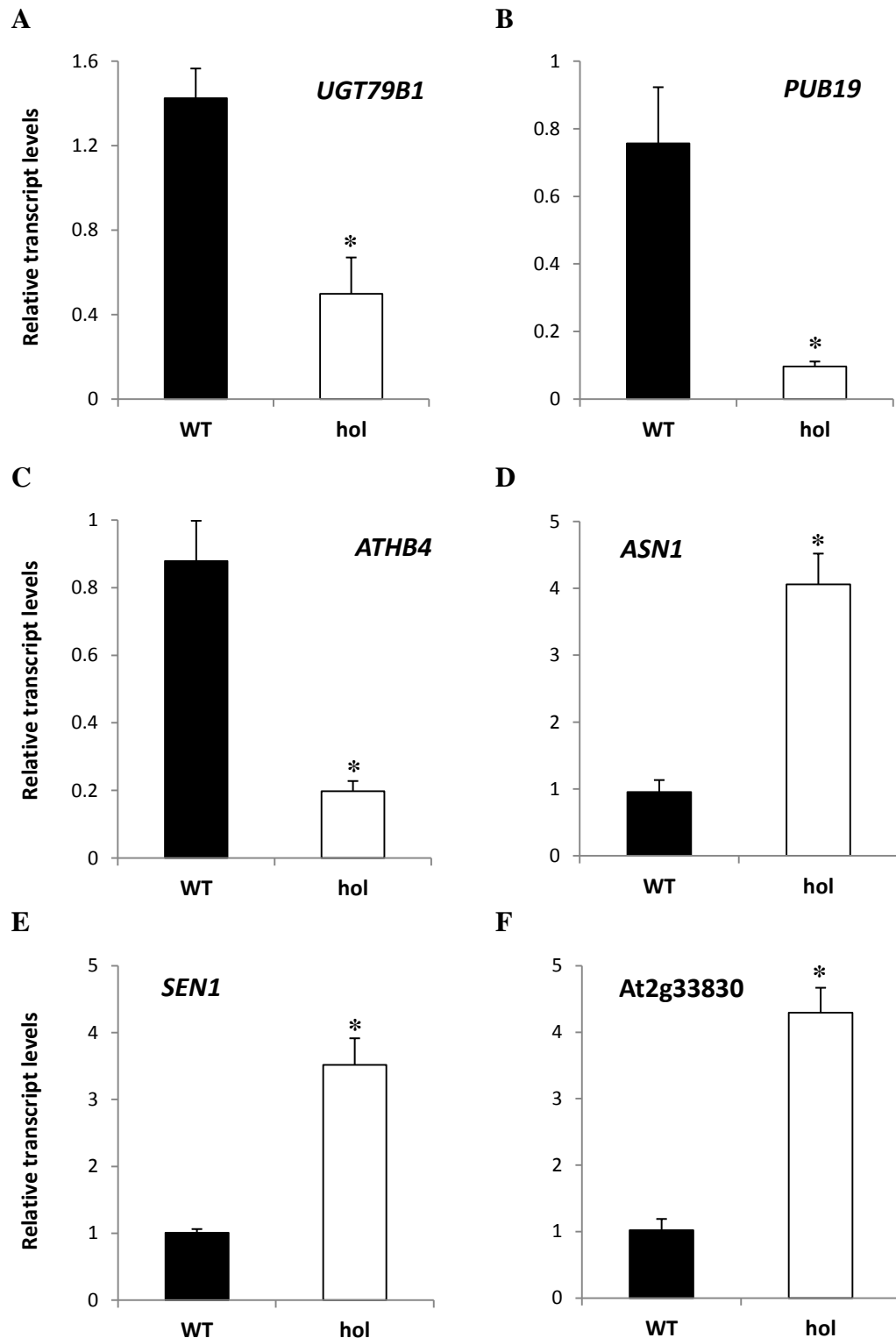
### Chapter 3



**Supplemental Figure 3.1.** *A. thaliana* *HOL* and *HOL*-like (*HLL*) genes. Location, structure and predicted transcripts of *HOL* (At2g43910), *HLL1* (At2g43920) and *HLL2* (At2g43940) on chromosome II. Image taken from the *A. thaliana* Genome Browser at [www.phytozome.net](http://www.phytozome.net).



**Supplemental Figure 3.2. Methyl halide emissions from WT and *hol* seedlings.** Emission profiles (nmol per plate) of CH<sub>3</sub>Cl (A), CH<sub>3</sub>Br (B) and CH<sub>3</sub>I (C) from 20-day-old *A. thaliana* WT (black) and *hol* seedlings (grey) grown on agar plates. Air samples were taken 1, 3, 6 or 14 h after enclosure. Background methyl halide emissions were also determined from agar control plates and subtracted from the amounts detected from enclosed seedlings.



**Supplemental Figure 3.3. Verification of expression levels of six genes differentially expressed in the *hol* mutant (microarray).** Transcript levels were determined in 7-day-old seedlings grown on MS media by qPCR. Expression levels of *UGT79B1* (A), *PUB19* (B), *ATHB4* (C), *ASN1* (D), *SEN1* (E) and dormancy/auxin associated protein (*At2g33830*) (F) were normalised to the expression of *EF1 $\alpha$* . Data points are the mean  $\pm$  s.e. of four biological replicates. Asterisks represent significant differences from WT (t-test,  $p < 0.01$ ).



**Supplemental Table 3.1. Treatments which produce similar changes to genes down-regulated in the *hol* mutant.** Treatments were identified by iterative group analysis (P-value < 0.001) comparing the list of down-regulated genes in the *hol* mutant with lists of genes significantly up/down-regulated by different stress and hormone treatments in the AtGenExpress database.

<b>Group name</b>	<b>Group members</b>	<b>Number changed</b>	<b>P-value</b>	<b>Percent changed</b>
1 min red light 45 min dark (up)	83	9	1.7E-09	10.8
Red light 45 min (up)	96	9	6.2E-09	9.4
Far red light 45 min (up)	89	8	6.2E-08	9.0
Proteasome inhibitor MG132 (10 µM) 3h (up)	94	8	8.0E-08	8.5
Sulphate starvation 2-8 h (up)	5	3	1.1E-07	60.0
UV-B root 0.25-3 h (up)	98	7	2.9E-06	7.1
Sulphate starvation 12-24 h (up)	16	3	5.9E-06	18.8
Flagellin (down)	59	4	3.9E-05	6.8
DC3000 hrcC (down)	33	3	0.00023	9.1
Oxidative shoot 6-24 h (down)	5	3	0.00025	60.0
ACC (down)	5	3	0.00029	60.0
<i>Erysiphe orontii</i> infection 1-2 d (down)	56	4	0.00038	7.1
Wounding root 6-24 h (down)	8	5	0.00039	62.5
Osmotic shoot 0.5-3 h (down)	86	2	0.00046	2.3
<i>Erysiphe orontii</i> infection 6-18 h (down)	15	8	0.00049	53.3
Ethylene inhibitor aminoethoxyvinylglycine (10 µM) 3h (up)	117	3	0.00054	2.6
Sulphate starvation 12-24 h (down)	19	8	0.00064	42.1
<i>Erysiphe orontii</i> infection 3-5d (down)	102	3	0.00080	2.9
White light 45 min (up)	108	4	0.00080	3.7
6-deoxocathasterone (1 µM) 3 h (down)	116	3	0.00089	2.6
24h 30µM ABA during 48 h seed imbibition (down)	89	3	0.00090	3.4
Blue light 45 min (up)	102	3	0.00094	2.9
HarpinZ (down)	80	4	0.00100	5.0

**Supplemental Table 3.2. Treatments which produce similar changes to genes up-regulated in the *hol* mutant.** Treatments were identified by iterative group analysis (P-value < 0.001) comparing the list of up-regulated genes in the *hol* mutant with lists of genes significantly up/down-regulated by different stress and hormone treatments in the AtGenExpress database.

Group name	Group members	Number changed	P-value	Percent changed
Salt shoot 0.5-3 h (down)	71	9	6.1E-12	12.7
<i>Erysiphe orontii</i> infection 6-18 h (up)	20	11	9.6E-12	55.0
UV-B shoot 0.25-3 h (down)	96	9	1.1E-11	9.4
Cold shoot 0.5-3 h (down)	59	9	1.1E-11	15.3
Drought shoot 0.25-3 h (down)	33	7	1.8E-11	21.2
Osmotic shoot 0.5-3 h (down)	86	10	3.9E-11	11.6
UV-B root 0.25-3 h (down)	26	6	4.0E-09	23.1
Methyl jasmonate (down)	66	8	8.6E-09	12.1
Blue light 45 min (down)	54	7	4.4E-08	13.0
Wounding shoot 0.25-3 h (down)	26	5	8.2E-08	19.2
Heat root 0.25-3 h (down)	42	6	8.6E-08	14.3
Wounding root 6-24 h (up)	80	6	9.8E-08	7.5
Oxidative shoot 0.5-3h (down)	17	4	1.8E-07	23.5
Cathasterone (1 $\mu$ M) 3 h (up)	69	7	2.5E-07	10.1
6-Deoxocathasterone (1 $\mu$ M), 3 h (up)	52	6	8.6E-07	11.5
Brassinolide (up)	41	5	2.9E-06	12.2
White light 45 min (down)	40	5	4.2E-06	12.5
Drought shoot 6-24 h (up)	84	4	6.8E-06	4.8
UV-A/B 5 min + 45 min dark (down)	31	4	1.8E-05	12.9
ABA (down)	54	5	2.3E-05	9.3
Oxidative root 6-24 h (up)	44	2	7.9E-05	4.5
Auxin (up)	115	3	0.00033	2.6
Red light 45 min (down)	12	4	0.00040	33.3
UV-B root 6-24 h (down)	20	2	0.00044	10.0
GA biosynthesis inhibitor uniconazole (10 $\mu$ M) 3-12 h (down)	59	4	0.00052	6.8
Auxin inhibitor (down)	39	2	0.00056	5.1
SAR tissue from uninfiltreated half of <i>P. syringae</i> ES4326 infiltrated leaf 1-2 d (down)	63	4	0.00066	6.3
UV-A/B 5 min + 4 h dark (down)	115	2	0.00070	1.7
Osmotic root 0.5-3 h (down)	93	2	0.00074	2.2
<i>Erysiphe orontii</i> infection 1-2 d (up)	12	1	0.00078	8.3
UV-A 5 min + 45 dark (down)	20	8	0.00081	40.0
SAR tissue from uninfiltreated half of <i>P. syringae</i> ES4326 avrrpt2 infiltrated leaf 1-2 d (down)	23	5	0.00083	21.7

Group name	Group members	Number changed	P-value	Percent changed
Lipopolysaccharide (up)	25	18	0.00084	72.0
6-Deoxoteasterone (1 $\mu$ M) 3 h (up)	112	4	0.00088	3.6
Brassinolide (down)	25	14	0.00095	56.0

**Supplemental Table 3.3. Genes which are co-expressed with *HOL* (positive correlation).** Genes were identified using the Genevestigator database. *HOL* expression patterns were compared with anatomy meta-profiles and genes with a Pearson's correlation coefficient (PCC)  $\geq 0.7$  are shown.

AGI code	Functional classes and gene description	PCC
<b>Response to abiotic/biotic stress</b>		
At1g13930	Involved in response to salt stress	0.81
At3g26520	Tonoplast intrinsic protein 2 (TIP2)	0.79
At5g46790	PYR1-like 1 (PYL)	0.78
At3g53420	Plasma membrane intrinsic protein 2 (PIP2)	0.78
At2g15970	Cold-regulated 413 plasma membrane 1	0.78
At2g26690	Major facilitator superfamily protein	0.78
At4g23670	Polyketide cyclase/dehydrase and lipid transport superfamily protein	0.76
At1g30360	Early-responsive to dehydration stress protein (ERD4)	0.75
At2g36830	Tonoplast intrinsic protein 1 (TIP1)	0.75
At5g65310	Homeodomain-leucine zipper protein (ATHB5)	0.71
At5g28770	Transcription factor (ATBZIP63)	0.71
At2g31790	UDP-Glucosyltransferase 74C1 (UGT74C1)	0.71
At5g16000	NSP-interacting kinase 1 (NIK1)	0.71
<b>Response to light/auxin</b>		
At1g34000	ONE-HELIX PROTEIN 2 (OHP2)	0.79
At2g30520	ROOT PHOTOTROPISM 2 (RPT2)	0.78
At3g45780	ROOT PHOTOTROPISM 1 (RPT1)	0.74
At1g04240	AUX/IAA transcriptional regulator family protein (IAA3)	0.74
AtCg00220	Photosystem II reaction center protein M (PSBM)	0.73
<b>Structure/Cell wall</b>		
At3g14310	Pectin methylesterase 3 (PME3)	0.78
At1g75500	WALLS ARE THIN 1 (WAT1)	0.75
At1g12090	Extensin-like protein (ELP)	0.74
At5g60920	COBRA-like extracellular glycosyl-phosphatidyl inositol-anchored protein	0.73
At4g25570	Cytochrome b561/ferric reductase transmembrane protein family	0.71

<b>AGI code</b>	<b>Functional classes and gene description</b>	<b>PCC</b>
<b>Metabolism</b>		
At1g65960	Glutamate decarboxylase 2 (GAD2)	0.79
At2g45180	Bifunctional inhibitor/lipid-transfer protein/seed storage 2S albumin protein	0.76
At3g11945	Homogentisate prenyltransferase (HST)	0.73
<b>Seed germination</b>		
At3g47620	Transcription factor (TCP14)	0.73
At1g49510	Embryo defective 1273 (EMB 1273)	0.71
<b>Miscellaneous</b>		
At3g06750	Hydroxyproline-rich glycoprotein family protein	0.74
At4g27710	Cytochrome P450, family 709, subfamily B, polypeptide 3 (CYP709B3)	0.74
At5g40950	Ribosomal protein large subunit 27 (RPL27)	0.73
At5g14880	Potassium transporter family protein	0.71
At2g16740	Ubiquitin-conjugating enzyme 29 (UBC29)	0.70
<b>Unknown</b>		
At5g23920	Unknown protein	0.81
At5g59350	Unknown protein	0.78
At2g34310	Unknown protein	0.75
At1g73650	Unknown protein	0.73
At5g04440	Unknown protein	0.73
At2g42320	Nucleolar protein gar2-related	0.72
At1g49500	Unknown protein	0.72
At1g50020	Unknown protein	0.71

**Supplemental Table 3.4. Genes which are co-expressed with *HOL* (negative correlation).** Genes were identified using the Genevestigator database. *HOL* expression patterns were compared with anatomy meta-profiles and genes with a Pearson's correlation coefficient (PCC)  $\leq -0.7$  are shown.

<b>AGI code</b>	<b>Functional classes and gene description</b>	<b>PCC</b>
<b>Response to abiotic/biotic stress</b>		
At1g79610	Na <sup>+</sup> /H <sup>+</sup> antiporter 6 (NHX6)	-0.76
At5g41610	Cation/H <sup>+</sup> exchanger 18 (CHX18)	-0.75
At4g24680	Modifier of SNC1	-0.72
<b>Metabolism</b>		
At3g25440	LAG ONE HOMOLOGUE 1 (LOH1)	-0.70
At1g06030	pfkB-like carbohydrate kinase family protein	-0.70
<b>DNA repair</b>		
At4g38780	Pre-mRNA-processing-splicing factor	-0.75
At5g66130	RADIATION SENSITIVE 17 (RAD17)	-0.73
At1g72270	Ribosome 60S biogenesis N-terminal-domain containing protein	-0.72
At2g06510	Replication protein A 1A (RPA1A)	-0.70
<b>Miscellaneous</b>		
At3g28730	High mobility group (HMG)	-0.72
At2g36370	Ubiquitin-protein ligase	-0.72
At2g42640	Mitogen activated protein kinase kinase kinase-related	-0.71
At2g20540	Mitochondrial editing factor 21 (MEF21)	-0.71
At5g27660	Trypsin family protein with PDZ domain (DEG14)	-0.71
At3g10780	emp24/gp25L/p24 family/GOLD family protein	-0.70
<b>Unknown</b>		
At3g20730	Tetratricopeptide repeat (TPR)-like superfamily protein	-0.72
At2g44630	Galactose oxidase/kelch repeat superfamily protein	-0.72
At5g46640	AT hook motif DNA-binding family protein	-0.72
At2g22070	Pentatricopeptide (PPR) repeat-containing protein	-0.71
At5g33390	Glycine-rich protein	-0.71
At2g07676	Unknown protein	-0.71
At1g15300	Transposable element gene	-0.71
At1g55040	Zinc finger (Ran-binding) family protein	-0.70
At1g55050	Unknown protein	-0.70
At1g06270	Pentatricopeptide repeat (PPR) superfamily protein	-0.70
At2g07714	Transcription factor-related	-0.70

**Supplemental Table 3.5. Treatments and genotypes which down-regulate *HOL*.** Treatments and genotypes were identified using the Genevestigator database. Fold change is calculated from the mean signal ratio of experimental samples over control samples applying a fold change threshold < 0.5 and a P-value < 0.05.

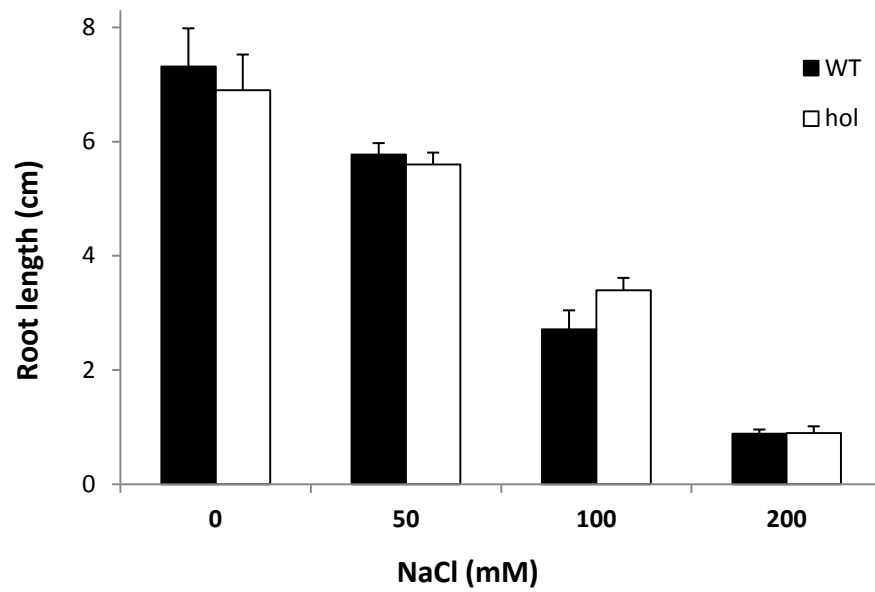
Experiment/control	Fold change	P-value
ABA study 2 / untreated embryo endosperm samples	0.02	3.7E-08
BL/H3BO3 (2d) / untreated cell culture samples	0.05	0.006
Paclobutrazole study 2 / untreated embryo endosperm samples	0.06	0.007
BL/H3BO3 (6d) / untreated cell culture samples	0.07	0.006
BL/H3BO3 (4d) / untreated cell culture samples	0.08	0.007
BL/H3BO3 (8d) / untreated cell culture samples	0.14	0.016
ABA study 7 (Col-0) / solvent treated guard cell samples (Col-0)	0.18	0.007
Syringolin study 3 (late) / solvent treated leaf samples (Col-0; late)	0.19	0.002
BL/H3BO3 (10d) / untreated cell culture samples	0.20	0.017
<i>P. syringae</i> pv. <i>tomato</i> study 9 (DC3118 Cor-) / mock inoculated leaf samples	0.21	0.011
Heat study 4 / untreated plant samples	0.23	0.005
<i>P. syringae</i> pv. <i>tomato</i> study 10 (DC3000) / mock inoculated leaf samples	0.24	0.004
Night extension (late) / untreated rosette samples	0.25	1.3E-04
Cycloheximide / mock treated seedlings	0.27	0.026
<i>P. syringae</i> pv. <i>tomato</i> study 3 (DC3000) / mock inoculated leaf samples (24h)	0.28	7.3E-05
Hypoxia study 6 (Col-0) / untreated plant samples (Col-0)	0.28	0.001
<i>P. syringae</i> pv. <i>maculicola</i> (Col-0) / mock treated leaf samples (Col-0)	0.31	7.0E-05
ABA + DMTU (20h) / solvent treated cell suspension samples (20h)	0.32	0.006
Salt study 2 (late) / untreated root samples (late)	0.33	0.002
Iron deficiency study 2 (late) / mock treated root samples	0.33	0.004
<i>P. syringae</i> pv. <i>tomato</i> study 11 (Ler) / untreated leaf disc samples (Ler)	0.34	0.004
FLG22 study 5 (Col-0) / untreated leaf disc samples (Col-0)	0.34	0.029
<i>P. syringae</i> pv. <i>tomato</i> study 3 (DC3000 avrRpm1) / mock inoculated leaf samples (24h)	0.36	0.006
Paclobutrazole study 3 / untreated leaf disc samples (Ler)	0.38	0.030
<i>A. brassicicola</i> (Ler) / untreated leaf disc samples (Ler)	0.39	0.005
OXUPB1-2 / Col-0	0.40	0.034
Drought study 2 (Col-0) / untreated leaf samples (Col-0)	0.40	0.047
ABA study 10 (20h) / solvent treated cell suspension samples (20h)	0.40	0.023
KCl treated root samples (early) / untreated root samples	0.40	0.001
csn4-1 / Col-0	0.41	0.019
NAA + FLG22 (2h) / untreated leaf disc samples (Col-0)	0.41	0.005
FLG22 study 9 (2h) / FLG22 study 9 (0h)	0.42	0.015
FLG22 study 7 (Ler) / FLG22 study 8 (2h)	0.42	0.037
ABA study 8 (Col-0) / solvent treated leaf samples (Col-0)	0.42	0.002

Experiment/control	Fold change	P-value
Shift to pH 4.6 (LZ4) / mock treated root samples (LZ4)	0.43	0.027
<i>P. syringae</i> pv. <i>tomato</i> study 2 (DC3000 avrRpm1) / mock inoculated leaf samples (6h)	0.43	0.002
BL study 2 (Sav-0) / mock treated seedlings (Sav-0)	0.44	0.007
lrx1_rol1-2 / Col-0	0.47	0.005
Dark / 32°C (300-360min) / dark / 21°C (300-360min)	0.49	6.5E-05
FLG22 + GA (2h) / untreated leaf disc samples (Ler)	0.49	0.049
hy5-215 / Col-0	0.50	0.001

**Supplemental Table 3.6. Treatments and genotypes which up-regulate *HOL*.** Treatments and genotypes were identified using the Genevestigator database. Fold change is calculated from the mean signal ratio of experimental samples over control samples applying a fold change threshold > 2 and a P-value < 0.05.

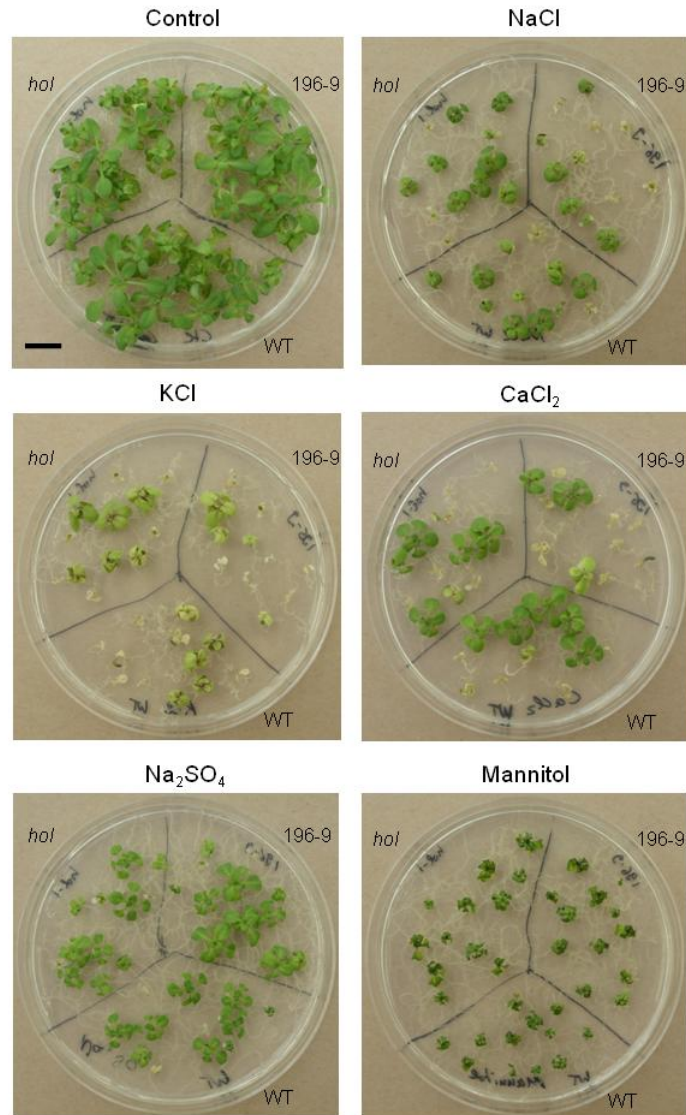
Experiment/control	Fold change	P-value
max4 / Col-0	4.97	3.6E-05
Heat study 2 (Ws) / untreated leaf samples (Ws)	3.36	0.044
<i>P. syringae</i> pv. <i>tomato</i> study 10 (DC3000 hrpA) / <i>P. syringae</i> pv. <i>tomato</i> study 10 (DC3000)	3.32	0.030
axr1-12 / Col-0	3.24	1.8E-04
<i>P. syringae</i> pv. <i>tomato</i> study 9 (DC3118 Cor-hrpS) / <i>P. syringae</i> pv. <i>tomato</i> study 9 (DC3118 Cor-)	3.21	0.010
Red study 3 (1h) / dark grown seedlings (Col-0)	3.05	4.0E-04
rga-delta17 / empty cassette	3.01	0.001
aba1-1 / Ler-0	2.99	0.021
Red study 3 (45h) / dark grown seedlings (Col-0)	2.94	5.1E-05
Far red / dark grown Col-0 seedlings	2.72	0.005
cngc4 / ws-2	2.49	0.004
Blue / dark grown Col-0 seedlings	2.36	0.007
Dark / 4°C (640 and 1280min) / dark / 21°C (640 and 1280min)	2.27	0.048
bri1-116 / Col-0	2.26	0.003
<i>P. syringae</i> pv. <i>tomato</i> study 2 (DC3000 hrcC-) / <i>P. syringae</i> pv. <i>tomato</i> study 2 (DC3000 avrRpm1)	2.19	0.002
White / dark grown Col-0 seedlings	2.05	0.007
ced1 / Col-5	2.03	0.037
pad4 / Col-0	2.01	0.020

## Chapter 4

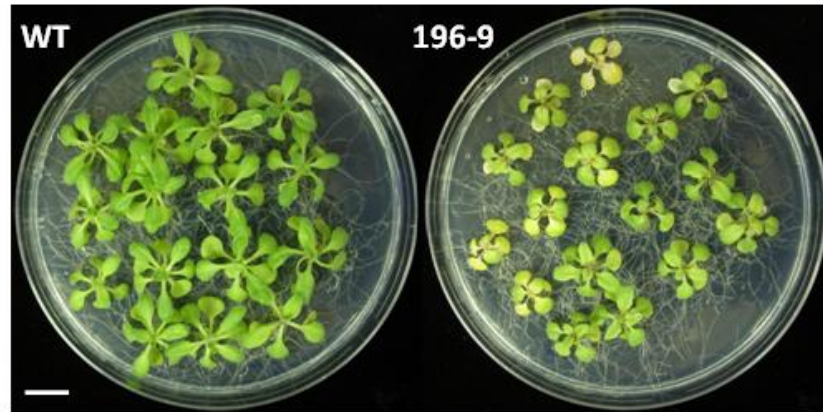


**Supplemental Figure 4.1. Root growth of WT and *hol* seedlings on sodium chloride (NaCl).** Three-day-old seedlings were transferred to MS agar plates containing 0, 50, 100 or 200 mM NaCl. Root length was measured 7 days after transfer. Data points are the mean  $\pm$  s.e. of seven seedlings. No significant differences were observed between genotypes within each treatment group (t-test).

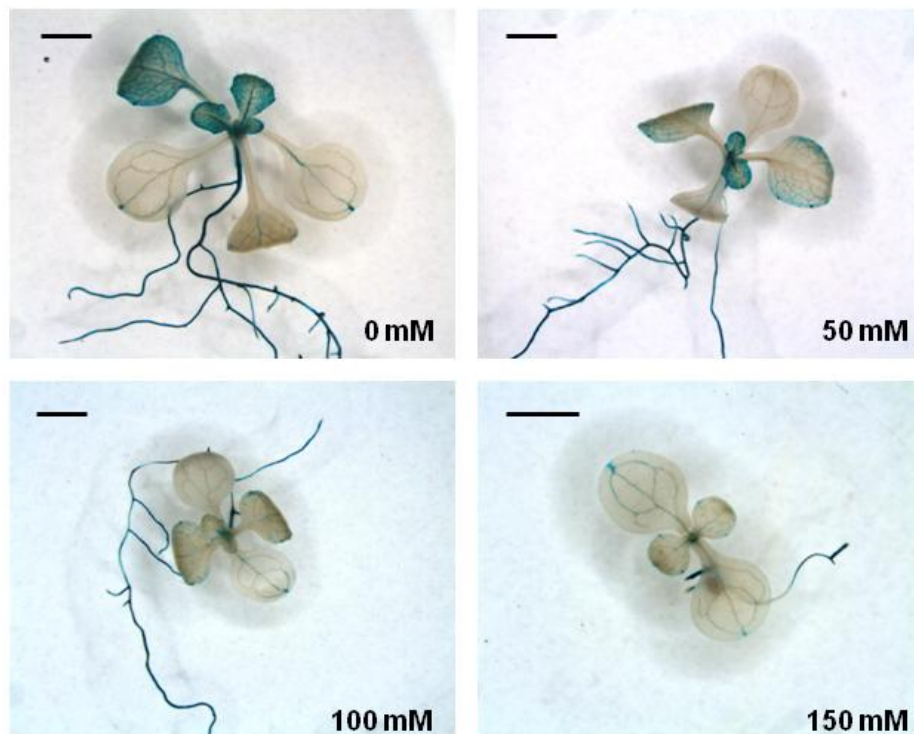




**Supplemental Figure 4.2. Growth of WT, *hol* and 35S::*HOL* (196-9) seedlings on various salts and mannitol.** Four-day-old seedlings were transferred to MS agar plates containing no salt (control), 100 mM NaCl, 100 mM KCl, 50 mM CaCl<sub>2</sub>, 50 mM Na<sub>2</sub>SO<sub>4</sub> or 200 mM mannitol. Pictures were taken after 12 days of treatment. Scale bar = 1 cm.

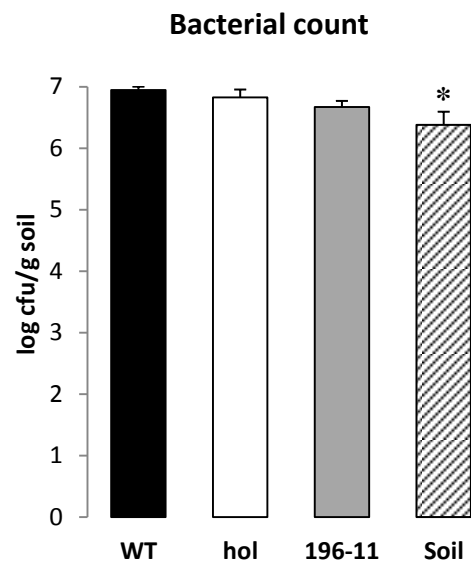


**Supplemental Figure 4.3. Growth of WT and 35S::HOL (196-9) seedlings on sodium iodide (NaI).** Ten-day-old seedlings were transferred to MS agar plates containing 10 mM NaI. Pictures were taken after 10 days of treatment. Scale bar = 1 cm.

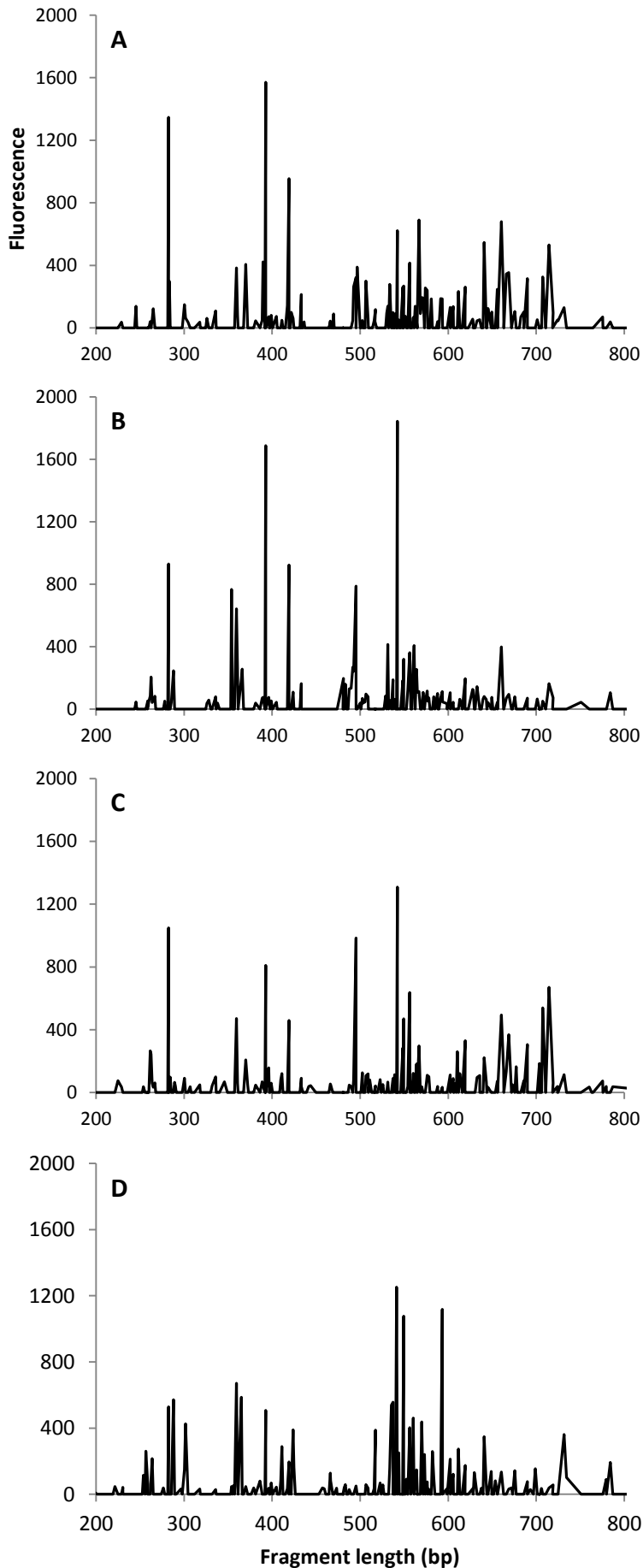


**Supplemental Figure 4.4. Expression patterns of *HOL* in a *HOL::GUS* reporter line under NaBr stress.** Four-day-old seedlings were transferred to MS agar plates containing 0, 50, 100 or 200 mM NaBr and stained for GUS activity after 5 days. Scale bars = 1 mm.

## Chapter 5



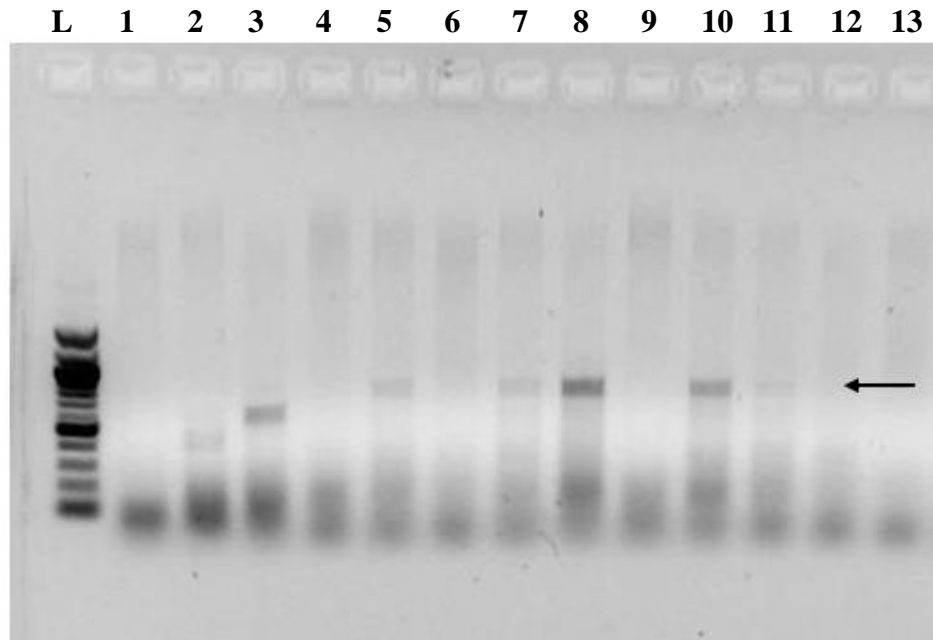
**Supplemental Figure 5.1. Bacterial population count in the rhizosphere of WT, *hol* and *35S::HOL* (196-11) roots.** Soil samples were collected from the rhizosphere or from the unplanted soil control 4 weeks after the start of the experiment. Soil solution was plated on TY agar plates and colony-forming units (cfu) were counted 1 day after inoculation. Asterisks represent significant differences from WT (ANOVA with Fisher's LSD post-hoc test,  $p < 0.05$ ).



**Supplemental Figure 5.2. Examples of ARISA profiles.** Profiles were obtained from DNA extracted from the rhizosphere soil of WT (A), *hol* (B) and *35S::HOL* (196-11) (C) plants or from the unplanted soil control (D) one week after the start of the experiment.

**Supplemental Table 5.1. MANOVA p-values for pairwise comparisons between genotypes and time points.** Reported values are the proportion of p-values from 1000 simulations that were significant at a significance level of  $p < 0.05$ .

<b>Pairwise comparison</b>	<b>Proportion of significant differences (%)</b>
<b>Genotype/treatment</b>	
<b>Week 1</b>	
Control vs. WT	100
Control vs. <i>hol</i>	100
Control vs. <i>35S::HOL</i>	100
WT vs. <i>hol</i>	0
WT vs. <i>35S::HOL</i>	0
<i>hol</i> vs. <i>35S::HOL</i>	0
<b>Week 2</b>	
Control vs. WT	100
Control vs. <i>hol</i>	0
Control vs. <i>35S::HOL</i>	0
WT vs. <i>hol</i>	0
WT vs. <i>35S::HOL</i>	0
<i>hol</i> vs. <i>35S::HOL</i>	0
<b>Week 4</b>	
Control vs. WT	12
Control vs. <i>hol</i>	0
Control vs. <i>35S::HOL</i>	1
WT vs. <i>hol</i>	0
WT vs. <i>35S::HOL</i>	0
<i>hol</i> vs. <i>35S::HOL</i>	0
<b>Time point</b>	
<b>Control</b>	
Start vs. week 1	0
Start vs. week 4	0
Start vs. week 3	0
Week 1 vs. Week 2	0
Week 1 vs. Week 4	0
Week 2 vs. Week 4	0
<b>WT</b>	
Week 1 vs. Week 2	100
Week 1 vs. Week 4	100
Week 2 vs. Week 4	100
<b><i>hol</i></b>	
Week 1 vs. Week 2	100
Week 1 vs. Week 4	100
Week 2 vs. Week 4	100
<b><i>35S::HOL</i></b>	
Week 1 vs. Week 2	100
Week 1 vs. Week 4	100
Week 2 vs. Week 4	100



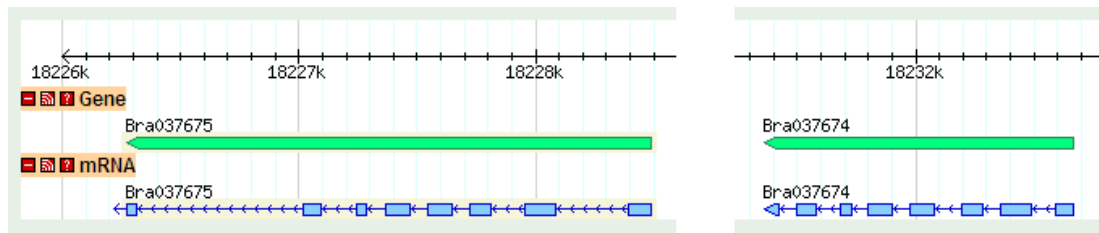
**Supplemental Figure 5.3. Examples of *cmuA* fragments obtained by PCR from DNA extracted from rhizosphere samples of *A. thaliana*.** Primers *cmuA802f* and *cmuA1609r* were used to amplify a *cmuA* fragment from DNA samples extracted from rhizosphere soil 2 weeks after the start of the experiment. Fragments were separated on a 1% agarose gel. Arrow indicates bands of the expected size (807 bp). L, 100 bp ladder (NEB); 1-7, WT; 8-13, *hol* mutant.

Chapter 6

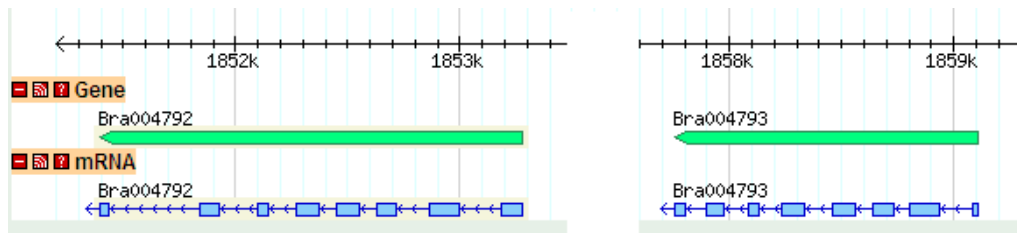
AtHOL	1	MAEEQONS	DQSN	GNV	IPT	PEEVAT	FLH	KTV	EEGG	WEKC	WEE	EIT	TPW	DQGR	ATPL	IVHLV
AtHLL1	1	MAEEQONS	SSYS	IGNI	IPT	PEEAAT	EQP	QVVA	EGGW	DKC	WEDG	VTP	WDQ	GRAT	PLI	IHL
BoTMT1	1	MAEEQOKA	CHSN	GENI	IIP	PEEVAK	FLPE	TV	EEGG	WEKC	WEDG	IT	TPW	DQGR	ATPL	VVHLV
BraA.HOL.b	1	MAEEQOKT	GQSN	GENI	IIP	PEEVAK	FLPE	TV	EEGG	WEKC	WEDG	IT	TPW	DQGR	ATPL	VVHLV
BoTMT2	1	MAEVQONS	SGNS	NGENI	IIP	PEDVAK	FLPK	TV	DEGG	WEKC	WEDG	VTP	WDQ	GRAT	PLV	VHLV
BraA.HOL.a	1	MAEEQONS	SAHIN	GENI	IIP	PEDVAK	FLPK	TV	EEGG	WEKC	WEDG	VTP	WDQ	GRAT	PLV	VHLV
AtHLL2	1	-----	MENAG	KATSI	QSSR	DLF	HL	MSEN	SSGG	WEKS	SWEA	GAT	PWD	LCK	PTP	VI
BraA.HLL.a	1	-----	MCNS	GKAP	AVES	PSDI	FQRL	VRED	SSGG	WEK	TWK	GAT	PWD	LGR	PTPI	IKHLA
BraA.HLL.b	1	-----	MDH	-----	-----	-----	-----	-----	-----	-----	-----	-----	-----	-----	-----	-----
AtHOL	61	DTSS	LPLGR	ALV	PGCG	GGHD	VVAM	ASPER	FVV	GLD	ISE	SALAK	ANET	YGSS	PKAE	YFSFV
AtHLL1	61	DSS	ALPLGR	TLPV	PGCG	GGHD	VVAM	ASPER	FVV	GLD	IS	DKALN	KANET	YGSS	PKAE	YFSFV
BoTMT1	60	DSS	LPLGR	ALV	PGCG	GGHD	VVAM	ASPER	FVV	GLD	ISE	SALEKA	AET	YGSS	PKAK	YTFV
BraA.HOL.b	60	DSS	LPLGR	ALV	PGCG	GGHD	VVAM	ASPER	YVV	GLD	ISE	SALEKA	AET	YGSS	PKSK	YFTFV
BoTMT2	60	ESS	LPLGR	CLV	PGCG	GGHD	VVAM	ASPER	YVV	GLD	ISE	SALEKA	AET	YGSS	PKAK	YTFV
BraA.HOL.a	60	ESS	LPLGR	ALV	PGCG	GGHD	VVAM	ASPER	YVV	GLD	ISE	SALEKA	AET	YGSS	PKAK	YTFV
AtHLL2	54	ET	GS	LPLGR	ALV	PGCG	TGY	DV	VAM	AS	DR	HV	VGL	D	IS	KTA
BraA.HLL.a	54	ET	GS	LPLGR	ALV	PGCG	TGY	DV	VAM	AS	DR	YV	VGL	D	IS	R
BraA.HLL.b	36	ET	SS	LPLGR	ALV	PGCG	TGY	DV	VV	MA	DR	HV	I	G	L	S
AtHOL	121	KED	VFTWR	PTEL	FDLI	FDY	VV	FCA	IE	PE	MR	PAW	AKS	MY	ELL	KPD
AtHLL1	121	KED	VFTWR	PNEL	FDLI	FDY	VV	FCA	IE	PE	MR	PAW	AKS	MY	ELL	KPD
BoTMT1	120	KED	FFTWR	PNEL	FDLI	FDY	VV	FCA	IE	PE	MR	PAW	AKS	MY	ELL	KPD
BraA.HOL.b	120	KED	FFTWR	PNEL	FDLI	FDY	VV	FCA	IE	PE	MR	PAW	AKS	MY	ELL	KPD
BoTMT2	120	KED	FFTWR	PNEL	FDLI	FDY	VV	FCA	IE	PE	TR	PAW	AKS	MY	ELL	KPD
BraA.HOL.a	120	KED	FFTWR	PNEL	FDLI	FDY	VV	FCA	IE	PE	TR	PAW	AKS	MY	ELL	KPD
AtHLL2	114	SE	FFTWE	PAEK	FDLI	FDY	T	FFCA	FE	AS	VR	PL	WA	QR	ME	KL
BraA.HLL.a	114	CE	FFTWE	PAEK	FDLI	FDY	T	FFCA	FE	AS	VR	PL	WA	QR	ME	KL
BraA.HLL.b	96	KE	FFTWE	PT	EKF	FDLI	FDY	N	FFCA	FE	PK	VR	PL	WA	KR	MO
AtHOL	181	PP	YK	V	D	V	S	T	F	E	V	L	V	P	I	G
AtHLL1	181	AP	YK	V	A	L	S	S	Y	E	D	V	L	V	P	V
BoTMT1	180	PP	YK	V	A	V	S	T	Y	E	D	V	L	V	P	V
BraA.HOL.b	180	PP	YK	V	A	V	S	T	Y	E	D	V	L	V	P	V
BoTMT2	180	PP	YK	V	A	V	S	T	Y	E	D	V	L	V	P	V
BraA.HOL.a	180	PP	YK	V	A	V	S	T	Y	E	D	V	L	V	P	V
AtHLL2	174	PP	Y	V	S	V	S	E	Y	E	K	V	L	I	P	I
BraA.HLL.a	174	PP	Y	K	V	S	V	S	D	Y	E	K	V	L	I	P
BraA.HLL.b	156	PP	Y	R	V	S	V	S	A	Y	E	E	L	L	I	P

**Supplemental Figure 6.1. Alignment of HOL and HLL protein sequences from *A. thaliana*, *B. rapa* and *B. oleracea*.** Full-length protein sequences were aligned using ClustalX. The corresponding phylogenetic tree is shown in Fig. 6.3.

A



B



**Supplemental Figure 6.2. *B. rapa* *HOL* and *HOL-like (HLL)* genes.** Location, structure and predicted transcripts of *BraA.HOL.a* (Bra037675) and *BraA.HLL.a* (Bra037674) on chromosome A4 (A) and *BraA.HOL.b* (Bra004792) and *BraA.HLL.b* (Bra004793) on chromosome A5 (B). Image taken and modified from the *B. rapa* Genome Browser at [brassicadb.org](http://brassicadb.org).

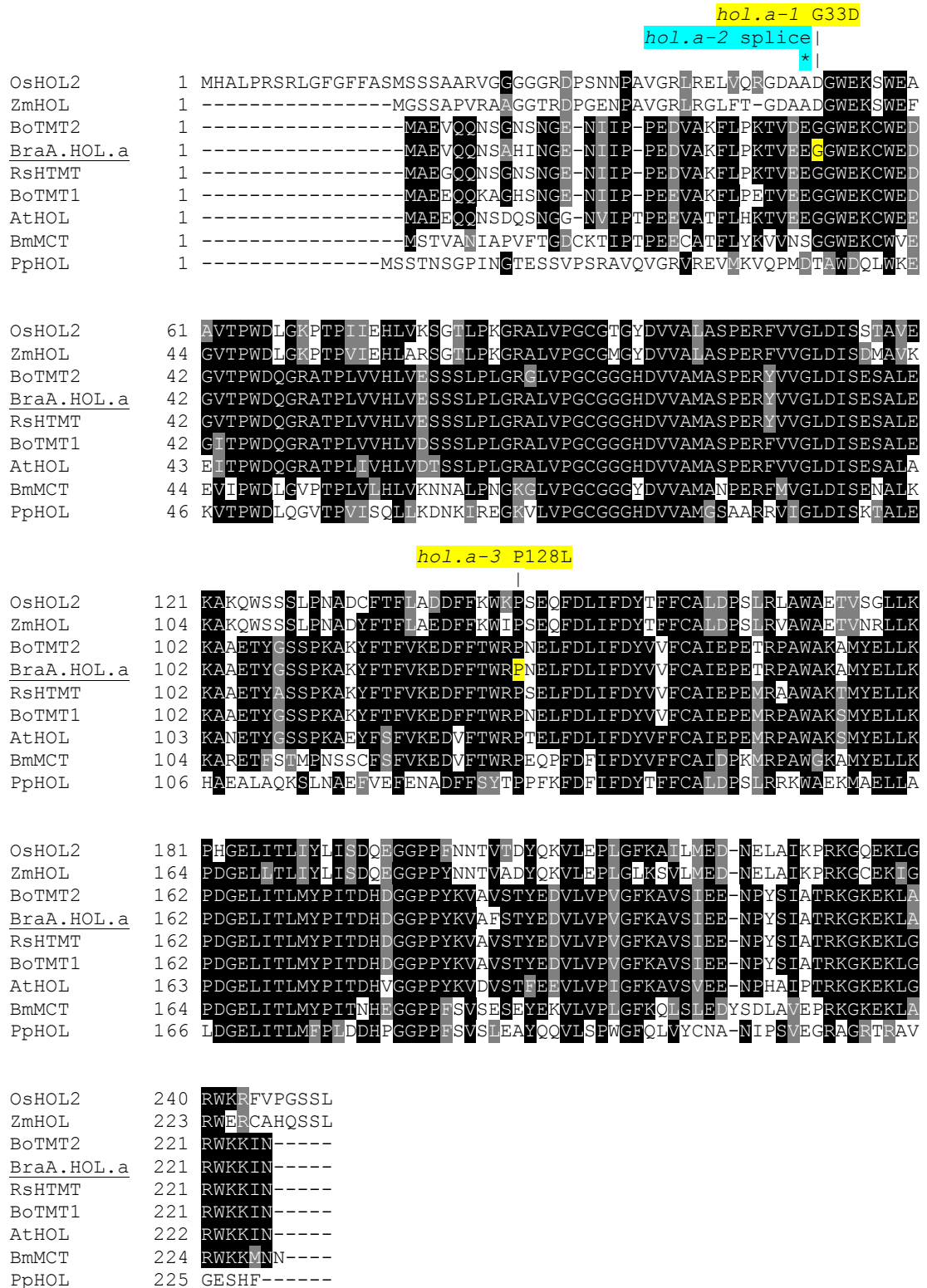


```

1 cgcgaaattca TGGCTGAGGT ACAACAAAAC TCAGCTCACA TCAATGGTGA AAACATCATC
61 CCTCCAGAAG ATGTTGCTAA GTTCCTGCCC AAAACTGTTG AAGAAGgtga ttcggttcctc
121 cctcaatatt acttataaaa ttttttttga tcaatattac ttatacaatt gtaacagagt
181 tttaggtcctt tgttctctag taatatgaga aaaatcatta cggattttgtg acaaatgagt
241 cacactaatc aatatcatat gctttttgat tggatctata tggtttcttt ttttttcgcg
301 ctatatgggtt tccttatcca tagccacaaa atggatggaa ctatttttga tttcgttagg
361 tagagaaaaa aaatagtaat actaatgtga atactattaa ataaaaataa aagTGGATG
421 GGAAAAATGT TGGGAAGATG GGGTAACACC ATGGGACCAA GGAAGAGCCA CACCTCTTGT
481 TGTCCATCTT GTTGAATCTT CTTCTCTTCC TgTTGGTCGT GCTCTTGTCC CgGGCTGTGG
541 CGGAgttagt cttcttttta ctcttcatat attttttccg gctcggttta gagaacaaat
601 atactgacca aactaagatc caagctagtt tgaattgtgc ataaggtaat tatctattat
661 ttttggtaaa aatcatgaat ggagcagGGT CgATGTGG TTGCGATGGC AAGCCCCGAA
721 CGTTACGTTG TTGTTTGGG TATTTGTGAA AGTGCCTCC AGAAAGCTGC TGAGgttaat
781 catattctca ctatgttact ttcacgtca attactgaat tttttattaa ttacctttgg
841 attacatata gACTTACGGC TCCTCACCGA AGGCCAAGTA CTTTACGTTT GTGAAGGAAG
901 ACTTCTTCAC ATGGCGTCCT AACGAATTAT TCGATCTCAT TTTCGATTAT GTgtgagttta
961 gttaactatt ttaacataat ctttgaaatc agaaagaaaa aaagaaacca atattccaag
1021 taacagGGTC TTCTGTGCCA TTGAGCCGGA GACGAGACCT GCATGGGCCA AAGCCATGTA
1081 TGAACTCTTA AAACCCGATG GCGAACTCAT TACTCTCATG TATCCGgtaa ttatttgata
1141 ttttggtgtaa ttattccatt tttaatcaat taaaaaaaaa cttgcacttt ttgtttatta
1201 gATTACCGAT CATGATGGTG GACCGCCATA CAAAGTAGCT TTCTCTACgt acgtaaatag
1261 cctcttaatt ttcggtatgt acatagctat tctaataattt atgacatgaa aatctgtagt
1321 tacagtaaca attacaagta gattaagtaa tcaactactaa actgttaatt ttgcttgtgt
1381 ttcttgggtt ttagCTACGA AGATGTTTTG GTCCGGTAG GATCAAGGC AGTGCCATT
1441 GAAGAGAATC CATACTCCAT TGCCACTCGT AAGgtatata cactgaccac attttgcggc
1501 acatatagtt taagctcgca ttagttaaagc cgtatggaat ggaacagatt gaacttatca
1561 aaaccgcatc acattgttac actaatcatt cttcgtatgc ttcatgcgcc ccggttcata
1621 cacataaatg tatataactta tatatactag agtctaagtt ggaactatat gactttgtgt
1681 aaatacatat cccaatacca ttatactata tatataagaa attagtacat ggactacagt
1741 ataggccata ttgaacagaa caatgtcatt tatagatcta cttacaattc caaacatata
1801 tcaaattttg aataacttag gagttactat tgtaagtttt aatattagat gtaccttcta
1861 acaatataac tagttatcac caaattttaa taatttgttta acattatatt ttcttacctt
1921 tttgtaacca aactaacata actaatactc ttcttgtatt atattagaaa tgggtgtttc
1981 aagaaagcga aattagtcag attttactat ttatattcgt aaaatcattt taacattttt
2041 taaaaattat agattaattg ttcgattttt tatctggttta attacataat cagaattgta
2101 gttgcaattt aaatacacgt aactgattgt tcattacttc attggattgg tatatgtatt
2161 tgaaaaaata acaggaacc aggattacca atttgatttt caggaactat cagatatatc
2221 actcgagatg agacataata tgtcagaaat accaatgcca tacaccaagg agagcaagga
2281 atctactctg ggagctccaa actccacatt aatattgat gtggctactt acaccaactc
2341 agcaaacggt ttgacacctg aaacggaatg ttgcagggta cttttccctg atcaagagag
2401 tgaagggcaa aacaaaaccg gttgagaaga gtcaacagac ctacctcgtt gagactgatg
2461 gctcctctag taccactact tgtagtcagG GTAAAGAGAA GCTTGCTAGG TGAAGAAGA
2521 TCAACTGAgT cgacgcg

```

**Supplemental Figure 6.3. Genomic DNA sequence of *BraA.HOL.a* showing the mutations identified in the TILLING assay.** Exons are depicted in coloured capital letters. Primer annealing sequences used to generate the 1.2 kb fragment for TILLING are underlined. Silent and mis-sense mutations identified in the TILLING screen are highlighted in yellow and green, respectively. The splicing-site mutation is highlighted in pink.



**Supplemental Figure 6.4. Amino acid substitutions in *B. rapa* hol.a mutant lines identified in the TILLING assay.** ClustalX alignment of protein sequences from *Brassica rapa*, *Brassica oleracea*, *Arabidopsis thaliana*, *Raphanus sativus*, *Batis maritima*, *Zea mays*, *Oryza sativa* and *Physcomitrella patens*. Amino acid substitutions of the *B. rapa* mutant lines are highlighted in yellow. The position of the splice-site mutation is highlighted in blue.

```

AtHOL      1  -----MEEQQNSDQSNCGNVIPTPEEVATFLHKTVEEG-----GWEKC
AtHLL1    1  -----MEEQQNSSYSICGNILPTPEEAATFQPQVVAEG-----GWDKC
AtHLL2    1  -----MENAGKATS-----LOSSRDLFHRLMSSENSSG-----GWEKS
OsHOL1    1  -----MASAIVDVAGGGRCQALDGSNPAVARLRQLIGGQESSDGWSRC
OsHOL2    1  MHALPRSRLGFGFFASMSSSAARVGGGGGRDPSN--NPVAVGRRLRELVRG--DAADGWEKS

AtHOL      40  WEEETTPWDQGRATPLIVHLVDTSSSLPLGRA---LVPGCGGHDVVAMASPERFVVGLDI
AtHLL1    40  WEDGVTTPWDQGRATPLIHLHLDSSALPLGRT---LVPGCGGHDVVAMASPERFVVGLDI
AtHLL2    33  WEAGATPVDLGKPTPIAHLVETGSLPNGRA---LVPGCGTGYDVVAMASPERFVVGLDI
OsHOL1    45  WEEGVTTPVDLQRTPAVVELVHSGTLPAGDATTVLVPGCGAGYDVVALSGPGRFVVGLDI
OsHOL2    58  WEAAVTPVDLGKPTPIIEHLVKSGTLPKGRA---LVPGCGTGYDVVALASPERFVVGLDI

AtHOL      97  SESALAKANETYGSSPKAE-----YFSFVKEDVFTWRPELFDLIFDYVFFCAIEPE
AtHLL1    97  SDKALNKANETYGSSPKAE-----YFSFVKEDVFTWRPENLFDLIFDYVFFCAIEPE
AtHLL2    90  SKTAVERSSTKKFSTLPNAK-----YFSFISEDFFTWEPAEKFDLIFDYVFFCAFEPG
OsHOL1    105 CDTATQKAKQLSAAAAAADGGDSSSEFAFVADDFFTWEPPEPFHLIFDYVFFCALHPS
OsHOL2    115 SSTAVEKAKQWSSSLPNAD-----CFTFLADDFKWKPESEQFDLIFDYVFFCALDPS

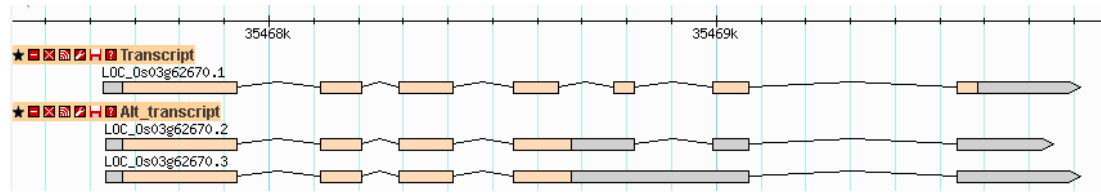
AtHOL      149  MRPAAKSMYELLKPDGELITLMYPIIDFVGGPPYKVDVSTFEVVLVPIGFKAVSVEENP
AtHLL1    149  MRPAAKSMHELLKPDGELITLMYPMIDHEGGAPYKVALSSYEDVLVPIGFKAVSVEENP
AtHLL2    142  VRPLWAQRMKLLKPGGELITLMFPIDERSGGPPYEVSVSEYEKVLIPLGFBAISIVDNE
OsHOL1    165  MRPAAKRMADLLRPDGELITLMYLAEGQEAAGPPFNTIVLDYKEVLNPLGLVITSIEDNE
OsHOL2    167  LRLAWAETVSGLLKPHGELITLIYLIISDQEGGPPFNNTIVTDYQKVLPLGFKAILMEDNE

AtHOL      209  HAIPTRKGKEKLGWRWKKLN-----
AtHLL1    209  DSIPTRKGKEKLGWRWKKLN-----
AtHLL2    202  LAVGPRKGMKLGWRWKKSSTFHSTL
OsHOL1    225  VAVEPRKGMKGIARWKRMTKSD---
OsHOL2    227  LAIKPRKGMKLGWRWKRIVPVGSSL-

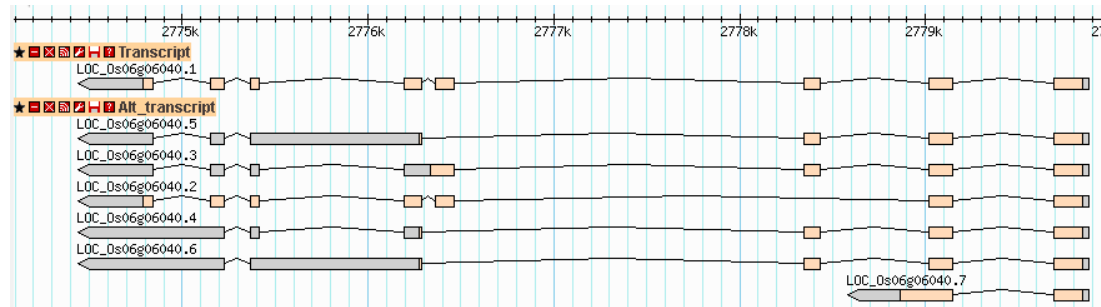
```

**Supplemental Figure 6.5. Alignment of HOL and HLL protein sequences from *A. thaliana* and *O. sativa*.** Full-length protein sequences were aligned using ClustalX.

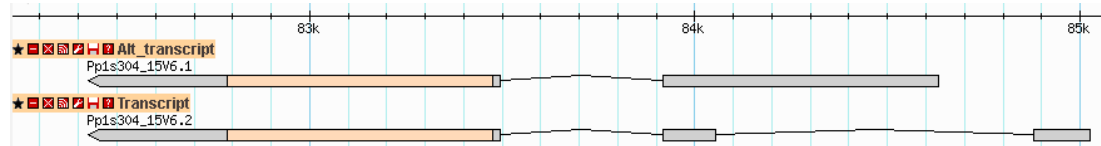
A



B



**Supplemental Figure 6.6. Rice *HOL* genes.** Location, structure and predicted transcripts of *OsHOL1* (LOC\_Os03g62670) on chromosome III (A) and *OsHOL2* (LOC\_Os06g06040) on chromosome VI (B). Image taken from the *O. sativa* Genome Browser at [www.phytozome.net](http://www.phytozome.net).



**Supplemental Figure 6.7. Location, structure and predicted transcripts of the *P. patens* *HOL* gene** (Pp1s304\_15V6, Phypa\_60954). Image taken from the *P. patens* Genome Browser at [www.phytozome.net](http://www.phytozome.net).

```

AtHOL      1 MAEEQ----QNSDQSNNGNVIPTEEVATFLHKTVEEGGWKCEWEEETTPWDQGRATPLI
AtHLL1     1 MAEEQ----QNSSYSIGGNIIPTEEAATEQPQVVAEGGWKCEWEDGVTPWDQGRATPLI
AtHLL2     1 MENAG----KATS-----LOSSRDLFHRLMSENSSGGWKESWEAGATPWDLGKPTPVI
PpHOL      1 MSSTNSGPIINGTESSVPSRAVQVGR-VREVVKVQPMDTAWDQLWKEKVTPWDLQGVTPVI

AtHOL      57 VHLVDTSSLPLGRALVPGCGGGHDVVAMASPERFVVGLDISESALAKANETYGSSPKAEY
AtHLL1     57 LHLIDSALPLGRITLVPGCGGGHDVVAMASPERFVVGLDISDKALNKANETYGSSPKAEY
AtHLL2     50 AHLVETGSLFNGRALVPGCGTGYDVVAMASPD RHVVGLDISKTAVERSTKKESTLPNAKY
PpHOL      60 SQLLKDNKIREGKVLVPGCGGGHDVVAMCSAARRVIGLDISKTALEHAEALAQKSLNAEF

AtHOL      117 FSFVKEDVFTWRPTELFDLIFDYVFFCAIEPEMRPAWAKSMYELLKPDGELITLMYPITD
AtHLL1     117 FSFVKEDVFTWRPNELFDLIFDYVFFCAIEPEMRPAWCKSMHELLKPDGELITLMYPMTD
AtHLL2     110 FSFLSEDFFTWEPAEKFDLIFDYTFFCALPEPGVRPLWAQRMEKLLKPGGELITLMFPIDE
PpHOL      120 VEFENADFFSYTTPPFKDFDFIFDYTFFCALDPSLRKWAEEKMAELLALDGLITLMFPLDD

AtHOL      177 HVGGPPYKVDVSTFEVLVPIGFKAVSVEENPHAIPTKKGKEKLGKRWKIN-----
AtHLL1     177 HEGGAPYKVALSSYEDVLPVVGFKAVSVEENPDSIPTKKGKEKLARWKIN-----
AtHLL2     170 RSGGPPYEVSVSEYEKVLIPIGFEATSTVDNELAVGPRKGMKLGKRWKKSSTFFHSTL
PpHOL      180 HPGGPPFESVSL EAYQQVLSFWGFLVYCNANIPSV EGRAGRTRAVGESHF-----

```

**Supplemental Figure 6.8. Alignment of HOL and HLL protein sequences from *A. thaliana* and *P. patens*.** Full-length protein sequences were aligned using ClustalX.

## Chapter 7

**Supplemental Table 7.1. Names and sources of HTMT protein sequences used for phylogenetic analysis in this study.**

Name	Original name/accession number	Species	Source*
AtHOL	AT2G43910.1 HARMLESS TO OZONE LAYER 1	<i>Arabidopsis thaliana</i>	MIPS
AtHLL1	AT2G43920.1 SAM-dependent methyltransferase	<i>Arabidopsis thaliana</i>	MIPS
AtHLL2	AT2G43940.1 SAM-dependent methyltransferase	<i>Arabidopsis thaliana</i>	MIPS
BoTMT1	gi 75331625 sp Q93V78.1 TMT1_BRAOL	<i>Brassica oleracea</i>	NCBI
BoTMT2	gi 75331717 sp Q93XC4.1 TMT2_BRAOL	<i>Brassica oleracea</i>	NCBI
RsHTMT	gi 253787624 dbj BAH84870.1	<i>Raphanus sativus</i>	NCBI
BrHOLa	gi 119655911 gb ABL86248.1	<i>Brassica rapa</i>	NCBI
BmMCT	gi 4588479 gb AAD26120.1 AF109128_1	<i>Batis maritima</i>	NCBI
PtrHOL	Ptrichocarpa POPTR_0017s03980  POPTR_0017s03980.1	<i>Populus trichocarpa</i>	Phytozome
VvHOL1	Vvinifera GSVIVG01038246001  GSVIVT01038246001	<i>Vitis vinifera</i>	Phytozome
VvHOL2	Vvinifera GSVIVG01038247001  GSVIVT01038247001	<i>Vitis vinifera</i>	Phytozome
VvHOL3	gi 147783616 emb CAN68137.1	<i>Vitis vinifera</i>	NCBI
VvHOL4	gi 225434217 ref XP_002275789.1	<i>Vitis vinifera</i>	NCBI
MeHOL	Mesculenta cassava4.1_014307m.g  cassava4.1_014307m	<i>Manihot esculenta</i>	Phytozome
PpeHOL	Ppersica ppa010661m.g ppa010661m	<i>Prunus persica</i>	Phytozome
CpHOL1	Cpapaya evm.TU.supercontig_151.2  evm.model.supercontig_151.2	<i>Carica papaya</i>	Phytozome
CpHOL2	Cpapaya evm.TU.supercontig_151.3  evm.model.supercontig_151.3	<i>Carica papaya</i>	Phytozome
CpHOL3	Cpapaya evm.TU.supercontig_151.4  evm.model.supercontig_151.4	<i>Carica papaya</i>	Phytozome
MgHOL	Mguttatus mgv1a012055m.g mgv1a012055m	<i>Mimulus guttatus</i>	Phytozome
AcHOL	Acoerulea AcoGoldSmith_v1.025805m.g  AcoGoldSmith_v1.025805m	<i>Aquilegia coerulea</i>	Phytozome
SiHOL1	Sitalica SiPROV035223m.g SiPROV035223m	<i>Setaria italica</i>	Phytozome
SiHOL2	Sitalica SiPROV014068m.g SiPROV014068m	<i>Setaria italica</i>	Phytozome
BdHOL	Bdistachyon Bradi1g49130 Bradi1g49130.1	<i>Brachypodium distachyon</i>	Phytozome
EgHOL	Egrandis Egrandis_v1_0.025224m.g  Egrandis_v1_0.025224m	<i>Eucalyptus grandis</i>	Phytozome
CsHOL	Csinensis orange1.1g024021m.g  orange1.1g024008m	<i>Citrus sinensis</i>	Phytozome
CcHOL	Cclementina clementine0.9_018340m.g  clementine0.9_018336m	<i>Citrus clementina</i>	Phytozome
RcHOL	Rcommunis 30042.t000021 30042.m000483	<i>Ricinus communis</i>	Phytozome
OsHOL1	Osativa LOC_Os03g62670 LOC_Os03g62670.1	<i>Oryza sativa</i>	Phytozome
OsHOL2	Osativa LOC_Os06g06040 LOC_Os06g06040.1	<i>Oryza sativa</i>	Phytozome
SbHOL	Sbicolor Sb10g003780 Sb10g003780.1	<i>Sorghum bicolor</i>	Phytozome
ZmHOL	gi 226507030 ref NP_001147771.1	<i>Zea mays</i>	NCBI
SmHOL	Smoellindorffii 15402622_locus 100790	<i>Selaginella moellendorffii</i>	Phytozome
PpHOL	Ppatens Pp1s304_15V6 Pp1s304_15V6.1	<i>Physcomitrella patens</i>	Phytozome
PtHTMT	gi 217409314 gb EEC49246.1	<i>Phaeodactylum tricorutum</i>	NCBI

\* MIPS, <http://mips.helmholtz-muenchen.de/plant/genomes.jsp>

NCBI, <http://www.ncbi.nlm.nih.gov/>

Phytozome v6.0, <http://www.phytozome.net/>

**Motif I**

PtHTMT	1	SPWELLWVKDGLTPWDLGRPTPLCKEIERFSLVGSKRITLVPGCCAGYDLATLAADSASVTGLDISENALQ
PpHOL	1	TAWDQLWKEKVTTPWDLQGVTPWIS-QHLKDNKIREGKVLVPGCGGGHDVVMGSAARFVIGLDISKTALE
SmHOL	1	--WEKCWAERVTPWDLGGVTPLIQ-HLVSQEQLPQGRCLVPGCCSGYDVLALANPSRHVVGLDISETALE
SiHOL1	1	DGWSRCWEEGVTTPWDLGQPTPAVV-ELAKSGTLP-CDALVPGCCAGYDVAALSGPGRFVVGLDICEATAVA
OsHOL1	1	DGWSRCWEEGVTTPWDLGQRTPAVV-ELVHSGTLPAGDALVPGCCAGYDVAALSGPGRFVVGLDICTATAQ
SiHOL2	1	DGWEKSWIEFGVTTPWDLGKPTPIE-HLVRSGLLPKGRALVPGCGMGYDVAALACPERFVVGLDVSIDLAIK
BdHOL	1	DGWEKSWESGVTTPWDLGKPTPIE-HLVKSGSLPKGRALVPGCGMGYDVAALASPERFVVGLDISNTIATE
OsHOL2	1	DGWEKSWEAAVTPWDLGKPTPIE-HLVKSGTLPKGRALVPGCGTYDVAALASPERFVVGLDISSTAVE
SbHOL	1	DGWEKSWIEFGVTTPWDLGKPTPIE-HLVRSGLLPKGRALVPGCGMGYDVAALASPERFVVGLDISIDLAVK
ZmHOL	1	DGWEKSWIEFGVTTPWDLGKPTPIE-HLARSGLLPKGRALVPGCGMGYDVAALASPERFVVGLDISDMAVK
<b>BmMCT</b>	1	GGWEKCWVEEVIPTWDLGVPTPLVL-HLVKNALPNKGLVPGCGGGYDVAAMANPERFMVGLDISENALK
<b>AtHLL1</b>	1	GGWDKCWEDGVTTPWDLQGRATPLIL-HLLDSSALPLGRTLVPGCCGGHDVVMASPERFVVGLDISDKALN
<b>AtHOL</b>	1	GGWEKCWEEETTPWDLQGRATPLIV-HLVDTSSLPKGRALVPGCGGGHDVVMASPERFVVGLDISESALA
<b>BoTMT1</b>	1	GGWEKCWEDGVTTPWDLQGRATPLVV-HLVDTSSLPKGRALVPGCGGGHDVVMASPERFVVGLDISESALE
<b>RsHTMT</b>	1	GGWEKCWEDGVTTPWDLQGRATPLVV-HLVDTSSLPKGRALVPGCGGGHDVVMASPERFVVGLDISESALE
<b>BoTMT2</b>	1	GGWEKCWEDGVTTPWDLQGRATPLVV-HLVDTSSLPKGRALVPGCGGGHDVVMASPERFVVGLDISESALE
<b>BrHOLa</b>	1	GGWEKCWEDGVTTPWDLQGRATPLVV-HLVDTSSLPKGRALVPGCGGGHDVVMASPERFVVGLDISESALE
AtHLL2	1	GGWEKSWEACIPTWDLGKPTPIA-HLVEETSLPNGRALVPGCGTYDVAALASPERFVVGLDISKTAVE
MgHOL	1	NCWDKWEETTPWDLGRPTPLVL-HLHNTGSLPKGRALVPGCGSGHDVVALASSDLHVGLDISENALK
AcHOL	1	GGWDKCWEQAITPWDLGGPTPVL-NLLKTCALPKGRVLIIPGCCSGHDVVALACPERFVVGLDISENALN
EgHOL	1	DCWEKWEQGLTPWDLGKPTPIQ-QLHQMGALPKGRALVPGCGTYDVAALACPERFVVGLDISENALN
PpHOL	1	SGWDKCWEQGLTPWDLGQPTPIA-HLHQSGALPKGRALVPGCGTYDVAALASPERFVVGLDISENALK
CsHOL	1	GGWEKWEEGTTPWDLGQPTPIV-HLHQSGALPKGRALVPGCGTYDVAALASPERFVVGLDISDLAIK
CcHOL	1	GGWEKWEEGTTPWDLGQPTPIV-HLHQSGALPKGRALVPGCGTYDVAALASPERFVVGLDISDLAIK
PtHOL	1	GGWEKWEQGLTPWDLGRPTPLIL-HLHQTCALPKGRALVPGCGSGYDVAALACSERFVVGLDVSHTAIE
MeHOL	1	GGWEKWEQGLTPWDLGQPTPALI-HLHHTGSLPKGRALVPGCGSGHDVVALACPERFVVGLDVSIDLAIK
RcHOL	1	GGWEKWEQGLTPWDLGQPTPII-HLHHTGSLPKGRALVPGCGSGHDVVALACPERFVVGLDIAEKAVK
CpHOL3	1	GAWEKRWEIGTTPWDLGQPTPIVL-HLQQHGSALPKGRALVPGCGTYDVAALASLERFVVGLDISENALK
CpHOL1	1	SGWEKSWELGLTPWDLGQPTPVL-HLQQGALPNGRALVPGCGTYDVAALASPERFVVGLDISENALK
CpHOL2	1	GGWEKSWEQGLTPWDLGQPTPII-HLQQGTLPNGRALVPGCGTYDVAALASPERFVVGLDISENALK
VvHOL1	1	GGWEKSWQQCHTPWDLGKPTPIQ-HLHQGTLPKSGRTLVPGCGCGYDVAALACPERFVVGLDISDSAIK
VvHOL4	1	GGWEKSWQQCHTPWDLGKPTPIQ-HLHQGTLPKSGRTLVPGCGCGYDVAALACPERFVVGLDISDSAIK
VvHOL2	1	GSWEKSWQQGLTPWDLGKATPIE-HLHQAGALPNGRALVPGCGRKYDVAALACPERFVVGLDISDSAIK
VvHOL3	1	SSWEKSWQQGLTPWDLGKATPIE-HLHQAGALPNGRALVPGCGRKYDVAALACPERFVVGLDISDSAIK

PtHTMT	71	SARRLSSNLSDK-LCLNLICGDFFTWKGSPIVDFDIFDYT-----FFCALSPSMRPAWGR
PpHOL	70	HAEALAQKSLNA-EFVEFENADFFSYTPFKFDIFDYT-----FFCALDPSLRKWAIE
SmHOL	68	RAKELTSKNTTSQNYVEFKAVDFFSYSEPKFDFLIDYD-----FFCAIEPSTRPAWAK
SiHOL1	69	KAKQWSAAADDG-SLFAFVAADFFTWEPPELFDLIDYTKNDFSCPLDRSCVFRFFCAFHPSMRPAWAK
OsHOL1	70	KAKQLSAAAAAADFAFVADFFTWEPPEPEHLIDYD-----FFCALHPSMRPAWAK
SiHOL2	70	KAKQWSSSLPNA-DYFTFLAEDFFKWPSEOFDLIDYD-----FFCALDPSLRVAWAE
BdHOL	70	KAKKWSSSLPNA-DCFTFLAADFFKWRPSEPEFDLIDYD-----FFCALDPSLRVAWAE
OsHOL2	70	KAKQWSSSLPNA-DCFTFLAADFFKWRPSEOFDLIDYD-----FFCALDPSLRVAWAE
SbHOL	70	KAKQWSSSLPNA-DYFTFLAEDFFKWPSEOFDLIDYD-----FFCALDPSLRVAWAE
ZmHOL	70	KAKQWSSSLPNA-DYFTFLAEDFFKWPSEOFDLIDYD-----FFCALDPSLRVAWAE
<b>BmMCT</b>	70	KARETFSTMPNS-SCFSFVKEDVFTWRNELEFDLIDYV-----FFCAIEPEMRPAWAK
<b>AtHLL1</b>	70	KANETYGSSPKA-EYFSFVKEDVFTWRNELEFDLIDYV-----FFCAIEPEMRPAWAK
<b>AtHOL</b>	70	KANETYGSSPKA-EYFSFVKEDVFTWRNELEFDLIDYV-----FFCAIEPEMRPAWAK
<b>BoTMT1</b>	70	KAAETYGSSPKA-KYFTFVKEDFFTWRELEFDLIDYV-----VFCALPEMRPAWAK
<b>RsHTMT</b>	70	KAAETYASSPKA-KYFTFVKEDFFTWRELEFDLIDYV-----VFCALPEMRPAWAK
<b>BoTMT2</b>	70	KAAETYGSSPKA-KYFTFVKEDFFTWRELEFDLIDYV-----VFCALPEMRPAWAK
<b>BrHOLa</b>	70	KAAETYGSSPKA-KYFTFVKEDFFTWRELEFDLIDYV-----VFCALPEMRPAWAK
AtHLL2	70	RSTKKFSTLPNA-KYFSFLSEDFFTWEPAEKFDLIDYD-----FFCAIEPEMRPAWAK
MgHOL	70	KATELCSSEPKM-DHVSFLKDFFTWCPAQLFDLIDYD-----FFCAIEPKLRSLWAR
AcHOL	70	KARELFSSSONA-SHVAFVKEDFFTWNEPSLFDLIDYD-----FFCAIEPSKRPWAS
EgHOL	70	RAVKLFSSSPNA-NHFTFLKEDFFTWNELEFDLIDYD-----FFCAIEPEMRVAWAE
PpHOL	70	KAAELFSSLPNA-RYYSFLKVDFFTWNELEFDLIDYD-----FFCAIEPEMRVWAR
CsHOL	70	KAEELSSSLPNA-KEVSFLKADFFTWCPTELEFDLIDYD-----FFCAIEPEMRAWAK
CcHOL	70	KAEELSSSLPNA-KEVSFLKADFFTWCPTELEFDLIDYD-----FFCAIEPEMRAWAK
PtHOL	70	KAIELSSSLPNS-SYFTFLKADFFTWEPPELFDLIDYD-----FFCAIEPEMRSRWAC
MeHOL	70	KAEELSSSLPNA-NCFIFLRAADFFSWHPELEFDLIDYD-----FFCAIEPEMRSRWAM
RcHOL	70	KAEELSSSLPNA-NCFIFLKAADFFSWHPELEFDLIDYD-----FFCAIEPEMRSQWAI
CpHOL3	70	KAKEMSSSSPNA-NCFIFLKAADFFTWCPSELEFDLIDYD-----FFCAIEPEMRSWAK
CpHOL1	70	KAKEMSSSSPNA-NCFIFLKAADFFTWCPSELEFDLIDYD-----FFCAIEPEMRSWAK
CpHOL2	70	KAEEMSSSSPNA-NCFIFLKAADFFTWCPSELEFDLIDYD-----FFCAIEPEMRSWAK
VvHOL1	70	KAKELSSSLWNA-NHFTFLKEDFFTWNELEFDLIDYD-----FFCAIEPEMRSWAK
VvHOL4	70	KAKELSSSLWNA-NHFTFLKEDFFTWNELEFDLIDYD-----FFCAIEPEMRSWAK
VvHOL2	70	KAKESSSSSWNA-SHFTFLKADFFTWNELEFDLIDYD-----FFCAIEPEMRPAWAS
VvHOL3	70	KAKESSSSSWNA-SHFTFLKADFFTWNELEFDLIDYD-----FFCAIEPEMRPAWAS

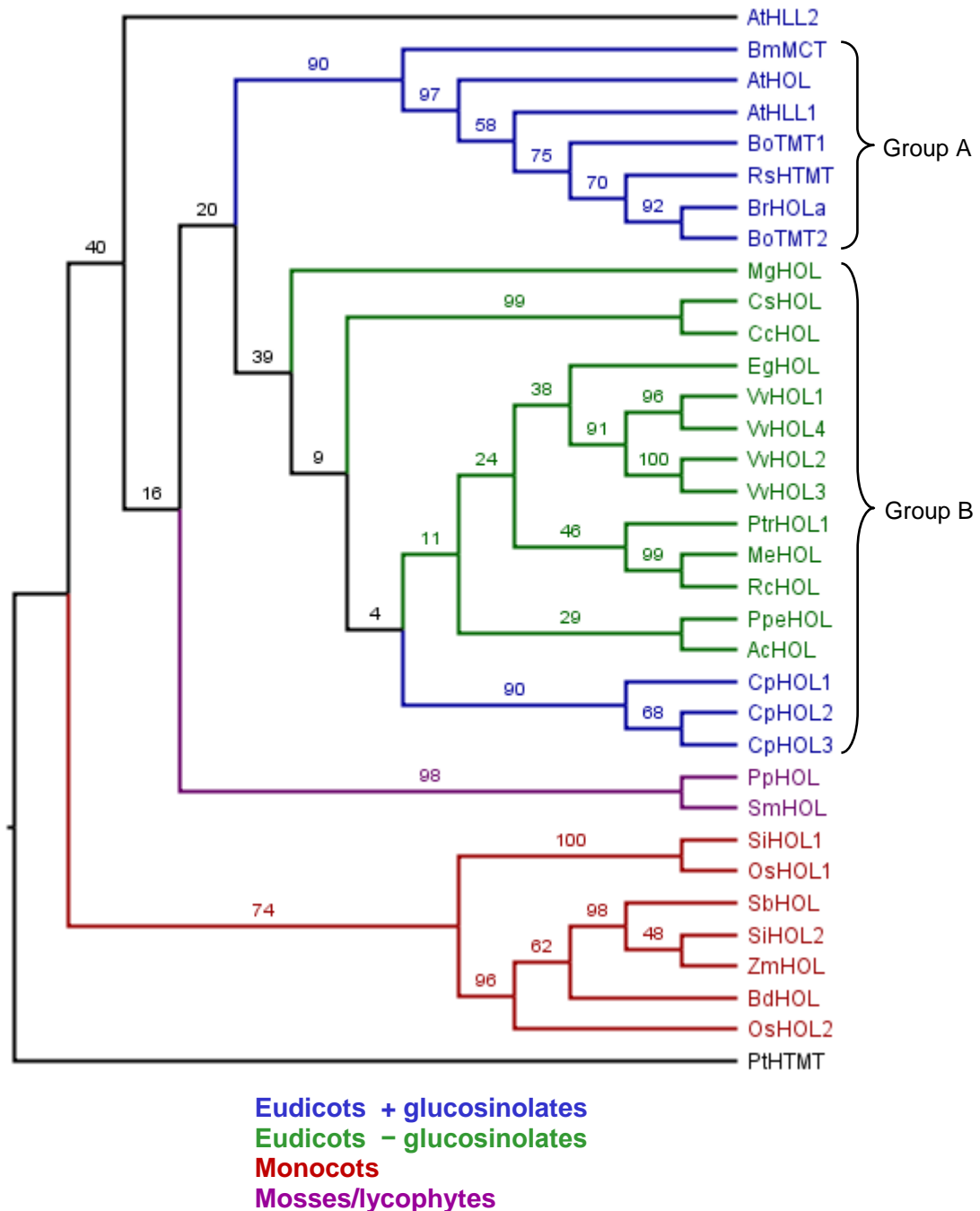
		Motif II	Motif III
PtHTMT	124	QTSLLDPEETCQLITLIFPITPEEDAEKGGPPYFVSVADYRKALEPIVIRTGPYES-EE-TIRQRKGIHQV	
PpHOL	123	KMAELLALD-GELITLMFPID---DHEGGPPESVSLIAYQQVLSPPWGFQLVYCNA-NIPSEVGRAGRT--	
SmHOL	122	KMAELLARD-GELITLMYPVG---DHEGGPPYAASPKAYEAVLHPCGLHAISEED-NKFSICARKGREITL	
SiHOL1	138	RVADLLKPN-GELITLMYLAQ---GQEAAGPPENTTVLE-----	
OsHOL1	124	RMADLLKPD-GELITLMYLAE---GQEAAGPPENTTVLDYKEVLNPIGLVITSTED-NEVAVEPRKGMKEI	
SiHOL2	123	TVNRLKPD-GELITLTYLAP---DPLQGPPLSHTTCGYGTRGEEELGQRAAAMET-AAVAYRLREEAEEI	
BdHOL	123	TVTRLLKPD-GELITLTYLIS---DHEGGPPYNNITVADYKVLVLEPLGFKAVLMED-NELAIKPRKGEFKL	
OsHOL2	123	TVSGLLKP-H-GELITLTYLIS---DHEGGPPYNNITVADYKVLVLEPLGFKAVLMED-NELAIKPRKGEFKL	
SbHOL	123	TVNRLKPD-GELITLTYLIS---DHEGGPPYNNITVADYKVLVLEPLGFKAVLMED-NEVAIKPRKGCCKI	
ZmHOL	123	TVNRLKPD-GELITLTYLIS---DHEGGPPYNNITVADYKVLVLEPLGFKAVLMED-NELAIKPRKGCCKI	
<b>BmMCT</b>	123	AMYELLKPD-GELITLMYPIT---DHEGGPPYFVSVSESEYKVLVPLGFKQVLEEDYSPLAVEPRKGMKEI	
<b>AtHLL1</b>	123	SMHELLKPD-GELITLMYPIT---DHEGGAPYKVALSSYEIVLVPVGFKAVSVEE-NPDSIPTRKGMKEI	
<b>AtHOL</b>	123	SMYELLKPD-GELITLMYPIT---DHEGGPPYKVDVSTFEEVLPVIGFKAVSVEE-NPHAIPTRKGMKEI	
<b>BoTMT1</b>	123	SMYELLKPD-GELITLMYPIT---DHEGGPPYKVAVSTYEDVLPVGFKAVSVEE-NPYSIATRKGKKEI	
<b>RsHTMT</b>	123	TMYELLKPD-GELITLMYPIT---DHEGGPPYKVAVSTYEDVLPVGFKAVSVEE-NPYSIATRKGKKEI	
<b>BoTMT2</b>	123	AMYELLKPD-GELITLMYPIT---DHEGGPPYKVAVSTYEDVLPVGFKAVSVEE-NPYSIATRKGKKEI	
<b>BrHOLa</b>	123	AMYELLKPD-GELITLMYPIT---DHEGGPPYKVAVSTYEDVLPVGFKAVSVEE-NPYSIATRKGKKEI	
AtHLL2	123	RMEKLLKPG-GELITLMFPID---DHEGGPPYFVSVSESEYKVLVPLGFKAVLMED-NELAIKPRKGMKEI	
MgHOL	123	KMSDLLKSD-GELITLMYPIT---DHEGGPPYKVSVDYEEVLPVIGFKAVLMED-NELAIAPRMGRKEI	
AcHOL	123	RIHDLKPD-GELITLMFPID---DHEGGPPYKVSVDYEEVLPVIGFKAVLMED-NELAVGARKGKKEI	
EgHOL	123	QMSGLLKPD-GELITLMFPIS---DHEGGPPYKVSISDYEEVLPVIGFKAVLMED-NELAVGPRKGMKEI	
PpeHOL	123	KIRDLLKPD-GELITLMFPIS---DHEGGPPYKVSISDYEEVLPVIGFKAVLMED-NELAVGPRKGMKEI	
CsHOL	123	KIKDFLKPD-GELITLMFPIS---DHEGGPPYKVSVDYEEVLPVIGFKAVLMED-NELAIAPRMGRKEI	
CcHOL	123	KIKDFLKPD-GELITLMFPIS---DHEGGPPYKVSVDYEEVLPVIGFKAVLMED-NELAIAPRMGRKEI	
PtrHOL	123	KVQEMLKPD-GELITLMYPIS---DHEGGPPYKVSVDYEEVLPVIGFKAVLMED-NELAIAPRMGRKEI	
MeHOL	123	QIQNLLKPD-GELITLMFPID---DHEGGPPYKVSVDYEEVLPVIGFKAVLMED-NELAIKARK---VC	
RcHOL	123	RIQDLLKPD-GELITLIFPID---DHEGGPPYKVSVDYEEVLPVIGFKAVLMED-NELAIKVR-----L	
CpHOL3	123	RMHELLKLD-GELITLMFPIT---DHEGGPPYFVSVAAAYEEVLCPIGFRPVSIVD-NNLATASRQGEKEL	
CpHOL1	123	RMCKLLKPD-GELITLMFPIS---DHEGGPPYFVSVADYEEVLRPMGFKSVSVVD-NELAIAPRMGRKEI	
CpHOL2	123	RMYELLKPD-GELITLMFPIS---DHEGGPPYFVSVADYEEVLRPMGFKSVSVVD-NELAIAPRMGRKEI	
VvHOL1	123	RMRHLLKPD-GELITLMFPIS---DHEGGPPYKVSVDYEEVLPVIGFKAVLMED-NELAIAPRMGRKEI	
VvHOL4	123	RMRHLLKPD-GELITLMFPIS---DHEGGPPYKVSVDYEEVLPVIGFKAVLMED-NELAIAPRMGRKEI	
VvHOL2	123	RMQQLKPD-GELITLMFPIS---DHEGGPPYKVSVDYEEVLPVIGFKAVLMED-NELAIAPRMGRKEI	
VvHOL3	123	RMQQLKPD-GELITLMFPIS---DHEGGPPYKVSVDYEEVLPVIGFKAVLMED-NELAIAPRMGRKEI	

PtHTMT	192	CWNT-----
PpHOL	186	---EAVG-ESH
SmHOL	187	GRWKKITP---R
SiHOL1		-----
OsHOL1	189	ARWKRMTK-SD-
SiHOL2	188	ARRDAEER-RHA
BdHOL	188	GRWRRCGP-QSC
OsHOL2	188	GRWKRFPV-GSS
SbHOL	188	GRWRRCAH-QSS
ZmHOL	188	GRWERCAH-QSS
<b>BmMCT</b>	189	ARWKKMNN----
<b>AtHLL1</b>	188	ARWKKIN----
<b>AtHOL</b>	188	GRWKKIN----
<b>BoTMT1</b>	188	GRWKKIN----
<b>RsHTMT</b>	188	GRWKKIN----
<b>BoTMT2</b>	188	ARWKKIN----
<b>BrHOLa</b>	188	ARWKKIN----
AtHLL2	188	GRWKKSTFHST
MgHOL	188	GRWKRSTS-QSS
AcHOL	188	GRWKRSLA-ESC
EgHOL	188	GRWKRIRV-NSL
PpeHOL	188	GRWKRSL-ESS
CsHOL	188	GRWKRSVR-HSL
CcHOL	188	GRWKRSVR-HSL
PtrHOL	188	GRWRRDTT-QSI
MeHOL	185	G-----
RcHOL	183	GLYKA-----
CpHOL3	188	GRWKKLVD-KPS
CpHOL1	188	GRWKFVA--KPS
CpHOL2	188	GRWKKLVG-KPS
VvHOL1	188	GRWKRTPS-KSL
VvHOL4	188	GRWKRTPS-KSL
VvHOL2	188	GRWKRTPD--EPL
VvHOL3	188	GRWKRTPS-KSL

**Supplemental Figure 7.1. Alignment of HTMT protein sequences used for phylogenetic analysis.**

Full-length protein sequences were prealigned using Muscle. The alignment was then manually edited in BioEdit to remove ambiguously aligned positions. Amino acid (AA) residues forming the putative nucleophile-binding site in *A. thaliana* HOL are marked with triangles: black triangles indicate conserved AAs whereas red triangles indicate variation of AAs between HTMTs. HTMTs belonging to group A are in bold. Highly conserved motifs found in other MTs are marked with a line. Species names: Ac, *Aquilegia coerulea*; At, *Arabidopsis thaliana*; Bd, *Brachypodium distachyon*; Bm, *Batis maritima*; Bo, *Brassica oleracea*; Br, *Brassica rapa*; Cc, *Citrus clementina*; Cp, *Carica papaya*; Cs, *Citrus sinensis*; Eg, *Eucalyptus grandis*; Me, *Manihot esculenta*; Mg, *Mimulus guttatus*; Os, *Oryza sativa*; Pp, *Physcomitrella patens*; Ppe, *Prunus persica*; Pt, *Phaeodactylum tricornutum*; Ptr, *Populus trichocarpa*; Rc, *Ricinus communis*; Rs, *Raphanus sativus*; Si, *Setaria italica*; Sm, *Selaginella moellendorffii*; Sb, *Sorghum bicolor*; Vv, *Vitis vinifera*; Zm, *Zea mays*.





**Supplemental Figure 7.2. Maximum Likelihood tree of plant HTMT proteins.** A Maximum Likelihood analysis was performed on an alignment of plant HTMT protein sequences (Suppl. Fig. 7.1). The tree was rooted using the *Phaeodactylum tricornutum* TMT (diatom) as an outgroup. The numbers on the clades are Bootstrap values. Species names: Ac, *Aquilegia coerulea*; At, *Arabidopsis thaliana*; Bd, *Brachypodium distachyon*; Bm, *Batis maritima*; Bo, *Brassica oleracea*; Br, *Brassica rapa*; Cc, *Citrus clementina*; Cp, *Carica papaya*; Cs, *Citrus sinensis*; Eg, *Eucalyptus grandis*; Me, *Manihot esculenta*; Mg, *Mimulus guttatus*; Os, *Oryza sativa*; Pp, *Physcomitrella patens*; Ppe, *Prunus persica*; Pt, *Phaeodactylum tricornutum*; Ptr, *Populus trichocarpa*; Rc, *Ricinus communis*; Rs, *Raphanus sativus*; Si, *Setaria italica*; Sm, *Selaginella moellendorffii*; Sb, *Sorghum bicolor*; Vv, *Vitis vinifera*; Zm, *Zea mays*.

## References

- Abascal, F., Zardoya, R. and Posada, D. (2005). ProtTest: selection of best-fit models of protein evolution. *Bioinformatics* **21**: 2104-2105.
- Abramoff, M. D., Magalhaes, P. J. and Ram, S. J. (2004). Image Processing with ImageJ. *Biophotonics International* **11**: 36-42.
- Agerbirk, N., De Vos, M., Kim, J. H. and Jander, G. (2009). Indole glucosinolate breakdown and its biological effects. *Phytochemistry Reviews* **8**: 101-120.
- Agerbirk, N. and Olsen, C. E. (2012). Glucosinolate structures in evolution. *Phytochemistry* **77**: 16-45.
- Alboresi, A., Gerotto, C., Giacometti, G. M., Bassi, R. and Morosinotto, T. (2010). *Physcomitrella patens* mutants affected on heat dissipation clarify the evolution of photoprotection mechanisms upon land colonization. *Proceedings of the National Academy of Sciences of the United States of America* **107**: 11128-11133.
- Alcazar, R., Altabella, T., Marco, F., Bortolotti, C., Reymond, M., Koncz, C., Carrasco, P. and Tiburcio, A. F. (2010). Polyamines: molecules with regulatory functions in plant abiotic stress tolerance. *Planta* **231**: 1237-1249.
- Alonso-Ramirez, A., Rodriguez, D., Reyes, D., Angel Jimenez, J., Nicolas, G., Lopez-Climent, M., Gomez-Cadenas, A. and Nicolas, C. (2009). Evidence for a role of gibberellins in salicylic acid-modulated early plant responses to abiotic stress in *Arabidopsis* seeds. *Plant Physiology* **150**: 1335-1344.
- Amachi, S., Kamagata, Y., Kanagawa, T. and Muramatsu, Y. (2001). Bacteria mediate methylation of iodine in marine and terrestrial environments. *Applied and Environmental Microbiology* **67**: 2718-2722.
- Armeanu-D'Souza, K. (2009) Saving the ozone layer from oilseed rape. *MSc Thesis*. University of East Anglia. Norwich, UK
- Attieh, J., Djiana, R., Koonjul, P., Etienne, C., Sparace, S. A. and Saini, H. S. (2002). Cloning and functional expression of two plant thiol methyltransferases: a new class of enzymes involved in the biosynthesis of sulfur volatiles. *Plant Molecular Biology* **50**: 511-521.
- Attieh, J., Kleppinger-Sparace, K. F., Nunes, C., Sparace, S. A. and Saini, H. S. (2000a). Evidence implicating a novel thiol methyltransferase in the detoxification of glucosinolate hydrolysis products in *Brassica oleracea* L. *Plant Cell and Environment* **23**: 165-174.
- Attieh, J., Sparace, S. A. and Saini, H. S. (2000b). Purification and properties of multiple isoforms of a novel thiol methyltransferase involved in the production of volatile sulfur compounds from *Brassica oleracea*. *Archives of Biochemistry and Biophysics* **380**: 257-266.
- Attieh, J. M., Hanson, A. D. and Saini, H. S. (1995). Purification and characterization of a novel methyltransferase responsible for biosynthesis of halomethanes and methanethiol in *Brassica oleracea*. *Journal of Biological Chemistry* **270**: 9250-9257.
- Bailey, C. D., Koch, M. A., Mayer, M., Mummenhoff, K., O'Kane, S. L., Jr., Warwick, S. I., Windham, M. D. and Al-Shehbaz, I. A. (2006). Toward a global phylogeny of the *Brassicaceae*. *Molecular Biology and Evolution* **23**: 2142-2160.
- Bais, H. P., Weir, T. L., Perry, L. G., Gilroy, S. and Vivanco, J. M. (2006). The role of root exudates in rhizosphere interactions with plants and other organisms. *Annual Review of Plant Biology* **57**: 233-266.
- Baldwin, I. T., Halitschke, R., Paschold, A., von Dahl, C. C. and Preston, C. A. (2006). Volatile signaling in plant-plant interactions: "Talking trees" in the genomics era. *Science* **311**: 812-815.
- Barker, M. S., Vogel, H. and Schranz, M. E. (2009). Paleopolyploidy in the Brassicales: Analyses of the cleome transcriptome elucidate the history of genome duplications in *Arabidopsis* and other Brassicales. *Genome Biology and Evolution* **1**: 391-399.

- Barth, C. and Jander, G.** (2006). *Arabidopsis* myrosinases TGG1 and TGG2 have redundant function in glucosinolate breakdown and insect defense. *Plant Journal* **46**: 549-562.
- Batard, Y., Hehn, A., Nedelkina, S., Schalk, M., Pallett, K., Schaller, H. and Werck-Reichhart, D.** (2000). Increasing expression of P450 and P450-reductase proteins from monocots in heterologous systems. *Archives of Biochemistry and Biophysics* **379**: 161-169.
- Bayer, T. S., Widmaier, D. M., Temme, K., Mirsky, E. A., Santi, D. V. and Voigt, C. A.** (2009). Synthesis of methyl halides from biomass using engineered microbes. *Journal of the American Chemical Society* **131**: 6508-6515.
- Bednarek, P., Pislewska-Bednarek, M., Svatos, A., Schneider, B., Doubisky, J., Mansurova, M., Humphry, M., Consonni, C., Panstruga, R., Sanchez-Vallet, A., Molina, A. and Schulze-Lefert, P.** (2009). A glucosinolate metabolism pathway in living plant cells mediates broad-spectrum antifungal defense. *Science* **323**: 101-106.
- Bell, N., Hsu, L., Jacob, D. J., Schultz, M. G., Blake, D. R., Butler, J. H., King, D. B., Lobert, J. M. and Maier-Reimer, E.** (2002). Methyl iodide: Atmospheric budget and use as a tracer of marine convection in global models. *Journal of Geophysical Research-Atmospheres* **107**.
- Blasco, B., Rios, J. J., Cervilla, L. M., Sanchez-Rodriguez, E., Ruiz, J. M. and Romero, L.** (2008). Iodine biofortification and antioxidant capacity of lettuce: potential benefits for cultivation and human health. *Annals of Applied Biology* **152**: 289-299.
- Blei, E., Hardacre, C. J., Mills, G. P., Heal, K. V. and Heal, M. R.** (2010). Identification and quantification of methyl halide sources in a lowland tropical rainforest. *Atmospheric Environment* **44**: 1005-1010.
- Bouchenak-Khelladi, Y., Salamin, N., Savolainen, V., Forest, F., van der Bank, M., Chase, M. W. and Hodkinson, T. R.** (2008). Large multi-gene phylogenetic trees of the grasses (*Poaceae*): Progress towards complete tribal and generic level sampling. *Molecular Phylogenetics and Evolution* **47**: 488-505.
- Breitling, R., Amtmann, A. and Herzyk, P.** (2004). Iterative Group Analysis (iGA): A simple tool to enhance sensitivity and facilitate interpretation of microarray experiments. *BMC Bioinformatics* **5**.
- Bressan, M., Roncato, M.-A., Bellvert, F., Comte, G., Haichar, F. e. Z., Achouak, W. and Berge, O.** (2009). Exogenous glucosinolate produced by *Arabidopsis thaliana* has an impact on microbes in the rhizosphere and plant roots. *ISME Journal* **3**: 1243-1257.
- Brown, P. D. and Morra, M. J.** (1997). Control of soil-borne plant pests using glucosinolate-containing plants. *Advances in Agronomy, Vol 61* **61**: 167-231.
- Butler, J. H., King, D. B., Lobert, J. M., Montzka, S. A., Yvon-Lewis, S. A., Hall, B. D., Warwick, N. J., Mondeel, D. J., Aydin, M. and Elkins, J. W.** (2007). Oceanic distributions and emissions of short-lived halocarbons. *Global Biogeochemical Cycles* **21**.
- Cardinale, M., Brusetti, L., Quatrini, P., Borin, S., Puglia, A. M., Rizzi, A., Zanardini, E., Sorlini, C., Corselli, C. and Daffonchio, D.** (2004). Comparison of different primer sets for use in automated ribosomal intergenic spacer analysis of complex bacterial communities. *Applied and Environmental Microbiology* **70**: 6147-6156.
- Chinnusamy, V. and Zhu, J.** (2004). Plant salt tolerance. In H. Hirt and K. Shinozaki. *Plant Responses to Abiotic Stress*, Springer Verlag Berlin Heidelberg.
- Clerbaux, C., Cunnold, D. M., Anderson, J., Engel, A., Fraser, P. J., Mahieu, E., Manning, A., Miller, J., Montzka, S. A., Nassar, R., Prinn, R., Reimann, S., Rinsland, C. P., Simmonds, P., Verdonik, D., Weiss, R., Wuebbles, D. and Yokouchi, Y.** (2007). Long-Lived Compounds. In *Scientific Assessment of Ozone Depletion: 2006*. Geneva, Switzerland, World Meteorological Organization.
- Clough, S. J. and Bent, A. F.** (1998). Floral dip: a simplified method for *Agrobacterium*-mediated transformation of *Arabidopsis thaliana*. *Plant Journal* **16**: 735-743.
- Coiner, H., Schröder, G., Wehinger, E., Liu, C. J., Noel, J. P., Schwab, W. and Schröder, J.** (2006). Methylation of sulfhydryl groups: a new function for a family of small molecule plant O-methyltransferases. *Plant Journal* **46**: 193-205.

- Colmenero-Flores, J. M., Martinez, G., Gamba, G., Vazquez, N., Iglesias, D. J., Brumos, J. and Talon, M.** (2007). Identification and functional characterization of cation-chloride cotransporters in plants. *Plant Journal* **50**: 278-292.
- Colomb, A., Yassaa, N., Williams, J., Peeken, I. and Lochte, K.** (2008). Screening volatile organic compounds (VOCs) emissions from five marine phytoplankton species by head space gas chromatography/mass spectrometry (HS-GC/MS). *Journal of Environmental Monitoring* **10**: 325-330.
- Cove, D.** (2005). The moss *Physcomitrella patens*. *Annual Review of Genetics* **39**: 339-358.
- Cox, M. L., Fraser, P. J., Sturrock, G. A., Siems, S. T. and Porter, L. W.** (2004). Terrestrial sources and sinks of halomethanes near Cape Grim, Tasmania. *Atmospheric Environment* **38**: 3839-3852.
- Dameris, M.** (2010). Climate change and atmospheric chemistry: how will the stratospheric ozone layer develop? *Angewandte Chemie-International Edition* **49**: 8092-8102.
- Davis, D., Crawford, J., Liu, S., McKeen, S., Bandy, A., Thornton, D., Rowland, F. and Blake, D.** (1996). Potential impact of iodine on tropospheric levels of ozone and other critical oxidants. *Journal of Geophysical Research-Atmospheres* **101**: 2135-2147.
- Desai, P. N., Shrivastava, N. and Padh, H.** (2010). Production of heterologous proteins in plants: Strategies for optimal expression. *Biotechnology Advances* **28**: 427-435.
- Dicke, M. and Baldwin, I. T.** (2010). The evolutionary context for herbivore-induced plant volatiles: beyond the 'cry for help'. *Trends in Plant Science* **15**: 167-175.
- Dimmer, C. H., Simmonds, P. G., Nickless, G. and Bassford, M. R.** (2001). Biogenic fluxes of halomethanes from Irish peatland ecosystems. *Atmospheric Environment* **35**: 321-330.
- Ding, Z. J., Galvan-Ampudia, C. S., Demarsy, E., Langowski, L., Kleine-Vehn, J., Fan, Y. W., Morita, M. T., Tasaka, M., Fankhauser, C., Offringa, R. and Friml, J.** (2011). Light-mediated polarization of the PIN3 auxin transporter for the phototropic response in *Arabidopsis*. *Nature Cell Biology* **13**: 447-452.
- Dudareva, N., Negre, F., Nagegowda, D. A. and Orlova, I.** (2006). Plant volatiles: Recent advances and future perspectives. *Critical Reviews in Plant Sciences* **25**: 417-440.
- Edgar, R. C.** (2004). MUSCLE: a multiple sequence alignment method with reduced time and space complexity. *BMC Bioinformatics* **5**: 1-19.
- Edwards, K., Johnstone, C. and Thompson, C.** (1991). A simple and rapid method for the preparation of plant genomic DNA for PCR analysis. *Nucleic Acids Research* **19**: 1349-1349.
- Emanuelsson, O., Brunak, S., von Heijne, G. and Nielsen, H.** (2007). Locating proteins in the cell using TargetP, SignalP and related tools. *Nature Protocols* **2**: 953-971.
- Fahey, D. W. and Hegglin, M. I.** (2011). Twenty questions and answers about the ozone layer: 2010 Update. In *Scientific Assessment of Ozone Depletion: 2010*. Geneva, Switzerland, World Meteorological Organization.
- Fahey, J. W., Zalcmann, A. T. and Talalay, P.** (2001). The chemical diversity and distribution of glucosinolates and isothiocyanates among plants. *Phytochemistry* **56**: 5-51.
- Falk, K. L., Tokuhisa, J. G. and Gershenzon, J.** (2007). The effect of sulfur nutrition on plant glucosinolate content: Physiology and molecular mechanisms. *Plant Biology* **9**: 573-581.
- Fall, R.** (2003). Abundant oxygenates in the atmosphere: A biochemical perspective. *Chemical Reviews* **103**: 4941-4951.
- Feng, Z. and Kobayashi, K.** (2009). Assessing the impacts of current and future concentrations of surface ozone on crop yield with meta-analysis. *Atmospheric Environment* **43**: 1510-1519.
- Fior, S. and Gerola, P. D.** (2009). Impact of ubiquitous inhibitors on the GUS gene reporter system: evidence from the model plants *Arabidopsis*, tobacco and rice and correction methods for quantitative assays of transgenic and endogenous GUS. *Plant Methods* **5**.

- Fisher, M. M. and Triplett, E. W.** (1999). Automated approach for ribosomal intergenic spacer analysis of microbial diversity and its application to freshwater bacterial communities. *Applied and Environmental Microbiology* **65**: 4630-4636.
- Flowers, T. J.** (2004). Improving crop salt tolerance. *Journal of Experimental Botany* **55**: 307-319.
- Flowers, T. J. and Colmer, T. D.** (2008). Salinity tolerance in halophytes. *New Phytologist* **179**: 945-963.
- Flury, M. and Papritz, A.** (1993). Bromide in the natural-environment - occurrence and toxicity. *Journal of Environmental Quality* **22**: 747-758.
- Frank, W., Decker, E. L. and Reski, R.** (2005). Molecular tools to study *Physcomitrella patens*. *Plant Biology* **7**: 220-227.
- Friml, J., Vieten, A., Sauer, M., Weijers, D., Schwarz, H., Hamann, T., Offringa, R. and Jurgens, G.** (2003). Efflux-dependent auxin gradients establish the apical-basal axis of *Arabidopsis*. *Nature* **426**: 147-153.
- Fujimori, T., Yoneyama, Y., Taniai, G., Kurihara, M., Tamegai, H. and Hashimoto, S.** (2012). Methyl halide production by cultures of marine proteobacteria *Erythrobacter* and *Pseudomonas* and isolated bacteria from brackish water. *Limnology and Oceanography* **57**: 154-162.
- Gachon, C. M. M., Langlois-Meurinne, M., Henry, Y. and Saindrenan, P.** (2005). Transcriptional co-regulation of secondary metabolism enzymes in *Arabidopsis*: functional and evolutionary implications. *Plant Molecular Biology* **58**: 229-245.
- Gan, J., Yates, S. R., Ohr, H. D. and Sims, J. J.** (1998). Production of methyl bromide by terrestrial higher plants. *Geophysical Research Letters* **25**: 3595-3598.
- Gentleman, R. C., Carey, V. J., Bates, D. M., Bolstad, B., Dettling, M., Dudoit, S., Ellis, B., Gautier, L., Ge, Y. C., Gentry, J., Hornik, K., Hothorn, T., Huber, W., Iacus, S., Irizarry, R., Leisch, F., Li, C., Maechler, M., Rossini, A. J., Sawitzki, G., Smyth, C., Smyth, G., Tierney, L., Yang, J. Y. H. and Zhang, J. H.** (2004). Bioconductor: open software development for computational biology and bioinformatics. *Genome Biology* **5**.
- Girin, T., Paicu, T., Stephenson, P., Fuentes, S., Körner, E., O'Brien, M., Sorefan, K., Wood, T. A., Balanza, V., Ferrandiz, C., Smyth, D. R. and Østergaard, L.** (2011). INDEHISCENT and SPATULA interact to specify carpel and valve margin tissue and thus promote seed dispersal in *Arabidopsis*. *Plant Cell* **23**: 3641-3653.
- Griffiths, R. I., Whiteley, A. S., O'Donnell, A. G. and Bailey, M. J.** (2000). Rapid method for coextraction of DNA and RNA from natural environments for analysis of ribosomal DNA- and rRNA-based microbial community composition. *Applied and Environmental Microbiology* **66**: 5488-5491.
- Guindon, S. and Gascuel, O.** (2003). A simple, fast, and accurate algorithm to estimate large phylogenies by maximum likelihood. *Systematic Biology* **52**: 696-704.
- Halkier, B. A. and Gershenzon, J.** (2006). Biology and biochemistry of glucosinolates. *Annual Review of Plant Biology* **57**: 303-333.
- Hall, J. C., Iltis, H. H. and Sytsma, K. J.** (2004). Molecular phylogenetics of core Brassicales, placement of orphan genera *Emblingia*, *Forchhammeria*, *Tirania*, and character evolution. *Systematic Botany* **29**: 654-669.
- Hall, T. A.** (1999). BioEdit: a user-friendly biological sequence alignment editor and analysis program for Windows 95/98/NT. *Nucleic Acids Symposium Series* **41**: 95-98.
- Hamilton, J. T. G., McRoberts, W. C., Keppler, F., Kalin, R. M. and Harper, D. B.** (2003). Chloride methylation by plant pectin: An efficient environmentally significant process. *Science* **301**: 206-209.
- Harper, D. B.** (1985). Halomethane from halide ion - a highly efficient fungal conversion of environmental significance. *Nature* **315**: 55-57.
- Harper, D. B.** (2000). The global chloromethane cycle: biosynthesis, biodegradation and metabolic role. *Natural Product Reports* **17**: 337-348.

- Harper, D. B., Buswell, J. A., Kennedy, J. T. and Hamilton, J. T. G.** (1990). Chloromethane, methyl donor in veratryl alcohol biosynthesis in *Phanerochaete*, *Chrysosporium* and other lignin-degrading fungi. *Applied and Environmental Microbiology* **56**: 3450-3457.
- Harper, D. B., Hamilton, J. T. G., Kennedy, J. T. and McNally, K. J.** (1989). Chloromethane, a novel methyl donor for biosynthesis of esters and anisoles in *Phellinus pomaceus*. *Applied and Environmental Microbiology* **55**: 1981-1989.
- Haseloff, J.** (1999). GFP variants for multispectral imaging of living cells. *Methods in Cell Biology* **58**: 139.
- Hein, J. W., Wolfe, G. V. and Blee, K. A.** (2008). Comparison of rhizosphere bacterial communities in *Arabidopsis thaliana* mutants for systemic acquired resistance. *Microbial Ecology* **55**: 333-343.
- Howarth, J. R., Parmar, S., Barraclough, P. B. and Hawkesford, M. J.** (2009). A sulphur deficiency-induced gene, *SDII*, involved in the utilization of stored sulphate pools under sulphur-limiting conditions has potential as a diagnostic indicator of sulphur nutritional status. *Plant Biotechnology Journal* **7**: 200-209.
- Hruz, T., Laule, O., Szabo, G., Wessendorp, F., Bleuler, S., Oertle, L., Widmayer, P., Gruissem, W. and Zimmermann, P.** (2008). Genevestigator v3: a reference expression database for the meta-analysis of transcriptomes. *Advances in Bioinformatics* **2008**: 420747-420747.
- Huelsenbeck, J. P. and Ronquist, F.** (2001). MRBAYES: Bayesian inference of phylogenetic trees. *Bioinformatics* **17**: 754-755.
- Ibekwe, A. M., Papiernik, S. K., Gan, J., Yates, S. R., Yang, C. H. and Crowley, D. E.** (2001). Impact of fumigants on soil microbial communities. *Applied and Environmental Microbiology* **67**: 3245-3257.
- Ibekwe, A. M., Papiernik, S. K., Grieve, C. M. and Yang, C. H.** (2010). Influence of fumigants on soil microbial diversity and survival of *E. coli* O157:H7. *Journal of Environmental Science and Health Part B-Pesticides Food Contaminants and Agricultural Wastes* **45**: 416-426.
- Irizarry, R. A., Hobbs, B., Collin, F., Beazer-Barclay, Y. D., Antonellis, K. J., Scherf, U. and Speed, T. P.** (2003). Exploration, normalization, and summaries of high density oligonucleotide array probe level data. *Biostatistics* **4**: 249-264.
- Itoh, N., Toda, H., Matsuda, M., Negishi, T., Taniguchi, T. and Ohsawa, N.** (2009). Involvement of S-adenosylmethionine-dependent halide/thiol methyltransferase (HTMT) in methyl halide emissions from agricultural plants: isolation and characterization of an HTMT-coding gene from *Raphanus sativus* (daikon radish). *BMC Plant Biology* **9**.
- Itoh, N., Tsujita, M., Ando, T., Hisatomi, G. and Higashi, T.** (1997). Formation and emission of monohalomethanes from marine algae. *Phytochemistry* **45**: 67-73.
- Jaillon, O., Aury, J.-M., Noel, B., Policriti, A., Clepet, C., Casagrande, A., Choisne, N., Aubourg, S., Vitulo, N., Jubin, C., Vezzi, A., Legeai, F., Hugueney, P., Dasilva, C., Horner, D., Mica, E., Jublot, D., Poulain, J., Bruyere, C., Billault, A., Segurens, B., Gouvenoux, M., Ugarte, E., Cattonaro, F., Anthouard, V., Vico, V., Del Fabbro, C., Alaux, M., Di Gaspero, G., Dumas, V., Felice, N., Paillard, S., Juman, I., Moroldo, M., Scalabrin, S., Canaguier, A., Le Clainche, I., Malacrida, G., Durand, E., Pesole, G., Laucou, V., Chatelet, P., Merdinoglu, D., Delledonne, M., Pezzotti, M., Lecharny, A., Scarpelli, C., Artiguenave, F., Pe, M. E., Valle, G., Morgante, M., Caboche, M., Adam-Blondon, A.-F., Weissenbach, J., Quetier, F. and Wincker, P.** (2007). The grapevine genome sequence suggests ancestral hexaploidization in major angiosperm phyla. *Nature* **449**: 463-U5.
- Janowitz, T., Trompeter, I. and Piotrowski, M.** (2009). Evolution of nitrilases in glucosinolate-containing plants. *Phytochemistry* **70**: 1680-1686.
- Jefferson, R. A., Kavanagh, T. A. and Bevan, M. W.** (1987). Gus fusions: beta-glucuronidase as a sensitive and versatile gene fusion marker in higher plants. *Embo Journal* **6**: 3901-3907.

- Jensen, P. J., Hangarter, R. P. and Estelle, M. (1998). Auxin transport is required for hypocotyl elongation in light-grown but not dark-grown *Arabidopsis*. *Plant Physiology* **116**: 455-462.
- Jiao, Y., Wickett, N. J., Ayyampalayam, S., Chanderbali, A. S., Landherr, L., Ralph, P. E., Tomsho, L. P., Hu, Y., Liang, H., Soltis, P. S., Soltis, D. E., Clifton, S. W., Schlarbaum, S. E., Schuster, S. C., Ma, H., Leebens-Mack, J. and dePamphilis, C. W. (2011). Ancestral polyploidy in seed plants and angiosperms. *Nature* **473**: 97-U113.
- Joshi, C. P., Zhou, H., Huang, X. Q. and Chiang, V. L. (1997). Context sequences of translation initiation codon in plants. *Plant Molecular Biology* **35**: 993-1001.
- Jossier, M., Kroniewicz, L., Dalmas, F., Le Thiec, D., Ephritikhine, G., Thomine, S., Barbier-Brygoo, H., Vavasseur, A., Filleur, S. and Leonhardt, N. (2010). The *Arabidopsis* vacuolar anion transporter, AtCLCc, is involved in the regulation of stomatal movements and contributes to salt tolerance. *Plant Journal* **64**: 563-576.
- Kafkafi, U., Xu, G., Imas, P., Magen, H. and Tarchitzky, J. (2001). Potassium and chloride in soils. In A. E. Johnston. *IPI Research Topics No. 22 Potassium and chloride in crops and soils: The role of potassium chloride fertilizer in crop nutrition*. Basel, Switzerland, International Potash Institute.
- Kagan, R. M. and Clarke, S. (1994). Widespread occurrence of 3 sequence motifs in diverse S-Adenosylmethionine-dependent methyltransferases suggests a common structure for these enzymes. *Archives of Biochemistry and Biophysics* **310**: 417-427.
- Kenrick, P. and Crane, P. R. (1997). The origin and early evolution of plants on land. *Nature* **389**: 33-39.
- Keppler, F., Harper, D. B., Rockmann, T., Moore, R. M. and Hamilton, J. T. G. (2005). New insight into the atmospheric chloromethane budget gained using stable carbon isotope ratios. *Atmospheric Chemistry and Physics* **5**: 2403-2411.
- Knudsen, J. T., Eriksson, R., Gershenzon, J. and Stahl, B. (2006). Diversity and distribution of floral scent. *Botanical Review* **72**: 1-120.
- Köllmer, I., Werner, T. and Schmölling, T. (2011). Ectopic expression of different cytokinin-regulated transcription factor genes of *Arabidopsis thaliana* alters plant growth and development. *Journal of Plant Physiology* **168**: 1320-1327.
- Koornneef, M. and Meinke, D. (2010). The development of *Arabidopsis* as a model plant. *Plant Journal* **61**: 909-921.
- Koprivova, A., Mugford, S. T. and Kopriva, S. (2010). *Arabidopsis* root growth dependence on glutathione is linked to auxin transport. *Plant Cell Reports* **29**: 1157-1167.
- Koprivova, A., North, K. A. and Kopriva, S. (2008). Complex signaling network in regulation of adenosine 5'-phosphosulfate reductase by salt stress in *Arabidopsis* roots. *Plant Physiology* **146**: 1408-1420.
- Kozbial, P. Z. and Mushegian, A. R. (2005). Natural history of S-adenosylmethionine-binding proteins. *BMC Structural Biology* **5**.
- Krishnan, A., Guiderdoni, E., An, G., Hsing, Y.-i. C., Han, C.-d., Lee, M. C., Yu, S.-M., Upadhyaya, N., Ramachandran, S., Zhang, Q., Sundaresan, V., Hirochika, H., Leung, H. and Pereira, A. (2009). Mutant resources in rice for functional genomics of the grasses. *Plant Physiology* **149**: 165-170.
- Krizek, B. A. and Meyerowitz, E. M. (1996). Mapping the protein regions responsible for the functional specificities of the *Arabidopsis* MADS domain organ-identity proteins. *Proceedings of the National Academy of Sciences of the United States of America* **93**: 4063-4070.
- Kunihiro, A., Yamashino, T., Nakamichi, N., Niwa, Y., Nakanishi, H. and Mizuno, T. (2011). PHYTOCHROME-INTERACTING FACTOR 4 and 5 (PIF4 and PIF5) activate the homeobox ATHB2 and auxin-inducible IAA29 genes in the coincidence mechanism underlying photoperiodic control of plant growth of *Arabidopsis thaliana*. *Plant and Cell Physiology* **52**: 1315-1329.
- Landini, M., Gonzali, S., Kiferle, C., Tonacchera, M., Agretti, P., Dimida, A., Vitti, P., Alpi, A., Pinchera, A. and Perata, P. (2012). Metabolic engineering of the iodine content in *Arabidopsis*. *Scientific Reports* **2**.

- Landini, M., Gonzali, S. and Perata, P.** (2011). Iodine biofortification in tomato. *Journal of Plant Nutrition and Soil Science* **174**: 480-486.
- Laothawornkitkul, J., Taylor, J. E., Paul, N. D. and Hewitt, C. N.** (2009). Biogenic volatile organic compounds in the Earth system. *New Phytologist* **183**: 27-51.
- Laternus, F., Adams, F. C. and Wiencke, C.** (1998). Methyl halides from Antarctic macroalgae. *Geophysical Research Letters* **25**: 773-776.
- Lee-Taylor, J. and Redeker, K. R.** (2005). Reevaluation of global emissions from rice paddies of methyl iodide and other species. *Geophysical Research Letters* **32**: 5.
- Li, L., Foster, C. M., Gan, Q., Nettleton, D., James, M. G., Myers, A. M. and Wurtele, E. S.** (2009). Identification of the novel protein QQS as a component of the starch metabolic network in *Arabidopsis* leaves. *Plant Journal* **58**: 485-498.
- Lichtenthaler, H. K.** (1987). Chlorophylls and Carotenoids - Pigments of Photosynthetic Biomembranes. *Methods in Enzymology* **148**: 350-382.
- Lindow, S. E. and Brandl, M. T.** (2003). Microbiology of the phyllosphere. *Applied and Environmental Microbiology* **69**: 1875-1883.
- Liu, Y.-C., Wu, Y.-R., Huang, X.-H., Sun, J. and Xie, Q.** (2011). AtPUB19, a U-Box E3 ubiquitin ligase, negatively regulates Abscisic acid and drought responses in *Arabidopsis thaliana*. *Molecular Plant* **4**: 938-946.
- Lysak, M. A., Koch, M. A., Pecinka, A. and Schubert, I.** (2005). Chromosome triplication found across the tribe Brassiceae. *Genome Research* **15**: 516-525.
- Manley, S. L.** (2002). Phyto-genesis of halomethanes: A product of selection or a metabolic accident? *Biogeochemistry* **60**: 163-180.
- Manley, S. L., Goodwin, K. and North, W. J.** (1992). Laboratory production of bromoform, methylene bromide, and methyl-iodide by macroalgae and distribution in nearshore southern California waters. *Limnology and Oceanography* **37**: 1652-1659.
- Manley, S. L., Wang, N.-Y., Walser, M. L. and Cicerone, R. J.** (2007). Methyl halide emissions from greenhouse-grown mangroves. *Geophysical Research Letters* **34**.
- Manley, S. L., Wang, N. Y., Walser, M. L. and Cicerone, R. J.** (2006). Coastal salt marshes as global methyl halide sources from determinations of intrinsic production by marsh plants. *Global Biogeochemical Cycles* **20**.
- Maruyama-Nakashita, A., Nakamura, Y., Watanabe-Takahashi, A., Inoue, E., Yamaya, T. and Takahashi, H.** (2005). Identification of a novel cis-acting element conferring sulfur deficiency response in *Arabidopsis* roots. *Plant Journal* **42**: 305-314.
- McAnulla, C., Woodall, C. A., McDonald, I. R., Studer, A., Vuilleumier, S., Leisinger, T. and Murrell, J. C.** (2001). Chloromethane utilization gene cluster from *Hyphomicrobium chloromethanicum* strain CM2(T) and development of functional gene probes to detect halomethane-degrading bacteria. *Applied and Environmental Microbiology* **67**: 307-316.
- Mead, M. I., White, L. R., Nickless, G., Wang, K. Y. and Shallcross, D. E.** (2008). An estimation of the global emission of methyl bromide from rapeseed (*Brassica napus*) from 1961 to 2003. *Atmospheric Environment* **42**: 337-345.
- Menand, B., Yi, K. K., Jouannic, S., Hoffmann, L., Ryan, E., Linstead, P., Schaefer, D. G. and Dolan, L.** (2007). An ancient mechanism controls the development of cells with a rooting function in land plants. *Science* **316**: 1477-1480.
- Micallef, S. A., Channer, S., Shiaris, M. P. and Colon-Carmona, A.** (2009a). Plant age and genotype impact the progression of bacterial community succession in the *Arabidopsis* rhizosphere. *Plant signaling & behavior* **4**: 777-80.
- Micallef, S. A., Shiaris, M. P. and Colon-Carmona, A.** (2009b). Influence of *Arabidopsis thaliana* accessions on rhizobacterial communities and natural variation in root exudates. *Journal of Experimental Botany* **60**: 1729-1742.
- Miles, A. A., Misra, S. S. and Irwin, J. O.** (1938). The estimation of the bactericidal power of the blood. *The Journal of hygiene* **38**: 732-49.



- Miller, L. G., Warner, K. L., Baesman, S. M., Oremland, R. S., McDonald, I. R., Radajewski, S. and Murrell, J. C. (2004). Degradation of methyl bromide and methyl chloride in soil microcosms: Use of stable C isotope fractionation and stable isotope probing to identify reactions and the responsible microorganisms. *Geochimica Et Cosmochimica Acta* **68**: 3271-3283.
- Mockaitis, K. and Estelle, M. (2008). Auxin receptors and plant development: A new signaling paradigm. *Annual Review of Cell and Developmental Biology* **24**: 55-80.
- Moffatt, B. A. and Weretilnyk, E. A. (2001). Sustaining S-adenosyl-L-methionine-dependent methyltransferase activity in plant cells. *Physiologia Plantarum* **113**: 435-442.
- Montzka, S. A., Reimann, S., Engel, A., Krüger, K., O'Doherty, S., Sturges, W. T., Blake, D., Dorf, M., Fraser, P., Froidevaux, L., Jucks, K., Kreher, K., Kurylo, M. J., Mellouki, A., Miller, J., Nielsen, O., Orkin, V. L., Prinn, R. G., Rhew, R., Santee, M. L., Stohl, H. and Verdonik, D. (2011). Ozone-Depleting Substances (ODSs) and Related Chemicals. In *Scientific Assessment of Ozone Depletion: 2010*. Geneva, Switzerland, World Meteorological Organization.
- Moore, R. M. and Zafiriou, O. C. (1994). Photochemical production of methyl iodide in seawater. *Journal of Geophysical Research-Atmospheres* **99**: 16415-16420.
- Muday, G. K. (2001). Auxins and tropisms. *Journal of Plant Growth Regulation* **20**: 226-243.
- Mudd, S. H. and Datko, A. H. (1990). The S-methylmethionine cycle in *Lemna paucicostata*. *Plant Physiology* **93**: 623-630.
- Mugford, S. G., Yoshimoto, N., Reichelt, M., Wirtz, M., Hill, L., Mugford, S. T., Nakazato, Y., Noji, M., Takahashi, H., Kramell, R., Gigolashvili, T., Fluegge, U.-I., Wasternack, C., Gershenzon, J., Hell, R., Saito, K. and Kopriva, S. (2009). Disruption of Adenosine-5'-Phosphosulfate Kinase in *Arabidopsis* reduces levels of sulfated secondary metabolites. *Plant Cell* **21**: 910-927.
- Munns, R. (2002). Comparative physiology of salt and water stress. *Plant Cell and Environment* **25**: 239-250.
- Munns, R. and Tester, M. (2008). Mechanisms of salinity tolerance. *Annual Review of Plant Biology* **59**: 651-681.
- Muramatsu, Y. and Yoshida, S. (1995). Volatilization of methyl iodide from the soil-plant system. *Atmospheric Environment* **29**: 21-25.
- Nadalig, T., Farhan Ul Haque, M., Roselli, S., Schaller, H., Bringel, F. and Vuilleumier, S. (2011). Detection and isolation of chloromethane-degrading bacteria from the *Arabidopsis thaliana* phyllosphere, and characterization of chloromethane utilization genes. *Fems Microbiology Ecology* **77**: 438-448.
- Nagatoshi, Y. and Nakamura, T. (2007). Characterization of three halide methyltransferases in *Arabidopsis thaliana*. *Plant Biotechnology* **24**: 503-506.
- Nagatoshi, Y. and Nakamura, T. (2009). *Arabidopsis* HARMLESS TO OZONE LAYER protein methylates a glucosinolate breakdown product and functions in resistance to *Pseudomonas syringae* pv. *maculicola*. *Journal of Biological Chemistry* **284**: 19301-19309.
- Nakamichi, N., Kiba, T., Henriques, R., Mizuno, T., Chua, N. H. and Sakakibara, H. (2010). PSEUDO-RESPONSE REGULATORS 9, 7, and 5 are transcriptional repressors in the *Arabidopsis* circadian clock. *Plant Cell* **22**: 594-605.
- Neal, C. S., Fredericks, D. P., Griffiths, C. A. and Neale, A. D. (2010). The characterisation of AOP2: a gene associated with the biosynthesis of aliphatic alkenyl glucosinolates in *Arabidopsis thaliana*. *BMC Plant Biology* **10**.
- Newton, H. (2011) Tropospheric composition of organohalogens and alkyl nitrates: Tropical and temperate case studies. *PhD Thesis*. University of East Anglia. Norwich, UK
- Ni, X. H. and Hager, L. P. (1998). cDNA cloning of *Batis maritima* methyl chloride transferase and purification of the enzyme. *Proceedings of the National Academy of Sciences of the United States of America* **95**: 12866-12871.
- Ni, X. H. and Hager, L. P. (1999). Expression of *Batis maritima* methyl chloride transferase in *Escherichia coli*. *Proceedings of the National Academy of Sciences of the United States of America* **96**: 3611-3615.

- Nishiyama, T., Fujita, T., Shin-I, T., Seki, M., Nishide, H., Uchiyama, I., Kamiya, A., Carninci, P., Hayashizaki, Y., Shinozaki, K., Kohara, Y. and Hasebe, M. (2003). Comparative genomics of *Physcomitrella patens* gametophytic transcriptome and *Arabidopsis thaliana*: Implication for land plant evolution. *Proceedings of the National Academy of Sciences of the United States of America* **100**: 8007-8012.
- Noctor, G., Arisi, A. C. M., Jouanin, L., Kunert, K. J., Rennenberg, H. and Foyer, C. H. (1998). Glutathione: biosynthesis, metabolism and relationship to stress tolerance explored in transformed plants. *Journal of Experimental Botany* **49**: 623-647.
- Nouchi, I., Hosono, T. and Sasaki, K. (1997). Seasonal changes in fluxes of methane and volatile sulfur compounds from rice paddies and their concentrations in soil water. *Plant and Soil* **195**: 233-245.
- Ohr, H. D., Sims, J. J., Grech, N. M., Becker, J. O. and McGiffen, M. E. (1996). Methyl iodide, an ozone-safe alternative to methyl bromide as a soil fumigant. *Plant Disease* **80**: 731-735.
- Oksanen, J., Blanchet, F. G., Kindt, R., Legendre, P., O'Hara, R. B., Simpson, G. L., Solymos, P., Stevens, M. H. H. and Wager, H. (2010). vegan: Community Ecology Package. R package version 1.17-3.
- Osborne, C. A., Zwart, A. B., Broadhurst, L. M., Young, A. G. and Richardson, A. E. (2011). The influence of sampling strategies and spatial variation on the detected soil bacterial communities under three different land-use types. *FEMS Microbiology Ecology* **78**: 70-79.
- Østergaard, L. and King, G. J. (2008). Standardized gene nomenclature for the *Brassica* genus. *Plant Methods* **4**.
- Parkin, I. A. P., Gulden, S. M., Sharpe, A. G., Lukens, L., Trick, M., Osborn, T. C. and Lydiate, D. J. (2005). Segmental structure of the *Brassica napus* genome based on comparative analysis with *Arabidopsis thaliana*. *Genetics* **171**: 765-781.
- Paul, N. A., de Nys, R. and Steinberg, P. D. (2006a). Chemical defence against bacteria in the red alga *Asparagopsis armata*: linking structure with function. *Marine Ecology-Progress Series* **306**: 87-101.
- Paul, N. A., de Nys, R. and Steinberg, P. D. (2006b). Seaweed-herbivore interactions at a small scale: direct tests of feeding deterrence by filamentous algae. *Marine Ecology-Progress Series* **323**: 1-9.
- Petersen, B. L., Chen, S. X., Hansen, C. H., Olsen, C. E. and Halkier, B. A. (2002). Composition and content of glucosinolates in developing *Arabidopsis thaliana*. *Planta* **214**: 562-571.
- Pfalz, M., Vogel, H. and Kroymann, J. (2009). The gene controlling the Indole Glucosinolate Modifier1 quantitative trait locus alters indole glucosinolate structures and aphid resistance in *Arabidopsis*. *Plant Cell* **21**: 985-999.
- Price, N. R. (1985). The mode of action of fumigants. *Journal of Stored Products Research* **21**: 157-164.
- Quatrano, R. S., McDaniel, S. F., Khandelwal, A., Perroud, P.-F. and Cove, D. J. (2007). *Physcomitrella patens*: mosses enter the genomic age. *Current Opinion in Plant Biology* **10**: 182-189.
- Raaijmakers, J. M., Paulitz, T. C., Steinberg, C., Alabouvette, C. and Moenne-Loccoz, Y. (2009). The rhizosphere: a playground and battlefield for soilborne pathogens and beneficial microorganisms. *Plant and Soil* **321**: 341-361.
- Ranjard, L., Poly, F., Lata, J. C., Mougél, C., Thioulouse, J. and Nazaret, S. (2001). Characterization of bacterial and fungal soil communities by automated ribosomal intergenic spacer analysis fingerprints: Biological and methodological variability. *Applied and Environmental Microbiology* **67**: 4479-4487.
- Ratzka, A., Vogel, H., Kliebenstein, D. J., Mitchell-Olds, T. and Kroymann, J. (2002). Disarming the mustard oil bomb. *Proceedings of the National Academy of Sciences of the United States of America* **99**: 11223-11228.
- Reddy, M. P. (2009). Bromide tolerance in *Salicornia brachiata* Roxb, an obligate halophyte. *Water Air and Soil Pollution* **196**: 151-160.

- Redeker, K. R., Andrews, J., Fisher, F., Sass, R. and Cicerone, R. J.** (2002). Interfield and intrafield variability of methyl halide emissions from rice paddies. *Global Biogeochemical Cycles* **16**: 1125.
- Redeker, K. R. and Cicerone, R. J.** (2004). Environmental controls over methyl halide emissions from rice paddies. *Global Biogeochemical Cycles* **18**: Gb1027.
- Redeker, K. R., Manley, S. L., Walser, M. and Cicerone, R. J.** (2004). Physiological and biochemical controls over methyl halide emissions from rice plants. *Global Biogeochemical Cycles* **18**: Gb1007.
- Redeker, K. R., Wang, N. Y., Low, J. C., McMillan, A., Tyler, S. C. and Cicerone, R. J.** (2000). Emissions of methyl halides and methane from rice paddies. *Science* **290**: 966-969.
- Rhew, R. C., Miller, B. R. and Weiss, R. F.** (2000). Natural methyl bromide and methyl chloride emissions from coastal salt marshes. *Nature* **403**: 292-295.
- Rhew, R. C., Østergaard, L., Saltzman, E. S. and Yanofsky, M. F.** (2003). Genetic control of methyl halide production in *Arabidopsis*. *Current Biology* **13**: 1809-1813.
- Ristaino, J. B. and Thomas, W.** (1997). Agriculture, methyl bromide, and the ozone hole: Can we fill the gaps? *Plant Disease* **81**: 964-977.
- Roje, S.** (2006). S-Adenosyl-L-methionine: Beyond the universal methyl group donor. *Phytochemistry* **67**: 1686-1698.
- Ryan, F. J., Leesch, J. G., Palmquist, D. E. and Aung, L. H.** (2007). Glutathione concentration and phytotoxicity after fumigation of lemons with methyl iodide. *Postharvest Biology and Technology* **45**: 141-146.
- Saini, H. S., Attieh, J. M. and Hanson, A. D.** (1995). Biosynthesis of halomethanes and methanethiol by higher plants via a novel methyltransferase reaction. *Plant Cell and Environment* **18**: 1027-1033.
- Saito, T. and Yokouchi, Y.** (2006). Diurnal variation in methyl halide emission rates from tropical ferns. *Atmospheric Environment* **40**: 2806-2811.
- Saito, T. and Yokouchi, Y.** (2008). Stable carbon isotope ratio of methyl chloride emitted from glasshouse-grown tropical plants and its implication for the global methyl chloride budget. *Geophysical Research Letters* **35**: L08807.
- Sakakibara, K., Nishiyama, T., Kato, M. and Hasebe, M.** (2001). Isolation of homeodomain-leucine zipper genes from the moss *Physcomitrella patens* and the evolution of homeodomain-leucine zipper genes in land plants. *Molecular Biology and Evolution* **18**: 491-502.
- Saxena, D., Aouad, S., Attieh, J. and Saini, H. S.** (1998). Biochemical characterization of chloromethane emission from the wood-rotting fungus *Phellinus pomaceus*. *Applied and Environmental Microbiology* **64**: 2831-2835.
- Schäfer, H., Miller, L. G., Oremland, R. S. and Murrell, J. C.** (2007). Bacterial cycling of methyl halides. *Advances in Applied Microbiology* **61**: 307-346.
- Schena, M., Lloyd, A. M. and Davis, R. W.** (1993). The HAT4 gene of *Arabidopsis* encodes a developmental regulator. *Genes & Development* **7**: 367-379.
- Schiestl, F. P.** (2010). The evolution of floral scent and insect chemical communication. *Ecology Letters* **13**: 643-656.
- Schmidberger, J. W., James, A. B., Edwards, R., Naismith, J. H. and O'Hagan, D.** (2010). Halomethane biosynthesis: Structure of a SAM-dependent halide methyltransferase from *Arabidopsis thaliana*. *Angewandte Chemie-International Edition* **49**: 3646-3648.
- Schröder, F., Lisso, J. and Muessig, C.** (2011). EXORDIUM-LIKE1 promotes growth during low carbon availability in *Arabidopsis*. *Plant Physiology* **156**: 1620-1630.
- Schubert, H. L., Blumenthal, R. M. and Cheng, X. D.** (2003). Many paths to methyltransfer: a chronicle of convergence. *Trends in Biochemical Sciences* **28**: 329-335.
- Seo, P. J., Kim, M. J., Ryu, J.-Y., Jeong, E.-Y. and Park, C.-M.** (2011). Two splice variants of the IDD14 transcription factor competitively form nonfunctional heterodimers which may regulate starch metabolism. *Nature Communications* **2**.

- Smith, C. J., Danilowicz, B. S., Clear, A. K., Costello, F. J., Wilson, B. and Meijer, W. G.** (2005). T-Align, a web-based tool for comparison of multiple terminal restriction fragment length polymorphism profiles. *Fems Microbiology Ecology* **54**: 375-380.
- Smyth, G. K.** (2005). Limma: Linear models for microarray data. In R. Gentleman, V. Carey, S. Dudoit, R. Irizarry and W. Huber. *Bioinformatics and Computational Biology Solutions using R and Bioconductor*. New York, Springer: 397-420.
- Soler, R., Harvey, J. A., Kamp, A. F. D., Vet, L. E. M., Van der Putten, W. H., Van Dam, N. M., Stuefer, J. F., Gols, R., Hordijk, C. A. and Bezemer, T. M.** (2007). Root herbivores influence the behaviour of an aboveground parasitoid through changes in plant-volatile signals. *Oikos* **116**: 367-376.
- Solfanelli, C., Poggi, A., Loreti, E., Alpi, A. and Perata, P.** (2006). Sucrose-specific induction of the anthocyanin biosynthetic pathway in *Arabidopsis*. *Plant Physiology* **140**: 637-646.
- Sorefan, K., Booker, J., Haurogne, K., Goussot, M., Bainbridge, K., Foo, E., Chatfield, S., Ward, S., Beveridge, C., Rameau, C. and Leyser, O.** (2003). MAX4 and RMS1 are orthologous dioxygenase-like genes that regulate shoot branching in *Arabidopsis* and pea. *Genes & Development* **17**: 1469-1474.
- Sorefan, K., Girin, T., Liljegren, S. J., Ljung, K., Robles, P., Galvan-Ampudia, C. S., Offringa, R., Friml, J., Yanofsky, M. F. and Østergaard, L.** (2009). A regulated auxin minimum is required for seed dispersal in *Arabidopsis*. *Nature* **459**: 583-U114.
- Sorin, C., Salla-Martret, M., Bou-Torrent, J., Roig-Villanova, I. and Martinez-Garcia, J. F.** (2009). ATHB4, a regulator of shade avoidance, modulates hormone response in *Arabidopsis* seedlings. *Plant Journal* **59**: 266-277.
- Steindler, C., Matteucci, A., Sessa, G., Weimar, T., Ohgishi, M., Aoyama, T., Morelli, G. and Ruberti, I.** (1999). Shade avoidance responses are mediated by the ATHB-2 HD-Zip protein, a negative regulator of gene expression. *Development* **126**: 4235-4245.
- Stephenson, P., Baker, D., Girin, T., Perez, A., Amoah, S., King, G. J. and Østergaard, L.** (2010). A rich TILLING resource for studying gene function in *Brassica rapa*. *BMC Plant Biology* **10**: 62.
- Sun, T.-P.** (2008). Gibberellin metabolism, perception and signaling pathways in *Arabidopsis*. *The Arabidopsis book / American Society of Plant Biologists* **6**: e0103-e0103.
- Takekawa, Y. and Nakamura, T.** (2012). Rice OsHOL1 and OsHOL2 proteins have S-adenosyl-L-methionine-dependent methyltransferase activities toward iodide ions. *Plant Biotechnology* **29**: 103-108.
- Tang, H., Bowers, J. E., Wang, X. and Paterson, A. H.** (2010). Angiosperm genome comparisons reveal early polyploidy in the monocot lineage. *Proceedings of the National Academy of Sciences of the United States of America* **107**: 472-477.
- Tanimoto, E.** (2005). Regulation of root growth by plant hormones - Roles for auxin and gibberellin. *Critical Reviews in Plant Sciences* **24**: 249-265.
- Tatematsu, K., Nakabayashi, K., Kamiya, Y. and Nambara, E.** (2008). Transcription factor AtTCP14 regulates embryonic growth potential during seed germination in *Arabidopsis thaliana*. *Plant Journal* **53**: 42-52.
- Taylor, R. W. D.** (1994). Methyl-bromide - Is there any future for this noteworthy fumigant. *Journal of Stored Products Research* **30**: 253-260.
- Teakle, N. L. and Tyerman, S. D.** (2010). Mechanisms of Cl<sup>-</sup> transport contributing to salt tolerance. *Plant Cell and Environment* **33**: 566-589.
- Till, B. J., Cooper, J., Tai, T. H., Colowit, P., Greene, E. A., Henikoff, S. and Comai, L.** (2007). Discovery of chemically induced mutations in rice by TILLING. *BMC Plant Biology* **7**.
- Toda, H. and Itoh, N.** (2011). Isolation and characterization of a gene encoding a S-adenosyl-L-methionine-dependent halide/thiol methyltransferase (HTMT) from the marine diatom *Phaeodactylum tricorutum*: Biogenic mechanism of CH<sub>3</sub>I emissions in oceans. *Phytochemistry* **72**: 337-343.

- Tzafrir, I., Pena-Muralla, R., Dickerman, A., Berg, M., Rogers, R., Hutchens, S., Sweeney, T. C., McElver, J., Aux, G., Patton, D. and Meinke, D.** (2004). Identification of genes required for embryo development in *Arabidopsis*. *Plant Physiology* **135**: 1206-1220.
- U, N.** (1935). Genome analysis in *Brassica* with special reference to the experimental formation of *B. napus* and peculiar mode of fertilization. *Japanese Journal of Botany* **7**: 389-452.
- Unsicker, S. B., Kunert, G. and Gershenzon, J.** (2009). Protective perfumes: the role of vegetative volatiles in plant defense against herbivores. *Current Opinion in Plant Biology* **12**: 479-485.
- Vandesompele, J., De Preter, K., Pattyn, F., Poppe, B., Van Roy, N., De Paepe, A. and Speleman, F.** (2002). Accurate normalization of real-time quantitative RT-PCR data by geometric averaging of multiple internal control genes. *Genome Biology* **3**.
- Vanneste, S. and Friml, J.** (2009). Auxin: A trigger for change in plant development. *Cell* **136**: 1005-1016.
- Vaughan, M. M., Tholl, D. and Tokuhisa, J. G.** (2011). An aeroponic culture system for the study of root herbivory on *Arabidopsis thaliana*. *Plant Methods* **7**.
- Verkhusha, V. V., Kuznetsova, I. M., Stepanenko, O. V., Zaraisky, A. G., Shavlovsky, M. M., Turoverov, K. K. and Uversky, V. N.** (2003). High stability of *Discosoma* DsRed as compared to *Aequorea* EGFP. *Biochemistry* **42**: 7879-7884.
- Vickers, C. E., Gershenzon, J., Lerdau, M. T. and Loreto, F.** (2009). A unified mechanism of action for volatile isoprenoids in plant abiotic stress. *Nature Chemical Biology* **5**: 283-291.
- Vig, A. P., Rampal, G., Thind, T. S. and Arora, S.** (2009). Bio-protective effects of glucosinolates - A review. *Lwt-Food Science and Technology* **42**: 1561-1572.
- Wenke, K., Kai, M. and Piechulla, B.** (2010). Belowground volatiles facilitate interactions between plant roots and soil organisms. *Planta* **231**: 499-506.
- Whitehead, D. C.** (1984). The distribution and transformations of iodine in the environment. *Environment International* **10**: 321-339.
- Winter, D., Vinegar, B., Nahal, H., Ammar, R., Wilson, G. V. and Provart, N. J.** (2007). An "Electronic Fluorescent Pictograph" Browser for Exploring and Analyzing Large-Scale Biological Data Sets. *Plos One* **2**.
- Wishkerman, A., Gebhardt, S., McRoberts, C. W., Hamilton, J. T. G., Williams, J. and Keppler, F.** (2008). Abiotic methyl bromide formation from vegetation, and its strong dependence on temperature. *Environmental Science & Technology* **42**: 6837-6842.
- Wuosmaa, A. M. and Hager, L. P.** (1990). Methyl chloride transferase - a carbocation route for biosynthesis of halometabolites. *Science* **249**: 160-162.
- Yamaguchi, K., Takahashi, Y., Berberich, T., Imai, A., Miyazaki, A., Takahashi, T., Michael, A. and Kusano, T.** (2006). The polyamine spermine protects against high salt stress in *Arabidopsis thaliana*. *FEBS Letters* **580**: 6783-6788.
- Yan, X. and Chen, S.** (2007). Regulation of plant glucosinolate metabolism. *Planta* **226**: 1343-1352.
- Yang, Y. W., Lai, K. N., Tai, P. Y. and Li, W. H.** (1999). Rates of nucleotide substitution in angiosperm mitochondrial DNA sequences and dates of divergence between *Brassica* and other angiosperm lineages. *Journal of Molecular Evolution* **48**: 597-604.
- Yokouchi, Y., Ikeda, M., Inuzuka, Y. and Yukawa, T.** (2002). Strong emission of methyl chloride from tropical plants. *Nature* **416**: 163-165.
- Yokouchi, Y., Nojiri, Y., Barrie, L. A., Toom-Sauntry, D., Machida, T., Inuzuka, Y., Akimoto, H., Li, H. J., Fujinuma, Y. and Aoki, S.** (2000). A strong source of methyl chloride to the atmosphere from tropical coastal land. *Nature* **403**: 295-298.
- Yokouchi, Y., Saito, T., Ishigaki, C. and Aramoto, M.** (2007). Identification of methyl chloride emitting plants and atmospheric measurements on a subtropical island. *Chemosphere* **69**: 549-553.

- Yonekura-Sakakibara, K., Fukushima, A., Nakabayashi, R., Hanada, K., Matsuda, F., Sugawara, S., Inoue, E., Kuromori, T., Ito, T., Shinozaki, K., Wangwattana, B., Yamazaki, M. and Saito, K.** (2012). Two glycosyltransferases involved in anthocyanin modification delineated by transcriptome independent component analysis in *Arabidopsis thaliana*. *Plant Journal* **69**: 154-167.
- Yoshida, Y., Wang, Y. H., Zeng, T. and Yantosca, R.** (2004). A three-dimensional global model study of atmospheric methyl chloride budget and distributions. *Journal of Geophysical Research-Atmospheres* **109**: D24309.
- Youn, D., Patten, K. O., Wuebbles, D. J., Lee, H. and So, C. W.** (2010). Potential impact of iodinated replacement compounds CF<sub>3</sub>I and CH<sub>3</sub>I on atmospheric ozone: a three-dimensional modeling study. *Atmospheric Chemistry and Physics* **10**: 10129-10144.
- Zhang, W. M., McGiffen, M. E., Becker, J. O., Ohr, H. D., Sims, J. J. and Kallenbach, R. L.** (1997). Dose response of weeds to methyl iodide and methyl bromide. *Weed Research* **37**: 181-189.
- Zhu, Y. G., Huang, Y. Z., Hu, Y. and Liu, Y. X.** (2003). Iodine uptake by spinach (*Spinacia oleracea* L.) plants grown in solution culture: effects of iodine species and solution concentrations. *Environment International* **29**: 33-37.